

**UNIVERSITAT POLITECNICA DE VALÈNCIA**

**DEPARTAMENTO DE INGENIERÍA DE LA CONSTRUCCIÓN Y  
PROYECTOS DE INGENIERÍA CIVIL**



**EVALUATION OF THE DEGRADATION PROCESS OF CEMENT-BASED  
MATERIALS EXPOSED TO AGGRESSIVE ENVIRONMENT BY USING  
ULTRASONIC TECHNIQUES AND PHYSICAL CHARACTERIZATION**

**Ph.D. Thesis**

Presented by:

Tarek Ibrahim Mahmoud Selouma

**Supervisor** Dr. José Vicente Fuente Ramírez  
**Tutor** Dr. José María Monzó Balbuena

Valencia, Spain in February 2013



**EVALUATION OF THE DEGRADATION PROCESS OF CEMENT-BASED  
MATERIALS EXPOSED TO AGGRESSIVE ENVIRONMENT BY USING  
ULTRASONIC TECHNIQUES AND PHYSICAL CHARACTERIZATION**

By

Tarek Ibrahim Mahmoud Selouma

Dissertation Submitted to the Department of Construction Engineering and  
Civil Engineering Projects in Partial Fulfillment of the Requirements for the  
Degree of

Doctor of PHILOSOPHY

At the

Polytechnic University of Valencia- Spain

February 2013

Certified by

Accepted by ...

Accepted by ...

Accepted by ...

Accepted by ...

Accepted by ...





## **ABSTRACT**

Reinforced Portland cement concrete was invented approximately more than one hundred years ago and it has become one of the most widely used industrial materials in the world. Thus, durability of concrete structures is one of the most important considerations in the design of the structures elements and when assessing the condition of existing structures. On the other hand, when the concrete is exposed to a severe environment such as highway bridges or marine structures whether it contains uncommon materials such as high alumina cement or re-cycled aggregates, thus, the knowledge of the concrete durability is a potential key to the long term performance.

Non-destructive tests are one of the greatest economic and social importance techniques, and it can be used to determine the durability of civil engineering structures where these materials are widely used. However, the usage of non-destructive techniques in these materials is not widespread around of the world, motivated mainly by the heterogeneous microstructural characteristics that shown by these materials. Between all non-destructive testing methods available for concrete examining, the use of ultrasonic waves is very essential to characterize the microstructure and material properties of inhomogeneous materials.

The objective of this work is to obtain an evaluation procedure of the cycle-life of precast concrete prepared and put into the service in marine environments. Also, the incorporation of various methodologies (destructive and non-destructive techniques), is studied and analyzed to characterize the degradation process of concrete and mortar degraded by sodium sulfate and ammonium nitrate solution. For this purpose, accurate integration of different techniques is used in order to characterize the properties and to follow the degradation process that affects the concrete.

As additional objectives, the relationship between destructive and non-destructive parameters is studied, also the relationship between the non-destructive parameters each other was studied. Most of the previous studies used the ultrasonic techniques to calculate the w/c ratio of concrete, mortar and cement paste to follow the effect of

variation of w/c ratio on the microstructure changes of such materials during the curing process. However, in this research, we study the effect of the variation of w/c ratio on ultrasonic parameters due to the degradation process by aggressive elements.

For this purpose, Limestone Portland Cement type II A-L 45.5R (LPC), and Sulfo-Resistant Portland Cement type I 42.5R/SR (SRPC) were used to fabricate two precast concrete frames, which were used in this study as a concrete in service (real case). On the other hand, for studying the effect of variation of w/c ratio on ultrasonic parameters due to the degradation process, mortar samples with different water-cement ratios 0.30, 0.375, 0.45 and 0.525 were fabricated by using cement type (LPC) to obtain different degradation levels.

To follow the degradation processes, an integration of ultrasonic techniques was used. For example, Ultrasonic Pulse-echo technique using frequencies (1 and 3.5MHz) is used to obtain the parameter of attenuation profile area (APA) which estimated by (Vergara et al., 2003) and used by (Fuente, 2004) to follow the curing process of mortar and cement paste; this parameter has a high sensitivity to characterize the changing of microstructure of cement based materials along the curing processes. Ultrasonic transmission-reception method is used to calculate wave velocity of ultrasonic longitudinal wave using frequency 1MHz and ultrasonic shear wave using frequency 500 KHz. Velocity of ultrasonic waves also has ability to follow the microstructural changes easily, because it is related by the variation of porosity. Ultrasonic image technique (UIT) using frequency 2MHz also was used for the same purpose.

As a destructive testing, compressive and flexural strength tests are used to follow the change in the strength of mortar and concrete, open porosity is used to observe the variation of porosity inside the material by the effect of the aggressive elements which penetrates the material and causes degradation, Mercury intrusion porosimetry (MIP) is used to observe the variation of the pores volume and finally Scanning Electron Microscopy (SEM) is used to allow quantifying and detecting the changes in the microstructure of concrete and mortar samples due to the attack by the aggressive elements.

The obtained results showed that, the degradation by sodium sulfate solution has two steps; the first step is due to the formation of ettringite and filling the pores by it, but yet it is not produced cracks. In this step it was observed a variation in the obtained parameters, for example increasing of ultrasonic wave velocity, the compressive and flexural strength or decreasing of porosity. This variation may indicates an increasing of the mechanical performance of materials under investigation, but in fact, this is not true because the pores are filled by ettringite and soon it will be expanded and causes degradation as showed in the second step. In the second step it was observed cracks and micro cracks due to the expansion of ettringite and increasing of its volume inside the pores. This changed the measured parameters to the contrast that was observed in the first step, for example a decreasing of ultrasonic wave velocity, compressive and flexural strength, and increasing of porosity etc. On the other hand one step degradation was observed for the degradation by ammonium nitrate solution due to the decalcification process from the start to the end of exposure time. For both cases the conjunction of the used techniques found to be successful to follow and estimate the degradation process, also it is found a good relationship between the destructive and non-destructive parameters.



## **RESUMEN**

El hormigón armado compuesto de cemento Portland fue inventado hace algo más de un siglo aproximadamente y se ha convertido en el material más utilizado en la construcción. La durabilidad de este hormigón es una de las consideraciones más importantes a ser tenidas en cuenta en el diseño de nuevas estructuras y en la evaluación estructural de las ya existentes. Cuando un hormigón sujeto a un ambiente o cargas que puede degradarlo, como puede ser su uso en puentes y ambientes marinos o si contiene grandes cantidades de alúmina o áridos reciclados, el conocimiento o predicción de su durabilidad es un aspecto crítico para su comportamiento en servicio.

Los ensayos no destructivos se han mostrado como unos de los ensayos preceptivos con una importancia económica y social más relevante desde que se han aplicado para la auscultación de la durabilidad de las estructuras de hormigón pertenecientes a la ingeniería civil, donde estos materiales son ampliamente utilizados. En cualquier caso, el uso de las técnicas no destructivas en estos materiales no está suficientemente implementado, hecho este motivado por las características heterogéneas de su microestructura. De todos los métodos no destructivos aplicables para el hormigón, el uso de pulsos ultrasónicos es de gran interés para la caracterización de la microestructura y las propiedades de materiales heterogéneos.

El objetivo del presente trabajo es obtener un procedimiento de evaluación del ciclo de vida del hormigón preparado y puesto en servicio para ambientes marinos. Además, será estudiado y analizado la incorporación de varias metodologías (destructivas y no destructivas) para caracterizar el proceso de degradación de morteros y hormigones expuestos a disolución de sulfato de sodio y a exposición en disolución de nitrato amónico. Con esta finalidad, una integración adecuada de diferentes técnicas será usada para la caracterización de propiedades y el seguimiento del proceso de degradación que afectan al hormigón.

Como objetivos adicionales, destaca que fueron estudiadas las relaciones entre los parámetros destructivos y no destructivos, así como la relación entre los distintos parámetros no destructivos entre sí. Muchos de los estudios anteriores que han usado

la inspección ultrasónica las cuáles fueron utilizadas para determinar la relación agua/cemento del mortero, de la pasta de cemento y del hormigón, o para monitorizar los cambios estructurales, para diferentes relaciones a/c, en el proceso de curado. En este trabajo de investigación fue analizado el efecto que tiene para diferentes relaciones a/c en los parámetros ultrasónicos durante el proceso de degradación.

Para este objetivo, se utilizaron un Cemento Portland tipo II A L 42.5 (LPC), y otro sulforresistente tipo I 42.5R/SR (SRPC) que fueron usados en la fabricación de dos marcos de hormigón, los cuales fueron utilizados como hormigón en servicio (caso real). Para el estudio del efecto de la variación de a/c en los parámetros ultrasónicos durante la degradación se utilizaron muestras de mortero con diferentes relaciones agua cemento 0.30, 0.375, 0.45 y 0.525 a partir de LPC para obtener diferentes niveles de degradación.

Para monitorizar el proceso de degradación se utilizó la inspección por pulso/eco (1 y 3.5 MHz) para la obtención del parámetro del área del perfil de atenuaciones (APA) el cual fue estimado por L Vergara et al., 2003 y usado por Fuente, 2004.

Para seguir el proceso de curado de pasta de cemento y morteros, este parámetro ha demostrado una alta sensibilidad para caracterizar los cambios microestructurales de materiales derivados del cemento a lo largo de su curado. El método de transmisión se ha utilizado para la determinación de las velocidades de ondas longitudinales con la frecuencia de 1MHz y transversales con la frecuencia de 500 kHz. La velocidad ultrasónica también ha demostrado la capacidad para seguir los cambios microestructurales de un modo sencillo porque dicho parámetro está relacionado con la variación de las propiedades mecánicas, y bajo ciertas premisas, con la variación de la porosidad. El análisis con la imagen ultrasónica con 2 MHz fue también usada para la consecución de los mismos objetivos.

Como métodos destructivos, los ensayos de resistencia a la compresión y flexión fueron los utilizados para determinar la pérdida de actividad resistente de morteros y hormigones, y la porosidad conectada al agua para analizar los cambios en la matriz porosa por el efecto de la difusión de elementos agresivos que penetran en el material provocando su degradación.

La porosimetría de mercurio (MIP) fue usada para observar las variaciones del volumen y tamaño de poro y, por último, la microscopía electrónica de barrido (MEB) que fue utilizada para cuantificar y detectar los cambios en la microestructura por el ataque de elementos agresivos.

Los resultados obtenidos muestran que, la degradación producida por exposición a sulfato de sodio, tiene dos etapas, en la primera etapa se forma la etringita que llena los poros pero que no produce microfisuración. En esta etapa se observó una variación en los parámetros obtenidos por ejemplo, incremento de la velocidad de la onda ultrasónica, de las resistencias a compresión y a la flexión o la disminución de la porosidad. Esta variación en los parámetros podría indicar una mejora en las prestaciones mecánicas del material objeto de la investigación, pero en realidad esto no es cierto porque los poros están llenos de etringita, provocando una expansión, que es la causa de la degradación en la segunda etapa. En dicha segunda etapa, se produce una microfisuración generalizada por la expansión de la etringita e incrementando su volumen dentro de los poros. Este hecho produjo un cambio en los parámetros medidos que contrastan con la evolución en la primera etapa, disminución de la velocidad de las ondas ultrasónicas, y de las resistencias mecánicas y consecuentemente un aumento de la porosidad. Por otro lado, la degradación por ataque de nitrato amonio tiene una única etapa debida al proceso de descalcificación que comienza desde el principio del proceso de exposición y es lineal durante todo el periodo de exposición. Para ambos casos, la integración de las diversas técnicas se revela como satisfactoria para el seguimiento del proceso de degradación, encontrando buenas correlaciones entre los parámetros no destructivos y los parámetros destructivos de técnicas de análisis físico-químico.





## **RESUM**

El formigó armat compost de ciment Portland va ser inventat fa poc més d'un segle aproximadament i s'ha revelat com al material amb més ús en la construcció. La durabilitat d'aquest formigó és una de les consideracions més importants a tenir en compte en el disseny de noves estructures i en l'avaluació estructural de les ja existents. Quan un formigó subjecte a un entorn o tensions que poden degradar-lo, com pot ser el seu ús en ponts i ambients marins o si conté grans quantitats d'alúmina o àrids reciclats, el coneixement o predicció de la seva durabilitat és una aspecte crític per al seu comportament en servei.

Els assajos no destructius s'han mostrat com uns dels assajos preceptius amb una importància econòmica i social més rellevant des que s'han aplicat per a la auscultació de la durabilitat de les estructures de formigó al marc de l'enginyeria civil, on aquests materials són àmpliament utilitzats. En qualsevol cas, l'ús de les tècniques no destructives en aquests materials no està prou implementada, aquest fet està motivat per les característiques heterogènies de la seua microestructura. De tots els mètodes no destructius aplicables per al formigó, l'ús de polsos ultrasònics és de gran interès per a la caracterització de la microestructura i les propietats de materials heterogenis.

L'objectiu d'aquest treball és obtindre un procediment d'avaluació del cicle de vida del formigó preparat i posat en servei als entorns marins. Més enllà, serà estudiat i analitzat la incorporació de diverses metodologies (destructives i no destructives) per caracteritzar el procés de degradació de morters i formigons exposats a dissolució de sulfat de sodi i l'exposició en dissolució de nitrat amònic. Amb aquesta finalitat, una integració adequada de diferents tècniques serà introduïda per a la caracterització de propietats i el seguiment del procés de degradació que afecten el formigó.

Com objectius addicionals, destaca que van ser estudiades les relacions entre els paràmetres destructius i no destructius, així com la relació entre els diferents paràmetres no destructius entre si. Molts dels estudis anteriors que han fet servir la inspecció ultrasònica les quals van ser introduïdes per determinar la relació aigua/ciment del morter, de la pasta de ciment i del formigó, o per monitoritzar els

canvis estructurals, per a diferents relacions a/c, al voltant del procés de curat. En aquest treball de recerca va ser analitzat l'efecte que té per a diferents relacions a/c en els paràmetres ultrasònics a lo llarg del procés de degradació.

Per aquest objectiu, es van utilitzar un ciment Portland del tipus II AL 42.5 (LPC), i un altre sulfurresistent del tipus I 42.5R/SR (SRPC) que van ser usats en la fabricació de dos marcs de formigó, els quals van ser destinats com formigó en servei (cas real). Per a l'estudi de l'efecte de la variació de a/c en els paràmetres ultrasònics a lo llarg de la degradació es van fer servir mostres de morter amb diferents relacions aigua/ciment 0.30, 0.375, 0.45 i 0.525 a partir de LPC per obtenir diferents estadis de degradació.

Per monitoritzar el procés de degradació es va fer servir la inspecció per pols/eco (1 i 3.5 MHz) per obtenir el paràmetre de l'àrea del perfil de atenuacions (APA) el qual va ser estimat per L. Vergara et al., 2003 i usat per Fuente et al, 2004. Per seguir el procés de curat de pasta de ciment i morters, aquest paràmetre ha demostrat una alta sensibilitat per caracteritzar els canvis microestructurals de materials derivats del ciment al llarg de la seua maduració. El mètode de transmissió s'ha fet servir per a la determinació de les velocitats d'ones longitudinals amb la freqüència de 1MHz i transversals amb la freqüència de 500 kHz. La velocitat ultrasònica també ha permès seguir els canvis microestructurals d'una manera senzilla perquè aquest paràmetre està relacionat amb la variació de les propietats mecàniques, i sota certes premisses, amb la variació de la porositat. L'anàlisi amb la imatge ultrasònica amb 2 MHz va ser també usada per a la consecució dels mateixos objectius.

Com mètodes destructius, els assaigs de resistència a la compressió i flexió van ser els utilitzats per determinar la pèrdua d'activitat resistent de morters i formigons, i la porositat connectada en l'aigua per analitzar els canvis en la matriu porosa per l'efecte de la difusió d'elements agressius que penetren en el material provocant la seva degradació.

La porosimetria de mercuri (MIP) va ser usada per observar les variacions del volum i la mida del porus i, finalment, la microscòpia electrònica de rastreig o d'escombratge

(MER) per a quantificar i detectar els canvis en la microestructura per l'atac d'elements agressius.

Els resultats obtinguts mostren que, la degradació produïda per exposició a sulfat de sodi, té dues etapes, en la primera etapa es forma la etringita que ompli els poros però que no produeix micro-fisuració. En aquesta etapa es va observar una variació en els paràmetres obtinguts per exemple, increment de la velocitat de l'ona ultrasònica, de les resistències a compressió i a la flexió o la disminució de la porositat. Aquesta variació en els paràmetres podria indicar una millora en les prestacions mecàniques del material objecte de la recerca, però en realitat això no és cert perquè els poros estan plens de etringita i aviat expandirà essent la causa de la degradació en la segona etapa. En aquesta segona etapa, es produeix una microfisuració generalitzada per l'expansió de la etringita i el increment del seu volum dins dels poros. Això va conduir al canvi dels paràmetres mesurats per causa del procés de degradació que posa el contrast amb el que es va observar en la primera etapa.

D'altra banda, la degradació per atac de nitrat d'amoniac té una única etapa deguda al procés de desqualificació que comença des del principi del procés d'exposició i és lineal a lo llarg de tot el període d'exposició. Per a ambdós casos, la integració de les diverses tècniques es revela com satisfactòria per al seguiment del procés de degradació, trobant bones correlacions entre els paràmetres no destructius i els paràmetres destructius de tècniques d'anàlisi físic-químic.



## DEDICATION

*I dedicate this work to whom my heartfelt thanks; to my parents, wife, daughters and my brothers for their patience and help. These times have been very hard for you and for me. Thank you for your strength and support, for your understanding and your love.*

*As well as to my friends for all the support they lovely offered along the period of my post-graduation.*

## **ACKNOWLEDGEMENTS**

First of all, praise to Allah the greatest, the most merciful, the all beneficent, the omniscient, who guided the man to know which he did not know.

Then, as recognition of gratitude, I introduce my great respect and thanks for my parents for their continuous material and moral assistance in hole my life until being in the current position.

I'd like also to thank my wife who was besides me at the good and bad moments in this work with sharing me both of them with complete happiness and satisfaction. My thanks also to all my family and my friends, how was besides me during this work.

I would like to express my deep thanks to my research supervisor, Dr. José Vicente Fuente for his continuous encouragement, helpful suggestions, valuable supervision and reading throughout the manuscript which have rendered the realization of this work to be possible. I would like to express also my deep thanks to Prof. José María Monzo Balbuena for his help during all years of this work.

Special and deep thanks to AIDICO Instituto Tecnológico de la Construcción, where the tests of this work were realized during many years. Also I wish to thank the AIDICO director D. Ramón Congost Valles for many things, especially, his help for renovation of my NIE.

I would like to knowledge the help I received from all the people, deep thank to Dr. José Javier Anaya and to all people who helped me for realizing ultrasonic Imaging test. Many thanks to Pepe Azorin who realized Mercury Intrusion Porosity test. Also I would like to thank Stephanie, Pilar Lozano and Isabel Girbés for their help in Scanning electron microscope test (SEM). Also have to thank Fernando Mohedano and Angel Carcer for their help in the laboratory work during the research period.

I'd like also to thank my brothers Eng. Mahmoud, Dr. Mustafa, Eng. Mohamed, Eng. Ahmed and my sisters Rasha and Shima. Also many and deep especial thanks to Dr. Mohamed Abdelkader and my brother Dr. Safwat Abdelkader

Thanks for all my friends, Egyptian friends especially, Abeer. Deep thanks to my friends Ayman el Nagar, Mohamed Ragab, Ramy Shaltout, Mohammed Ali, Abd Allah, Mohamed Alaa, Khaled Harby, Ahmed Yehia and his wife.

Also I would like to thank the new Egyptian collages, Abdelrahman, Abdel Sattar, Ragab, Amr and Ahmed Izzat. Deep thanks to my Tunisian friends Nidhal Ammar and Abelhedi Chaieb and many thanks to my friends Youssef Aluni, Naufal, Amaal, Zoulaikha, and Sara.

I also wish to thank my colleagues of the structural assessment and non-destructive test department for their help and friendship during more than 4 years, many thanks to Javier Yuste, Dolores Rodríguez, Rafael Martinez, Nuria González, Juan Vicente Sabater, Santiago Martínez, Vicente Albert and Vicente Císcar. Thanks are also to Marina, Belén, Alejandro, Isabel González, Pilar Lozano, Susana, María José, Elena, Diana, Pau, Nacho, Carlos, Sara, Ana, Paco Martínez, Juan Cuenca and Javier Mohedano.

Many thanks to all the people of AIDICO





## TABLE OF CONTENTS

<b>Abstract</b>	<b>i</b>
<b>Resumen</b>	<b>v</b>
<b>Resum</b>	<b>ix</b>
<b>Acknowledgements</b>	<b>xiv</b>
<b>Table of Contents</b>	<b>xvii</b>
<b>list of tables</b>	<b>xix</b>
<b>List of figure</b>	<b>xxi</b>
<b>Nomenclature</b>	<b>xxvii</b>
<b>1 Introduction</b>	<b>1</b>
1.1. Objectives.....	3
1.2. Structure of Thesis .....	5
<b>2 Literature Review</b>	<b>9</b>
2.1. Literature Review on Cement Based Materials .....	9
2.1.1. Composition and Hydration of Cement .....	10
2.1.1.1. Hydration of Tricalcium Silicate and Dicalcium Silicate.....	13
2.1.1.2. Hydration of Tricalcium Aluminate and Tetracalcium Aluminoferrite .....	13
2.1.2. Microstructure of Hardened Cement Paste .....	14
2.1.2.1 Pores in cement paste, mortar and concrete .....	15
Gel pores .....	16
Capillary pores.....	18
2.1.3. Durability of concrete structure in marine environment .....	18
2.1.3.1. Causes of concrete degradation.....	21
Sulfate Attack.....	22
Sea water Attack .....	24
Chloride Attack.....	26
Freeze-thaw Degradation.....	27
2.2. Literature Review of Ultrasonic Techniques .....	29
2.2.1. Non-destructive Testing .....	29
2.2.2. Non-destructive analysis by Ultrasonic Techniques .....	32
2.2.3. Characterization of Cement-based Materials using Ultrasonic Testing .....	34
2.2.3.1. Sulfate attack degradation characterized by Ultrasonic Techniques .....	38
2.2.3.2 Freeze-thaw Characterization by Ultrasonic Techniques.....	39
2.2.3.3. Compressive and flexural strength characterization by Ultrasonic techniques .....	41

2.2.3.4. Porosity characterization by Ultrasonic techniques.....	42
<b>3 Materials, Samples Preparation and Methods</b>	<b>49</b>
3.1. Materials.....	49
3.1.1. Cement.....	49
3.1.2. Aggregate and sand used for precast concrete.....	50
3.1.3. Water.....	51
3.1.4. Admixtures.....	51
3.2. Experimental development.....	52
3.2.1. Mixture proportions and manufacture of concrete frames.....	52
3.2.2. Coring procedures.....	53
3.2.3. Mixture proportions and manufacture of mortar.....	54
3.2.4. Chemical dissolutions.....	56
3.2.5. Compressive strength test.....	57
3.2.6. Flexural strength test.....	58
3.2.7. Porosity measurement.....	59
3.2.8. Ultrasonic testing.....	60
3.2.8.1. Equipment Calibration.....	61
3.2.8.2. Pulse-echo method.....	63
3.2.8.3. Through-Transmission.....	69
Velocity Estimation.....	71
3.2.8.4. Ultrasonic Image.....	72
3.2.9. Scanning Electron Microscopy.....	74
3.2.10. Mercury Intrusion Porosimetry.....	77
<b>4 Results and Discussion the Degradation process by Sodium Sulfate</b>	<b>83</b>
4.1. Analysis and Discussion the Results of Mortar.....	83
4.1.1. Visual Examination.....	83
4.1.2. Scanning Electron Microscopy (SEM).....	85
4.1.3. Compressive and Flexural Strength.....	89
4.1.4. Open Porosity.....	91
4.1.5. Mercury Intrusion Porosimetry (MIP).....	93
4.1.6. Ultrasound Longitudinal and Transversal Wave Velocity.....	99
4.1.7. Ultrasonic Attenuation Profile Area (APA).....	102
4.1.8. Ultrasonic Tomography Imaging.....	116
4.2. Correlation the Measured Parameters for Mortar.....	123
4.2.1. Correlation Ultrasonic P and S-Wave Velocity versus Porosity.....	123
4.2.2. Correlation Attenuation Profile Area versus Porosity.....	126
4.2.3. Correlation P and S-Wave Velocity vs Compressive and Flexural Strength.....	129
4.2.4. Correlation Attenuation Profile Area vs Compressive and Flexural Strengt.....	133
4.2.5. Correlation P and S- Wave Velocity versus APA.....	136
4.3. Analysis and Discussion the Results of Concrete.....	139
4.3.1. Scanning Electron Microscopy (SEM).....	139
4.3.2. Compressive Strength.....	145
4.3.3. Open Porosity.....	146
4.3.4. Ultrasound Longitudinal and Transversal Wave Velocity.....	147
4.3.5. Ultrasonic Attenuation Profile Area (APA).....	149
4.3.6. Ultrasonic Tomography Imaging.....	156
4.4. Correlation the Measured Parameters for Concrete.....	166

4.4.1. Correlation Ultrasonic P and S-Wave Velocity versus Porosity .....	166
4.4.2. Correlation Attenuation Profile Area versus Porosity .....	168
4.4.3. Correlation P and S-wave Velocity versus Compressive Strength.....	169
4.4.4. Correlation Attenuation profile Area versus Compressive Strength .....	170
4.4.5. Correlation P- Wave and S-wave versus APA .....	171
<b>5 Results and Discussion the Degradation Process Ammonium Nitrate</b>	<b>179</b>
5.1. Analysis and Discussion the Results of Mortar .....	179
5.1.1. Compressive and Flexural Strength .....	179
5.1.2. Open Porosity.....	182
5.1.3. Ultrasonic Longitudinal and Transversal Wave Velocity.....	183
5.1.4. Ultrasonic Attenuation Profile Area (APA) 1 and 3.5 MHz.....	185
5.2. Correlation the Measured Parameters for Mortar .....	194
5.2.1. Correlation Ultrasonic P and S-wave Velocity versus Porosity .....	194
5.2.2. Correlation Ultrasonic Attenuation Profile Area versus Porosity.....	195
5.2.3. Correlation P and S-wave Velocity vs Compressive and Flexural Strength .	196
5.2.4. Correlation Attenuation Profile Area vs Compressive and Flexural Strength	199
5.2.5. Correlation P and S-wave versus APA .....	200
5.3. Analysis and Discussion the Results of Concrete .....	202
5.3.1. Compressive Strength .....	202
5.3.2. Open Porosity.....	204
5.3.3. Ultrasonic Longitudinal and Transversal Wave Velocity.....	205
5.3.4. Ultrasonic Attenuation Profile Area (APA).....	208
5.4. Correlation the Measured Parameters for Concrete .....	214
5.4.1. Correlation Ultrasonic P and S-Wave Velocity versus Porosity .....	214
5.4.2. Correlation Attenuation Profile Area versus Porosity .....	216
5.4.3. Correlation P and S-Wave Velocity versus Compressive Strength.....	217
5.4.4. Correlation Attenuation Profile Area versus Compressive Strength .....	219
5.4.5. Correlation P and S- waves versus APA.....	220
<b>6 Conclusions</b>	<b>227</b>
<b>7 Future Work</b>	<b>231</b>
<b>8 References</b>	<b>233</b>

## LIST OF TABLES

<b>TABLE 2-1</b> CHEMICAL FORMULA AND CEMENT NOMENCLATURE FOR MAJOR CONSTITUENTS OF PORTLAND CEMENT. ABBREVIATION NOTATION: C = CAO, S = SiO <sub>2</sub> , A = AL <sub>2</sub> O <sub>3</sub> , F = Fe <sub>2</sub> O <sub>3</sub> . (ANDREW.B, 2010).....	11
<b>TABLE 2-2</b> COMPOSITION OF HARDENED CEMENT PASTE (w/c = 0.5) (BENSTED, 2001) .....	15
<b>TABLE 2-3</b> CLASSIFICATIONS OF THE PORE SIZES IN HYDRATED CEMENT (GI-SUNG PANG, 2009).....	18
<b>TABLE 2-4</b> CONCENTRATION OF MAJOR IONS IN SOME OF THE WORLD SEAS (MEHTA ET AL., 2006).21	
<b>TABLE 3-1</b> CHEMICAL COMPOSITION OF PORTLAND CEMENT.....	49
<b>TABLE 3- 2</b> PARTICLE SIZE DISTRIBUTION OF USED AGGREGATES AND SAND.....	51
<b>TABLE 3- 3</b> ANALYSIS OF WATER USED IN PREPARING PREFABRICATED CONCRETE.....	51
<b>TABLE 3- 4</b> FEATURES OF SIKAPAVER.....	51
<b>TABLE 3-5</b> MIXTURE PROPORTIONS FOR PRECAST CONCRETE FRAMES.....	53

<b>TABLE 3- 6</b>	<b>TEST TYPES AND CORE NUMBERS.....</b>	<b>54</b>
<b>TABLE 3- 7</b>	<b>MIXTURE PROPORTION OF MORTAR SPECIMENS.....</b>	<b>55</b>
<b>TABLE 3- 8</b>	<b>TEST TYPES AND MORTAR TOTAL SAMPLES NUMBER.....</b>	<b>55</b>
<b>TABLE 3-9</b>	<b>CHEMICAL DISSOLUTION USED.....</b>	<b>56</b>
<b>TABLE 3- 10</b>	<b>EQUIPMENT SETTING/CONFIGURATION FOR PULSE-ECHO TEST (MORTAR).....</b>	<b>64</b>
<b>TABLE 3- 11</b>	<b>EQUIPMENT SETTING FOR PULSE-ECHO TEST (CONCRETE).....</b>	<b>64</b>
<b>TABLE 3- 12</b>	<b>EQUIPMENT SETTING FOR THROUGH-TRANSMISSION TEST (MORTAR).....</b>	<b>69</b>
<b>TABLE 3- 13</b>	<b>EQUIPMENT SETTING FOR THROUGH-TRANSMISSION TEST (CONCRETE).....</b>	<b>70</b>
<b>TABLE 4- 1</b>	<b>EDS ANALYSIS FOR A SIMPLE DEGRADED BY 10% OF SODIUM SULFATE SOLUTION FOR 450 DAYS.....</b>	<b>86</b>
<b>TABLE 4- 2</b>	<b>VALUES OF ATTENUATION PROFILE AREA (APA) OF FREQUENCY 1MHZ FOR CONTROL AND SAMPLES DEGRADED BY SODIUM SULFATE SOLUTION FOR 450 DAYS.....</b>	<b>115</b>
<b>TABLE 4- 3</b>	<b>VALUES OF ATTENUATION PROFILE AREA (APA) OF FREQUENCY 3.5MHZ FOR CONTROL AND SAMPLES DEGRADED BY SODIUM SULFATE SOLUTION FOR 450 DAYS.....</b>	<b>115</b>
<b>TABLE 4- 4</b>	<b>% VARIATION OF ATTENUATION PROFILE AREA (APA) OF FREQUENCY 1MHZ DUE TO THE DEGRADATION PROCESS BY 10% OF SODIUM SULFATE SOLUTION.....</b>	<b>115</b>
<b>TABLE 4- 5</b>	<b>% VARIATION OF ATTENUATION PROFILE AREA (APA) OF FREQUENCY 3.5MHZ DUE TO THE DEGRADATION PROCESS BY 10% OF SODIUM SULFATE SOLUTION.....</b>	<b>115</b>
<b>TABLE 4- 6</b>	<b>VALUES MEAN VELOCITY FOR CONTROL AND SAMPLES DEGRADED BY SODIUM SULFATE SOLUTION FOR 450 DAYS. ....</b>	<b>122</b>
<b>TABLE 4- 7</b>	<b>REGRESSION COEFFICIENT FACTORS FOR CONTROL AND DEGRADED SAMPLES FOR BOTH FREQUENCIES 1 AND 3.5MHZ.....</b>	<b>127</b>
<b>TABLE 4- 8</b>	<b>ULTRASONIC MEAN VELOCITY OF THE DEGRADED SAMPLES IN THE DIRECTION OF SAMPLE AXIS (AXIAL) .....</b>	<b>162</b>
<b>TABLE 4- 9</b>	<b>ULTRASONIC MEAN VELOCITY OF THE DEGRADED SAMPLES IN THE DIRECTION PERPENDICULAR TO THE SAMPLE AXIS (RADIAL).....</b>	<b>162</b>
<b>TABLE 4-10</b>	<b>ULTRASONIC MEAN VELOCITY OF THE CONTROL SAMPLES IN THE DIRECTION OF SAMPLE AXIS (AXIAL) .....</b>	<b>163</b>
<b>TABLE 4-11</b>	<b>ULTRASONIC MEAN VELOCITY OF THE CONTROL SAMPLES IN THE DIRECTION PERPENDICULAR TO THE SAMPLE AXIS (RADIAL).....</b>	<b>163</b>
<b>TABLE 5- 1</b>	<b>COMPRESSIVE STRENGTH AND COMPRESSIVE STRENGTH LOSS FOR CONTROL AND AMMONIUM NITRATE SIMPLES .....</b>	<b>181</b>
<b>TABLE 5- 2</b>	<b>FLEXURAL STRENGTH AND FLEXURAL STRENGTH LOSS FOR CONTROL AND AMMONIUM NITRATE SIMPLES.....</b>	<b>181</b>
<b>TABLE 5- 3</b>	<b>ATTENUATION PROFILE AREA (APA) FOR FREQUENCY 1MHZ FOR CONTROL AND AMMONIUM NITRATE SIMPLES .....</b>	<b>191</b>
<b>TABLE 5- 4</b>	<b>ATTENUATION PROFILE AREA (APA) FOR FREQUENCY 3.5MHZ FOR CONTROL AND AMMONIUM NITRATE SIMPLES .....</b>	<b>192</b>
<b>TABLE 5- 5</b>	<b>THE THICKNESS DEPTH OF THE DEGRADED SAMPLES ESTIMATED BY PHENOLPHTHALEIN .....</b>	<b>193</b>
<b>TABLE 5- 6</b>	<b>COMPRESSIVE STRENGTH AND COMPRESSIVE STRENGTH LOSS FOR CONTROL AND AMMONIUM NITRATE SIMPLES .....</b>	<b>203</b>
<b>TABLE 5- 7</b>	<b>POROSITY VARIATION OF CONTROL AND AMMONIUM NITRATE SIMPLES .....</b>	<b>204</b>
<b>TABLE 5- 8</b>	<b>P-WAVE VELOCITY VARIATION OF CONTROL AND AMMONIUM NITRATE SIMPLES.....</b>	<b>207</b>
<b>TABLE 5- 9</b>	<b>VARIATION OF S-WAVE VELOCITY FOR CONTROL AND AMMONIUM NITRATE SIMPLES ....</b>	<b>207</b>

<b>TABLE 5- 10</b>	APA 1MHZ FOR CONTROL AND AMMONIUM NITRATE SAMPLES .....	213
<b>TABLE 5- 11</b>	APA 3.5 MHZ FOR CONTROL AND AMMONIUM NITRATE SAMPLES .....	214

## LIST OF FIGURES

<b>FIGURE 2-1</b>	COMPLEXITY OF CONCRETE MICROSTRUCTURE GARBOCZI, 1995 .....	10
<b>FIGURE 2-2</b>	A PICTORIAL REPRESENTATION OF A CROSS-SECTION OF A CEMENT GRAIN. ADAPTED FROM CEMENT MICROSCOPY, HALLIBURTON SERVICES, DUNCAN, OK. (ANDREW AND JOHNSON, 2008) .....	12
<b>FIGURE 2-3</b>	SCHEMATIC REPRESENTATION OF ANHYDROUS CEMENT (A) AND THE EFFECT OF HYDRATION AFTER (B) 10 MINUTES, (C) 10 HOURS, (D) 18 HOURS, (E) 1-3 DAYS, AND (F) 2 WEEKS. ADAPTED FROM M. BISHOP, PHD THESIS, RICE UNIVERSITY, 2001, (ANDREW AND JOHNSON, 2008).....	17
<b>FIGURE 2-4</b>	PROPOSED DEGRADATION MECHANISMS ACTING ON CONCRETE EXPOSED TO SEA WATER (MALHORTA 2000). .....	20
<b>FIGURE 2-5</b>	PHYSICAL CAUSES OF CONCRETE DETERIORATION (MEHTA, 2003).....	21
<b>FIGURE 2-6</b>	TYPES OF CHEMICAL REACTIONS RESPONSIBLE FOR CONCRETE DETERIORATION (MEHTA, 2003) A, SOFT-WATER ATTACK ON CALCIUM HYDROXIDE AND C-S-H PRESENTS IN HYDRATED PORTLAND CEMENTS: B(I), ACIDIC SOLUTION FORMING SOLUBLE CALCIUM COMPOUNDS SUCH AS CALCIUM CHLORIDE, CALCIUM SULFATE, CALCIUM ACETATE, OR CALCIUM BICARBONATE; B(II), SOLUTIONS OF OXALIC ACID AND ITS SALTS, FORMING CALCIUM OXALATE; B(III), LONG-TERM SEAWATER ATTACK WEAKENING THE C-S-H BY SUBSTITUTION OF $Mg^{2+}$ FOR $Ca^{2+}$ ; C, (1) SULFATE ATTACK FORMING ETTRINGITE AND GYPSUM, (2) ALKALI AGGREGATE ATTACK, (3) CORROSION OF STEEL IN CONCRETE, (4) HYDRATION OF CRYSTALLINE MGO AND CAO .....	22
<b>FIGURE 2-7</b>	(A) ANODIC AND CATHODIC REACTIONS IN THE CORROSION OF STEEL IN CONCRETE, (B) VOLUMETRIC EXPANSION AS A RESULT OF OXIDATION OF METALLIC IRON (MEHTA, 2003).....	27
<b>FIGURE 2-8</b>	DEGRADATION BY FREEZE-THAW CYCLES (WWW.ENGR.PSU.EDU) .....	29
<b>FIGURE 2-9</b>	THE SCOPE OF NON-DESTRUCTIVE TESTING (SMITH, 1998).....	31
<b>FIGURE 2-10</b>	NDT TECHNIQUES FOR LOCATING SURFACE FLAWS (SMITH, 1998).....	31
<b>FIGURE 2-11</b>	NDT TECHNIQUES FOR MONITORING STRUCTURAL VARIABILITY (SMITH, 1998) .....	32
<b>FIGURE 2-12</b>	NDT TECHNIQUES FOR LOCATING INTERNAL FLAWS (SMITH, 1998) .....	32
<b>FIGURE 2-13</b>	MULTI-LENGTH SCALES EXISTING IN CEMENT-BASED MATERIALS MICROSTRUCTURE (MEHTA AND MONTEIRO, 1993; WONSIRI, 2006). .....	34
<b>FIGURE 3-1</b>	CURVE OF GRADING OF FINE AND COARSE AGGREGATES.....	50
<b>FIGURE 3-2</b>	PRECAST CONCRETE FRAMES ON AIDICO FACILITIES.....	52
<b>FIGURE 3-3</b>	CORING PROCEDURES.....	53
<b>FIGURE 3-4</b>	PROCEDURE OF MORTAR PREPARING .....	55
<b>FIGURE 3-5.</b>	SOME OF THE PLASTIC BOXES USED IN THE ENTIRE RESEARCH WITH 120 x 80 x 25 CM. OF DIMENSIONS, IN THE DURABILITY CHAMBER AT AIDICO.....	57
<b>FIGURE 3-6</b>	PROCEDURE OF COMPRESSIVE STRENGTH FOR CONCRETE CORES AND MORTAR SAMPLES. 58	
<b>FIGURE 3-7</b>	PROCEDURE OF FLEXURAL TEST.....	59
<b>FIGURE 3-8</b>	PROCEDURE OF POROSITY MEASUREMENT .....	60
<b>FIGURE 3-9</b>	REFERENCE BLOCKS USED FOR THE EQUIPMENT CALIBRATION .....	62
<b>FIGURE 3-10</b>	PROCEDURE OF ULTRASONIC TESTING.....	63
<b>FIGURE 3-11</b>	ULTRASONIC TRANSDUCERS USED .....	63
<b>FIGURE 3-12</b>	PROCEDURE OF THE MEASUREMENT BY PULSE-ECHO METHOD.....	65
<b>FIGURE 3-13</b>	SCHEME OF INSPECTION FOR PULSE/ECHO.....	66
<b>FIGURE 3-14</b>	SCHEME OF TIME-FREQUENCY ANALYSIS PROCEDURE.....	68

<b>FIGURE 3-15</b>	PROCEDURE OF THE MEASUREMENT BY THROUGH-TRANSMISSION METHOD.....	70
<b>FIGURE 3-16</b>	AN EXAMPLE FOR P AND S-WAVE SIGNALS OBTAINED BY ULTRASONIC THROUGH-TRANSMISSION MODE.....	72
<b>FIGURE 3-18</b>	AN EXAMPLE OF ULTRASONIC IMAGE RESULTS.....	73
<b>FIGURE 3-17</b>	PHOTOS OF (A) THE AUTOMATIC POSITIONING SYSTEM FOR X, Y, Z COORDINATES AND THE TANK; (B) A SAMPLE ROW SUBMERGED INTO WATER; AND (C) THE TRANSMISSION MODE APPLIED TO THE MORTAR SAMPLES (M. MOLERO ET AL, 2009).....	74
<b>FIGURE 3-19</b>	EQUIPMENT OF SCANNING ELECTRON MICROSCOPY AT AIDICO FACILITIES.....	76
<b>FIGURE 3-20</b>	EXAMINATION POINTS OF SEM SAMPLE.....	76
<b>FIGURE 3-21</b>	THE EQUIPMENT USED FOR MIP TEST, AUTOPORE IV 9520 POROSIMETER MODEL.....	79
<b>FIGURE 4-1</b>	VISUAL RATINGS OF DETERIORATION DUE TO SULFATE ATTACK, AL-AMOUDI, 1992.....	84
<b>FIGURE 4-2</b>	VISUAL EXAMINATIONS, 340 DAYS OF DEGRADATION BY SOLUTION OF SODIUM SULFATE.....	84
<b>FIGURE 4-3</b>	VISUAL EXAMINATIONS, 450 DAYS OF DEGRADATION BY SOLUTION OF SODIUM SULFATE.....	85
<b>FIGURE 4-4</b>	SEM AND EDS ANALYSIS OF MORTAR SAMPLES IMMERSSED IN SODIUM SULFATE SOLUTION FOR A 200 DAYS, SHOWING THE MICRO CRACKS PRODUCED BY THE EFFECT OF ETTRINGITE FORMATION.....	87
<b>FIGURE 4-5</b>	SEM AND EDS ANALYSIS OF MORTAR SAMPLES IMMERSSED IN SODIUM SULFATE SOLUTION FOR A 450 DAYS, SHOWING THE MICRO CRACKS PRODUCED BY THE EFFECT OF ETTRINGITE FORMATION FOR A POINT FALLS AT DISTANCE OF 18.904MM FROM THE ATTACKED SURFACE.....	88
<b>FIGURE 4-6</b>	COMPRESSIVE AND FLEXURAL STRENGTH OF MORTAR SAMPLES.....	90
<b>FIGURE 4-7</b>	COMPRESSIVE AND FLEXURAL STRENGTH LOSS OF MORTAR SAMPLES.....	91
<b>FIGURE 4-8</b>	POROSITY OF MORTAR SUBMERGED IN 10% SODIUM SULFATE AND CONTROL.....	93
<b>FIGURE 4-9</b>	LOG DIFFERENTIAL INTRUSION $w/c = 0.30$ CONTROL.....	95
<b>FIGURE 4-10</b>	CUMULATIVE PORE SIZE DISTRIBUTION $w/c=0.30$ CONTROL.....	95
<b>FIGURE 4-11</b>	LOG DIFFERENTIAL INTRUSION $w/c = 0.30$ SODIUM SULFATE.....	95
<b>FIGURE 4-12</b>	CUMULATIVE PORE SIZE DISTRIBUTION $w/c=0.30$ SODIUM SULFATE.....	95
<b>FIGURE 4-13</b>	LOG DIFFERENTIAL INTRUSION $w/c = 0.375$ CONTROL.....	96
<b>FIGURE 4-14</b>	CUMULATIVE PORE SIZE DISTRIBUTION $w/c=0.375$ CONTROL.....	96
<b>FIGURE 4-15</b>	LOG DIFFERENTIAL INTRUSION $w/c = 0.375$ SODIUM SULFATE.....	96
<b>FIGURE 4-16</b>	CUMULATIVE PORE SIZE DISTRIBUTION $w/c=0.375$ SODIUM SULFATE.....	96
<b>FIGURE 4-17</b>	LOG DIFFERENTIAL INTRUSION $w/c = 0.45$ CONTROL.....	97
<b>FIGURE 4-18</b>	CUMULATIVE PORE SIZE DISTRIBUTION $w/c=0.45$ CONTROL.....	97
<b>FIGURE 4-19</b>	LOG DIFFERENTIAL INTRUSION $w/c = 0.45$ SODIUM SULFATE.....	97
<b>FIGURE 4-20</b>	CUMULATIVE PORE SIZE DISTRIBUTION $w/c=0.45$ SODIUM SULFATE.....	97
<b>FIGURE 4-21</b>	LOG DIFFERENTIAL INTRUSION $w/c = 0.525$ CONTROL.....	98
<b>FIGURE 4-22</b>	CUMULATIVE PORE SIZE DISTRIBUTION $w/c=0.525$ CONTROL.....	98
<b>FIGURE 4-23</b>	LOG DIFFERENTIAL INTRUSION $w/c = 0.525$ SODIUM SULFATE.....	98
<b>FIGURE 4-24</b>	CUMULATIVE PORE SIZE DISTRIBUTION $w/c=0.525$ SODIUM SULFATE.....	98
<b>FIGURE 4-25</b>	LONGITUDINAL WAVE VELOCITY WITH TIME.....	101
<b>FIGURE 4-26</b>	TRANSVERSAL WAVE VELOCITY WITH TIME.....	101
<b>FIGURE 4-27</b>	(A) AVERAGED DEPTH-FREQUENCY SPECTROGRAM (CONTOUR), (B) AVERAGED DEPTH-AND FREQUENCY-DEPENDENT SPECTROGRAM (PCOLOR) FOR EACH DEGRADATION TIME FOR $w/c = 0.525$ MORTAR DEGRADED BY SODIUM SULFATE SOLUTION, CENTRAL FREQUENCY 3.5MHz.....	104
<b>FIGURE 4-28</b>	(A) AVERAGED DEPTH-FREQUENCY SPECTROGRAM (CONTOUR), (B) AVERAGED DEPTH-AND FREQUENCY-DEPENDENT SPECTROGRAM (PCOLOR) FOR EACH DEGRADATION TIME FOR $w/c = 0.45$ MORTAR DEGRADED BY SODIUM SULFATE SOLUTION, CENTRAL FREQUENCY 3.5MHz.....	105
<b>FIGURE 4-29</b>	(A) AVERAGED DEPTH-FREQUENCY SPECTROGRAM (CONTOUR), (B) AVERAGED DEPTH-AND FREQUENCY-DEPENDENT SPECTROGRAM (PCOLOR) FOR EACH DEGRADATION TIME FOR $w/c = 0.375$ MORTAR DEGRADED BY SODIUM SULFATE SOLUTION, CENTRAL FREQUENCY 3.5MHz.....	106

<b>FIGURE 4-30</b> (A) AVERAGED DEPTH–FREQUENCY SPECTROGRAM (CONTOUR), (B) AVERAGED DEPTH- AND FREQUENCY-DEPENDENT SPECTROGRAM (PCOLOR) FOR EACH DEGRADATION TIME FOR W/C =0.30 MORTAR DEGRADED BY SODIUM SULFATE SOLUTION, CENTRAL FREQUENCY 3.5MHz. ....	107
<b>FIGURE 4-31</b> (A) AVERAGED DEPTH–FREQUENCY SPECTROGRAM (CONTOUR), (B) AVERAGED DEPTH- AND FREQUENCY-DEPENDENT SPECTROGRAM (PCOLOR) FOR EACH DEGRADATION TIME FOR W/C =0.525 MORTAR DEGRADED BY SODIUM SULFATE SOLUTION, CENTRAL FREQUENCY 1MHz.....	108
<b>FIGURE 4-32</b> (A) AVERAGED DEPTH–FREQUENCY SPECTROGRAM (CONTOUR), (B) AVERAGED DEPTH- AND FREQUENCY-DEPENDENT SPECTROGRAM (PCOLOR) FOR EACH DEGRADATION TIME FOR W/C =0.45 MORTAR DEGRADED BY SODIUM SULFATE SOLUTION, CENTRAL FREQUENCY 1MHz.....	109
<b>FIGURE 4-33</b> (A) AVERAGED DEPTH–FREQUENCY SPECTROGRAM (CONTOUR), (B) AVERAGED DEPTH- AND FREQUENCY-DEPENDENT SPECTROGRAM (PCOLOR) FOR EACH DEGRADATION TIME FOR W/C =0.375 MORTAR DEGRADED BY SODIUM SULFATE SOLUTION, CENTRAL FREQUENCY 1MHz.....	110
<b>FIGURE 4-34</b> (A) AVERAGED DEPTH–FREQUENCY SPECTROGRAM (CONTOUR), (B) AVERAGED DEPTH- AND FREQUENCY-DEPENDENT SPECTROGRAM (PCOLOR) FOR EACH DEGRADATION TIME FOR W/C =0.30 MORTAR DEGRADED BY SODIUM SULFATE SOLUTION, CENTRAL FREQUENCY 1MHz.....	111
<b>FIGURE 4-35</b> ATTENUATION PROFILE AREA 1 MHz WITH TIME.....	114
<b>FIGURE 4-36</b> ATTENUATION PROFILE AREA 3.5 MHz WITH TIME.....	114
<b>FIGURE 4-37</b> ATTENUATION AND VELOCITY OF ULTRASONIC WAVES FOR W/C RATIO 0.30.....	118
<b>FIGURE 4-38</b> ATTENUATION AND VELOCITY OF ULTRASONIC WAVES FOR W/C RATIO 0.375.....	119
<b>FIGURE 4-39</b> ATTENUATION AND VELOCITY OF ULTRASONIC WAVES FOR W/C RATIO 0.45.....	120
<b>FIGURE 4-40</b> ATTENUATION AND VELOCITY OF ULTRASONIC WAVES FOR W/C RATIO 0.525.....	121
<b>FIGURE 4-41</b> AVERAGE OF ULTRASONIC WAVE VELOCITY OBTAINED BY UTI TECHNIQUE FOR W/C RATIOS 0.30, 0.375, 0.45 AND 0.525, CONTROL AND SAMPLES DEGRADED BY SODIUM SULFATE. ....	122
<b>FIGURE 4-42</b> CORRELATION POROSITY WITH P- WAVE CONTROL.....	125
<b>FIGURE 4-43</b> CORRELATION POROSITY WITH S- WAVE CONTROL.....	125
<b>FIGURE 4-44</b> CORRELATION POROSITY WITH P- WAVE FOR SODIUM SULFATE SAMPLES.....	125
<b>FIGURE 4-45</b> CORRELATION POROSITY WITH S- WAVE FOR SODIUM SULFATE.....	125
<b>FIGURE 4-46</b> CORRELATION POROSITY WITH APA 1MHz CONTROL.....	128
<b>FIGURE 4-47</b> CORRELATION POROSITY WITH APA 3.5MHz CONTROL.....	128
<b>FIGURE 4-48</b> CORRELATION POROSITY WITH APA 1MHz SODIUM SULFATE.....	128
<b>FIGURE 4-49</b> CORRELATION POROSITY WITH APA 3.5MHz SODIUM SULFATE.....	128
<b>FIGURE 4-50</b> CORRELATION COMPRESSIVE STRENGTH WITH P-WAVE CONTROL.....	131
<b>FIGURE 4-51</b> CORRELATION COMPRESSIVE STRENGTH WITH S-WAVE CONTROL.....	131
<b>FIGURE 4-52</b> CORRELATION COMPRESSIVE STRENGTH WITH P-WAVE SODIUM SULFATE.....	131
<b>FIGURE 4-53</b> CORRELATION COMPRESSIVE STRENGTH WITH S-WAVE SODIUM SULFATE.....	131
<b>FIGURE 4-54</b> CORRELATION FLEXURAL STRENGTH WITH P-WAVE CONTROL.....	132
<b>FIGURE 4-55</b> CORRELATION FLEXURAL STRENGTH WITH S-WAVE CONTROL.....	132
<b>FIGURE 4-56</b> CORRELATION FLEXURAL STRENGTH WITH P-WAVE SODIUM SULFATE.....	132
<b>FIGURE 4-57</b> CORRELATION FLEXURAL STRENGTH WITH S-WAVE SODIUM SULFATE.....	132
<b>FIGURE 4-58</b> CORRELATION COMPRESSIVE STRENGTH APA 1MHz CONTROL.....	134
<b>FIGURE 4-59</b> CORRELATION COMPRESSIVE STRENGTH WITH APA 3.5MHz CONTROL.....	134
<b>FIGURE 4-60</b> CORRELATION COMPRESSIVE STRENGTH WITH APA 1MHz SODIUM SULFATE.....	134
<b>FIGURE 4-61</b> CORRELATION COMPRESSIVE STRENGTH WITH APA 3.5MHz SODIUM SULFATE.....	134
<b>FIGURE 4-62</b> CORRELATION FLEXURAL STRENGTH APA 1MHz CONTROL.....	135
<b>FIGURE 4-63</b> CORRELATION FLEXURAL STRENGTH WITH APA 3.5MHz CONTROL.....	135
<b>FIGURE 4-64</b> CORRELATION FLEXURAL STRENGTH WITH APA 1MHz SODIUM SULFATE.....	135
<b>FIGURE 4-65</b> CORRELATION FLEXURAL STRENGTH WITH APA 3.5MHz SODIUM SULFATE.....	135
<b>FIGURE 4-66</b> CORRELATION P-WAVE WITH APA 1MHz CONTROL.....	137

<b>FIGURE 4-67</b>	CORRELATION P-WAVE WITH APA 3.5MHZ CONTROL.....	137
<b>FIGURE 4-68</b>	CORRELATION P-WAVE WITH APA 1MHZ SODIUM SULFATE.....	137
<b>FIGURE 4-69</b>	CORRELATION P-WAVE WITH APA 3.5MHZ SODIUM SULFATE.....	137
<b>FIGURE 4-70</b>	CORRELATION S-WAVE WITH APA 1MHZ CONTROL.....	138
<b>FIGURE 4-71</b>	CORRELATION S-WAVE WITH APA 3.5MHZ CONTROL.....	138
<b>FIGURE 4-72</b>	CORRELATION S-WAVE WITH APA 1MHZ SODIUM SULFATE.....	138
<b>FIGURE 4-73</b>	CORRELATION S-WAVE WITH APA 3.5MHZ SODIUM SULFATE.....	138
<b>FIGURE 4-74</b>	SCANNING ELECTRON MICROGRAPH AND EDS OF CEM II A-L 42.5R CONCRETE SPECIMENS EXPOSURE TO 10% OF SODIUM SULFATE SOLUTION FOR 220 DAYS.....	142
<b>FIGURE 4-75</b>	SCANNING ELECTRON MICROGRAPH AND EDS OF CEM II A-L 42.5R CONCRETE SPECIMENS EXPOSURE TO 10% OF SODIUM SULFATE SOLUTION FOR 470 DAYS.....	143
<b>FIGURE 4-76</b>	SCANNING ELECTRON IMAGES FOR CEM I 42.5R/SR CONCRETE SPECIMENS EXPOSURE TO 10% OF SODIUM SULFATE SOLUTION FOR 220 AND 470 DAYS.....	144
<b>FIGURE 4-77</b>	COMPRESSIVE STRENGTH OF CONCRETE WITH TIME.....	146
<b>FIGURE 4-78</b>	POROSITY OF CONCRETE WITH TIME.....	147
<b>FIGURE 4-79</b>	P-WAVE VELOCITY WITH TIME.....	148
<b>FIGURE 4-80</b>	S-WAVE VELOCITY WITH TIME.....	148
<b>FIGURE 4-81</b>	(A) AVERAGED DEPTH–FREQUENCY SPECTROGRAM (CONTOUR), (B) AVERAGED DEPTH- AND FREQUENCY-DEPENDENT SPECTROGRAM (PCOLOR) FOR EACH DEGRADATION TIME FOR CEMI42.5R/SR DEGRADED BY SODIUM SULFATE SOLUTION, CENTRAL FREQUENCY 1MHZ.....	150
<b>FIGURE 4-82</b>	(A) AVERAGED DEPTH–FREQUENCY SPECTROGRAM (CONTOUR), (B) AVERAGED DEPTH- AND FREQUENCY-DEPENDENT SPECTROGRAM (PCOLOR) FOR EACH DEGRADATION TIME FOR CEMI42.5R/SR DEGRADED BY SODIUM SULFATE SOLUTION, CENTRAL FREQUENCY 3.5MHZ.....	151
<b>FIGURE 4-83</b>	(A) AVERAGED DEPTH–FREQUENCY SPECTROGRAM (CONTOUR), (B) AVERAGED DEPTH- AND FREQUENCY-DEPENDENT SPECTROGRAM (PCOLOR) FOR EACH DEGRADATION TIME FOR CEM II A-L 42.5R DEGRADED BY SODIUM SULFATE SOLUTION, CENTRAL FREQUENCY 1MHZ.....	152
<b>FIGURE 4-84</b>	(A) AVERAGED DEPTH–FREQUENCY SPECTROGRAM (CONTOUR), (B) AVERAGED DEPTH- AND FREQUENCY-DEPENDENT SPECTROGRAM (PCOLOR) FOR EACH DEGRADATION TIME FOR CEM II A-L 42.5R DEGRADED BY SODIUM SULFATE SOLUTION, CENTRAL FREQUENCY 3.5MHZ.....	153
<b>FIGURE 4-85</b>	ATTENUATION PROFILE AREA 1MHZ WITH TIME.....	155
<b>FIGURE 4-86</b>	ATTENUATION PROFILE AREA 3.5MHZ WITH TIME.....	155
<b>FIGURE 4-87</b>	ULTRASONIC TOMOGRAPHY FOR SODIUM SULFATE AND CONTROL SAMPLES FOR 90 DAYS OF IMMERSION TIME.....	158
<b>FIGURE 4-88</b>	ULTRASONIC TOMOGRAPHY FOR SODIUM SULFATE AND CONTROL SAMPLES FOR 220 DAYS OF IMMERSION TIME.....	159
<b>FIGURE 4-89</b>	ULTRASONIC TOMOGRAPHY FOR SODIUM SULFATE AND CONTROL SAMPLES FOR 370 DAYS OF IMMERSION TIME.....	160
<b>FIGURE 4-90</b>	ULTRASONIC TOMOGRAPHY FOR SODIUM SULFATE AND CONTROL SAMPLES FOR 480 DAYS OF IMMERSION TIME.....	161
<b>FIGURE 4-91</b>	VARIATION OF ULTRASONIC MEAN VELOCITY WITH TIME.....	164
<b>FIGURE 4-92</b>	COMPARISON BETWEEN ULTRASONIC MEAN VELOCITY AXIAL AND RADIAL.....	164
<b>FIGURE 4-93</b>	SCHEME OF A SAMPLE DEGRADED BY SODIUM SULFATE SOLUTION AND THE EFFECT OF THE DEGRADED PATH WAY ON THE ULTRASONIC PULSE .....	165
<b>FIGURE 4-94</b>	CORRELATION POROSITY WITH P- WAVE CONTROL AND SODIUM SULFATE.....	167
<b>FIGURE 4-95</b>	CORRELATION POROSITY WITH S- WAVE CONTROL AND SODIUM SULFATE.....	167
<b>FIGURE 4-96</b>	CORRELATION POROSITY WITH APA 1MHZ CONTROL AND SODIUM SULFATE.....	168
<b>FIGURE 4-97</b>	CORRELATION POROSITY WITH APA 3.5MHZ CONTROL AND SODIUM SULFATE.....	168
<b>FIGURE 4-98</b>	CORRELATION COMPRESSIVE STRENGTH WITH P-WAVE CONTROL AND SODIUM SULFATE .....	169



<b>FIGURE 4-99</b> CORRELATION COMPRESSIVE STRENGTH WITH S-WAVE CONTROL AND SODIUM SULFATE .....	169
<b>FIGURE 4-100</b> CORRELATION COMPRESSIVE STRENGTH WITH APA 1MHZ CONTROL AND SODIUM SULFATE.....	170
<b>FIGURE 4-101</b> CORRELATION COMPRESSIVE STRENGTH WITH APA 3.5MHZ CONTROL AND SODIUM SULFATE.....	170
<b>FIGURE 4-102</b> CORRELATION P-WAVE WITH APA 1MHZ CONTROL AND SODIUM SULFATE .....	171
<b>FIGURE 4-103</b> CORRELATION P-WAVE WITH APA 3.5MHZ CONTROL AND SODIUM SULFATE .....	171
<b>FIGURE 4-104</b> CORRELATION S-WAVE WITH APA 1MHZ CONTROL AND SODIUM SULFATE.....	172
<b>FIGURE 4-105</b> CORRELATION S-WAVE WITH APA 3.5MHZ FOR CONTROL AND SODIUM SULFATE..	172
<b>FIGURE 4-106</b> GENERAL TREND FOR ESTIMATION POROSITY USING S-WAVE VELOCITY OF MORTAR DEGRADED BY SS.....	175
<b>FIGURE 4-107</b> GENERAL TREND FOR ESTIMATION POROSITY USING APA 3.5MHZ OF MORTAR DEGRADED BY SS.....	175
<b>FIGURE 4-108</b> GENERAL TREND FOR ESTIMATION POROSITY USING APA 1MHZ OF CONTROL AND CONCRETE DEGRADED BY SS.....	175
<b>FIGURE 5-1</b> COMPRESSIVE AND FLEXURAL STRENGTH OF MORTAR SAMPLES SUBMERGED IN 4 MOLES OF AMMONIUM NITRATE .....	181
<b>FIGURE 5-2</b> COMPRESSIVE AND FLEXURAL STRENGTH LOSS OF MORTAR SAMPLES.....	182
<b>FIGURE 5-3</b> POROSITY OF MORTAR SUBMERGED IN 4 MOLES OF AMMONIUM NITRATE AND CONTROL	183
<b>FIGURE 5-4</b> LONGITUDINAL WAVE VELOCITY WITH TIME FOR AMMONIUM NITRATE AND CONTROL SAMPLES.....	184
<b>FIGURE 5-5</b> SHEAR WAVE VELOCITY WITH TIME FOR AMMONIUM NITRATE AND CONTROL SAMPLES.	184
<b>FIGURE 5-6</b> (A) AVERAGED DEPTH-FREQUENCY SPECTROGRAM (CONTOUR), (B) AVERAGED DEPTH- AND FREQUENCY-DEPENDENT SPECTROGRAM (PCOLOR) FOR EACH DEGRADATION TIME FOR W/C =0.40 MORTAR DEGRADED BY AMMONIUM NITRATE SOLUTION, CENTRAL FREQUENCY 1MHZ.	186
<b>FIGURE 5-7</b> (A) AVERAGED DEPTH-FREQUENCY SPECTROGRAM (CONTOUR), (B) AVERAGED DEPTH- AND FREQUENCY-DEPENDENT SPECTROGRAM (PCOLOR) FOR EACH DEGRADATION TIME FOR W/C =0.55 MORTAR DEGRADED BY AMMONIUM NITRATE SOLUTION, CENTRAL FREQUENCY 1MHZ.	187
<b>FIGURE 5-8</b> (A) AVERAGED DEPTH-FREQUENCY SPECTROGRAM (CONTOUR), (B) AVERAGED DEPTH- AND FREQUENCY-DEPENDENT SPECTROGRAM (PCOLOR) FOR EACH DEGRADATION TIME FOR W/C =0.40 MORTARS DEGRADED BY AMMONIUM NITRATE SOLUTION, CENTRAL FREQUENCY 3.5MHZ. ....	188
<b>FIGURE 5-9</b> (A) AVERAGED DEPTH-FREQUENCY SPECTROGRAM (CONTOUR), (B) AVERAGED DEPTH- AND FREQUENCY-DEPENDENT SPECTROGRAM (PCOLOR) FOR EACH DEGRADATION TIME FOR W/C =0.55 MORTAR DEGRADED BY AMMONIUM NITRATE SOLUTION, CENTRAL FREQUENCY 3.5MHZ. ....	189
<b>FIGURE 5-10</b> ATTENUATION PROFILE AREA 1 MHZ WITH TIME FOR AMMONIUM NITRATE AND CONTROL SAMPLES.....	192
<b>FIGURE 5-11</b> ATTENUATION PROFILE AREA 3.5 MHZ WITH TIME FOR AMMONIUM NITRATE AND CONTROL SAMPLES.....	193
<b>FIGURE 5-12</b> EVOLUTION OF THE DEGRADED THICKNESS WITH TIME.....	194
<b>FIGURE 5-13</b> CORRELATION POROSITY WITH P- WAVE VELOCITY FOR AMMONIUM NITRATE AND CONTROL SAMPLES.....	195
<b>FIGURE 5-14</b> CORRELATION POROSITY WITH S- WAVE VELOCITY FOR AMMONIUM NITRATE AND CONTROL SAMPLES.....	195
<b>FIGURE 5-15</b> CORRELATION POROSITY WITH APA 1MHZ FOR AMMONIUM NITRATE AND CONTROL SAMPLES.....	196

<b>FIGURE 5-16</b> CORRELATION POROSITY WITH APA 3.5MHZ FOR AMMONIUM NITRATE AND CONTROL SAMPLES.....	196
<b>FIGURE 5-17</b> CORRELATION FLEXURAL STRENGTH WITH P-WAVE VELOCITY FOR AMMONIUM NITRATE AND CONTROL SAMPLES .....	198
<b>FIGURE 5-18</b> CORRELATION FLEXURAL STRENGTH WITH S-WAVE VELOCITY FOR AMMONIUM NITRATE AND CONTROL SAMPLES .....	198
<b>FIGURE 5-19</b> CORRELATION COMPRESSIVE STRENGTH WITH P-WAVE VELOCITY FOR AMMONIUM NITRATE AND CONTROL SAMPLES .....	198
<b>FIGURE 5-20</b> CORRELATION COMPRESSIVE STRENGTH WITH S-WAVE VELOCITY FOR AMMONIUM NITRATE AND CONTROL SAMPLES .....	198
<b>FIGURE 5-21</b> CORRELATION FLEXURAL STRENGTH WITH APA 1MHZ FOR AMMONIUM NITRATE AND CONTROL SAMPLES.....	199
<b>FIGURE 5-22</b> CORRELATION FLEXURAL STRENGTH WITH APA 3.5MHZ FOR AMMONIUM NITRATE AND CONTROL SAMPLES.....	199
<b>FIGURE 5-23</b> CORRELATION COMPRESSIVE STRENGTH WITH APA 1MHZ FOR AMMONIUM NITRATE AND CONTROL SAMPLES .....	200
<b>FIGURE 5-24</b> CORRELATION COMPRESSIVE STRENGTH WITH APA 3.5MHZ FOR AMMONIUM NITRATE AND CONTROL SAMPLES .....	200
<b>FIGURE 5-25</b> CORRELATION P-WAVE WITH APA 1MHZ.....	201
<b>FIGURE 5-26</b> CORRELATION P-WAVE WITH APA 3.5MHZ.....	201
<b>FIGURE 5-27</b> CORRELATION S-WAVE WITH APA 1MHZ.....	201
<b>FIGURE 5-28</b> CORRELATION S-WAVE WITH APA 3.5MHZ.....	201
<b>FIGURE 5-29</b> (A) THE COMPRESSIVE STRENGTH OF THE PRECAST CONCRETE CORES DEGRADED BY 4 MOLES OF AMMONIUM NITRATE SOLUTION AND CONTROL SAMPLES; (B) THE LOSS IN THE STRENGTH DUE TO THE DEGRADATION PROCESS.....	203
<b>FIGURE 5-30</b> OPEN POROSITY OF PRECAST CONCRETE CORES DEGRADED BY AMMONIUM NITRATE AND CONTROL SAMPLES.....	205
<b>FIGURE 5-31</b> P AND S-WAVE VELOCITY OF THE PRECAST CONCRETE CORES FOR SAMPLES DEGRADED BY 4 MOLES OF AMMONIUM NITRATE SOLUTION AND CONTROL SAMPLES.....	207
<b>FIGURE 5-32</b> DEGRADATION DEPTH FOR A SAMPLE DEGRADED FOR 290 DAYS.....	208
<b>FIGURE 5-33</b> (A) AVERAGED DEPTH–FREQUENCY SPECTROGRAM (CONTOUR), (B) AVERAGED DEPTH- AND FREQUENCY-DEPENDENT SPECTROGRAM (PCOLOR) FOR EACH DEGRADATION TIME FOR CEMI42.5R/SR DEGRADED BY AMMONIUM NITRATE SOLUTION, CENTRAL FREQUENCY 1MHZ. ....	209
<b>FIGURE 5-34</b> (A) AVERAGED DEPTH–FREQUENCY SPECTROGRAM (CONTOUR), (B) AVERAGED DEPTH- AND FREQUENCY-DEPENDENT SPECTROGRAM (PCOLOR) FOR EACH DEGRADATION TIME FOR CEM II A-L 42.5R DEGRADED BY AMMONIUM NITRATE SOLUTION, CENTRAL FREQUENCY 1MHZ.....	210
<b>FIGURE 5-35</b> (A) AVERAGED DEPTH–FREQUENCY SPECTROGRAM (CONTOUR), (B) AVERAGED DEPTH- AND FREQUENCY-DEPENDENT SPECTROGRAM (PCOLOR) FOR EACH DEGRADATION TIME FOR CEMI42.5R/SR DEGRADED BY AMMONIUM NITRATE SOLUTION, CENTRAL FREQUENCY 3.5MHZ. ....	211
<b>FIGURE 5-36</b> (A) AVERAGED DEPTH–FREQUENCY SPECTROGRAM (CONTOUR), (B) AVERAGED DEPTH- AND FREQUENCY-DEPENDENT SPECTROGRAM (PCOLOR) FOR EACH DEGRADATION TIME FOR CEM II A-L 42.5R DEGRADED BY AMMONIUM NITRATE SOLUTION, CENTRAL FREQUENCY 3.5MHZ..	212
<b>FIGURE 5-37</b> ATTENUATION PROFILE AREA FOR FREQUENCIES (1 AND 3.5MHZ) OF THE PRECAST CONCRETE CORES FOR SAMPLES DEGRADED BY 4 MOLES OF AMMONIUM NITRATE SOLUTION AND CONTROL SAMPLES.....	214
<b>FIGURE 5-38</b> CORRELATION POROSITY WITH P- WAVE FOR AMMONIUM NITRATE SAMPLES.....	215
<b>FIGURE 5-39</b> CORRELATION POROSITY WITH S- WAVE FOR AMMONIUM NITRATE SAMPLES .....	215

<b>FIGURE 5-40</b>	CORRELATION POROSITY WITH APA 1MHZ FOR AMMONIUM NITRATE SAMPLES.....	217
<b>FIGURE 5-41</b>	CORRELATION POROSITY WITH APA 3.5MHZ FOR AMMONIUM NITRATE SAMPLES..	217
<b>FIGURE 5-42</b>	CORRELATION COMPRESSIVE STRENGTH WITH P-WAVE FOR AMMONIUM NITRATE SAMPLES.....	218
<b>FIGURE 5-43</b>	CORRELATION COMPRESSIVE STRENGTH WITH S-WAVE FOR AMMONIUM NITRATE SAMPLES.....	218
<b>FIGURE 5-44</b>	CORRELATION COMPRESSIVE STRENGTH WITH APA 1MHZ FOR AMMONIUM NITRATE SAMPLES.....	219
<b>FIGURE 5-45</b>	CORRELATION COMPRESSIVE STRENGTH WITH APA 3.5MHZ FOR AMMONIUM NITRATE SAMPLES.....	219
<b>FIGURE 5-46</b>	CORRELATION P-WAVE WITH APA 1MHZ FOR AMMONIUM NITRATE SAMPLES.....	221
<b>FIGURE 5-47</b>	CORRELATION P-WAVE WITH APA 3.5MHZ FOR AMMONIUM NITRATE SAMPLES.....	221
<b>FIGURE 5-48</b>	CORRELATION S-WAVE WITH APA 1MHZ FOR AMMONIUM NITRATE SAMPLES.....	221
<b>FIGURE 5-49</b>	CORRELATION S-WAVE WITH APA 3.5MHZ FOR AMMONIUM NITRATE SAMPLES.....	221
<b>FIGURE 5-50</b>	GENERAL TREND FOR ESTIMATION COMPRESSIVE STRENGTH USING P-WAVE VELOCITY OF MORTAR DEGRADED BY AM.....	224
<b>FIGURE 5-51</b>	GENERAL TREND FOR ESTIMATION OF COMPRESSIVE STRENGTH USING P-WAVE FOR CONCRETE DEGRADED BY AM.....	224

## NOMENCLATURE

<b>MIP</b>	Mercury Intrusion Porosimetry
<b>SEM</b>	Scanning Electronic Microscopy
<b>APA</b>	Attenuation profile area
<b>LPC</b>	Limestone Portland Cement type II A-L 45.5R
<b>SRPC</b>	Sulfo-Resistant Portland Cement type I 42.5R/SR
<b>C<sub>3</sub>S</b>	Tricalcium silicate
<b>C<sub>2</sub>S</b>	Dicalcium silicate
<b>C<sub>3</sub>A</b>	Tricalcium aluminate
<b>C<sub>4</sub>AF</b>	Tetracalcium aluminoferrite
<b>CH</b>	Calcium Hydroxide
<b>C-S-H</b>	Calcium silicate hydrate
<b>AFm</b>	Calcium monosulfate
<b>AFt</b>	Calcium trisulfate
<b>P-wave</b>	Longitudinal wave
<b>S-wave</b>	Transversal wave or shear wave

<b><i>DFF</i>(<math>\omega, z</math>)</b>	Depth-frequency function
<b><math>\alpha</math></b> ( $\omega, z$ )	Attenuation coefficient
<b><i>DTF</i></b> ( $\omega, z$ )	Time-frequency distribution
<b>(STFT)</b>	Short Time Fourier Transform
<b>(FP)</b>	Frequency profile
<b>(PA)</b>	Depth profile
<b>(UTI)</b>	Ultrasonic Tomography Imaging
<b>SEM/EDS</b>	Scanning Electron Microscopy with X-ray microanalysis
<b>SD</b>	Standard deviation
<b>CO</b>	Control
<b>SS</b>	Sodium Sulfate
<b>AM</b>	Ammonium nitrate

# CHAPTER 1

## **Introduction**

---



# 1 Introduction

Reinforced concrete has become the most commonly used material for structures subjected to marine environments. It is known that reinforced Portland cement concrete was invented approximately more than one hundred years ago and it has become one of the most widely used industrial materials in the world. This for the reasons that the excellent resistance of concrete to water and the capability of these structural concrete elements to be formed into a variety of shapes, sizes, on the other hand, the low cost and easy availability of concrete-making materials almost anywhere in the world (Mehta, 2003). The unfortunate trend in concrete structure is that people are bit over confident about the concrete strength and its durability. Concrete, however good it may be, deteriorates with the age when it is subjected to aggressive environment. It is never possible to prevent deterioration completely, but if the mechanics of concrete deterioration are understood, it can be retard the rate of it and thus achieve the desired life of concrete (Amita 2006).

The durability of concrete are related and mostly affected by its porous structure, which determines the interaction between concrete and its environment. Thus, in the interior of concrete, pores and capillaries will propitiate destructive processes, which commonly start on the surface. Aggressive elements are carried through the porous structure constituted by channel pores and cracks with different dimensions. Distribution and size of pores have a particular influence over the type and celerity of liquids and gases means of transport through the structure (Vergara et al., 2001; Gérard and Breysse, 1997).

Predictions of durability of the concrete structures are difficult to analyse the complexity of deleterious chemical and physical interactions between seawater, and the materials of structure element. The effect of marine environment on concrete may conveniently examined by considering of many factors; first, the factors characteristic of sea water exposure that can affect concrete, second, the elements of the specific concrete involved that may be affected by these factors, third, the consequences of the interaction of seawater with the concrete, and finally, the precautions that should be

## 1. Introduction

---

taken to avoid undesirable performance of concrete due to its interaction with sea water (Mather, 1964).

When concrete is exposed to sea water it will be wetted by a solution of salts, principally sodium chloride and magnesium sulfate. Degradation of concrete, if it occurs, usually results from failure to use good practices in concrete construction, and usually is the result of freezing and thawing or wetting and drying. Magnesium sulfate may be the most aggressive, if not all, of the constituents of hardened Portland cement paste, especially the aluminates constituent, while chlorides may promote corrosion of steel, and alkalis may participate in alkali-aggregate reaction. Thus, concrete when exposed to sea water it should be made with cement type controlled aluminates content and with nonreactive aggregate. On the other hand reinforced steel should be well covered by concrete of low permeability and finally a good construction practices should be followed (Mather, 1964).

Non-destructive evaluation techniques are of great importance for inspection of concrete structures and their usages have increased during the last few decades. On the other hand, new non-destructive evaluation techniques have been created and the ones that already existed have been perfected and their applicability extended. Due to the non-invasive nature, non-destructive evaluation techniques have several advantages when compared to conventional destructive techniques. Some non-destructive evaluation methods based on the propagation of the mechanical stress waves are frequently used to follow the damage in the tested materials. Properties of the propagating pulses after travelling through the damaged materials are compared with that of waves propagating through an undamaged sample to reveal microscopic changes and damaged in the inspected materials. Examples for the non-destructive methods widely used are, acoustic emission, electrical methods, , magnetic, radar, , surface hardness, thermography, sonic (impact-echo) and ultrasonic tests (Wonsiri, 2006).

Among all non-destructive testing methods available for concrete (Malhotra, 1991, IAEA, 2002), the use of ultrasonic waves is essentially to evaluate mechanical properties. Velocity and attenuation of such waves can be used to determine the viscoelastic properties (such as Young Modulus, Poisson ratio, or Lamé coefficients),



and also to characterise microstructural properties of materials (porosity, micro-cracks, grain size, etc.), (Chekroun et al., 2009).

In this work it will be studied and analyzed the incorporation of various methodologies (destructive and non-destructive tests) to characterize concrete and mortar degradation, which is approached from many points of view and there is no global solution to it. In particular, the research discusses the study and monitoring of degradation processes of precast concrete and mortar, the microstructure changes that occur through non-destructive techniques and physical analysis.

The following and estimation of the degradation processes by non-destructive techniques will be studied. We used the ultrasonic parameters to follow and estimate the degradation of precast concrete cores and mortar samples degraded by sodium sulphate and ammonium nitrate solutions, as will be seen in chapter 3.

### 1.1. Objectives

The general objective of this work is to obtain an evaluation procedure of the cycle life of precast concrete prepared and put into the service in marine environments. Also it will be studied and analyzed the incorporation of various methodologies (destructive and non-destructive techniques) to characterize the degradation process of concrete and mortar degraded by 10% sodium sulfate and 4moles of ammonium nitrate solution. For this purpose, accurate integration of different techniques is used for properties characterization that they affect to the concrete.

As additional objectives were to study the relationship between destructive and non-destructive parameters, also the relationship between the non-destructive parameters and each other was studied. The most previous studies of using ultrasonic techniques were used to calculate the w/c ratio of concrete, mortar and cement paste or to follow the variation of the microstructure changes of such materials during the curing process. Thus, in this research work as additional objective was to study the effect of different w/c ratio on ultrasonic parameters due to the degradation process by aggressive elements.

## 1. Introduction

---

For this purpose, Limestone Portland Cement type II A-L 45.5R (LPC), and Sulfo-Resistant Portland Cement type I 42.5R/SR (SRPC) were used to fabricate two precast concrete frames, which were used in this study as a concrete in service (real case). For studying the effect of variation of w/c ratio on ultrasonic parameters due to the degradation process, mortar samples with different water-cement ratios 0.30, 0.375, 0.45 and 0.525 were fabricated by using (LPC).

To follow the degradation processes, an integration of ultrasonic techniques was used. For example, Ultrasonic Pulse-echo technique using frequencies (1 and 3.5MHz) was used to obtain the parameter of attenuation profile area (APA) which estimated by (L Vergara et al., 2003) and used by (Fuente et al, 2004) to follow the curing process of mortar and cement paste; this parameter has a high sensitivity to characterize the changing of microstructure of cement based materials along the curing processes. Ultrasonic transmission-reception method is used to calculate wave velocity of ultrasonic longitudinal wave using frequency 1MHz and ultrasonic shear wave using frequency 500 KHz. Velocity of ultrasonic waves also has ability to follow the microstructural changes easily, because it is related by the variation of porosity. Ultrasonic image technique using frequency 2MHz also was used for the same purpose.

As a destructive testing, compressive and flexural strength test were used to observe the change in the strength of mortar and concrete, total porosity was used to observe the variation of porosity inside the material by the effect of the aggressive elements which penetrates the material and causes degradation, mercury porosimetry was used to observe the variation of the pores volume and size distribution, and finally scanning electron microscopy (SEM) was used to allow to quantify and detect the changes in the microstructure of concrete and mortar samples due to the attack by the aggressive elements.

### 1.2. Structure of Thesis

The current thesis doctoral is divided into six chapters. A summary to introduce the framework and problem under investigation and the objective of the present research are presented in the **Chapter 1**. The **Chapter 2** presents the literature review of the previous studies for durability of concrete structure and application of non-destructive testing to estimate and follow its degradation when it subjected to aggressive environments. This chapter is divided into two parts, the first one is a review on cement based materials to know the nature of the material under investigation and what are the factors which affect on it, and cause its deterioration when it is subjected to aggressive ambiances, such as marine environments. The second part is a review on non-destructive technique (ultrasonic techniques) which was used to estimate the curing process, strength and degradation of these materials. The **Chapter 3** presents a description of the experimental program, material properties, and experimental procedures used in this research. The results of concrete cores and mortar samples degraded by sodium sulfate solution (concentration 10%) are presented in the **Chapter 4** , this chapter is divided into two parts, the first one is divided into two sections, the first section presents the results of mortar samples examination tests; results of compressive and flexural strength, open porosity, mercury porosimetry, and scanning electron microscopy (SEM) as a destructive testing, and the results of ultrasonic wave velocities (P-wave and S-wave), attenuation profile area (APA) for frequencies (1 and 3.5MHz) and the results of ultrasonic image as a non-destructive testing. The second section presents the relationship between the destructive and non-destructive parameters, also the relationship between the non-destructive parameters and each other. The second part of this chapter presents the results of precast concrete cores and it has the same structure of the results as the part of mortar. The **Chapter 5** presents the results of concrete cores and mortar samples degraded by ammonium nitrate (4moles) as the same structure of Chapter 4. Finally, the conclusions of the entire research and the future work are presented in the **Chapter 6**.



# CHAPTER 2

**Literature Review**

---



## 2 Literature Review

This chapter is divided into two principal parts; the first part presents a review of cementitious or cement-based materials to understand the behaviour of the material under investigation and the changes that occur in the microstructure of it during the degradation process. In the second part is presented a review of non-destructive testing by ultrasonic techniques to understand the behaviour of ultrasonic waves and the changes of its parameters due to the degradation process and finally its applicability on concrete structures.

### 2.1. Literature Review on Cement Based Materials

The structure of hardened cement paste is fundamental for understanding of the performance of cement paste. To understanding the behaviour and for predicting the properties of cement paste, one has to understand the relationship structure–property. Also, the structural elements that affect the properties in cement paste have to be identified and quantified.

Cementitious materials are heterogeneous; its microstructure is random over a wide range of length scales. As can be seen, for example in Figure 2-1, concrete can be considered as a mortar-rock composite, at the largest length scale, where the randomness in the structure is on the order of centimetres. Mortar as a cement paste-sand composite with random structure on the order of millimetres can be considered. It can be considered that cement paste as a random composite material, forms from unreacted cement, CH, C-S-H gel, capillary pores, and other chemical phases. In cement paste microstructure the randomness is on the order of micrometres. On the other hand C-S-H itself is a complex material, on the order of nanometres. This variation range of random structure, from nanometres (as the case of C-S-H gel) to centimetres (as concrete) covers many orders of magnitude in size (Garboczi, 1995).

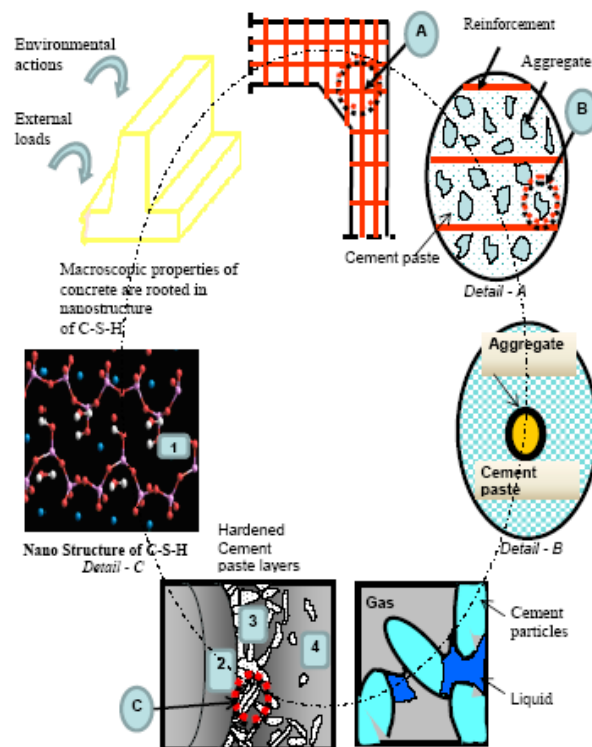


**Figure 2-1** Complexity of concrete microstructure  
Garboczi, 1995

### 2.1.1. Composition and Hydration of Cement

When cement chemically reacts with water, hardened cement paste is produced. For civil engineer applications (buildings, bridges, canals, tunnels, etc.,) Portland cement is used predominantly. It is known that dry cement consists of four main oxide phases (see Table 2-1), tricalcium silicate ( $C_3S$ ), dicalcium silicate ( $C_2S$ ), tricalcium aluminate ( $C_3A$ ), and tetracalcium aluminoferrite ( $C_4AF$ ) (Andrew, B., 2010).

The composition of cement is varied depending on its using. A typical example of cement contains 50–70%  $C_3S$ , 15–30%  $C_2S$ , 5–10%  $C_3A$ , 5–15%  $C_4AF$ , and 3–8% other additives or minerals (such as oxides of magnesium and calcium) (Andrew, B., 2010). On the other hand cement contains gypsum that is added to control the setting process.  $C_3S$  and  $C_2S$  constitute approximately 75% by mass of dry cement. The ratio of  $C_3S$  to  $C_2S$  helps to determine how fast the cement is setting, faster setting occurring with



## 2. Literature Review

---

higher C<sub>3</sub>S contents. The low content of C<sub>3</sub>A promotes resistance to sulfates. The higher amounts of ferrite lead to slower hydration; the ferrite phase causes the brownish gray colour in cements. Finally, calcium aluminoferrite (C<sub>4</sub>AF) forms a continuous phase around the other mineral crystallites, for example, the iron containing species act as a fluxing agent in the rotary kiln during cement production and are the last to solidify around the others. Figure 2-2 shows a typical cement grain.

**Table 2-1** Chemical formula and cement nomenclature for major constituents of Portland cement. Abbreviation notation: C = CaO, S = SiO<sub>2</sub>, A = Al<sub>2</sub>O<sub>3</sub>, F = Fe<sub>2</sub>O<sub>3</sub>. (Andrew.B, 2010)

Mineral	Chemical formula	Oxide composition	Abbreviation
Tricalcium silicate (alite)	Ca <sub>3</sub> SiO <sub>5</sub>	3CaO.SiO <sub>2</sub>	C <sub>3</sub> S
Dicalcium silicate (belite)	Ca <sub>2</sub> SiO <sub>4</sub>	2CaO.SiO <sub>2</sub>	C <sub>2</sub> S
Tricalcium aluminate	Ca <sub>3</sub> Al <sub>2</sub> O <sub>4</sub>	3CaO.Al <sub>2</sub> O <sub>3</sub>	C <sub>3</sub> A
Tetracalcium aluminoferrite	Ca <sub>4</sub> Al <sub>n</sub> Fe <sub>2-n</sub> O <sub>7</sub>	4CaO.Al <sub>n</sub> Fe <sub>2-n</sub> O <sub>3</sub>	C <sub>4</sub> AF

During the earliest stage of hydration, a series of rapid reactions are starting, that involve mainly clinker interstitial phases (i.e., aluminates, alkali sulfates, aluminoferrites, and free lime), addition to calcium sulfates (gypsum, hemihydrate and/or anhydrite) which have been interground into the cement (Gartner et al., 2002). After several hours of hydration, definite shells of hydration products will be formed, mostly C-S-H, CH, ettringite needles or thin calcium monosulfate (AFm Phase) plates which are sometimes present in the shells (Diamond, 1987). This layer of ettringite or AFt phase is often poorly crystalline and difficult to detect by X-ray diffraction (XRD) (Gartner et al, 2002 and Taylor, 1997).

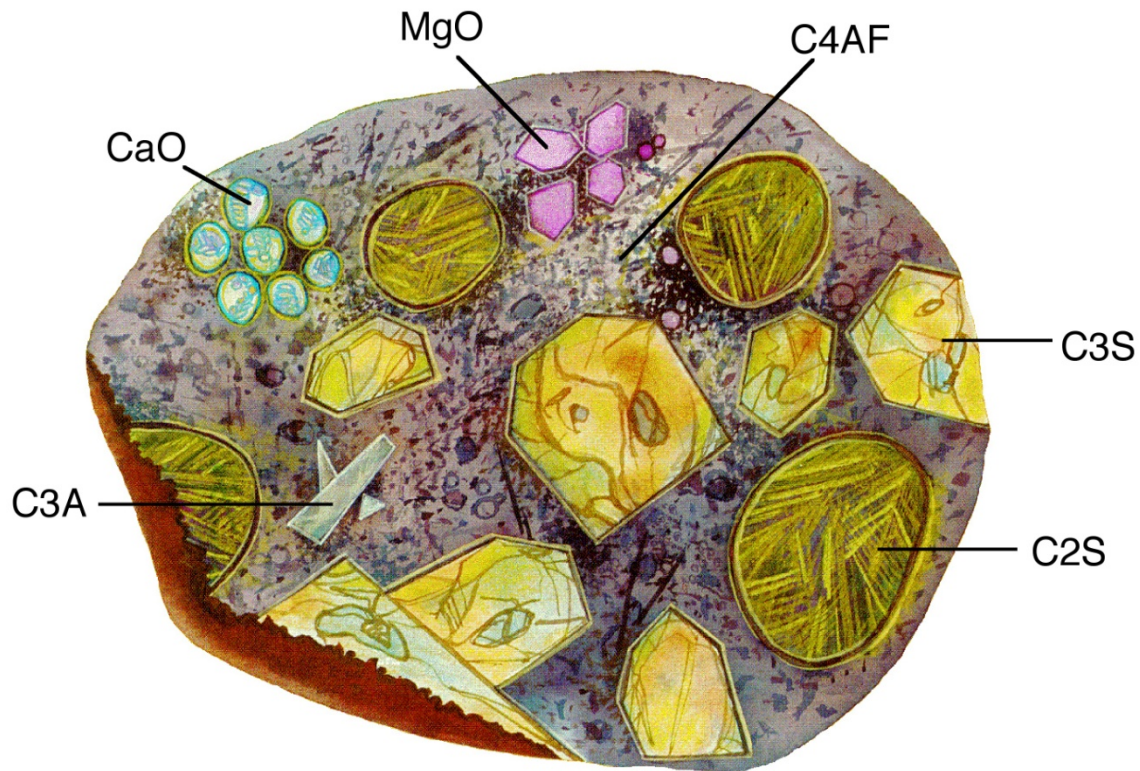


**Figure 2-2** A pictorial representation of a cross-section of a cement grain. Adapted from Cement Microscopy, Halliburton Services, Duncan, OK. (Andrew and Johnson, 2008)

The AFt phase contains lots of sulfate, which comes from the rapidly soluble sources such as alkali sulfates, gypsum and hemihydrate. The continued formation of AFt and AFm phases can affect on the workability, but the C-S-H formation leads to the onset of normal set concrete.

On the other hand shrinkage of cement paste due to drying process can be observed, as hydration continues for years if water is available. The hydration products are found around the grains and prohibit the access of water to the unhydrated particles, which prevent the late hydration (Azzam, 2002). This leads to strength increasing with time due to porosity, but at an ever low rate (Gartner et al, 2002).

Hydration can be seen as cross-linking of cement grains with the hydration products which may be occupy 2.1 times the volume of the unhydrated material, this leads to subdivide the spaces between the grains into smaller flow channels (Nyame1981). Different kinds of pores and solids can be formed at different stages during the

## 2. Literature Review

---

hydration process; the structure of these pores and solids formed after cement mixing with water is useful to understand the nature and performance of concrete.

### 2.1.1.1. Hydration of Tricalcium Silicate and Dicalcium Silicate

The two main cementitious compounds in cement are  $C_3S$  and the  $C_2S$ , and the physical behaviour of the overall cement during hydration is contributed to that of only these two compounds, (Flint and Wells 1934, Neville 1996). C-S-H and CH in different proportions are produced when both the  $C_3S$  and the  $C_2S$  react with water; C-S-H is the compound responsible for the strength characteristics in concrete. Nevertheless the  $C_3S$  hydrates much faster and it is responsible for the strength evolution in the early stages of hydration, in the first few days and weeks. On the other hand, the  $C_2S$  takes a much longer time to hydrate and is responsible for long term strength development, taking months or years. The hydration of both  $C_3S$  and  $C_2S$  are presented by the equations 1 and 2:



Both the  $C_3S$  and the  $C_2S$  need approximately the same amount of water for hydration; however the  $C_3S$  produces more than twice amount of CH than that produced from  $C_2S$ . Considering the reactions individually, the amount ratio of C-S-H to CH produced in the  $C_3S$  reaction is about 3 to 2 (Eq.1); whereas the ratio is 5 to 1 in the case of the  $C_2S$  reaction (Eq. 2) (Neville 1996).

### 2.1.1.2. Hydration of Tricalcium Aluminate and Tetracalcium Aluminoferrite

When tricalcium aluminate ( $C_3A$ ) reacts with water a condition known as flash setting occurs, this is due to the rapid and excessive formation of calcium aluminate hydrates. This reaction leads to the fast forming of concrete which is undesirable. The hydration is as follows:



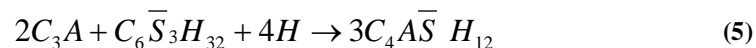
## 2. Literature Review

---

Gypsum is added to slow down the reaction between C<sub>3</sub>A and water by producing calcium sulfoaluminate hydrate which builds up as a layer on the C<sub>3</sub>A impeding hydration as follows:



When all the gypsum has been exhausted, the ettringite layer is no longer stable, and another reaction takes place. The ettringite reacts with tricalcium aluminate (C<sub>3</sub>A) to produce monosulfoaluminate, and is shown as:



The C<sub>4</sub>AF essentially will give a similar type of reaction as C<sub>3</sub>A; however since it is much less reactive it will only come in contact with a small amount of gypsum. In the presence of gypsum C<sub>4</sub>AF reacts with water to produce calcium sulfoferric as well as calcium sulfoaluminate (Neville 1996, Young 2002).

### 2.1.2. Microstructure of Hardened Cement Paste

As presented previously that hardened cement paste microstructure is composed of a highly heterogeneous level which has a several kinds of solids and pores of various sizes and shape. The composition of cured cement paste is shown in Table 2-2, from the table it can be seen that C-S-H gel is the principal hydration product in hardened cement paste and it has a poorly crystalline structure. There are two generic forms of C-S H were be found; low density C-S-H gel (outer product) and high density C-S-H gel (inner product). On the other hand another primary hydration product is calcium hydroxide (CaOH<sub>2</sub>) which has a crystalline structure. Also there are some minor components such as AFm and Aft phases (ettringite and monosulfate) which are generally crystalline and vary considerably in morphology and size. In addition, unhydrated cement particles may occupy the volume depending on the degree of hydration or w/c ratio (Rathinam, 2009).

Pores are considered also as components of hardened cement paste microstructure. It was recognized and classified two classes of pores as major classes. The first class is gel pores, is imaginary to be part of the C-S-H gel with characteristic diameters less than 10

## 2. Literature Review

---

nm. The second class is capillary pores, water not consumed in the hydration reaction and will remain in the microstructure pore space. These pores make the concrete weaker due to the lack of strength-forming Calcium Silicate Hydrate bonds (Garboczi and Bentz, 1995). On the other hand there may be incidental or deliberately entrained air voids, and larger empty spaces where the pastes have not been properly consolidated. The total pore volume depends on the curing condition, w/c ratio, degree of hydration, etc. The development of ordinary Portland cement microstructure during hydration process is illustrated in Figure 2-3.

**Table 2-2** Composition of Hardened Cement Paste (w/c = 0.5) (Bensted, 2001)

Component	Approximate Volume (%)	Remarks
Calcium Silicate Hydrate(C-S-H)	50	Amorphous structure, includes gel pores
Calcium Hydroxide (CH)	12	Crystalline structure
AFm and Aft phases	13	Crystalline structure
Unreacted Cement particles	5	Depends on hydration
Capillary pores	20	Depends on the water-cement-ratio

### 2.1.2.1 Pores in cement paste, mortar and concrete

When cement paste is combined with fine aggregate it forms a mortar, whereas, when cement paste is combined with fine and coarse aggregate it forms concrete. It is known that, mortar and concrete are the most used cement-based material for engineering applications and their properties are significantly controlled by the properties of cement paste. As seen in the previous paragraph that, pores in cement mortar and concrete vary in size, shape and origin, and can be subdivided into the following classes: (I) pores in the cement paste matrix, which include air voids, hollow-shell pores, capillary pores and gel pores, (II) pores in the aggregates, (III) pores associated with the interface between aggregates and cement paste, (IV) water voids, where voids under aggregate particles or reinforcing bars created by bleeding water of the concrete

## 2. Literature Review

---

mixture, and voids due to construction deficiencies, for example honeycombing due to inadequate compaction, (V) internal discontinuities in the cement paste associated with dimensional instabilities that occur during humidity and temperature changes (Aligizaki K., 2006).

### *Gel pores*

According to (Aligizaki K., 2006), the C-S-H gel found to be the main component of cement paste and is responsible for the strength and microstructure of cement paste. On the other hand the C-S-H gel is a colloidal amorphous gel that contains pores of approximately a few nanometers in size which are called gel pores, the C-S-H gel itself has about 28% of porosity, and it can only produce in the originally water filled capillary cavities in fresh cement paste. In addition, the bulk volume of C-S-H gel after cement grain is fully hydrated requires 60% more volume than the original volume of the unhydrated cement grain and water, and this expansion moves into capillary pores. The amount and distribution of capillary and gel pores changes considerably as the hydration proceeds, the reduced of capillary pore volume is found because the capillary pores become filled with the hydration products. Also it is found that, the gel pore volume increases as more gel is formed; in addition, there is a net reduction in total.

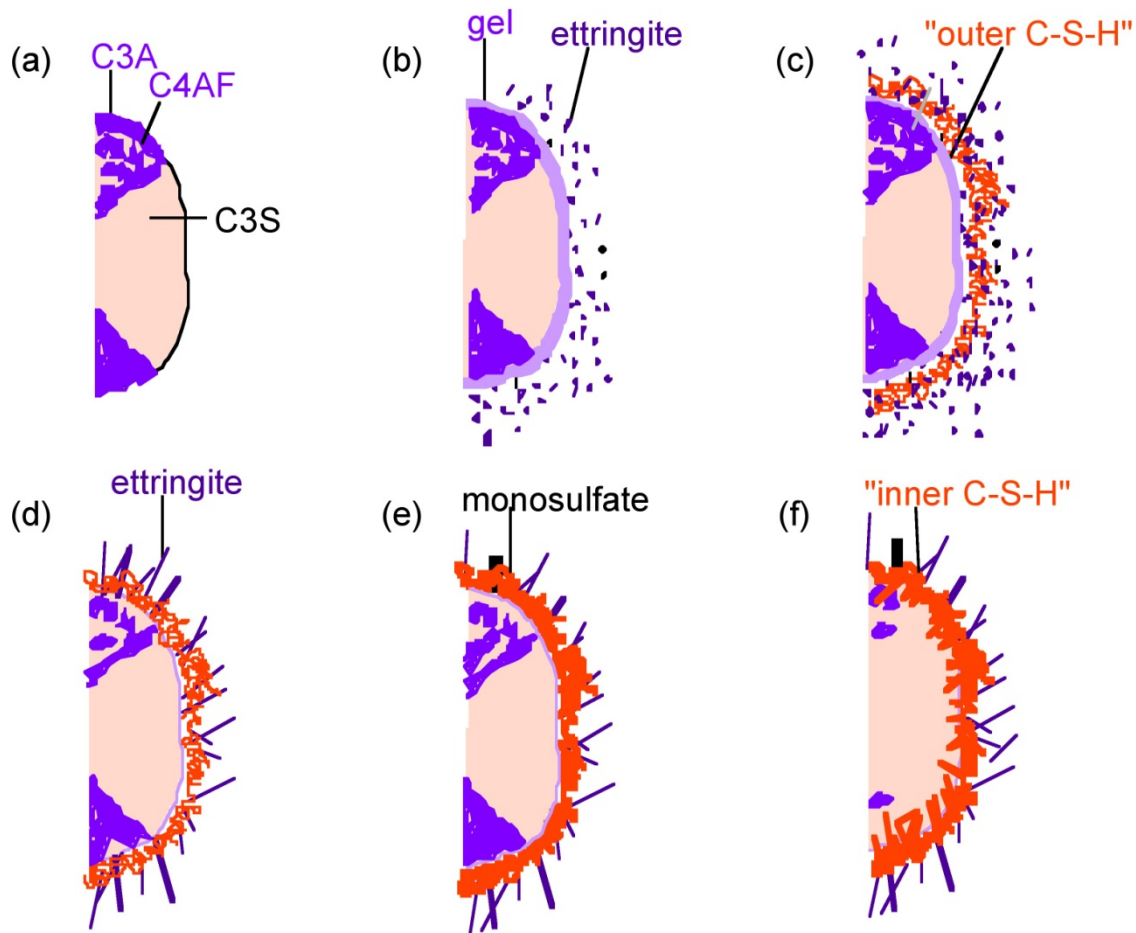


**Figure 2-3** Schematic representation of anhydrous cement (a) and the effect of hydration after (b) 10 minutes, (c) 10 hours, (d) 18 hours, (e) 1-3 days, and (f) 2 weeks. Adapted from M. Bishop, PhD Thesis, Rice University, 2001, (Andrew and Johnson, 2008).

Table 2-3 shows that there is a wide range of pore size distribution, from 10  $\mu\text{m}$  to less than 0.5 nm in diameter. It is known that the pore size distributions are mainly affected by the w/c ratio and the degree of hydration. As it can be seen in Table 2-3, that porosity over the whole size range of pores has an influence on paste properties. It is found that is difficult to get an exact assessment of pore-size distributions because no one measurement encompasses the whole size range and because it is difficult to interpret experimental data (Gi-Sung Pang, 2009).

## 2. Literature Review

**Table 2-3** Classifications of the pore sizes in hydrated cement (Gi-Sung Pang, 2009)

Type	Diameter (nm)	Description	Role of water	Paste properties affected
Capillary pores	50~10,000	Large capillaries	Behaves as bulk water	Strength, permeability
	10~50	Medium-sized capillaries	Moderate surface tension forces generated	Strength, permeability; shrinkage at high humidity
Gel pores	2.5~10	Small (gel) capillaries	Strong surface tension forces generated	Shrinkage to 50% RH
	0.5~2.5	Micropores	Strongly adsorbed water; no menisci form	Shrinkage, creep
	<~0.5	Micropores "interlayer"	Structural water involved in bonding	Shrinkage, creep

### ***Capillary pores***

The network interconnected channels on the cement pasted are filled by water at initial stage. If the cement matrix is dense enough, its porosity will be called gel pores, and capillary pores or capillary cavities. The capillary porosity is influenced by the original water cement ratio and the total amount of cement is the mixture. The capillarity pores structure change during the curing process at early times by precipitation oh hydrated components, mainly by C-S-H gel in the original water filled space. This forming process and the consequent shrinkage will lead a random structure formed by hydrated products, unreacted components of cement and the interfaces or boundaries between them and the gel and capillary pores (Aligizaki K., 2006).

### **2.1.3. Durability of concrete structure in marine environment**

Concrete durability as defined by the American Concrete Institute is the resistance of concrete to weathering action, chemical attack, abrasion and their degradation



## 2. Literature Review

---

processes. Concrete exposed to sea water is wetted by a solution of salts, as sodium, chloride, magnesium and sulfate. When concrete damage is produced, results failure to use good practices in concrete construction, and sometimes is the result of wetting and drying or freezing and thawing as much as or more than the results of the effects of sea water as such. Magnesium sulfate is more aggressive, if not all, of the constituents of hardened Portland cement paste, especially the aluminate constituent, alkalies may participate in alkali-aggregate reaction and chlorides lead to corrosion of steel. Thus, concrete exposed to sea water should be made with cement of controlled aluminate content and with non-reactive aggregate, for example using sulfate resisting Portland cement, on the other hand the embedded steel should be well covered by concrete of low permeability, and good construction practices should be followed (Mather 1964). The different degradation mechanisms which can act on concrete exposed to sea water are illustrated in Figure 2-4.

Many factors are considered when concrete is subjected to sea water the first factor is the characteristic factors of sea water which can affect on concrete, the second one, the elements of the specific concrete implicated that may be affected by these factors, the third is the consequences of the interaction of sea water with the concrete, and finally, the precautions that should be taken to avoid undesirable performance of concrete due to its interaction with sea water (Mather 1964).

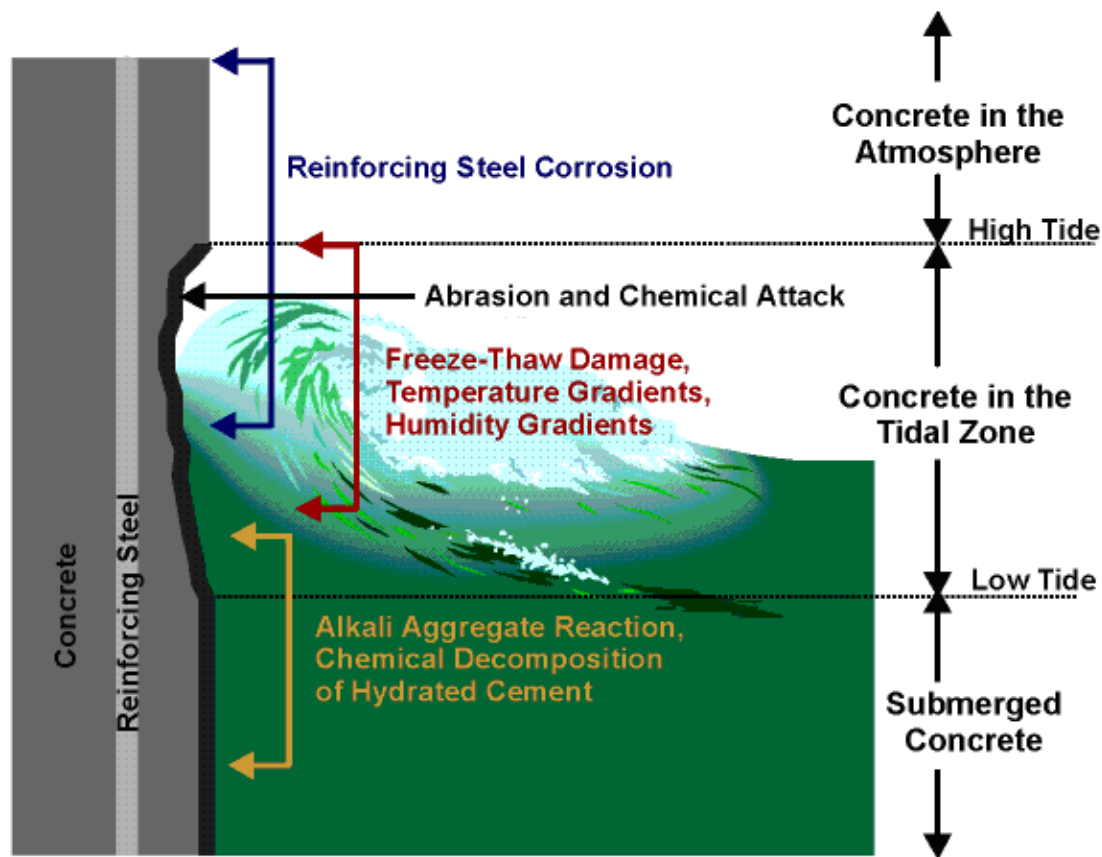


**Figure 2-4** Proposed degradation mechanisms acting on concrete exposed to sea water (Malhorta 2000).

It is reported that, most sea water is quite uniform in chemical composition, which is characterized in general by the presence of about 3.5% soluble salts by weight. The concentration of both ionic sodium ( $\text{Na}^+$ ) and chloride ( $\text{Cl}^-$ ) are the highest, and the values of their concentrations are 11,000 and 20,000 mg/liter, respectively. Also sufficient amounts of  $\text{Mg}^{2+}$  and  $\text{SO}_4^{2-}$  are presented, with concentrations of 1,400 and 2,700 mg/liter, respectively. The variation of pH of seawater is between 7.5 and 8.4, and the average value in equilibrium with the atmospheric  $\text{CO}_2$  being 8.2 under exceptional conditions (as in sheltered bays and estuaries). On the other hand pH values lower than 7.5, may be encountered due to the high concentration of dissolved  $\text{CO}_2$ , and this leads to that sea water will be more aggressive to Portland cement concrete (Mehta et al., 2006). The concentration of major ions in some of the world seas is presented in Table 2-4

## 2. Literature Review

**Table 2-4** Concentration of major ions in some of the world seas (Mehta et al., 2006)

Major Ions	Concentration (mg/l)								
	Black Sea	Marmara Sea	Mediterranean Sea	North Sea	Atlantic Ocean	Baltic Sea	Arabian Gulf	BRE** Exposure	Red Sea
Sodium	4,900	8,100	12,400	12,200	11,100	2,190	20,700	9,740	11,350
Magnesium	640	1,035	1,500	1,110	1,210	260	2,300	1,200	1,867
Chloride	9,500	14,390	21,270	16,550	20,000	3,960	36,900	18,200	22,660
Sulfate	1,362	2,034	2,596	2,220	2,180	580	5,120	2,600	3,050
TDS*	17,085	26,409	38,795	33,060	35,370	7,110	66,650	32,540	40,960
TDS Ratio	3.90	2.52	1.72	2.02	1.88	9.37	1.00	2.05	1.63

TDS>Total dissolved solids

### 2.1.3.1. Causes of concrete degradation

The understanding of the degradation processes of concrete is needed to predict the development before deterioration. Thus, it is reported by (Mehta, 2003) the physical and chemical causes of concrete deterioration which are classified and presented in the Figures 2-5 and 2-6.

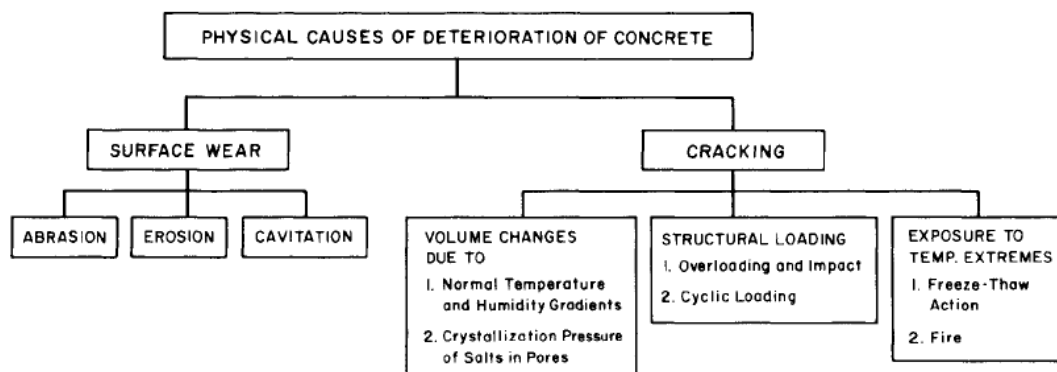


**Figure 2-5** physical causes of concrete deterioration (Mehta, 2003).

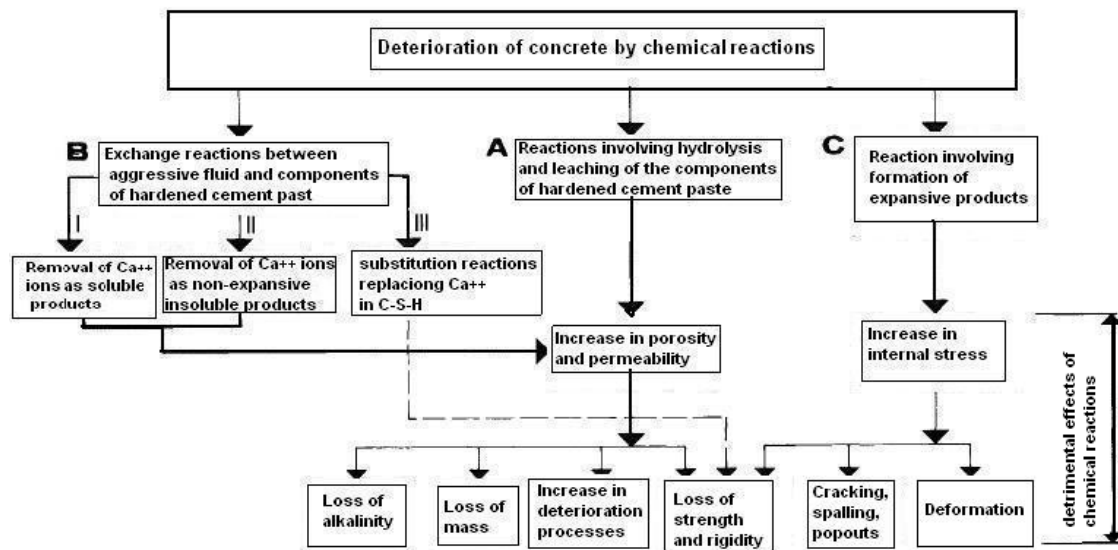


**Figure 2-6** Types of chemical reactions responsible for concrete deterioration (Mehta, 2003) A, Soft-water attack on calcium hydroxide and C-S-H presents in hydrated portland cements: B(I), acidic solution forming soluble calcium compounds such as calcium chloride, calcium sulfate, calcium acetate, or calcium bicarbonate; B(II), Solutions of oxalic acid and its salts, forming calcium oxalate; B(III), long-term seawater attack weakening the C-S-H by substitution of  $Mg^{2+}$  for  $Ca^{2+}$ ; C, (1) Sulfate attack forming ettringite and gypsum, (2) alkaliaggregate attack, (3) corrosion of steel in concrete, (4) hydration of crystalline MgO and CaO.

Woodson, (2009) also reported the causes of deterioration and distress of concrete, for example, chemical reaction, shrinkage, weathering and erosion. The damage of concrete by chemical reaction can be occurs when a suitable ambience is found, and small amounts of chemicals can do serious structural damage to concrete. On the other hand degradation by physical effects causes salt crystallization in concrete pores, which leads to expansion and microcracking of concreter elements (Mehta, 2003).

### ***Sulfate Attack***

Sulfate attack is the most common form of salt attack on concrete. Concrete can exposed to sulfates, due to environmental actions, in the cement binder or aggregates. Damages caused by sulfate attack can for example be expansion, strength loss and spalling. Solid salts do not attack concrete, but when present in solutions they can react with hydrated cement paste. The most common solutions are sulfates of sodium, potassium,

## 2. Literature Review

---

magnesium and calcium. The natural origins of sulfates are in ground water and also they may come from fertilizers and industrial activities.

When concretes are attacked by sulfates, damage usually starting at the edges and corners and followed by cracking. The reason for this is the formation of calcium sulphoaluminate (ettringite) and/or calcium sulfate (gypsum), both products occupying a greater volume than the compounds which they replace, so that expansion and disruption of hardened concrete takes place.

The effects of sulfate attacks in concrete can be reduced in two different ways as demonstrated by (Neville, 1997):

- Reduction of the  $C_3A$  amount in the binder, this can be enhanced by the usage of sulfate resistant cements in the concrete.
- Reduction of the quantities of  $Ca(OH)_2$  in the cement paste, this is done by using of blended cements, containing ground granulated blast-furnace slag (GGBS) or pozzolans. The effects of blended cements are; (1) Pozzolans react with the  $Ca(OH)_2$  so that  $Ca(OH)_2$  is no longer available for reaction and (2) Blended cements contain less  $Ca(OH)_2$  than PC.

In order to avoid flash set due to the hydration of the tricalcium aluminate ( $C_3A$ ), gypsum is added to the cement clinker and it quickly reacts with  $C_3A$  to produce ettringite which is harmless at this stage, where, the concrete is still in a non-hardened state so that expansion can be accommodated.

A similar reaction takes place when cement-based materials are exposed to sulfates from external sources. A typical sulfate solution is the groundwater of clay which contains calcium, sodium, or magnesium sulfates. And as mentioned previously the sulfates react with both  $Ca(OH)_2$  and the hydrated  $C_3A$  to form gypsum and ettringite, respectively. Magnesium sulfate has a more damaging effect than other sulfates because magnesium ions reacts with all cement components and this leads to the decomposition

## 2. Literature Review

---

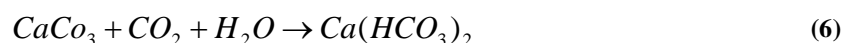
of the hydrated calcium silicates as well as of  $\text{Ca(OH)}_2$  and of hydrated  $\text{C}_3\text{A}$  (Neville, 1997).

The extent of sulfate attack depends on its concentration and on the permeability of the concrete, whereas sulfate can travel through the pore system. If the concrete is high permeable, water can be percolate right through its thickness,  $\text{Ca(OH)}_2$  will be leached out. On the other hand evaporation at the far surface of the concrete leaves behind deposits of calcium carbonate which formed by the reaction of  $\text{Ca(OH)}_2$  with carbon dioxide, this deposit of whitish appearance is known as efflorescence. Efflorescence is generally not harmful, however, extensive leaching of  $\text{Ca(OH)}_2$  leads to increasing of porosity, so that concrete becomes progressively weaker and more prone to chemical attack (Ferreira, 2004).

### ***Sea water Attack***

Sea water contains sulfates and could be expected to attack concrete in a similar manner as described in the previous section. However, as chlorides are also present, sea-water attack does not generally cause expansion of the concrete. This is because the expansive products (gypsum and ettringite), which formed due to the reaction of  $\text{C}_3\text{A}$  with sulfates in sea water, these expansive products are not accompanied by the extent of swelling seen in pure solutions of magnesium and sodium sulfate, because ettringite and gypsum are more soluble in solutions containing chlorides such as sea water (Mehta, 1975; Verbeck 1975; Ferreira, 2004).

In sea water containing a high degree of dissolved carbon dioxide, the degradation process can gradually progress inwards (Biczock, 1964; Ferreira, 2004). The calcium and hydroxyl ions transported to the surface and react with carbon dioxide to form aragonite. However, due to the high levels of carbon dioxide, aragonite is converted to calcium bicarbonate which is leached away.



## 2. Literature Review

---

Magnesium ions cause the precipitation of magnesium hydroxide in the new surface, while sulfate and chloride ions move in and form chloroaluminates and sulfoaluminates. When the hydroxyl ions are depleted at an advanced level of degradation, magnesium ion penetration into the paste can occur, thus exposing the calcium silicate hydrate to magnesium ion attack (Gutt 1977, Regourd 1978).

In the interior layers, the formation of ettringite and gypsum is responsible for removal of sulfate ions from sea water. Thus, chlorides can continue to penetrate into the interior. The observed penetration by chloride ions even at low w/c ratios of 0.3 can be explained by the fact that, except for chloride ions, the components of sea water (such as magnesium sulfate and carbon dioxide) are readily removed in the outer zones as a result of the chemical reactions with the cement paste (Gutt 1977).

Although  $C_3A$  and  $C_4AH_{19}$  are capable of removing chlorides as chloroaluminate hydrate, the compounds are not stable in a sulfate environment. Thus in sea water, chloroaluminate animals to ettringite releasing chloride ions. Also the  $C_3A$  content plays an important role in the minimum  $Cl^-/OH^-$  ratio needed to initiate corrosion. The threshold value for corrosion initiation (generally 0.63) is significantly influenced by cements with high  $C_3A$  content because of chloride removal (Mehta 1980).

The pH of the concrete is the important controlling factor in the corrosion process. From the several salts present in sea water, magnesium chloride is the most destructive because it replaces  $OH^-$  ions that lead to reduce the pH to threshold levels which initiate corrosion process. In addition, there is no disruption but only a very slow increase in porosity and, hence a decrease in strength. Concrete between tide marks, always subjected to alternating wetting and drying, and this is severely attacked, while permanently immersed concrete is lower attacked. However, the attack by sea water is slowed down by the blocking of pores in the concrete due to the deposition of magnesium hydroxide which is formed, together with gypsum, by the reaction both of magnesium sulfate and  $Ca(OH)_2$ . In some cases it can be seen that, the action of sea water on concrete is accompanied by the destructive action of frost of wave impact and of abrasion. Additional damage can be produced by rupture of concrete surrounding

## 2. Literature Review

---

reinforcement which has corroded due to electro-chemical action due to absorption of salts by the concrete (Ferreira, 2004).

Concrete density, cement content and type play an essential role in the resistance of concrete to sea water. Concretes made with supersulfated, calcium aluminate cements and also those containing supplementary cementing materials, resist sea water completely well. Such improved resistance as compared to 100% Type I ordinary Portland cement stems from reduced free lime content in such concretes. Regardless of the cement type used, deteriorated concrete generally contains the same constituents of calcium carbonate as calcite or, brucite, aragonite and magnesium silicate hydrate (Mehta 1980, Regourd 1978, Kalousek 1970).

### ***Chloride Attack***

A high concentration of chloride ions are found in sea water which is a common cause for the breakdown of the local passivity of reinforcing steel, due to its penetration to the steel surface. The chloride concentrations in the range of 0.6 to 0.9 kg/m<sup>3</sup> in concrete, or 300–1200 g/liter in the pore fluid, are enough to cause dissolution of the passive film (Mehta, 2003).

On the other hand, when the passivity of steel becomes partly or completely broken, the electrochemical potential locally becomes more negative. It can be said that, the area becomes anodic with respect to another area of steel which continues to remain passive and, therefore, acts as the cathode.



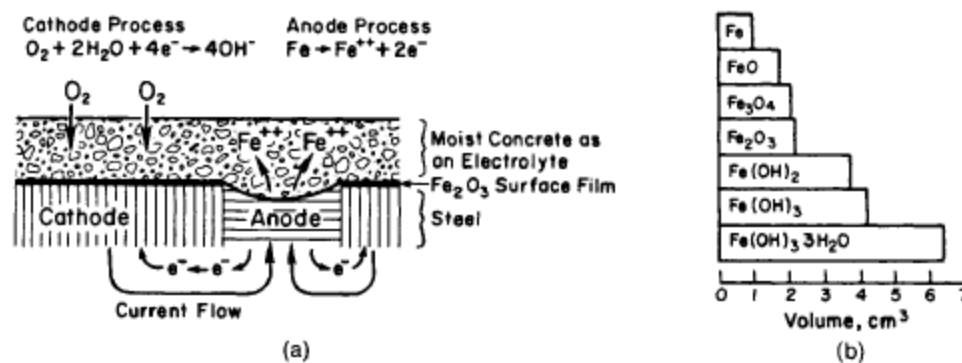


**Figure 2-7** (a) Anodic and cathodic reactions in the corrosion of steel in concrete, (b) Volumetric expansion as a result of oxidation of metallic iron (Mehta, 2003)

The chemical changes occurring at the anodic and cathodic areas are illustrated in Figure 2-7 (a). Also there are two other requirements in addition to the passivity breakdown; these requirements must be simultaneously fulfilled in order for the corrosion process to proceed at a significant rate. First is the continuous availability of oxygen and water at the cathode, the second requirement is the electrical conductivity of concrete (it should be noted that saturated concrete can act as an electrolyte). Depending on the oxidation state of iron, the transformation of metallic iron to rust may be accompanied by a considerable increase in volume as large as 600%, and this volumetric increase may be the principal cause of concrete expansion and cracking as can be seen in Figure 2-7 (b), (Mehta, 2003).

### ***Freeze-thaw Degradation***

The degradation of concrete due to freeze-thaw effect has been the subject of extensive research in the last century, because this type of deterioration is stilling represents a durability problem in many countries. This is primarily due to the widespread use of de-icing salt on concrete pavements (Gjørsv 2002).

While pure water in the open freezes at  $0^\circ C$ , in concrete the water is really a solution of various salts so that its freezing point is lower. On the other hand, the temperature at which water freezes is lower the small size of pores is full by water. It is known that, the gel pores are too small to permit the formation of ice, and the greater part of freezing

## 2. Literature Review

---

takes place in the capillary pores. It is observed that larger voids, arising from bad compaction, are usually air-filled and are not appreciably subjected to the initial action of frost. Thus, frost attack in concrete structures can be divided into two different types depend on the mechanism;

- First, freezing with fresh water pure frost attack. In this case the attack causes normally internal damages, while the surfaces are undamaged. The damages can be prevented if air is entrained in the concrete and a waterproof concrete is used.
- Second freezing with salt water or water that is polluted salt frost attack. In this case the attack causes external damages, i.e. scaling of the surface. The damage can be prevented if air is entrained and the w/c is kept low.

Figure 2-8 illustrates an example of concrete degradation by freeze- thaw cycles. When the water freezes its volume increases approximately 9 % due to the drop of the concrete temperature, freezing occurs gradually so that, the still unfrozen water in the capillary pores is subjected to hydraulic pressure by the volume expanding of formed ice. This pressure could result internal tensile stresses, and causing microstructural cracking in the concrete. Also this may occur, in porous of a saturated concrete containing no empty voids, where the liquid water can move. On subsequent thawing, the expansion caused by ice is maintained so that there is a new space for additional water which may be subsequently embedded on re-freezing further expansion occurs. Therefore, if there are a cumulative effect in the freezing and thawing cycles,

## 2. Literature Review

---



**Figure 2-8** Degradation by freeze-thaw cycles ([www.engr.psu.edu](http://www.engr.psu.edu))

the damage or cracking extends by the microstructure. However, the presence of neighbours air voids and empty capillaries around the ice presence allows a relief of hydraulic pressure by the flow of water into these spaces; and this is the entrance air (Ferreira, 2004).

### 2.2. Literature Review of Ultrasonic Techniques

#### 2.2.1. Non-destructive Testing

Non-destructive testing (NDT) forms an integral part of quality control, and used to describe the procedures which contribute to total quality assurance. A formal definition of the subject agreed by the International Committee for Non-destructive Testing (ICNDT) and accepted by the International Standards Organization (EO) states:

“Non-destructive testing is a procedure which covers the inspection and/or testing of any material, component or assembly by means that do not affect its ultimate service ability”.

The scope and importance of NDT can tend to be confused by the diffuseness of its boundaries as set by this definition, and by differing interpretations of how it should best be used with economy and effect to achieve its objectives. Figure 2-9 shows a range

## 2. Literature Review

---

of surface and internal variables that may need to be controlled and hence monitored non-destructively, again emphasizing that possible indications related to the flaw location and sizing represents only one of the many facets that may need to be considered when assessing overall quality (Smith, 1998).

The importance of non-destructive evaluation techniques in inspection of concrete structures has increased during the last few decades. New non-destructive evaluation techniques have been created and the ones that already existed have been perfected and their applicability extended. Because of the non-invasive nature, non-destructive evaluation techniques have several advantages when compared to conventional destructive techniques that most of them requires the sample extraction.

Some non-destructive evaluation methods based on the propagation of the mechanical stress waves are frequently used to detect and assess single and distributed damage in materials. On the other hand, properties of the pulses after propagation through the damaged materials can be compared with waves that were propagated through an undamaged sample to reveal microscopic changes and damaged in the inspected material's structure.

## 2. Literature Review

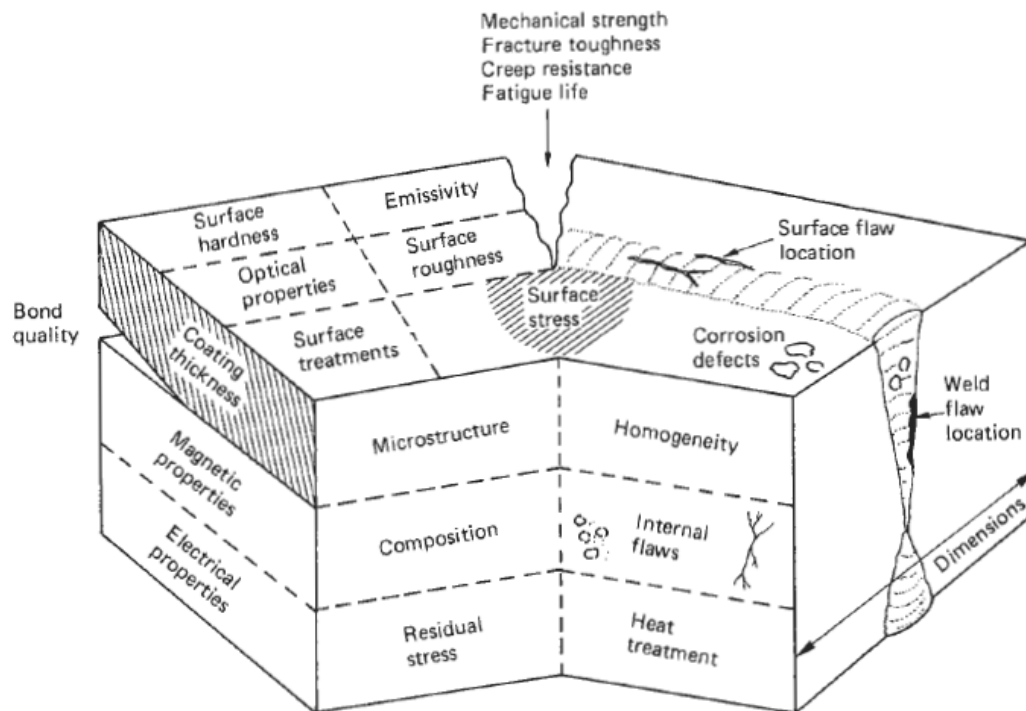


**Figure 2-9** the scope of non-destructive testing (Smith, 1998)

Examples are acoustic emission (AE), electrical methods (Eddy Current), nuclear (DRX or Gammagraphy) magnetic (Magnetic Particles), radar, sonic (Sonic Test), surface hardness (Indentation), thermography (IR), and impact-echo (Pile Test), ultrasonic testing. The Figure 2-10, Figure 2-12 and Figure 2-11 show a summary of the non-destructive methods for locating surface flaws, internal flaws and for monitoring structural variability (Smith, 1998)

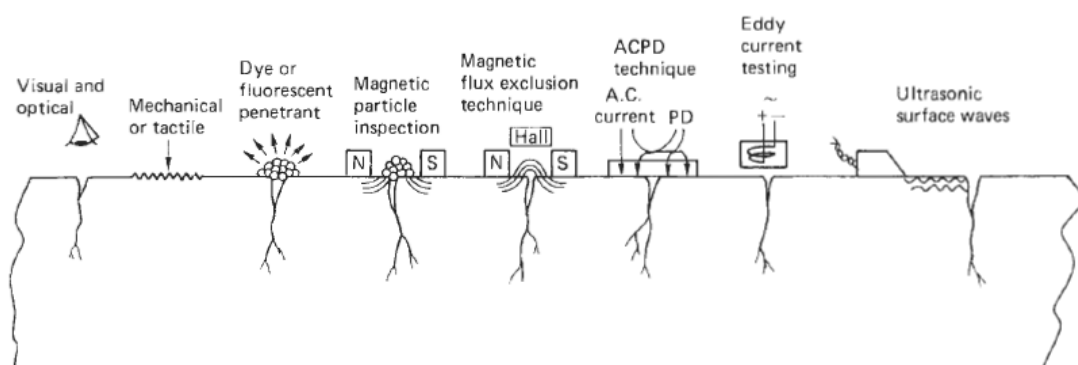


**Figure 2-10** NDT techniques for locating surface flaws (Smith, 1998)

## 2. Literature Review

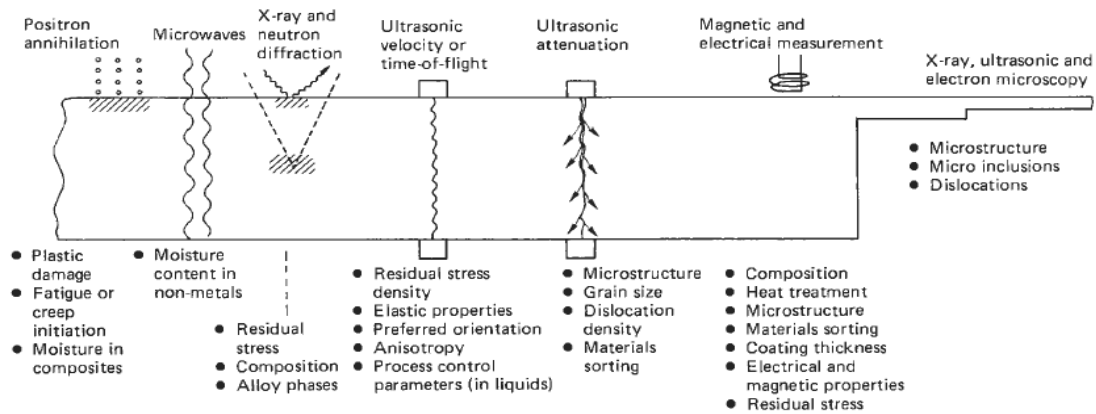


Figure 2-1 NDT techniques for monitoring structural variability (Smith, 1998)

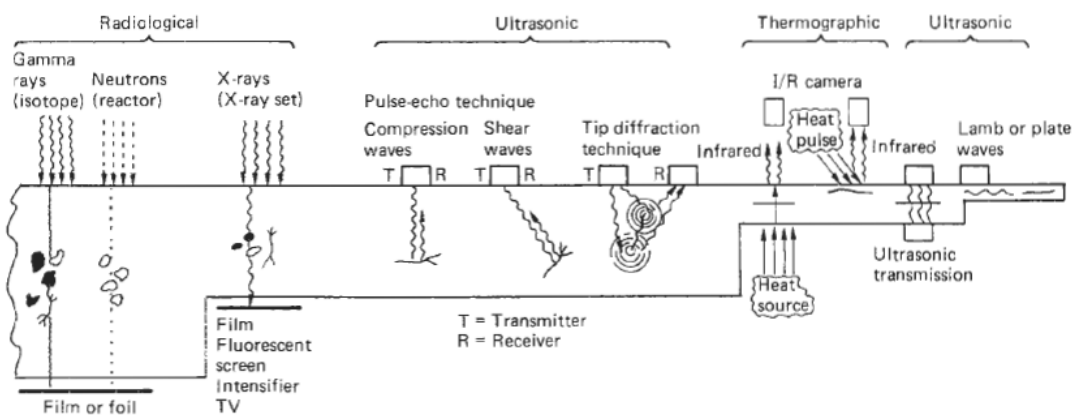


Figure 2-2 NDT techniques for locating internal flaws (Smith, 1998)

### 2.2.2. Non-destructive analysis by Ultrasonic Techniques

Among all non-destructive methods available for concrete testing (Malhotra, 1991; IAEA, 2002), the use of ultrasonic waves is of great interest to evaluate its mechanical properties. The velocity and attenuation are the typical parameters of such waves that are commonly used to determine the elastic properties (such as Young Modulus, Poisson ratio, or Lamé coefficients), and also to characterise micro-structural properties of materials (porosity, grain size, micro-cracks, etc.), (M. Chekroun, 2009).

There are different configurations available for the non-destructive evaluation as ultrasonic pulse-echo, ultrasonic pulse velocity, ultrasonic impact-echo and ultrasonic tomography. The ultrasonic impact-echo method, is a technique based on the use of

## 2. Literature Review

---

transient stress waves, has been used successfully for detecting and flawing the damage in many different types of concrete structures, including plate-like structures such as bridge decks, slabs, walls, beams, columns, layered structures and hollow cylindrical structures (Lin and Sansalone, 1996; Sansalone and Carino, 1989; Sansalone, 1997; Sansalone et al., 1996). In the ultrasonic pulse echo technique, a transducer is the sender and the receiver. The analysis of the frequency domain allows the user to determine the thickness and the crack depth by using the correspondent characteristic frequency equation.

$$f=V/2d, \text{ where } V \text{ is the velocity, and } d \text{ is the thickness.}$$

On the other hand, the wave velocity of ultrasonic wave depends on the inertia and elastic properties of the transmission material with an easy test procedure and accuracy at relatively low cost (Kaplan, 1960). This technique can detect and estimate areas of internal cracking, internal delamination and relative strength parameters (Tamn and Malhotra, 1991). The pulse velocity technique is usually employed to establish the uniformity and relative quality of concrete, such as permeability and porosity. The axial resolution (depth resolution) is very important to detect and locate defect quite close one to each other.

Previous researchers have been successful in relating the attributes of ultrasonic waves with specific material microstructure parameters in metal, ceramic, and cement based materials. (İsmail and Selami, 2006) used ultrasonic attenuation to estimate the mean grain size of marble, (Truell and Hikata, 1957; Bratina and Mill, 1962; Joshi and Green, 1972; Vergara and Fuente, 2004), for example, the usage of attenuation of longitudinal waves have successfully used as an indicator of the fatigue damage in metals in which dislocation, microcracks and non-uniform plastic deformation are the dominant attenuation mechanisms. And another example of the application of amplitude attenuation is its use in characterizing the grain size distribution in polycrystalline materials and the cavity in metals (Papadakis, 1965).

The theoretical background for used ultrasonic wave scattering by in-homogeneities, such as grains and air voids, can also be found in (Roney, 1950; Gubernatis and Domany,

## 2. Literature Review

1984; Sayers and Smith, 1982). As investigated by (Adler et al., 1986; Kumar et al., 1999; Smith, 1982; Nair et al., 1989;) there is a great deal of research on these works. On the other hand (Mal et al., 1992) investigated fibre-reinforced composites using attenuation of the ultrasonic longitudinal waves (Wonsiri, 2006).

### 2.2.3. Characterization of Cement-based Materials using Ultrasonic Testing

Cement-based materials provide a challenge for ultrasound diffusion and attenuation measurements due to the strong scattering produced by concrete and mortar microstructure as heterogeneous materials, due to the random distribution of aggregates and the variation of their length scales in the medium, as can be seen in Figure 2-13, following (Mehta and Monteiro, 1993) . The understanding of the effects of each of the components of the cement-based materials, including concrete, mortar, cement paste, aggregates, cracks, and voids on attenuation characteristics is important for the application of ultrasonic technique to characterize cement-based materials (Wonsiri, 2006).

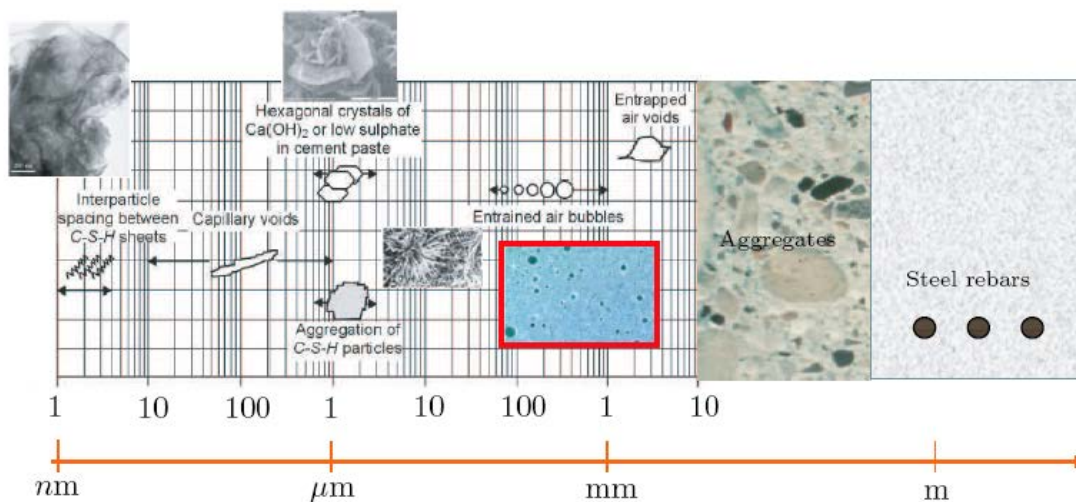


**Figure 2-3** Multi-length scales existing in cement-based materials microstructure (Mehta and Monteiro, 1993; Wonsiri, 2006).

As presented by Wonsiri, (2006) about the complexity and the variation of length scales of concrete “At a scale of meters, e.g. concrete is considered a homogeneous material with specific engineering properties such as compressive strength, elastic modulus, and



## 2. Literature Review

---

thermal expansion. At a scale of millimeters, concrete is a composite of entrained, entrapped air-filled voids and aggregates (0.1-30 mm in diameter) that are randomly dispersed in a matrix of cement paste (i.e., the solid that forms when cement reacts with water). At a scale of micrometers, cement paste is a composite of cement grains interspersed with hydration products, the two most prominent being an ionic solid that is slightly soluble in water  $\text{Ca(OH)}_2$  and a crystalline calcium silicate hydrate known as C-S-H; these products generally fail to fill all the space originally occupied by water, thus creating so called capillary pores in the paste. At a scale of tens of nanometers, the structure of C-S-H, resembling that of a particulate gel, is envisioned as agglomerates of approximately 10-20 nm in diameter that are subdivided into smaller particles approximately 5 nm across; this structure describes C-S-H at the particle level. At a scale of several nanometers, that is, at the sub-particle level, the structure of C-S-H resembles that of a disordered layered silicate”.

It is very important understanding the effects of each of the cement-based materials components, including concrete, mortar, paste, aggregates, cracks, and voids on ultrasonic parameters, this is essential for the application of ultrasonic technique to characterize cement-based materials (Wonsiri, 2006). In the next paragraphs is present a lot of research works whereas ultrasonic techniques were used for characterization of cement based materials.

Van Hawaert et al., (1998) used ultrasonic parameters (wave velocity, peak amplitude and wave energy) to follow the cracks growth of steel fiber reinforced concrete beam during a bending test. They found that both of peak amplitude and wave energy were dropped before the onset of a visible macro-crack, because of extensive micro-cracking, while ultrasonic wave velocity was changed after considerable crack growth. They concluded that, both of amplitude and energy of waveform, were found to be better indicators of crack growth than ultrasonic wave velocity, and this is due to their sensitivity to the extent of cracking. On the other hand, ultrasonic Leaky Rayleigh waves were used to investigate the topmost layer of mortar samples degraded by sulfate (Neuenschwander et al., 2006). Also ultrasonic Rayleigh waves were used to

## 2. Literature Review

---

characterize and detect the degraded concrete cover of concrete structure using a high frequency ultrasound (Piwakowski et al., 2004; Ould Naffa et al., 2002).

Yim et al., (2012) characterized the thermal damage of concrete using a nonlinear ultrasonic technique; an impact modulation method was used to obtain nonlinear parameters, because it shows better sensitivity than wave velocity as a linear method. To characterize the thermal damage of concrete, the authors compared the measured nonlinear parameters with another parameters such as wave velocity which calculated using low frequency (100-500 KHz), permeable pores which reflect the occurrence of opening pores in thermally damaged concrete, apparent density and SEM analysis. It was concluded that, it is possible to establish a correlation between compressive strength of thermal damage concrete and the measured nonlinearity parameters, it was found that, the measured nonlinearity parameters reflect the degree of thermal damage. The impact-modulation method found to be revealing remarkable sensitivity, showing earlier detection than ultrasonic wave velocity and dynamic Elastic modulus measurements.

Tsivilis et al., (2003) used ultrasonic pulse velocity to follow and estimate the formation of thaumasite in limestone Portland cement mortar samples subjected to sulfate attack. Also to estimate the parameters which affecting on thaumasite formation in limestone cement mortar, the compressive strength and ultrasonic wave velocity were used by (Kakali et al., 2003; Skaropoulou et al., 2009)

The effect of calcium leaching process of concrete on its mechanical properties was studied using ultrasonic wave velocity (Huang and Qian, 2011). The using of ultrasonic wave velocity to follow the setting process of fresh mortar is realized by (Robeyst, et al., 2009). Many investigators (Kozlov, (1988); Jacobs and Owino, (2000); Landis and Shah, (1995); Schicker, (2002); Anugonda et al., (2001); Popovics et al., (2000)) have performed experimental studies to understand of ultrasonic wave propagation in cement-based materials (Wonsiri, 2006).

(Selleck et al., 1998) measure attenuation of longitudinal waves in cement paste, fine mortar (sand aggregate diameter about 1 mm), coarse aggregate (aggregate diameter

## 2. Literature Review

---

about 5 mm) and concrete (maximum aggregate diameter about 10 mm). They use the fracture of glass capillary as a highly localized source, and detect the response with a point receiver. With this setup, the attenuation can be consistently determined up to 800 kHz for cement paste, 400 KHz for fine mortar and 300 KHz for coarse mortar and 150 KHz for concrete specimens. It is found that the frequency cut-off values depend on the size of the scatters, however no linear relationship is found between them. The specimens tested in this experiment are of the order of 30 – 40 mm and the transfer of the results to longer transmission lengths is unclear.

Naffa et al (2002) used velocity and attenuation of longitudinal, shear and surface waves to assess the feasibility of detecting concrete cover degraded by using a high concentration ammonium nitrate solution for 45 days exposure time. It was fabricated a slab mortar sample, the half of the sample was immersed into the solution and the other half was kept out of the solution and covered with an aluminium foil. Transducers between 0.5 and 1 MHz are used to characterize cover degradation with high sensitivity. The results showed that: (1) decreasing of ultrasonic pulse velocity and high increasing of attenuation in the degraded material relative to the sound material. For this they said that it is possible to detect and characterize cover degradation using high frequency ultrasound; (2) attenuation measurements in heterogeneous media are difficult, their sensitivity to degradation is very high; (3) surface wave seems to be the most appealing for cover detection: (I) it is high sensitive to cover degradation; (II) its depth of penetration is frequency dependent and for this it may be useful to inspect the concrete cover at different depths and thus to estimate the thickness of the degraded layer; (III) it is well a suited to on-site inspection as it requires access to one side of the structure only.

Chaix et al (2003) used backscattered ultrasonic waves to characterize concrete damage. They used a signal model to generate backscattered ultrasonic waves, and developed it to damaged concrete testing. Frequency range from 500 KHz to 2.25 MHz was used to obtain backscattered ultrasonic signals, thus the attenuation coefficient in the concrete can be deduced. The backscattered attenuation coefficient is measured by exploitation process for several thermal damage states of the concrete. They found a

## 2. Literature Review

---

relative variation between the different tests. They concluded that attenuation of ultrasonic waves is a good indicator to follow microstructural evolution and thus concrete damage if the work frequency is well chosen.

### **2.2.3.1. Sulfate attack degradation characterized by Ultrasonic Techniques**

Skaropoulou et al., (2009) studied the long term behavior of limestone cement mortars, in relation of variation limestone content replacement. Skaropoulou et al., (2012) studied the effect of cement composition, sand type and exposure temperature on thamasite formation due to sulfate attack. Skaropoulou et al., (2013) studied the using of the mineral admixture to improve the resistance of limestone cement concrete against thaumasit formation due to sulfate attack. In all these works, ultrasonic pulse velocity was used to follow the degradation level due to sulfate attack, and it is found that, ultrasonic wave velocity is a good parameter to follow the changes in the concrete and mortar microstructures due to sulfate attack. Yang and Luo, (2012) studied the damage of concrete subjected to sulfate attack under flexural loading. In their study ultrasonic propagation speed was used to calculate the dynamic elastic modulus of samples due to the degradation process. Also the dynamic elastic modulus was calculated by ultrasonic wave velocity in the work of (Zuquan et al., 2007).

Schmidt et al., (2009) investigated the consequences of external sulfate attack using traditional test methods, between these methods; the using of ultrasonic Leaky Rayleigh waves was realized to follow the degradation process of the topmost layer of the sample surface. It was concluded that, ultrasonic wave velocity is successfully applied for the investigation of the degradation process by sulfate attack.

Song and Chen, (2011) used ultrasonic wave velocity to study the effect of damage evolution on Poisson's ratio of concrete degraded by sulfate attack. It was concluded that the variation of ultrasonic wave velocity is caused by three factors; the first on is continuation of the hydration process of concrete samples, The second one is due to the formation and filling the pores by ettringite product, yet, it is not produced micro-

## 2. Literature Review

---

cracks, these two factors lead to the increasing of wave velocity. The third factor due to the expansion of ettringite which causes damage evolution, and this leads to decreasing of ultrasonic wave velocity due to the decreasing the effective modulus due to the erosion damage. The same conclusion is observed in a previous work for (Chen et al., 2008) when they studied the damage evolution of cement mortar due to sulfate attack.

Chu and Chen, (2013) presented an experimental and theoretical study using the attenuation coefficient of the ultrasonic expansion waves in concrete fabricated with different mixes and degraded by sulfate attack. Also it were derived the relationships between attenuation coefficient, relaxation time and ultrasonic wave velocity of the elastic expansion waves. The variation of the attenuation coefficient with time was determined during the degradation process, using a simple ultrasonic method. It was found that, an increasing in the magnitude of the attenuation coefficient with time, this reflects the concrete damage evolution caused by sulfate attack. Thus, it was suggested that the damage caused by sulfate attack in concrete can be estimated by using ultrasonic techniques.

Sun et al., (2013) proposed a new model to estimate the diffusion of sulfate ions in concrete, in this study ultrasonic test was used to evaluate the damage produced due to sulfate attack. It was concluded that "The damage evolution of the concrete caused by sulfate attack can be approximately represented by the damage function expressed in terms of the immersion time of the specimen in sulfate solution and the sulfate concentration in the specimen. The corresponding parameters of the evolution of damage can be determined by using ultrasonic tests"

### 2.2.3.2 Freeze-thaw Characterization by Ultrasonic Techniques

Akhras (1998) studied the damage in Portland cement concrete due to its exposed to freeze-thaw cycles. He used ultrasonic technique to calculate both of ultrasonic wave velocity and signal energy of ultrasonic waves. It was found that ultrasonic wave velocity is less sensitive than signal energy of ultrasonic to detect freezing and thawing

## 2. Literature Review

---

damage at the initial stage. But at sever damage, ultrasonic wave velocity found to be more sensitive than signal energy.

Kucharczyková et al., (2012) studied the influence of porous aggregate pre-soaking of lightweight concrete on the freeze-thaw resistance. They investigated three concrete mixtures with different degree of porous aggregate saturation; oven dried aggregate, aggregate with moisture of 13% and 30% pre-soaked aggregate. Non-destructive techniques (ultrasonic and resonance methods) were realized after every 25 cycles. Ultrasonic technique used to calculate wave velocity and the resonance method was used to detect the changes in the values of dynamic modulus of elasticity. On the other hand, destructive methods were used to determine the static modulus of elasticity, fracture and strength parameters. It was concluded that the fracture and strength tests found to be more sensitive to micro-cracks identification than ultrasonic wave velocity.

The ability of ultrasonic and laser impact tests to classify the ageing level of concrete samples damaged by freeze-thaw cycles, and also, to obtain an evaluation of elasticity coefficients were investigated by (Panet et al., 2002). Karakoç et al (2011) used ultrasonic wave velocity with compressive strength, porosity and the relative dynamic modulus of elasticity to study the freezing of pore solution in concrete subjected to freeze-thaw cycles. Also, the effects of pumice aggregate ratios on the high strength concrete properties were studied at 28 days. To model the relative changing in ultrasonic wave velocity and the relative changing of compressive strength, feed-forward artificial neural network techniques are used. Thereafter, a genetic algorithm was applied in order to determine optimum mix proportions subjected to 300 thermal days. It was found that, the increasing of pumice aggregate ratio led to decreasing both of relative dynamic modulus of elasticity, compressive strength and ultrasonic wave velocity. Also it is found that the neural network is capable of generalizing between input and output variables (ultrasonic wave velocity and compressive strength) and reasonably a good prediction.

## 2. Literature Review

---

Ultrasonic wave velocity with compressive strength and weight loss tests, are used to evaluate the durability of concrete with synthetic fiber addition and subjected to freeze-thaw cycles (Richardson et al., 2012). Also for following the damage of cementitious materials due to freeze-thaw process, ultrasonic wave velocity as (a non-destructive test) accompanied using compressive strength, mercury intrusion porosimetry and scanning electron microscope as (destructive tests) were used to study the frost resistance of blended cement containing calcined paper sludge as a partial cement replacement (Vegas et al., 2009).

Also many works are used ultrasound technique to study freeze-thaw durability of cement based materials as can be seen in the works of (Cao and Chung, 2002; Pospíchal et al., 2010; Molero et al., 2012; Uysal and Akyuncu 2012).

### **2.2.3.3. Compressive and flexural strength characterization by Ultrasonic techniques**

Rajagopalan et al (1973) reported a correlation between ultrasonic pulse velocity and compressive strength of concrete for some typical mixes. The study measured simultaneous measurements of pulse velocity and compressive strength made on 150 mm cubes, at different ages from 1 day to 28 days, indicates a linear relation between strength and velocity.

Kaplan, in 1958, investigated the compressive strength and UPV correlation both in the laboratory and on structural building columns; in 1959, reported the effects of w/c ratio and age, and concluded that the relation between UPV and compressive strength cannot be independent of age and w/c ratio; and in 1960, conducted to determine the effect of voids in specimens due to incomplete consolidation on the compressive strength, UPV, and dynamic modulus of elasticity of concrete. It was concluded that voids due to incomplete consolidation had much less effect on pulse velocity than on compressive and flexural strength (Kaplan, 1959).

Popovics et al. (1990) studied the difficulties of the estimation of concrete strength from pulse velocity measurement. In this study, the role of compositeness and dispersion were discussed. They used three pairs of narrowband transducers with the nominal

## 2. Literature Review

---

frequency of 24, 54, and 120 kHz. As a result of that study, they presented that the pulse velocity in the longitudinal direction of a concrete cylinder differs from the velocity in the lateral direction; more specifically, at low velocities the longitudinal velocities are greater, whereas at high velocities the lateral ones; this difference is more pronounced with lower frequencies; the dispersive nature of concrete decreases with age; and the pulse velocity is independent of the stresses in concrete to a large extent.

Gregor et al. (2009) studied the factors that affect on the ultrasonic wave velocity-compressive strength relationship, and also studied. The relationship between ultrasonic pulse velocity, static and dynamic young's modulus and shear modulus. They determined the influence of aggregate, initial concrete temperature, type of cement, environmental temperature and w/c ratio by their own experiment. They established a numerical model in order to evaluate the concrete's compressive strength by the determination of the ultrasonic pulse velocity in arbitrary concrete. The artificial neural network approach was used for this purpose. It was concluded that the influence of aggregate is very important and cannot be neglected for accurate prediction of compressive strength of concrete based on ultrasonic pulse velocity. The prediction of concrete compressive strength with the proposed by their numerical model, which was established within Matlab programming environment, showed a good degree of coherency with experimentally estimated compressive strength. Thus, their study showed that the determination of concrete compressive strength, based on ultrasonic pulse velocity alone, can be predicted very accurately if properly considered.

### **2.2.3.4. Porosity characterization by Ultrasonic techniques**

Wonsiri et al (2007) perform quantitative characterization of the capillary porosity and entrained air content in hardened cement paste with ultrasound. Direct measurements of ultrasonic attenuation are used to measure the volume fraction and average size of entrained air voids and to assess variations in intrinsic porosity, as influenced by water-to-cement ratio (w/c) in hardened cement paste specimens.

For the air entrained specimens, an inversion procedure based on a theoretical attenuation model is used to predict the average size and volume fraction of entrained



## 2. Literature Review

---

air voids in each specimen, producing results in very good agreement with results obtained by standard petrographic methods and by gravimetric analysis. In addition, ultrasonic attenuation measurements are related to w/c to quantify the relationship between increasing porosity (with increasing w/c) and ultrasonic wave characteristics.

L. Vergara et al (2001) used structural noise, wave velocity and attenuation of ultrasonic waves to estimate the porosity of mortar samples. They considered that mortar only formed by two phases solid and pores, the work was undertaken from two different approaches; the first one is analysis of the structural noise of ultrasonic waves to extract statistical parameters which might be correlated with porosity levels. The second is to study the relation between ultrasonic wave velocity and porosity, in transmission measurement mode, also to study the relation between porosity and ultrasonic attenuation in a similar manner. The authors studied mortar samples with different w/c ratios. They concluded that, from the three used method, the method based on ultrasonic velocity was offered satisfying results for mortar estimating porosity. While the methods based on attenuation and structural noise were presented a clear tendencies but yet, not with necessary precision considered to measure porosity, using these techniques.

L. Vergara et al (2004) have proposed a technique for material characterization by using centroid frequency profile of ultrasonic echo signals. They applied this technique to measure the degree of porosity of cement paste. Two different w/c ratios (0.4 and 0.5), and two different cement type (CEM 32.5 and CEM 42.5) were used to obtain various values of porosity and resistances. It was used 10MHz transducer to obtain enough amount of grain noise in the collected records. It was concluded that porosity has exhibited significant correlation with ultrasound penetration obtained after the centroid frequency profile.

Hernández et al (2000) applied a micromechanics model to estimate mortar porosity. It was fabricated mortar samples with various water-cement ratios to obtain different degrees of porosity. To measure ultrasonic wave velocity, transducers 2MHz, 1MHz and 500 KHz were used. It was concluded that "In order to use the model it is necessary to know the stiffness of mortar at zero porosity, and this is a difficult task because mortar

## 2. Literature Review

---

is always a porous material. However, it is possible to obtain these parameters by relating destructive and non-destructive measurements of mortar". Ultrasonic wave velocity is correlated with porosity.

Based on ultrasonic measurements, a three phase micromechanical model proposed by (Hernández et al., 2006) was used to estimate the porosity of mortar samples degraded by ammonium nitrate solution. In their study, a prismatic mortar samples ( $40 \times 40 \times 160 \text{mm}^3$ ) were used. Four series with different sand/cement and water/cement ratios were fabricated, using cement type III/B. porosity were measured according to RILEM standard. A Krautkramer K2K, broadband transducer with 2 MHz of central frequency, emitting in longitudinal mode, was used to measure P-wave velocity. Ultrasonic signals were acquired at 80 MHz of sampling frequency with SENDAS system, high precision equipment. Also S-waves were measured but only for non-degraded samples. Based on the obtained results, it was concluded that; an increasing in the capillary porosity due to the leaching process and a significant decreasing in the elastic properties of the cement matrix. The porosity variation was fitted linearly with the variation of Young's modulus of cement matrix obtained by the three phase micromechanical model proposed.

Lafhaj et al., (2006) used ultrasonic technique to correlate ultrasonic pulse velocity with porosity and permeability. It was used a simple model to relate ultrasonic pulse velocity with porosity and permeability. Various water-cement ratios (0.3 -0.6) was used. The ultrasonic parameters, pulse velocity and attenuation were measured for longitudinal and shear waves, using wideband spectroscopy in a frequency range from 0.5 to 1 MHz. It was concluded that: (1) pulse velocity decreases with increasing porosity and permeability, and it increases with the decreasing of water-cement ratio; (2) shear wave velocity is about half of the longitudinal wave velocity and seems to be less sensitive to the water content; (3) attenuation increases with porosity, permeability and water content; (4) shear wave attenuation is 2 to 4 times higher than that of longitudinal wave, depending in porosity.

The relationship between porosity and ultrasonic Rayleigh wave velocity was studied by (Goueygou, et al., 2009). A two single-phase model was used to compare the obtained

## 2. Literature Review

---

results using a statistical hypothesis test. They found a good agreements between the obtained result data (porosity and ultrasonic wave velocity) and the used models, it is concluded that, with this agreement it can be develop a simplified models of wave propagation in concrete, also the porosity concrete cover can be estimated by ultrasonic measurements. Also the relationship between porosity and ultrasonic wave velocity of mortar samples degraded by ammonium nitrate was studied by (Lafhaj and Goueygou, 2009)

To study the effect of moisture in the porosity measurements of mortar Poblete and Acebes Pascual, (2007) used ultrasonic wave velocity and a thermal non-destructive test (using thermographic camera) to achieve this purpose. They concluded that, it is found a good correlation between ultrasonic technique and thermal non-destructive test; also it is found that, both of the used techniques are good to measure the porosity of moisture mortar and for estimating the durability of concrete.

The relationship between porosity, concrete mixture and ultrasonic wave velocity of concrete was studied by (Benouis and Grini, 2011). Cylindrical specimens  $160 \times 320 \text{mm}^2$  were fabricated with seven different mixtures (W/C and S/S+G ratios) to obtain different porosity levels between (7 and 16%). Ultrasonic wave velocities were measured in the longitudinal direction using 7.5 mm and 49.5mm transducers diameter with 54 KHz central frequency. It was concluded that, ultrasonic wave velocity obtained by transducer 49.5mm if higher than that obtained by 7.5mm transducer, and the results obtained by transducer 49.5mm exhibits a better correlation with porosity than transducer 7.5mm. On the other hand they found that, the relationship between porosity and ultrasonic wave velocity can be described by a linear relationship. Also it is concluded that ultrasonic wave velocity is good for porosity estimation of ordinary or fluid concrete with w/c ratio higher 0.5. Soltani, et al., (2013) studied the relationship between ultrasonic Rayleigh wave velocity and capillary porosity of cement paste.

For all the previous studies mentioned above, it can be observed that ultrasonic techniques are used to estimate the compressive strength or to estimate w/c ratio of cementitious materials, also to estimate porosity of such materials during the curing stage and recently were used in a wide range to estimate the degradation of cement

## 2. Literature Review

---

based materials when they are subjected to aggressive environments, such as sulfate attack or degradation due to freezing- thawing cycles.

As a continuation to the previous studies, and as mentioned in the introduction (Chapter1), several ultrasonic techniques addition to other destructive techniques will be used to evaluate and estimate the degradation process by aggressive elements (sodium sulfate and ammonium nitrate) as will be seen later that are representative of different degradation process and rates, and also it is analysed by different purposes

It is known that both of sulfate and chloride are the more aggressive elements in marine environment, for this reason sulfate solution is used in this study to simulate the marine environment. By the other hand, ammonium nitrate degradation is used as example of decalcification. The use of ammonium nitrate solution to simulate and accelerate the leaching of cement pastes due to deionised water.

# **CHAPTER 3**

**Materials, Samples Preparation and Methods**



## 3 Materials, Samples Preparation and Methods

This chapter details the procedures followed in the preparation of the mortar specimens and the procedure of extracting prefabricated concrete cores. The materials used and corresponding specifications are outlined. The various test methods and test procedures are also detailed and explained.

### 3.1. Materials

#### 3.1.1. Cement

Portland cement type II (II A-L 42.5R) and type I (I 42.5R/SR) were used throughout the entire research. Cement II A-L 45.5R (Portland-limestone cement, containing 15% of limestone (PLC), according to the standard (UNE-EN 197:2000) was chosen because it has a percentage of (6-20%) of limestone which reacts with sulfate to form ettringite. For this, it is found a restrictions on the use of Portland limestone cement, not only in sulfate containing grounds, but perhaps also for marine structures exposed to sulfate containing sea water (Herald, 2003). Cement I 42.5R/SR (Sulfate resistant Portland cement (SRPC) was chosen according to the standard (UNE-EN 80303-1) that is the appropriate cement due to the low percentage of activated tri-calcium aluminate C3A and subsequently tetra-calcic ferrite aluminate C4AF. The reason for using two different types of cement is to obtain two different rates of degradation. The details of chemical composition of cement are presented in Table 3-1.

**Table 3-1** Chemical composition of Portland cement

Cement	SiO <sub>2</sub>	Al <sub>2</sub> O <sub>3</sub>	Fe <sub>2</sub> O <sub>3</sub>	CaO	MgO	SO <sub>3</sub>	K <sub>2</sub> O	Na <sub>2</sub> O	Loss on ignition (%)
IIA-L 42.5R	20.4	4.2	2.4	64.1	2.3	2.4	0.8	0.02	5.8
I 42.5R/SR	21.5	3,7	4.8	63.9	1,9	2,5	0.53	0.19	3.1

#### 3.1.2. Aggregate and sand used for precast concrete

The aggregate used is a crushed limestone aggregate. Also, it was used a gravel size 4/10 and 8/20mm, which has been provided in Lapidra kaolins (Llíria, Valencia). The physical tests carried out to characterize the coarse aggregate (see Table 3-2). Particle sizes were done according to the following standard (UNE-EN 933-1:97). Figure 3-1 shows size distribution of aggregates and sand used.

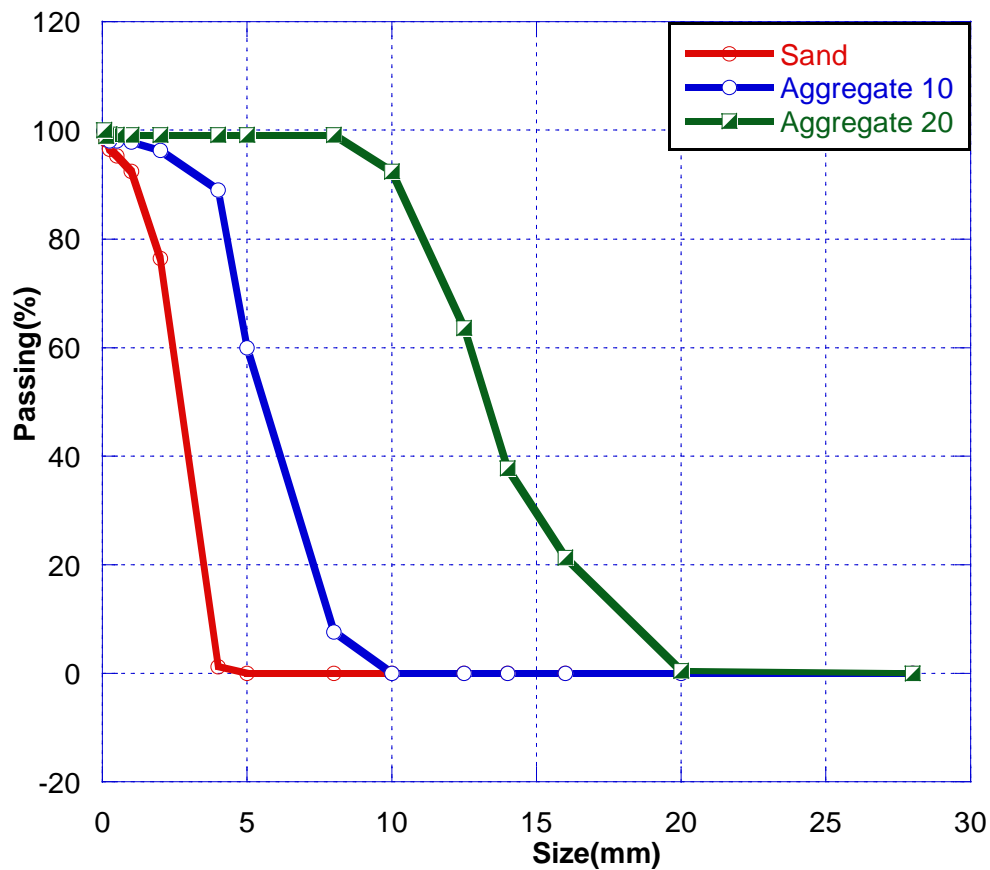


Figure 3-1 Curve of grading of fine and coarse aggregates



### 3. Materials, Samples preparation and Methods

**Table 3-2** Particle size distribution of used aggregates and sand

Sieve	Sand		Aggregate 10		Aggregate 20	
	% Retained	%Accumulated	% Retained	%Accumulated	% Retained	%Accumulated
28	0,0	100	0,0	100	0,0	100
20	0,0	100	0,0	100	0,4	99,6
16	0,0	100	0,0	100	21,3	28,7
14	0,0	100	0,0	100	37,8	62,2
12,5	0,0	100	0,0	100	63,6	36,4
10	0,0	100	0,0	100	92,4	7,6
8	0,0	100	7,6	92,4	99,1	0,9
5	0,0	100	60	40	99,2	0,8
4	1,2	98,8	89	11	99,2	0,8
2	76,4	26,6	96,3	3,7	99,2	0,8
1	92,4	7,6	97,8	2,2	99,2	0,8
0,5	95,3	4,7	98	2,0	99,2	0,8
0,25	96,5	3,5	98,1	1,9	99,3	0,7
0,125	98,3	1,7	99,3	0,7	99,9	0,1
0,063	99,8	0,2	99,9	0,1	100	0,0
Pass	100	0,0	100	0,00	100	0,0
<b>Grading module</b>	<b>4,601</b>		<b>6,461</b>		<b>10,089</b>	

#### 3.1.3. Water

The water used in preparing the concrete is drinking water. Table 3-3 presents the analysis of the used water.

**Table 3- 3** Analysis of water used in preparing prefabricated concrete

Acidity, by PH	Soluble substances	sulfates	chloride
8,41	0,96 g/l	0,25 g/l	0,10 g/l

#### 3.1.4. Admixtures

Sika Paver admixture ® HC-1 has been used according to the requirements of the standard (UNE-EN 934-2). The technical data supplied by the manufacturer are listed in Table 3-4.

**Table 3-4** Features of SikaPaver

Chemical base	Surfactante blend
Density	1,01 + 0,01 kg/l (a +20 °C)
pH	7 (neutral)
Chloride contain	≤ 0,1%
Dosage	0,2% - 0,5% weight of cement

## 3.2. Experimental development

### 3.2.1. Mixture proportions and manufacture of concrete frames

In a precast concrete factory Gadea Hermanos (Valencia- Spain), there have been fabricated two big frames of precast concrete with dimensions of 2000×1500×2000 mm<sup>3</sup>, (see Figure 3-2). Table 3-5 shows the mixture proportions of the frames, where frame1 manufactured using cement I 42.5R/SR (Sulfate resistant Portland cement (SRPC)), and frame2 with cement II A-L 45.5R (Limestone Portland cement (LPC)). The cure of the two frames was in natural environmental conditions.



**Figure 3-2** Precast concrete frames on AIDICO facilities.

### 3. Materials, Samples preparation and Methods

**Table 3-5** Mixture proportions for precast concrete frames

Dosage	Frame SRPC	Frame PLC
Crushed sand (kg/m <sup>3</sup> )	900	900
Gravel 20(kg/m <sup>3</sup> )	508	508
Gravel 10(kg/m <sup>3</sup> )	700	700
Relation w/c (kg/m <sup>3</sup> )	0.30	0.30
Cement (kg/m <sup>3</sup> )	325	300
Additives (l/m <sup>3</sup> )	1.3	1.3

#### 3.2.2. Coring procedures.

The coring procedures are shown in Figure 3-3; the coring apparatus consisted of a core drill with diamond-impregnated bits attached to a core barrel for obtaining cylindrical core specimens, the diameter of all cores is 75mm approximately and the length of the samples is 150mm and 75mm. Coring samples divided into three groups, depending of the test type (see Table 3-6). Cores were prepared for testing by removing top and bottom portions of core (by saw cutting) to provide a 2:1 length: diameter ratio for compressive strength and ultrasonic inspections and 1:1 for porosity test.



**Figure 3-3** Coring procedures

### 3. Materials, Samples preparation and Methods

---

**Table 3-6** Test types and core numbers

Test	N° of Cores	N° of dissolutions	L/d Slimness Ratio	Total
Compressive strength	18	3*2 types of cement	2:1	108
SEM				
Mercury intrusion porosimetry				
Open porosity	18	3	1:1	108
Ultrasonic transmission-reception	18	3	2:1	108
Ultrasonic pulse-echo				
Ultrasonic tomography				
<b>Total N° of cores</b>				<b>324</b>

#### 3.2.3. Mixture proportions and manufacture of mortar

In order to obtain various porosity values and various degradation rates, mortar samples were fabricated with mixture proportion of cement: sand equal to 1:2 and different water/cement ratios 0.30, 0.375, 0.45 and 0.525 for degradation process by sodium sulfate solution, and for the degradation process by ammonium nitrate solution w/c ratios 0.40 and 0.55 were used (Table 3-7). Cement II A-L42.5R type was used as mentioned previously (see Table 3-1) Mortar specimens 40×40×160 mm were prepared according to Spanish standard (UNE EN-196-1), and used as test specimens in our study (see Table 3-8). After 24 hours, the specimens were cured in water for 28 days. At the age of 28 days, the flexural, compressive strengths, porosity and ultrasound parameters were determined with three prisms of a series of the specimens and used as initial parameters of the mortar. Thereafter, the test specimens were immersed in sodium sulfate and ammonium nitrate solutions. The solutions were replaced as needed to maintain submersion of the samples, ensuring that the solution concentration was maintained. A series of specimens were immersed in water saturated by calcium hydroxide as reference, Figure 3-4 shows procedure of mortar preparing.

### 3. Materials, Samples preparation and Methods

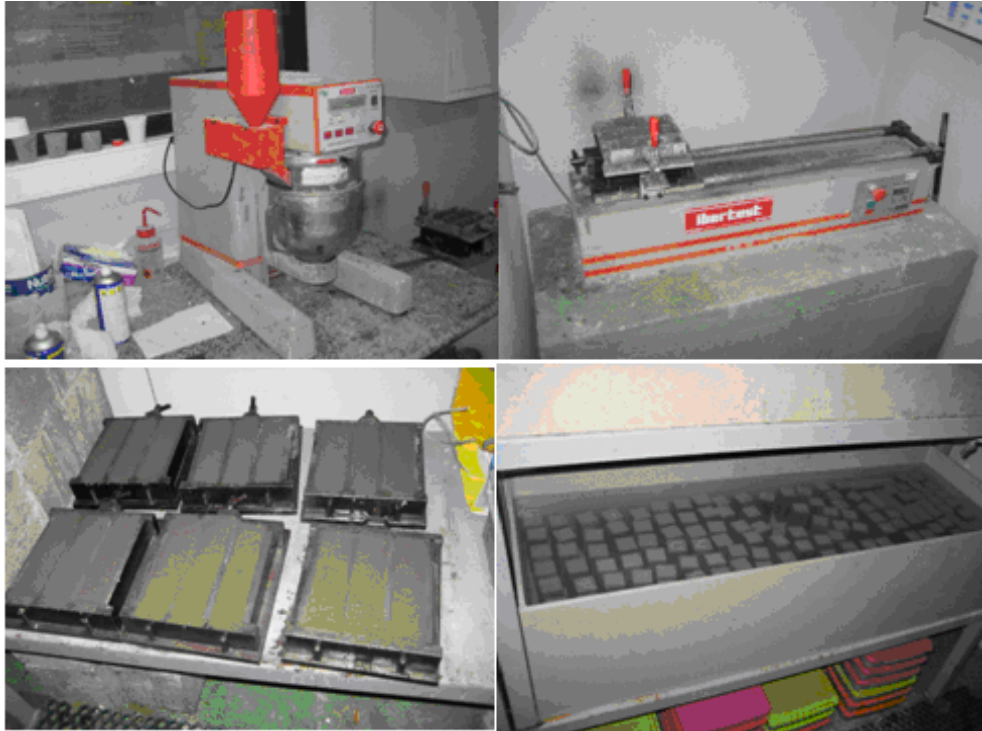


**Figure 3-4** Procedure of mortar preparing

**Table 3-7** Mixture proportion of mortar specimens

W/C ratio	C:S	Sand(kgm <sup>-3</sup> )	Cement(kgm <sup>-3</sup> )	Water(kgm <sup>-3</sup> )
0.55*	2	1350	675	432
0,525	2	1350	675	415,1
0,45	2	1350	675	364,5
0.40*	2	1350	675	330,8
0,375	2	1350	675	313,9
0,30	2	1350	675	263,3

\*w/c ratios for ammonium nitrate degradation process

**Table 3-8** Test types and Mortar total samples number

Test	N° of samples	N° of W/C ratio	N° of dissolutions	Total
Compressive strength	15	4	3	180
Flexural strength				
SEM				
Mercury intrusion porosimetry	15	4	3	180
Open porosity				
Ultrasonic transmission-reception	3	4	3	36
Ultrasonic pulse-echo				
Ultrasonic tomography				
<b>Total number of mortar samples</b>				<b>396</b>

### 3. Materials, Samples preparation and Methods

---

#### 3.2.4. Chemical dissolutions

In the entire research, it was used two chemical dissolutions to achieve the objectives of this work. Table 3-9 shows the dissolutions and its concentration. Sodium sulfate solution was refreshed every 2 months, while ammonium nitrate solution was refreshed every 3 weeks, to minimize the increase in pH due to the leaching of OH<sup>-</sup> ions from the prefabricated concrete cores and mortar specimens. The pH to be controlled, it was measured weekly using pH-meter sensION+ with sonde electrode in one glass tube joint with an electrode of reference, (Ag/AgCl) and KCl were used 3M potassium chloride KCl.

The samples were immersed in plastic boxes with dimensions 120 x 80 x 25 cm. as can be seen in Figure 3-5. As reference, prefabricated concrete cores and mortar specimens were immersed in water saturated by calcium hydroxide. The temperature of solution was kept at 20±1 °C during test period. For the entire realized tests, is presented the period where the samples were examined. The samples degraded by sodium sulfate solution, concrete samples were tested at 1, 90, 220, 360 and 470 days, while mortar samples were tested at 1, 90, 200, 340 and 450 immersion days. All tests were done at the same time, except SEM test, only it was realized in two periods as will be seen later in paragraph 3.2.9. On the other hand, for samples degraded by ammonium nitrate solution, concrete samples were tested at 1, 49, 96, 190 and 290 days, while mortar samples were tested at 1, 20, 35 and 50 day degradation time. Also all tests were realized at the same time, but both of Mercury Intrusion Porosimetry (MIP), SEM and ultrasonic image tests were not realized in the case of ammonium nitrate solution.

**Table 3-9** Chemical dissolution used.

<b>Dissolution</b>	<b>concentration</b>	<b>Notes</b>
Sodium sulfate	0.704Mol/liter	(10% from mass of water)- every liter of water has 100gm of NaSO <sub>4</sub>
Ammonium nitrate	4Mol/liter	



Figure 3-5. Some of the plastic boxes used in the entire research with 120 x 80 x 25 cm. of dimensions, in the durability chamber at AIDICO.

#### 3.2.5. Compressive strength test

Compressive strength is a common parameter used for quality control and quality assessment of concrete. Cores were prepared for compressive strength testing by removing top and bottom portions of core (by saw cutting) to provide a 2:1 length:diameter ratio. Sulphur caps were used. The testing machine used for the compression test was Ibertest model H/B150DAVA and the test was realized according to the standard UNE-EN 12504-1:200 (see Figure 3-6), the total maximum load indicated by the testing machine was recorded and the compressive strength values were calculated by dividing the total maximum load to loaded surface area as shown in next equation.



### 3. Materials, Samples preparation and Methods

---

$$f_c = \frac{P}{A}, \quad (1)$$

Where  $f_c$  the compressive strength in MPa, P is the total maximum load in kN, A is the area of loaded surface in cm<sup>2</sup>.



Mortar specimen



Concrete specimen

**Figure 3-6** Procedure of compressive strength for concrete cores and mortar samples.

#### 3.2.6. Flexural strength test

Flexural strength of mortar samples was measured using a simple beam with center-point loading (see Figure 3-7). The flexural strength values of mortar samples were calculated using the following equation according to standard UNE-EN 1015-11:200

$$R = \frac{3PL}{2bd^2}, \quad (2)$$

Where R is the modulus of rupture in MPa, P is the maximum applied load indicated by the testing machine in KN, L is the span length in cm, b is the average width of specimen in cm and d is the average depth of specimen in cm.





**Figure 3-7** Procedure of flexural test

#### 3.2.7. Porosity measurement

Vacuum saturation method described by RILEM CPC 11.3:1984 was used for the measurement of porosity of all mortar and concrete specimens. The procedure for the measurement is as follows:

The samples were oven dried for 24 hours at 105<sup>o</sup>C and then cooled in a desiccator for the next 24 hours and weighed. The samples were then kept in a desiccator under 1 bar of vacuum, for 24 hours. The desiccator was then filled with de-aired and de-ionised water, so that samples are fully submerged in water. Then the samples were kept under vacuum for 24 hours and were allowed to equilibrate for the next 24 hours. The samples were then weighed in air and water. Triplicate samples were tested for each age and the mean of three is reported as result. Figure 3-8 illustrates the procedures of porosity measurement.

$$\text{Porosity (\%)} = \frac{W1 - W2}{W1 - W3} \times 100 \quad (3)$$

W1 is oven-dry weight

W2 is saturated dry weight

W3 is Saturated submerged weight

### 3. Materials, Samples preparation and Methods

---



**Figure 3-8** Procedure of porosity measurement

#### **3.2.8. Ultrasonic testing**

In the entire research, we used the ultrasound technique as a non-destructive method to follow the microstructure changes of concrete cores and mortar samples submitted in a chemical dissolution. Two ultrasound techniques/configurations were used, pulse-echo to obtain the attenuation profile area (APA), and through-transmission to measure the velocities of both longitudinal wave (P-wave) and transversal wave (S-wave). For the acquisition of ultrasonic signals, it was used the following equipment:

### 3. Materials, Samples preparation and Methods

---

- Panametrics 5058PR equipment, transmitter-receiver high voltage pulses, high gain, whose bandwidth covers all frequencies of inspection (10 kHz to 10 MHz).
- Tektronics TDS3012 oscilloscope for displaying the signals.
- A 1MHz frequency transducers, Panametrics D703 for inspection the samples by the grain noise method.
- A 3.5MHz frequency transducer, Panametrics V412S for inspection the samples by the grain noise method.
- Two transducers with frequency of 1MHz Krautkammer K1SC to measure velocities of propagation (longitudinal wave).
- Two transducers Panametrics V151 with a frequency of 500 kHz for measuring velocities of propagation (transverse wave).

Figure 3-10 and Figure 3-11 show the equipment and the used transducers respectively.

#### 3.2.8.1. Equipment Calibration

“Calibration is necessary because most ultrasonic equipment can be reconfigured for use in a large variety of applications. The user must "calibrate" the system, which includes the equipment settings, the transducer, and the test setup, to validate that the desired level of precision and accuracy are achieved. The term calibration standard is usually only used when an absolute value is measured and in many cases, the standards are traceable back to standards at the National Institute for Standards and Technology” (<http://www.ndted.org>) .

Based on the ultrasonic system, calibration procedure and standards, the pulser/receiver apparatus, the digital oscilloscope, transducer and the couplants were adjusted in time and sensitive. The standards UNE-EN 12668-1, 2 and 3 show the procedures to the calibration in time (distance) or sensitive (amplitude) for ultrasonic equipments.

The ultrasonic systems were calibrated and adjusted periodically using different test reference block. The first reference sample was a stainless steel reference block DS (distance sensitivity) T-1018 as inverted rectangular block were the ultrasonic

### 3. Materials, Samples preparation and Methods

---

wavelength velocity is well known for each dimension. The steel properties show high velocity values and lower attenuation than the cement based materials.

The second reference block is a low weight polyethylene LWPE (plastic) with 65 us of travel time. Using this second probe, time calibration is observed in poor property value material.

It is difficult to get an equivalent acoustic performance reference sample for the ultrasonic concrete testing, so that it is calibrated using both samples, one with better propagation (high velocity, low attenuation) and other with low propagation (at least on velocities). Figure 3-9 shows the used reference blocks used for Calibration

The Vernier filter is used on attenuation coefficient measures for the transference loss between non-rough surfaces (as Calibration samples) and the roughness surface (as experimental samples).

The Calibration procedures were performed daily or in every transducer change to assure the correct determination of time/depth measuring and amplitude of ultrasonic register on the different samples.



**Figure 3-9** Reference blocks used for the equipment calibration

### 3. Materials, Samples preparation and Methods

---

#### 3.2.8.2. Pulse-echo method

Tests were conducted using a setup that consisted on an ultrasonic transducer, a pulser-receiver, and a digital oscilloscope. 1 and 3.5MHz centre frequency broadband transducers were used in the tests (see Figure 3-11). A high-gain, low-noise broadband (10 MHz) pulser-receiver with a signal repetition rate of 50 Hz is used to excite the transducer and send waves to the test material and also to receive the reflections from the test material.

The digital oscilloscope was used to view the waveforms and also to obtain a digital record of the waveforms for further processing (see Figure 3-10). The tests were conducted using the following settings on the pulser-receiver (see Table 3-10 for mortar samples and Table 3-11 for concrete cores).

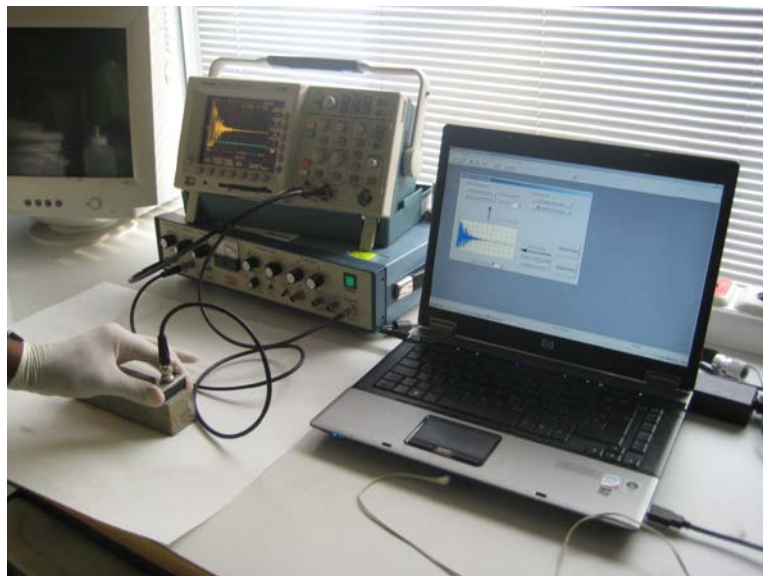


**Figure 3-10** Procedure of ultrasonic testing

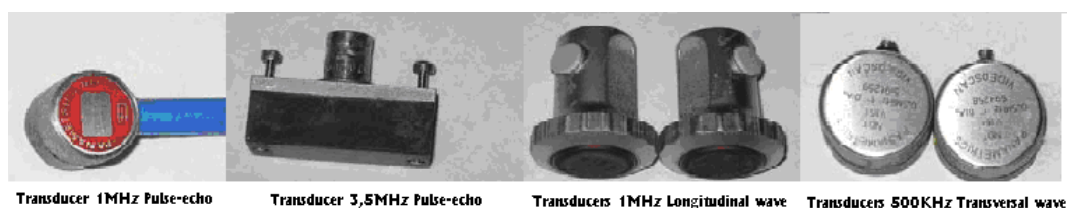


**Figure 3-11** Ultrasonic Transducers Used

### 3. Materials, Samples preparation and Methods

The settings were kept constant throughout the test program to ensure consistency of the measured waveforms. Although three samples were kept constant during all research time to observe the change of ultrasonic parameters with precise manner.

**Table 3- 10** Equipment setting/configuration for pulse-echo test (mortar)

Parameter	Settings for mortar	
	1MHz	3.5MHz
Repetition rate (Hz)	50	50
Damping ( $\Omega$ )	500	500
Pulse height	400	400
Attenuator left (dB)	0	0
Attenuator right (dB)	6	6
High pass filter (MHz)	0,3	0,3
Low pass filter (MHz)	3	5
Vernier (dB)*	0-1	0-1
Gain (dB)	40	40
Sampling rate (Msamples/s)	50	100
Phase	Normal (0°)	Normal (0°)

\*depending on the calibration

**Table 3- 11** Equipment setting for pulse-echo test (concrete)

Parameter	Settings	
	1MHz	3.5MHz
Repetition rate (Hz)	50	50
Damping ( $\Omega$ )	500	500
Pulse height	200	400
Attenuator left (dB)	0,0	0,0
Attenuator right (dB)	10	1
High pass filter (MHz)	0,3	0,3
Low pass filter (MHz)	3	5
Vernier (dB)*	0-1	0-1
Gain (dB)	50	40
Sampling rate (Msamples/s)	50	100
Phase	Normal (0°)	Normal (0°)

\*depending on the calibration



### 3. Materials, Samples preparation and Methods

A test is conducted by placing the transducer on the side of the specimen (each specimen has 4 sides and each side has 6 points of measurements), and then sending and receiving waves at the measurement location. The transducer is used for both sending and receiving the waves. A couplant is placed between the transducer and specimen to ensure full transmission of the waves into the test specimen and it has not produce attack or partial solution of the sample. For each specimen we obtained the average of 24 measurements (see Figure 3-12).

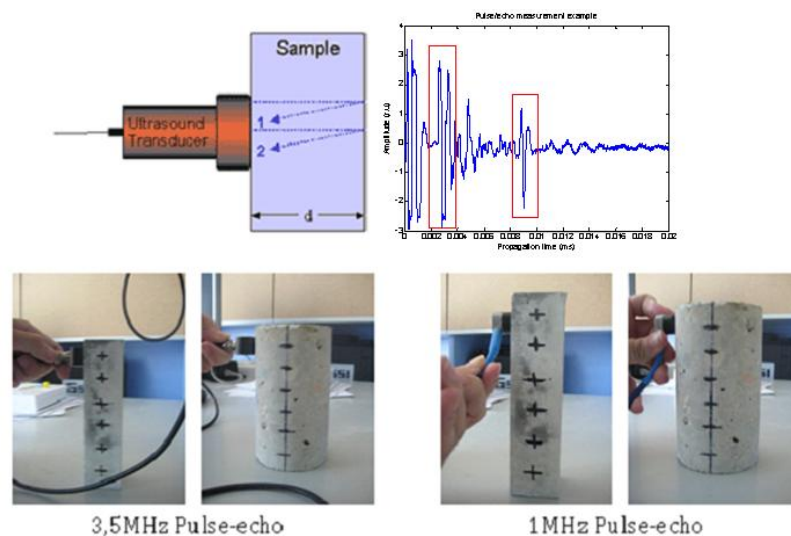


**Figure 3-12** Procedure of the measurement by Pulse-echo method

The medium and high ultrasonic frequency pulse interacts with the cement-based microstructure strongly than low frequency, because  $\lambda > \sim D$  (effective diameter of scatters) in the Rayleigh zone or region.

High scatters are the coarse grain that can show until 4 cm and they reveals high attenuation process for the most common ultrasonic frequencies. Regarding the typical frequencies for concrete ultrasonic testing a 20 kHz in a standard concrete has 20 cm of wavelength that is at least 5 times greater than the maximum scatter (coarse grain).

The sand grains could play the role of medium scatters that most of them they are between 0.5-2 mm. Lower than this diameter fine and cement pastes reveal the same attenuation process but sand can be seen as a grains embedded on the cement paste matrix. In the experimental work, lower frequencies are the 500 kHz with an average

### 3. Materials, Samples preparation and Methods

---

wavelength of 8 mm. This frequency is used to measure global parameters both in precast and mortar. Higher frequencies as 3.5 MHz implies near 1 mm of wavelength so that it is more related with the capilar porosity effects and the microstructure changes.

Since from the pulse/echo signals, the backscattering noise is composed by the multiple reflections of the ultrasonic pulse in the scatters of the microstructure, considering this scatters the different interfaces, grains, gravels and the different types of cemented phases, hydrated cement components and porosities (air voids, capillary porous and gel porosity). The interaction between the ultrasonic pulse and the complex microstructure cause multiple scattering or dispersion which can be described as a stochastic process.

The backscattering noise is an ultrasonic signal that overlaps the multiple reflections of the microstructure and the strong dispersion components could be analyzed in time and frequency signal domain.

The ultrasonic backscattering noise would reflect the possible changes in the cement-based material microstructure during the degradation process, so that it has been applied the time-frequency analysis that described in the thesis work of (Fuente, 2004).

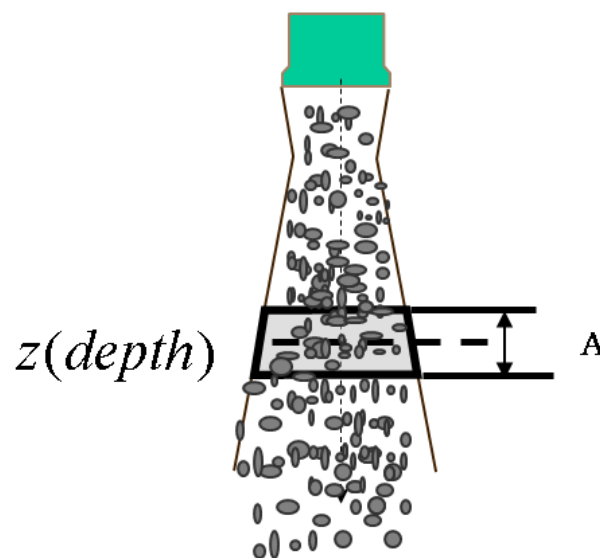


Figure 3-13 Scheme of inspection for pulse/echo.

In the abovementioned thesis work, it is reveal the complex mathematical description of the ultrasonic backscattering noise due to the composite effect of scattering process. Under some hypothesis, it is possible to describe a depth-frequency function  $DFF(\omega, z)$



### 3. Materials, Samples preparation and Methods

---

of some slabs or portion in depths with a depth  $A$  where multiple dispersion of the pulse are neglected, The attenuation coefficient  $\alpha(\omega, z)$  can be described in terms of  $DFE(\omega, z)$  and the novel approach is found how could be used the time-frequency distribution  $DTF(\omega, z)$  to estimate the  $DFE(\omega, z)$  and subsequently the  $\alpha(\omega, z)$ . This leads us to practical methods for estimation of depth- and frequency-dependent attenuation. Finally, the spectrograms was selected as the  $DTF(\omega, z)$  to estimate the attenuation in the  $f$  and  $z$  plane. The spectrograms were calculated with Short Time Fourier Transform (STFT) square modulus with an overlapping that assure stationary of the signal in the small slab with  $A$  thickness (see Figure 3-13). The attenuation coefficient  $\alpha(\omega, z)$  is calculated as follow in eq. 4.

$$\alpha_z(\omega) = \frac{\log\left(|STFT(\omega, 0)|^2\right) - \log\left(|STFT(\omega, z)|^2\right)}{4z} \quad (4)$$

Since from the pulse/echo signals, it has been applied the time-frequency analysis that described in the thesis work of (Fuente, 2004). However, it could be summarized in the following scheme (see Figure 3-14).

A battery of pulse/echo signals obtained by spatial diversity, i.e. several measurements, in the same material surface should be performed. After that, for each ultrasonic backscattering noise register, is calculated its time-frequency distribution using spectrogram algorithms, and using  $3 \mu s$  time *hanning* window and 50% of overlapping.

### 3. Materials, Samples preparation and Methods

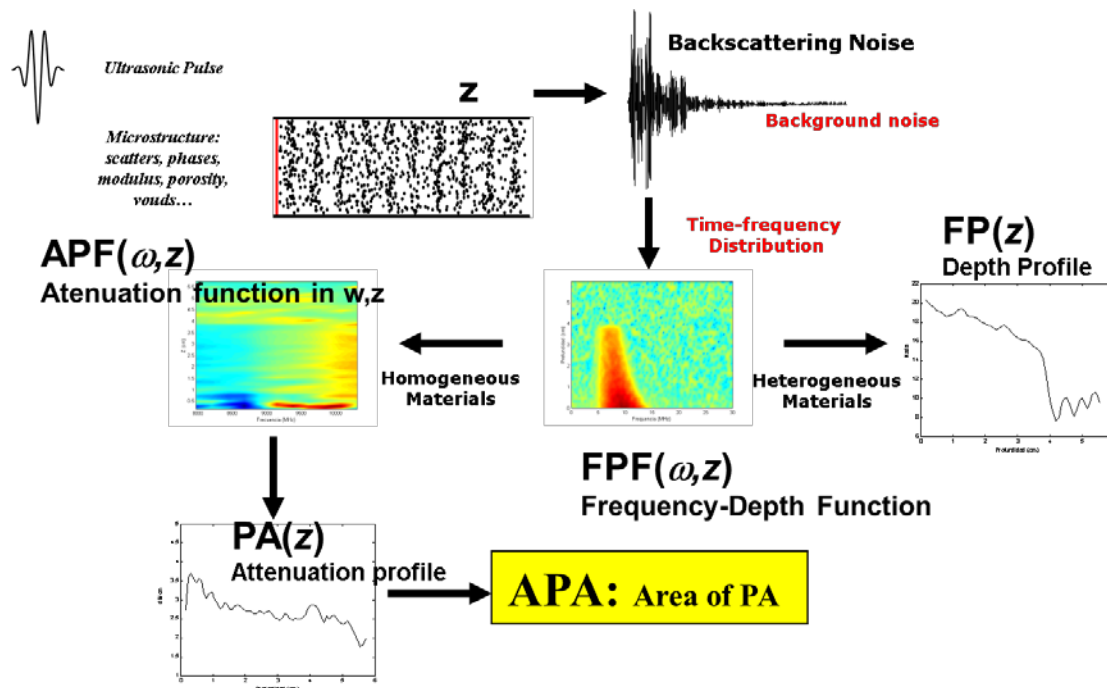


**Figure 3-14** Scheme of time-frequency analysis procedure

All the spectrograms (DTF), usually 10, should be averaged considering the same bandwidth and  $z_{min}$  and  $z_{max}$ , of course. Since from the averaged DTF, it is chosen the best  $z_0$  and calculating the APF (Attenuation function in terms of depth and bandwidth). After that, the APF shows the diffraction and scattering effects of the microstructure regarding the energy at different bands and depths. It is possible to characterize it, using frequency and depth profile (FP & PA). For the common cement based materials and the used frequencies in the testing campaign, it is suitable using depth profile averaged in the specific band of the nominal emitter (about 40% for low frequencies and 20% for higher frequencies) to see which is the power of pulse penetration for each microstructure. The 20% up to the nominal emitter transducer is sensible to diffraction effects and 40% of lower band is sensible the scattering and the subsequent low-pass filter effect of solid and granular solids.

#### 3.2.8.3. Through-Transmission

Ultrasonic through-transmission technique was used in this research to evaluate the velocity of longitudinal and transversal waves of mortar and precast concrete specimens. The tests were conducted using the following settings on Table 3-12 for mortar samples and Table 3-13 for concrete cores). Tests were conducted using a setup that consisted of 2 transducers, a pulser- receiver, and a digital oscilloscope. Two 1MHz-center frequency transducers were used for measurement of longitudinal wave velocities and two 500KHz-center frequency transducers were used for measurement of transversal wave velocities. The pulser-receiver and the oscilloscope were the same devices that were used in the pulse-echo tests. The pulser-receiver has a high-voltage pulser and a high-gain receiver, which are appropriate for testing high attenuation materials.

**Table 3- 12** Equipment setting for through-transmission test (mortar)

Parameter	Settings for mortar	
	1MHz	500KHz
Repetition rate (Hz)	50	50
Damping ( $\Omega$ )	500	500
Pulse height	variable	variable
Attenuator left (dB)	0,0	0,0
Attenuator right (dB)	variable	variable
High pass filter (MHz)	0,3	0,3
Low pass filter (MHz)	3	3
Vernier (dB)*	0-1	0-1
Gain (dB)	10	30
Sampling rate (Msamples/s)	100	100
Phase	Normal (0°)	Normal (0°)

\*depending on the calibration

### 3. Materials, Samples preparation and Methods

**Table 3-13** Equipment setting for through-transmission test (concrete)

Parameter	Settings	
	1MHz	500KHz
Repetition rate (Hz)	50	50
Damping ( $\Omega$ )	500	200
Pulse height	variable	variable
Attenuator left (dB)	0,0	0,0
Attenuator right (dB)	9	9
High pass filter (MHz)	0,3	0,3
Low pass filter (MHz)	3	3
Vernier (dB)*	0-1	0-1
Gain (dB)	50	60
Sampling rate (Msamples/s)	100	100
Phase	Normal ( $0^\circ$ )	Normal ( $0^\circ$ )

\*depending on the calibration

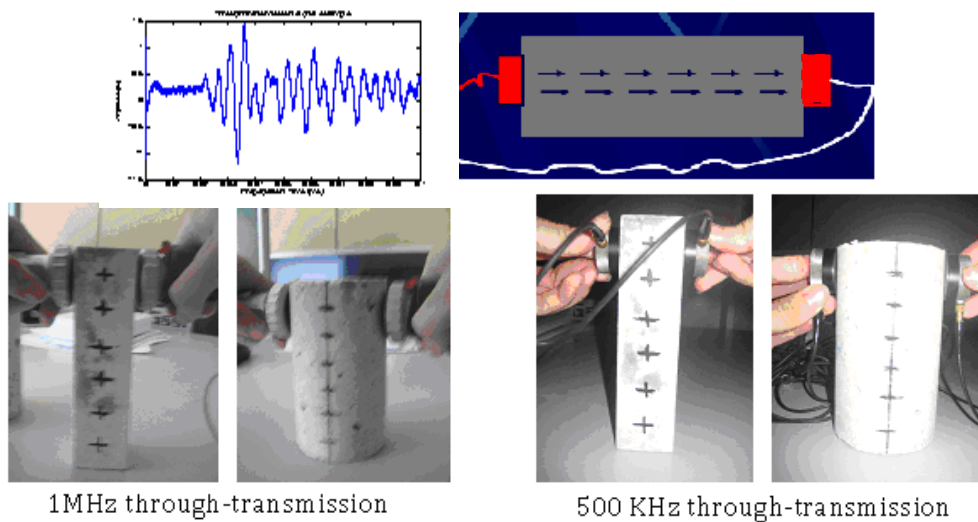


**Figure 3-15** Procedure of the measurement by through-transmission method.

A through-transmission test is conducted by placing one transducer on one surface of a test material and the second transducer on the opposite surface of the test material (see

### 3. Materials, Samples preparation and Methods

---

Figure 3-15). In this arrangement, one transducer is used to transmit waves and the other transducer is used to receive the transmitted waves. For each specimen we were obtained the average of 12 measurements.

#### *Velocity Estimation*

To estimate the ultrasonic velocity parameter, the method of double crossing zero is chosen, which was applied in a previous work of (Acebes, 2007). This method consists of taking the zero-crossing times of the signal, having offset subtracted conveniently possible. The time was taken to spread  $t_1$  and crossings of the first zero crossing and  $t_2$  as the second zero crossing as can be seen in Figure 3-16 which illustrate an example for P and S-wave signal. The equations 5 and 6 are used to calculate P and S-wave velocities respectively.

$$V_P = \frac{L}{t_{corr}} \quad (5) \quad t_{corr} = 2.t_2 - t_1 \quad V_S = \frac{L}{t_0} \quad (6)$$

On the other hand, it seeks to eliminate the low-pass filter effect of the material present in very highly dispersive and highly attenuating. On the other hand, the first pulse usually, is received with a slow beat or pulse or less frequently. This pulse has a slow rise in the waveform and this is where the threshold estimation methods could fail in many cases including the cementitious materials, while in the zero crossing, the slope is greater, so that the propagation time estimates are less biased and variance.

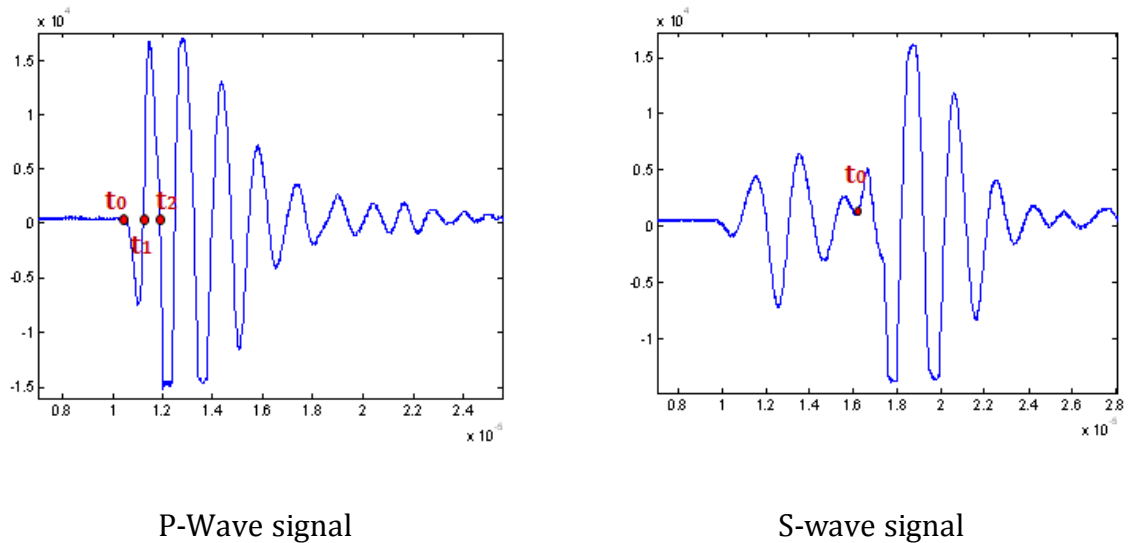


**Figure 3-16** An Example for P and S-wave Signals obtained by ultrasonic through-transmission mode

#### 3.2.8.4. Ultrasonic Image

The technique has been carried out by the Materials characterization by non-destructive testing Group of the “CAEND: Centro de Acústica Aplicada y Evaluación No Destructiva”, Research Centre of the “Consejo Superior de Investigaciones Científicas (CSIC)”. The systems procedure and results were produced by this group and it is used only as research purposes in the framework of the coordinated project EDHOREND as number reference of BIA-2006-15188-C03. This research involves activities on the BIA-2006-15188-C03-01 that have been coordinated by CAEND- (CSIC-UPM) and project BIA-2006-15188-C03-03 coordinated by AIDICO and where the FPI grant BES-2007-14314 is assigned.

This technique allows evaluating the properties distribution that can be evaluated by the ultrasonic velocity. It is known that aggregates can be lead to the increasing of the velocity of ultrasonic waves due to the high velocity which have sand and gravels. On the other hand, it can be said that the cement paste has a lower velocity, so that this method can inform of the effect of sand decay. Also, it could inform us the presence of voids. (Molero et al, 2011)

### 3. Materials, Samples preparation and Methods

The ultrasonic image is not a tomography technique, because is not a method that interpolates results from an ultrasonic path to other that is not propagated the ultrasonic pulse. The technique has been applied to prismatic specimens of mortar and cylindrical test of concrete.

The mortar specimens have been tested along the transversal dimension (40 mm. of length) while that concrete test have been tested along the radial & axial dimension. It is important to note that the cylindrical tests have been covered by an acrylic resin that prevents degradation in the longitudinal size, so that for the cylindrical test only is expected radial degradation process.

For the automatic scanning it is used an ultrasonic pool from the CAEND facilities (see Figure 3-17). The water acts perfect coupling method between transducer and the specimens. The specimens should be partially or fully saturated. The system uses two aligned transducer with the same distance along the scanning operation. The procedure depends on the specimen type. The automated system can reach the 1 m/s maximum speed of scan and an accuracy of 0.2 mm in the header position.

Figure 3-18 presents an example of the obtained results, where radial and axial images have been present respectively. It is noted that attenuation and velocity mark reveal changes of each parameters that correspond to a microstructural changes

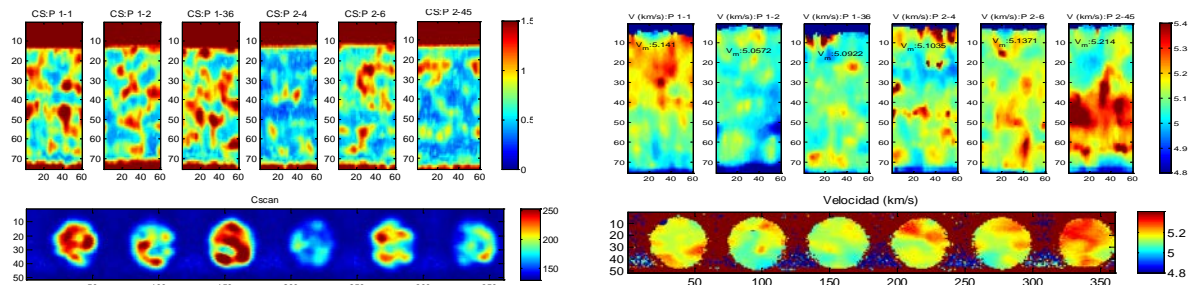
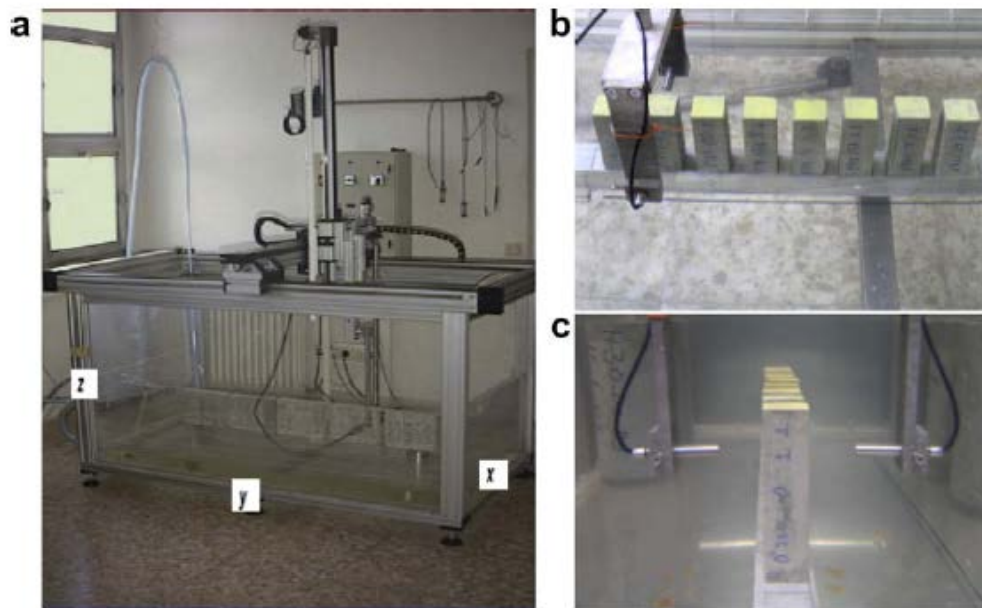


Figure 3-17 An example of ultrasonic image results



**Figure 3-18** Photos of (a) the automatic positioning system for x, y, z coordinates and the tank; (b) a sample row submerged into water; and (c) the transmission mode applied to the mortar samples (M. Molero et al, 2009).

#### 3.2.9. Scanning Electron Microscopy

A scanning electron microscope (SEM) equipped with energy dispersive analysis X-ray (EDS) testing is used on the samples to determine the chemical composition of the deposits within the microstructure and to help understanding and interpreting the results of destructive and non-destructive tests and the correlation between them.

The microstructural characterization was carried out with an electron microscope (SEM) model (HITACHI S-4800 II) and dispersive spectroscopy EDS, (see Figure 3-19). The images are obtained using the SEM equipment from the secondary electron generated by the following conditions:

- 10kV of voltage, 15 $\mu$ A current
- Working distance 15mm



#### **Sample Preparation**

To study the microstructure of the attacked concrete and mortar samples, A slice was cut from the exterior vertex (attacked area by sulfate) perpendicular to the longitudinal axis of the cylindrical concrete or longitudinal axis of mortar specimens, to inside of the specimen (not attacked area) by using a diamond blade saw. Samples were placed in acetone to stop the hydration process, thus, we can correlate the images obtained with SEM and microanalysis and EDX, with resistance values obtained in the mechanical characterization of the same ages. The portions obtained were introduced in small cylindrical mould and subsequently filled with resin (in order to not have influence the composition of the attacked concrete) and making vacuum for 15 to 20min, after this time polish and coat it. After obtaining the resin pellets are polished surfaces to study, and covered with graphite. Graphite is used as a bridge between the support driver electrons and the sample. Figure 3-20 shows a sample prepared for analysis (SEM), it can be seen that, several pointes were tested from the attacked surface toward the inside of the sample (non-attcked), with the objective of determination approximately the depth of ettringite formation, on the other hand, for mortar samples only w/c ratio 0.525 is examined at 200 and 450 days and for concrete both of types are tested at 220 and 470 days of immersion.

### 3. Materials, Samples preparation and Methods

---



**Figure 3-19** Equipment of scanning electron microscopy at AIDICO facilities.

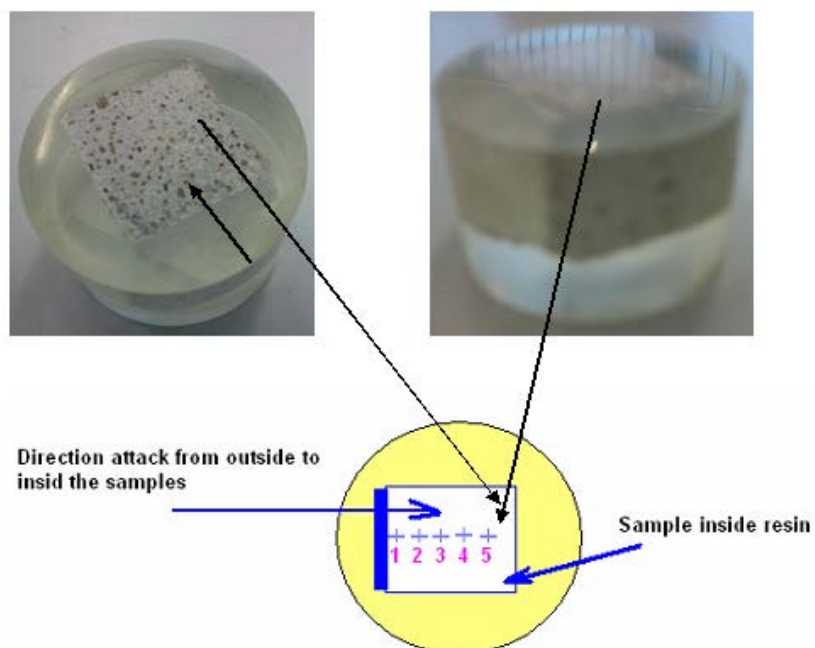


**Figure 3-20** Examination points of SEM Sample

#### 3.2.10. Mercury Intrusion Porosimetry

Mercury Intrusion Porosimetry (MIP) tests were conducted using autopore IV 9520 Porosimeter model (see Figure 3-21) to characterize a material's porosity by applying various levels of pressure to a sample immersed in mercury. The model used is 60.000 psia (414MPa) mercury porosimeter covering the pore diameter range from approximately 360 to 0.003  $\mu\text{m}$ . This model has four built-in low pressure ports and two high-pressure chambers.

Mercury intrusion porosimetry is based on the premise that a non-wetting liquid (one having a contact angle greater than  $90^\circ$ ) will only intrude capillaries under pressure. The relationship between the pressure and capillary diameter is described by Washburn eq. (7);

$$P = \frac{-4\gamma \cos \theta}{d} \quad (7)$$

Where;

$\gamma$  = the surface energy of the liquid

$\theta$  = the contact angle

$d$  = the pore diameter.

The procedure for determining the distribution and volume of pores in the concrete was as follows:

- The samples used were taken from specimens kept in a camera, curing at a temperature of 20 degree and a relative humidity of 95% during 28 days. The test was performed for concrete and mortars immersed in the aggressive solutions (for all solutions were realized in our study) at ages 90, 200, 340 and 450 days to study the variation of distribution and pore volume.
- Obtaining the sample followed by a process which removes a concrete and mortar fragment from the outside and inside of the cylinder 5 cm from the ends. By using a cutting plier coarse aggregate was extracted as possible and was

### 3. Materials, Samples preparation and Methods

---

separated by air pressure to remove the remains dust and fine aggregate surface which emerges from the die.

- These samples were kept in an oven dry at a temperature of 40 degree until they had a constant weight, with a precision weighing 0.01g.
- The samples were degassed by a vacuum pump 40kPa for 40 minutes before the test.
- The mercury intrusion was gradual and stabilization time for each condition of pressure was 10 seconds, the angle of contact used for the numerical calculations was 130 degrees, in both filling and emptying of the pores.

The mortar and concrete samples were tested, but only it is presented the results of mortar samples. The results of concrete are affected by the aggregate in the samples; it was difficult to remove it from the samples, due to the low w/c ratio and the high compact level using mechanical vibration.

The characterization dates (compressional, flexural and MIP or open porosity) for sulfate degradation experiences were 90, 200, 340 and 450 days from the initial degradation, after the 28 days of curing process. The degraded and control samples were tested

The nondestructive evaluation (TT, PE, UTI) was performed at the same dates. The SEM tests have been performed for specific times of 220 and 470 days of exposure.

For the ammonium nitrate degradation the steps or dates of degradation changes from mortar respect the precast specimens. Due to the high ammonium nitrate aggressive behavior, the degradation rate is different in mortar with higher porosity than the precast.

The characterization dates for mortars were 20, 35, 50 and 66 days and 49, 96, 190 and 290 immersion days for concrete specimens.



**Figure 3-21** The equipment used for MIP test, autopore IV 9520 Porosimeter model.



# CHAPTER 4

**Results and Discussion the Degradation  
process by Sodium Sulfate**

---





## 4 Results and Discussion the Degradation process by Sodium Sulfate

In this chapter, the results and discussion of mortar samples and precast concrete cores degraded by sodium sulfate solution are detailed and explained. The results of destructive and non-destructive tests are also presented and finally the relationship between these parameters is discussed.

### 4.1. Analysis and Discussion the Results of Mortar

#### 4.1.1. Visual Examination

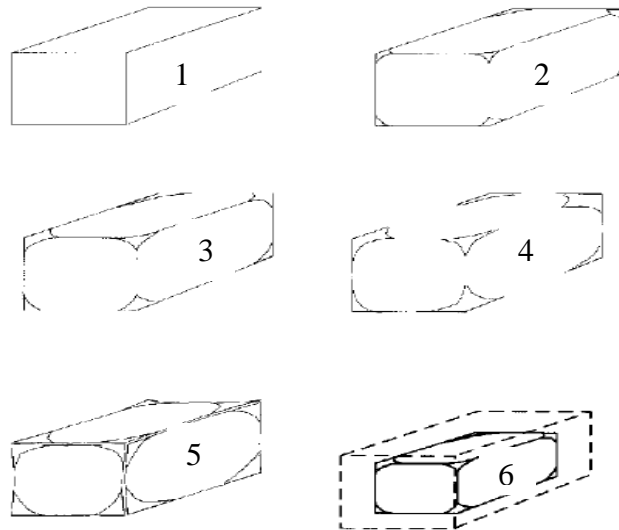
A thorough visual examination is carried out every test period to evaluate the visible signs of softening, cracking and spalling in the mortar specimens exposed to sulfate attack. Based on (Al-Amoudi, 1992) work, the ratings to evaluate visually the degree of the deterioration in tested mortar specimens are shown Figure 4-1. The visual ratings are divided into six stages.

Figure 4-2 and Figure 4-3 show examples of damage of mortar samples subjected to sulfate attack after 340 and 450 days of immersion, respectively. It is observed that the initial deterioration invariably started from the corners to inside the mortar samples. For high w/c ratios 0.525 and 0.45, after 450 days of immersion, a high deterioration stage (approximately between stages 5 and 6) is observed, for w/c ratio 0.375, the deterioration was approximately between stage 3 and stage 4, while for w/c ratio 0.30, the deterioration was not observed.

The top edges of the specimens which progressed along the sides to bottom edges, with an increase in the time of exposure, wider cracking at the edges and finally spalling off the surface skin at the sides is the predominant feature of the failure. After prolonged exposure, the side surfaces spalled off the core leading to the weakening and delamination of the top and bottom surfaces as well. Eventually, the inner core of the specimen was exposed due to this all round delamination of the surface layers. It is very

#### 4. Results and discussion the Degradation Process by Sodium Sulfate Solution

clear that the rate of degradation increases with increasing w/c ratio, thus, the water-cement ratio must be as low as possible to resist sulfate attack.



**Figure 4-1** Visual ratings of deterioration due to sulfate attack, Al-Amoudi, 1992

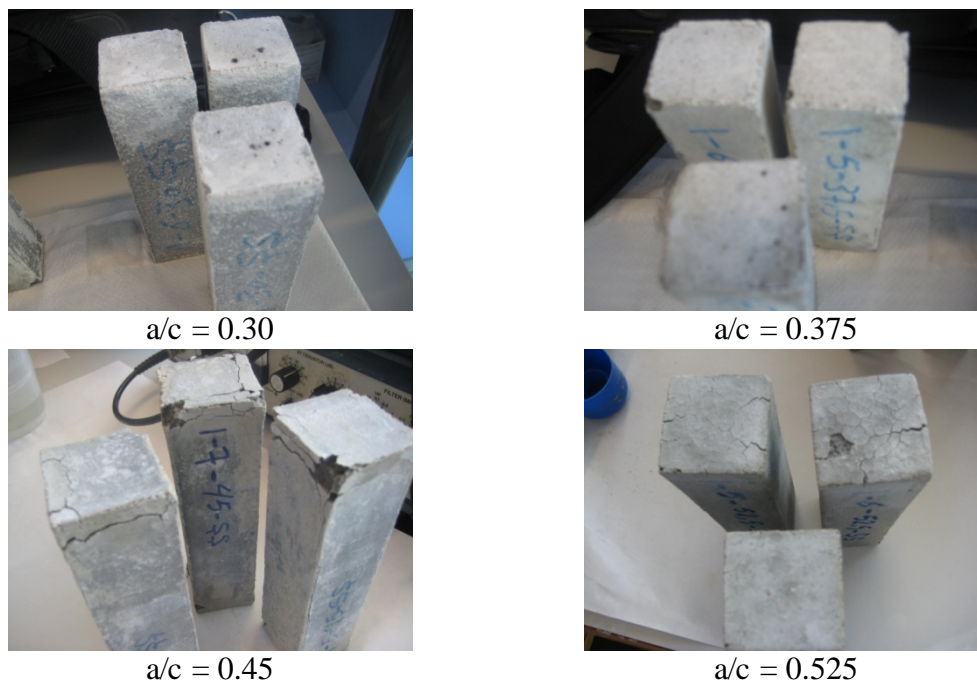


**Figure 4-2** Visual examinations, 340 days of degradation by solution of sodium sulfate

## 4. Results and discussion the Degradation Process by Sodium Sulfate Solution

---

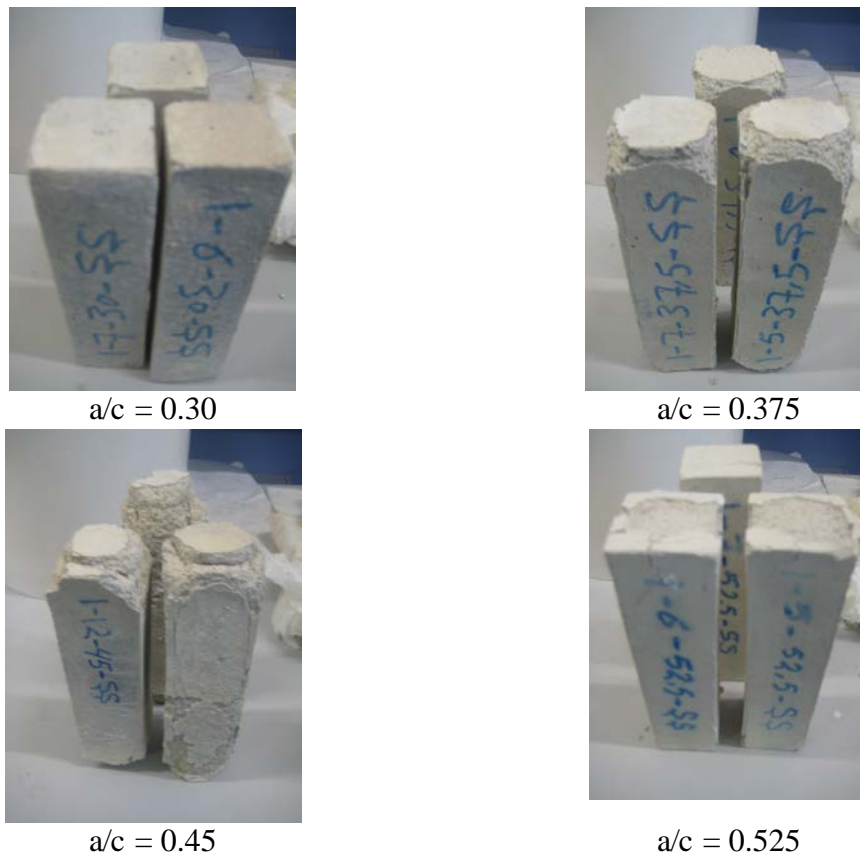


**Figure 4-3** Visual examinations, 450 days of degradation by solution of sodium sulfate

### 4.1.2. Scanning Electron Microscopy (SEM)

In this study, it is presented only the result of water-cement ratio 0.525 as an example to follow the changing in the microstructure of mortar samples. The micrograph and images for mortar samples immersed in sodium sulfate solution for 200 and 450 days are presented. As mentioned in Chapter3 (experimental method for SEM test), the sample was examined in several points from outside surface to inside the sample to see the degradation depth due to the penetration of sulfate ions into the mortar sample.

Figure 4-4 illustrates the results of SEM examination and EDS analysis for mortar sample immersed in sodium sulfate solution for 200days, the figure illustrates the results of points fall at distances range between (6.123mm and 9.783mm). It can be seen in the figure the micro-cracks produced inside the samples by the effect of the ettringite formation, due to the ingress of sulfate ions from the storage solution. The

#### 4. Results and discussion the Degradation Process by Sodium Sulfate Solution

related EDS spectrum indicates the relative Al, S and Ca peak intensities expected for ettringite.

By maintaining the samples immersed in sodium sulfate solution until 450 days, a point falls approximately at distance of 18.904mm from the attacked surface was studied, it can be seen that, ettringite crystals are participated into the air voids and cracks within the microstructure of the mortar samples. Figure 4-5 shows the SEM micrograph and EDS analysis of ettringite crystals forming at air voids and cracks. The EDS analysis revealed ettringite having a chemical composition of; Al= 3.45%wt, S= 6.75%wt, and Ca= 22.43%wt, as shown in Table 4-1

From the presented results of SEM test, it can be seen that, for w/c ratio 0.525, the sulfate ions were penetrated the samples approximately to 19mm from the surface, the dimensions of the samples are 40 ×40 ×160mm which means that after 450 days of immersion, ettringite was formed in whole the samples (for w/c 0.525). Thus, it is expected that for the other w/c ratios, the rate of penetration of sulfate ions and ettringite formation is decreasing as w/c ratio decreases.

**Table 4- 1** EDSanalysis for a simple degraded by 10% of sodium sulfate solution for 450 days

Element	Net un.	C norm.	C Atom.	C Compound	Comp.	C norm.	Comp.	C Error
	[wt. %]	[wt. %]	[at. %]		[wt. %]	[wt. %]	[wt. %]	
Carbon	47.00	37.25	51.05		37.25	47.00	14.9	
Oxygen	44.43	35.21	36.23		35.21	44.43	11.0	
Sodium	0.37	0.30	0.21		0.30	0.37	0.1	
Magnesium	0.17	0.14	0.09		0.14	0.17	0.1	
Aluminium	<b>3.45</b>	2.73	1.67		2.73	<b>3.45</b>	0.4	
Silicon	1.33	1.06	0.62		1.06	1.33	0.2	
Sulfur	<b>6.75</b>	5.35	2.75		5.35	<b>6.75</b>	0.5	
Chlorine	0.24	0.19	0.09		0.19	0.24	0.1	
Calcium	<b>22.43</b>	17.78	7.30		17.78	<b>22.43</b>	1.4	
Total:				126.18	100.00	100.00		

#### 4. Results and discussion the Degradation Process by Sodium Sulfate Solution

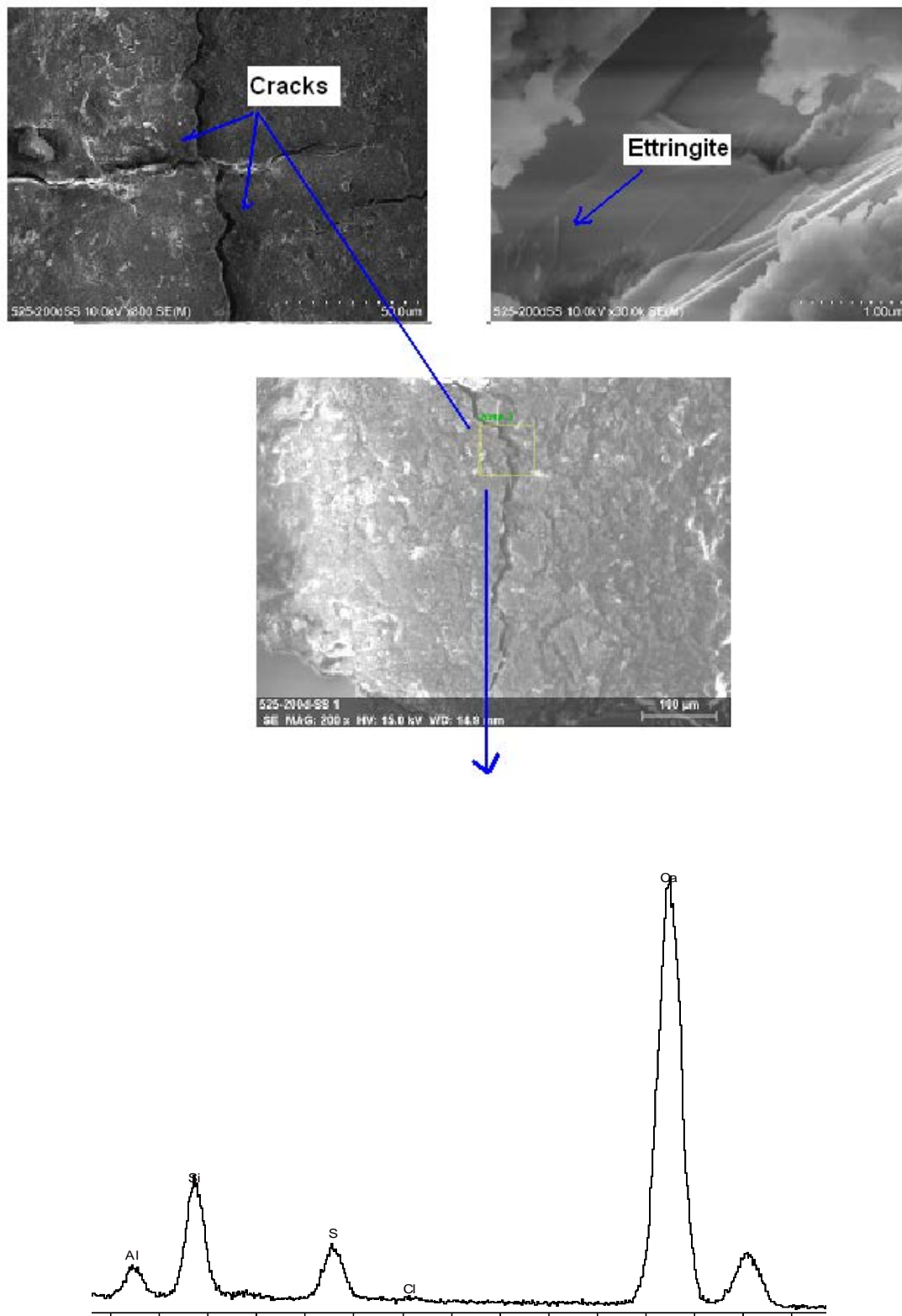


**Figure 4-4** SEM and EDS analysis of Mortar samples immersed in sodium sulfate solution for a 200 days, showing the micro cracks produced by the effect of ettringite formation

#### 4. Results and discussion the Degradation Process by Sodium Sulfate Solution

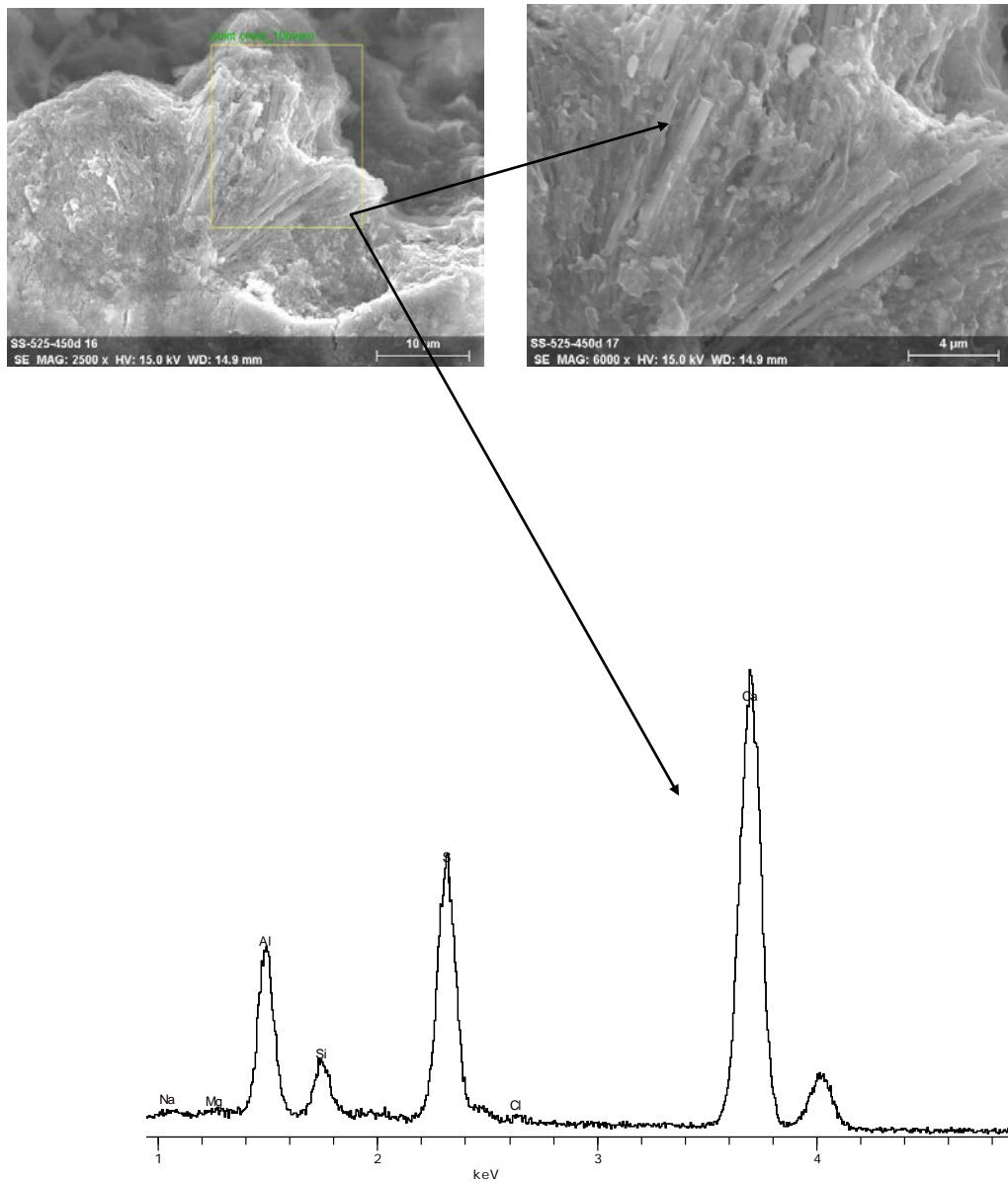


**Figure 4-5** SEM and EDS analysis of Mortar samples immersed in sodium sulfate solution for a 450 days, showing the micro cracks produced by the effect of ettringite formation for a point falls at distance of 18.904mm from the attacked surface.

### 4.1.3. Compressive and Flexural Strength

Figure 4-6 (A) and (B) illustrate the compressive and flexural strength for both mortar specimens exposed to sodium sulfate and control samples after 450 days of immersion. Figure 4-6 (A) shows that, the compressive strength of the two w/c ratios (0.525 and 0.45) were lower than that of control for all exposure period, while for w/c ratio (0.375), it is found that the compressive strength was increased up to 90 days of exposure after that it was decreased until the end of exposure time, for w/c ratio (0.30), it can be seen that the compressive strength is increased up to 200 days of immersion thereafter it was decreased until the end of exposure period. The same trend is observed for flexural strength as can be seen in Figure 4-6 (B).

In the case of w/c ratios 0.30 and 0.375, the increase in the strength of the specimens stored in sodium sulfate solution could be due to the formation of small volume of calcium sulpho-aluminates (ettringite) crystals which help to fill pores. With the increasing of immersion time, the volume of ettringite is increased inside the pores, until becoming higher than the pores volume (after 90 days for w/c=0.375 and after 200 days for w/c= 0.30). This produces micro-cracks due to the volume increasing of ettringite and results in decreasing the strength until the end of exposure time. In case of w/c ratios 0.525 and 0.45, the ettringite formation might take place and its volume is increased before 90 days of immersion, it can be seen that in Figure 4-6 (A and B), the compressive and flexural strength are decreased until the end of the immersion time, this could be due to the stresses produced by the increasing of ettringite volume. This was observed by SEM test as showed previously.

Figure 4-7 shows the compressive and flexural strength loss (CSL and FSL) of mortar samples immersed in 10% sulfate solution. The relative strength loss in the early stages of exposure indicates that the strength of the specimens exposed to sodium sulfate solution is greater than those cured in tap water for the same period. This has been previously reported (Al-Amoudi, 1998 and lee et al, 2005), and the negative values of CSL and FSL are attributed to the filling up of the pore space by the expansive products, identifying the mortar matrix in the early period of immersion, and prior to them being

#### 4. Results and discussion the Degradation Process by Sodium Sulfate Solution

subjected to high tensile strain. Figure 4-7 also confirms that the w/c ratio is a key factor in the strength loss of mortar samples exposed to sulfate attack. The strength loss increased as the w/c ratio increased.

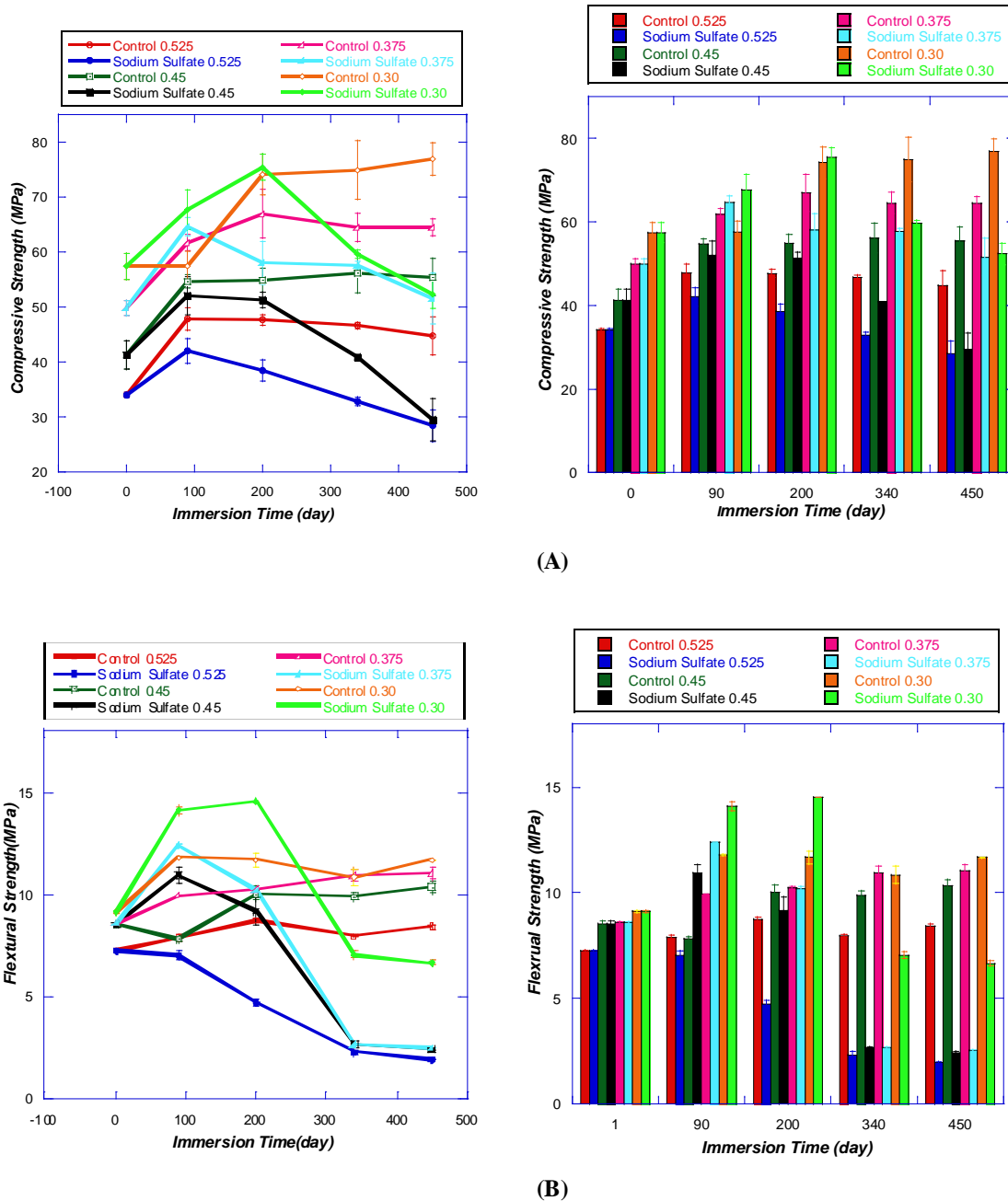


Figure 4-6 Compressive and flexural strength of mortar samples



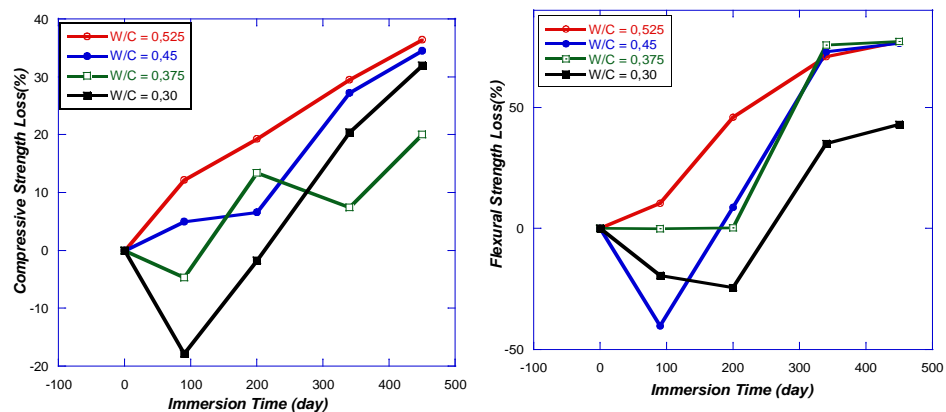


Figure 4-7 Compressive and flexural Strength loss of mortar samples

### 4.1.4. Open Porosity

Figure 4-8 shows the evolution of porosity of mortar samples immersed in sodium sulfate and tap water for 450 days of exposure time. It can be seen that for w/c ratio 0.525, the porosity of sodium sulfate samples is more than porosity of control during all exposure period. For w/c ratio 0.45, by comparing the porosity of sulfate samples with control samples, it can be seen that porosity decreased up to 90 days of immersion, thereafter, it was changed to be more than porosity of the control samples until the end of exposure time. For w/c ratio 0.375, it can be seen that porosity of samples degraded by sodium sulfate is less than porosity of control samples up to 200 days, after that it is changed to be more than the porosity of control samples until the end of exposure time. While for w/c ratio 0.30, it can be seen that the porosity of sulfate sample is lower than porosity of control samples during all experimental period.

As mentioned previously, due to sulfate ions penetration into the microstructure of mortar samples which led to formation of ettringite crystals that accumulated in pores of cement mortars, micro-cracks and cracks are caused, the rate of the produced cracks is related to both of w/c ratio and the increasing of immersion time. For example, as demonstrated previously for w/c ratio 0.525 by using SEM examination, it can be seen that the ettringite filled the pores and caused cracks production, this could be occurred at early age of immersion, but unfortunately the samples were tested at 200 days of

#### 4. Results and discussion the Degradation Process by Sodium Sulfate Solution

---

immersion in sodium sulfate solution. But it was found that the degradation due to the ingress of sulfate ions was clear. Thus, it is expected that the rate of degradation due to the ingress of sulfate ions is related to w/c ratio, and the presented results of open porosity confirmed this. As can be seen also in Figure 4-8, the changing of porosity for w/c ratio 0.45 for the degraded samples was after 90 days of immersion, and for w/c ratio 0.375 was after 200 days, while for w/c ratio 0.30 the porosity of the degraded samples remained lower than porosity of control until the end of exposure time.

The damage evolution may take place under the action of internal expansion force. Therefore, the porosity of concrete is composed of two parts, namely, initial porosity and volume fraction of damage. Hence the porosity of cementitious materials under sulfate attack can be expressed by the summation of initial porosity and volume fraction of damage (Song and Chen, 2011).

Thus, the initial damage of cementitious materials is related to the initial porosity, and the initial porosity increases with increasing of w/c ratio. As observed for the high w/c ratio 0.525, the initial porosity is increased at the initial stage of immersion, so it was easy for sulfate ions to penetrate mortar samples. When sulfate ions diffuse in pores of the cementitious materials, the chemical reaction between the hydration solution of cementitious materials and sulfate ions may take place. Therefore, ettringite crystals may nucleate and grow in pores; the internal expansion forces induced by ettringite crystals could lead to the micro-cracks evolution in mortar samples and enhance increasing of volume fraction of damage (Song and Chen, 2011).

For w/c ratios 0.45 and 0.375, the variation of porosity has two stages, in the first stage, the air voids are filled by ettringite crystals and this may lead to the decreasing of porosity after 90 days for w/c ratio 0.45 and after 200 days for w/c ratio 0.375. In the second stage, the ettringite crystals grow and touch to the boundary of the voids. It will produce an expansion force, and under the action of expansion force, the nucleation and growth of micro-cracks will also occur and lead to increasing the porosity in the second

#### 4. Results and discussion the Degradation Process by Sodium Sulfate Solution

stage (Chen et al., 2008). For w/c ratio 0.30, it can be seen that porosity until the end of exposure time is related to the first stage.

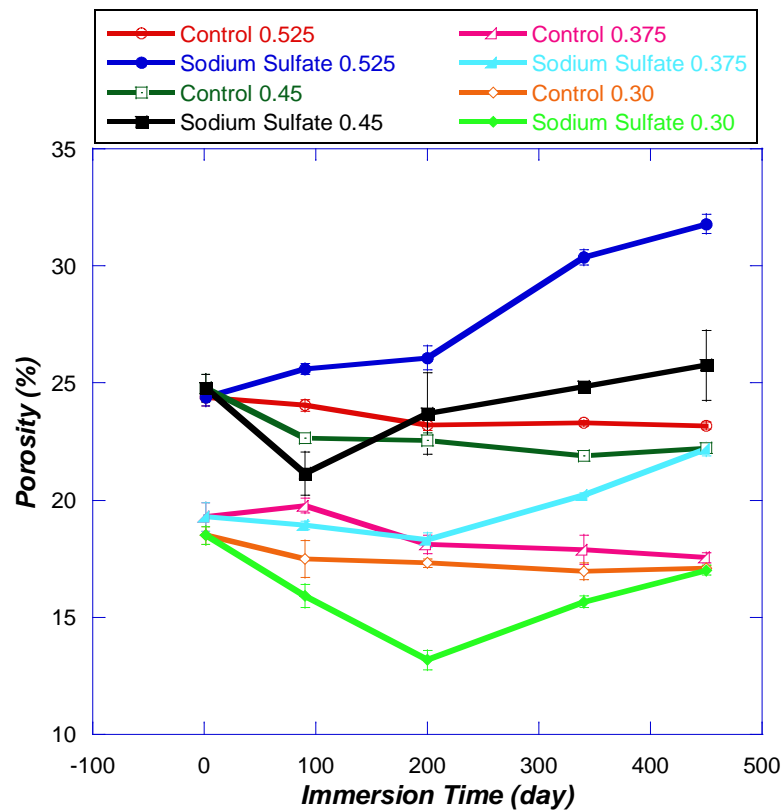


Figure 4-8 Porosity of mortar submerged in 10% sodium sulfate and control

#### 4.1.5. Mercury Intrusion Porosimetry (MIP)

The results of mercury intrusion porosimetry (MIP) are illustrated in the figures from 4-9 to 4-24, for both control and samples degraded by sodium sulfate. Cumulative pore size distribution and differential volume of mercury in a logarithm distribution are plotted against the pore diameter for w/c ratios 0.30, 0.375, 0.45 and 0.525, and for exposure time 1, 90, 200, 340 and 450 days.

#### 4. Results and discussion the Degradation Process by Sodium Sulfate Solution

---

For w/c ratio 0.30 cumulative pore size distribution curves of control and sulfate samples respectively are shown in Figure 4-10 and Figure 4-12, it can be seen that, the cumulative pore size decreases up to 200 days then, increases again until the end of exposure time, such control as sulfate samples, but in the case of sulfate samples at 450 days it was observed an increment in pore size than that of control, On the other hand, Figure 4-9 and Figure 4-11 show that the pores are concentrated between 0.03-0.156  $\mu\text{m}$  for control samples, and between 0.01-1 $\mu\text{m}$  for sulfate samples, it can be seen that, samples degraded by sulfate showed a shift toward large pore size at 450 day of immersion.

For w/c ratio 0.375 cumulative pore size distribution curves of control and sulfate samples respectively are shown in Figure 4-14 and Figure 4-16, it is observed that the sulfate samples had the same trend as w/c 0.30, the pore size diameter is decreased up to 200 days of exposure, then it is increased until the end of immersion time. In Figure 4-13 and Figure 4-15, it is observed that the critical peaks are between 0.030-0.150  $\mu\text{m}$  for control samples and between 0.01-2  $\mu\text{m}$  for sulfate samples, findings showed a clear shift toward large pore diameter, and the shift increases by increasing w/c ratio.

From Figure 4-17 to Figure 4-24, the results of (MIP) for water-cement ratios 0.45 and 0.525 are illustrated respectively. It can be observed that, the pore diameter increases due to the increasing of w/c ratio. From pore size distribution differential curves in Figure 4-17 and Figure 4-19, the critical peaks are between 0.040-0.182  $\mu\text{m}$  for control samples and for sulfate samples are between 0.01-5.6  $\mu\text{m}$  for w/c ratio 0.45. For w/c ratio 0.525, as can be seen in Figure 4-21 and Figure 4-23, the peaks are between 0.025-0.180  $\mu\text{m}$  for control samples and for sulfate samples the peaks are between 0.01-9.26  $\mu\text{m}$ . From the (MIP) test, it is seen how the pore size changes by the effect of sodium sulfate ions penetration into the mortar samples and how the changes in pore size are affected by the w/c ratio.

#### 4. Results and discussion the Degradation Process by Sodium Sulfate Solution

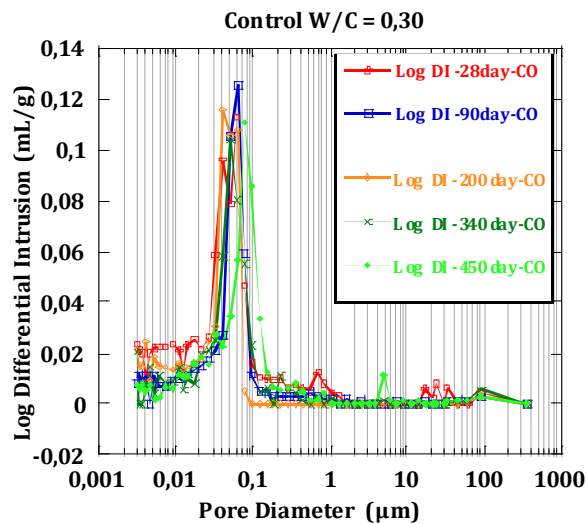


**Figure 4-9** Log differential intrusion w/c = 0.30 control

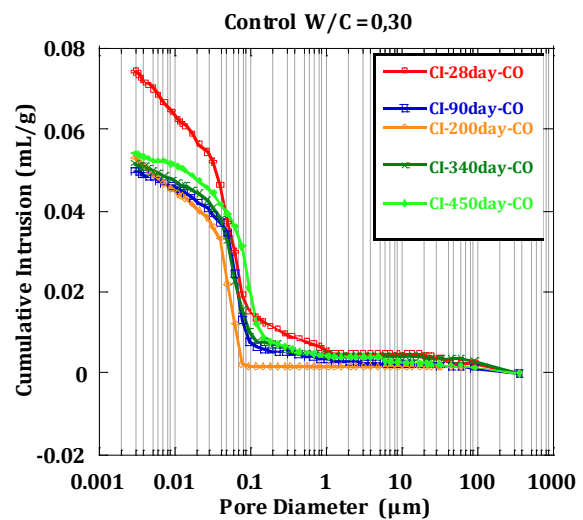


**Figure 4-10** Cumulative pore size distribution w/c=0.30 control

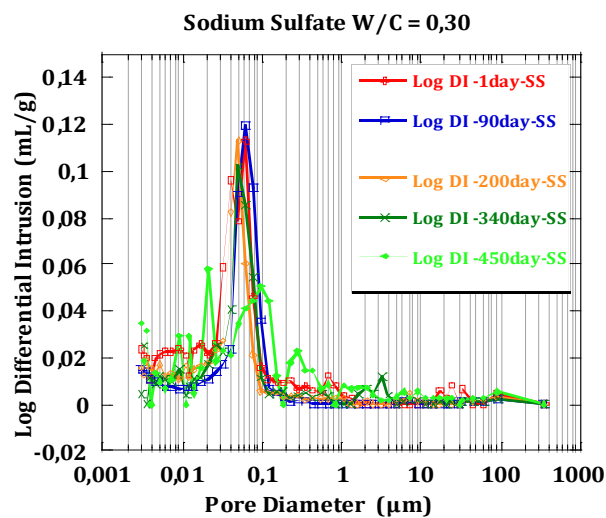


**Figure 4-11** Log differential intrusion w/c = 0.30 sodium sulfate

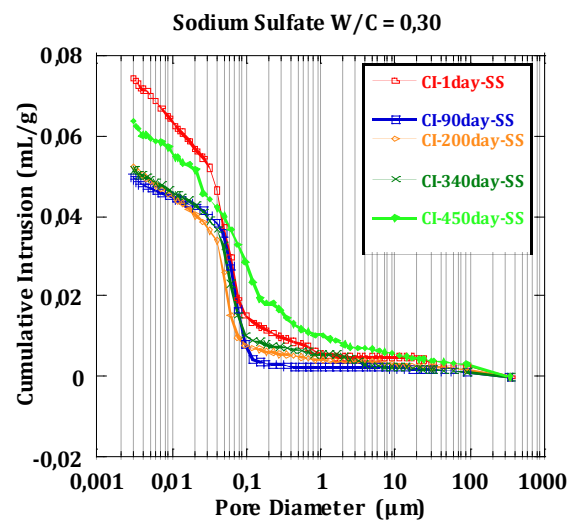


**Figure 4-12** Cumulative pore size distribution w/c=0.30 sodium sulfate

#### 4. Results and discussion the Degradation Process by Sodium Sulfate Solution

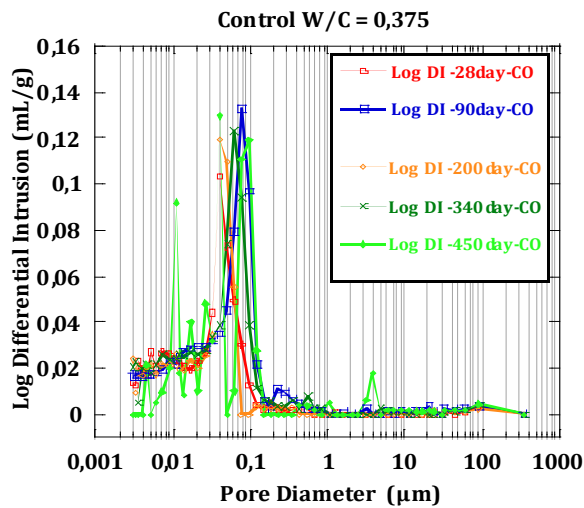


Figure 4-13 Log differential intrusion  $w/c = 0.375$  control

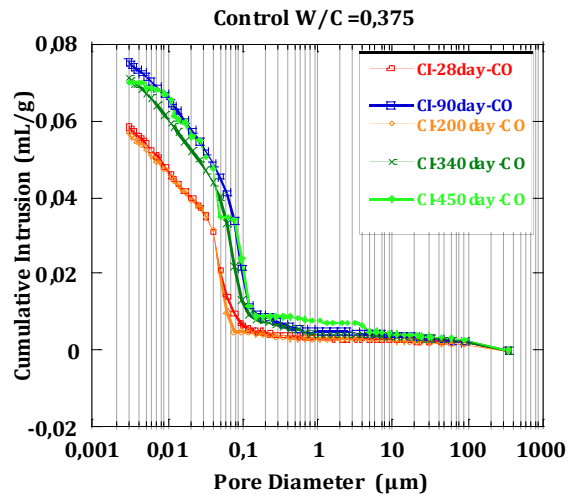


Figure 4-14 Cumulative pore size distribution  $w/c=0.375$  control

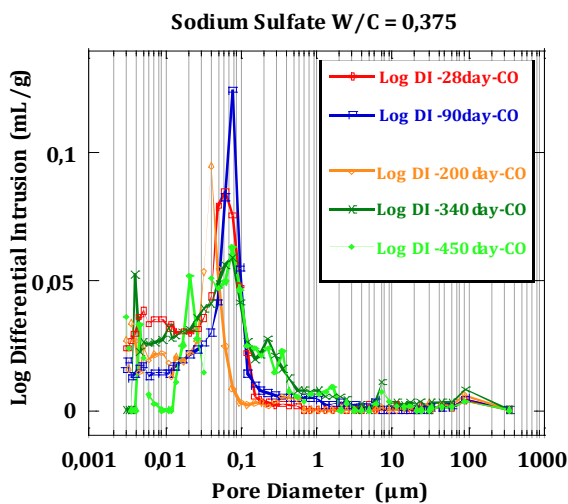


Figure 4-15 Log differential intrusion  $w/c = 0.375$  sodium sulfate

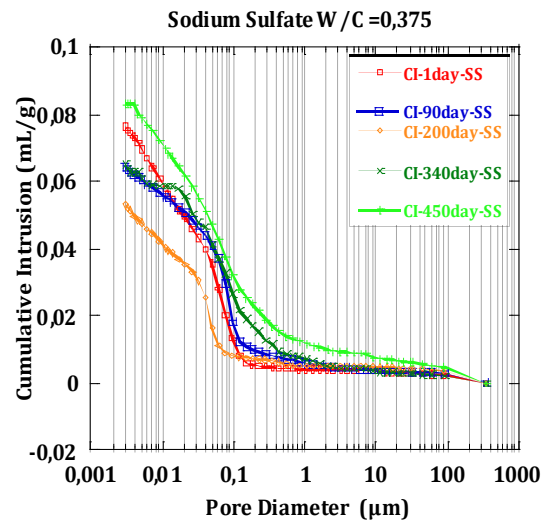
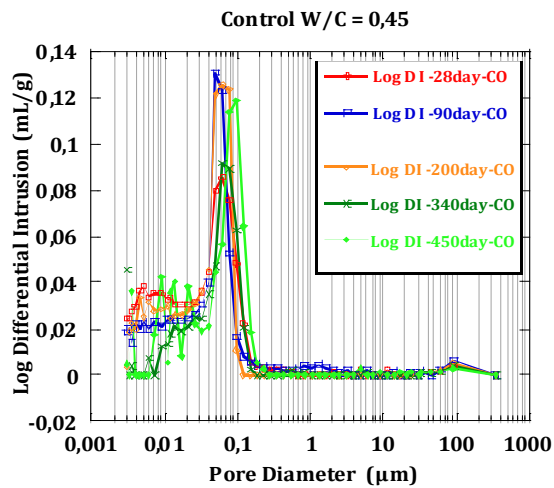
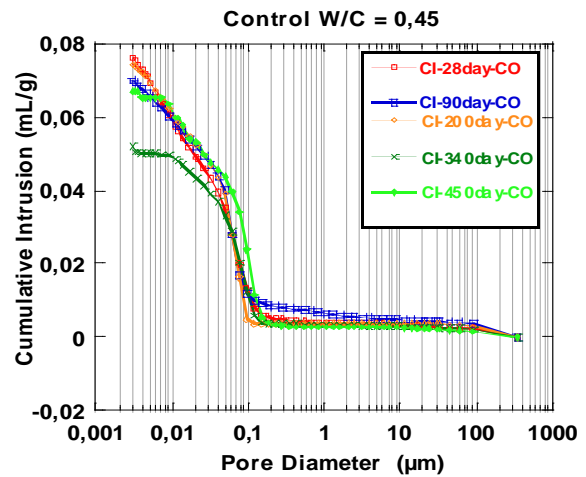


Figure 4-16 Cumulative pore size distribution  $w/c=0.375$  sodium sulfate

#### 4. Results and discussion the Degradation Process by Sodium Sulfate Solution



**Figure 4-17** Log differential intrusion w/c = 0.45 control



**Figure 4-18** Cumulative pore size distribution w/c=0.45 control

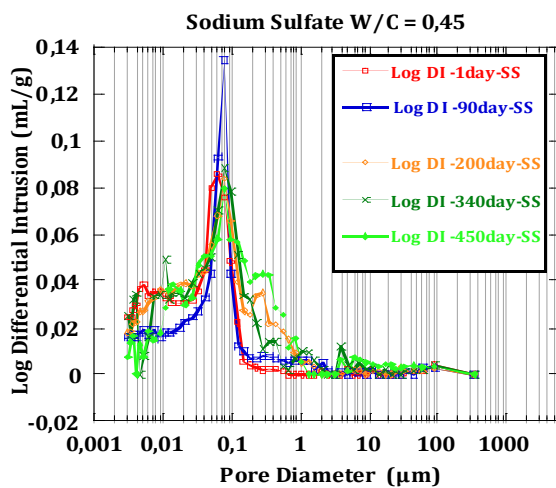


**Figure 4-19** Log differential intrusion w/c = 0.45 sodium sulfate

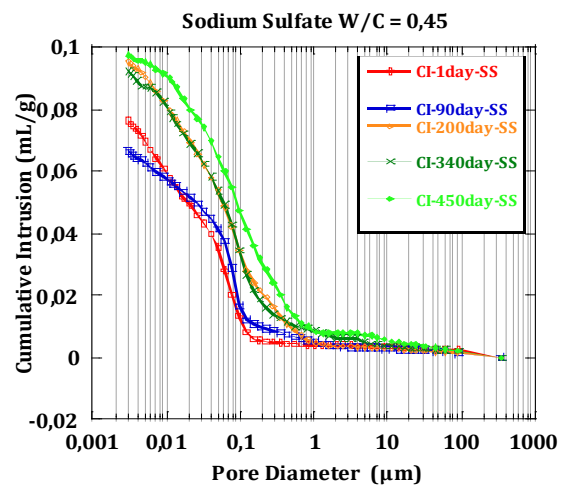


**Figure 4-20** Cumulative pore size distribution w/c=0.45 sodium sulfate

#### 4. Results and discussion the Degradation Process by Sodium Sulfate Solution

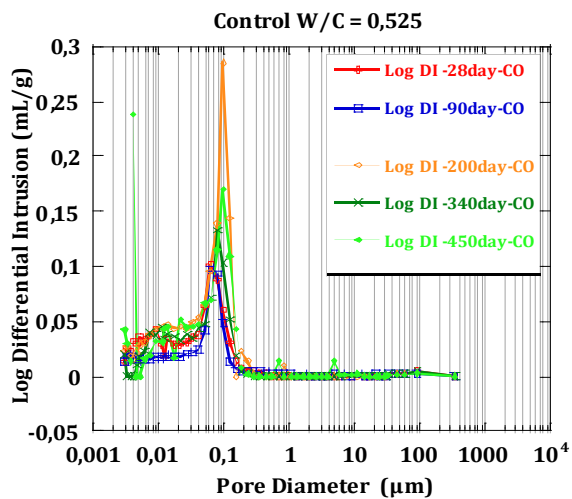


**Figure 4-21** Log differential intrusion w/c = 0.525 control

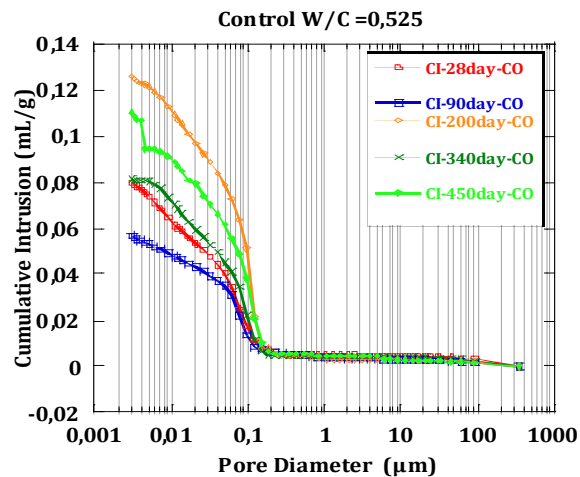


**Figure 4-22** Cumulative pore size distribution w/c=0.525 control

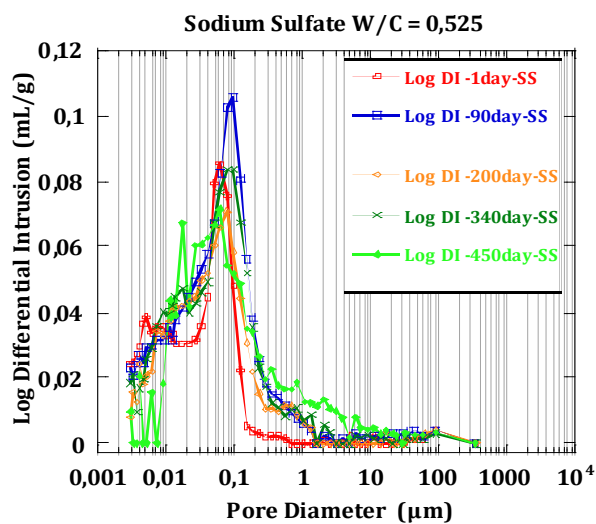


**Figure 4-23** Log differential intrusion w/c = 0.525 sodium sulfate

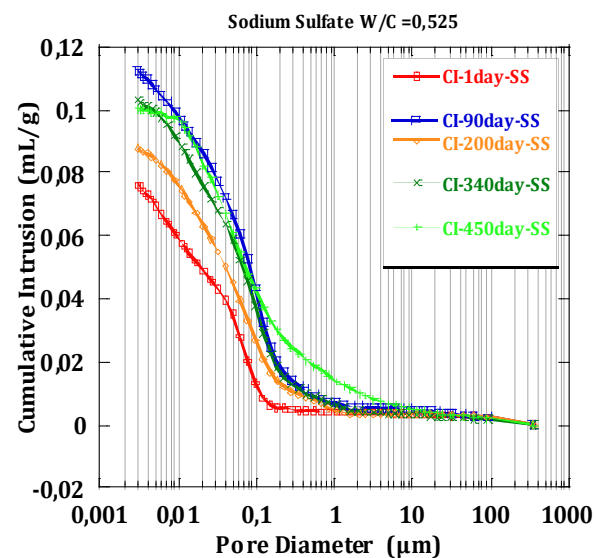


**Figure 4-24** Cumulative pore size distribution w/c=0.525 sodium sulfate



### 4.1.6. Ultrasound Longitudinal and Transversal Wave Velocity

Figure 4-25 illustrates the evolution of ultrasonic longitudinal wave velocity (P-wave) for both control and samples degraded by sodium sulfate solution for 450 days of immersion. The results have shown that change in w/c ratio affects the wave velocity, and it was found that the general trend of wave velocity is a decreasing of it with the increasing of w/c ratio. It is observed that, for control specimen, the wave velocity shows a slight increasing due to the progress of hydration process which led to the decreasing of porosity due to filling it by hydration products. In the figure, it can be seen that for w/c ratio 0.525 of sulfate samples, the wave velocity decreases until the end of exposure time, and also it was observed that the velocity of sulfate samples is less than that of control for all exposure time. This could be due to, in the early period of immersion in sulfate solution and when the w/c ratio is high, the sulfate ions are easy to penetrate the mortar samples and fill up the pore space by formation expansive products, results in development of micro-cracks which led to reduce the pulse velocity of ultrasonic wave.

For the two water-cement ratios 0.45 and 0.375, the wave velocity of sulfate samples increases up to 200 days of immersion, thereafter it decreases until the end of exposure period; it is found two steps for changing the wave velocity. The first step is filling the pores by the expansive products (ettringite), which causes an increasing in the wave velocity. And in the second step, by increasing the formation of expansive products until its volume becomes higher than the volume of pores, micro-cracks and cracks are produced, result in diffract the ultrasonic pulse wave, and hence it took more time to reach the receiving transducer.

For w/c ratio 0.30, the wave velocity of sulfate samples is higher than that of control for all exposure time. In this case (low w/c ratio), sulfate ions was penetrated mortar samples, but still in the first stage of ettringite formation which with time fills the pores. With this w/c ratio, long time is needed to produce expansive force into the pores, and the increment of these expansive products is slowly advanced. For this reason the wave velocity of sulfate sample was higher during all the exposure time.

#### 4. Results and discussion the Degradation Process by Sodium Sulfate Solution

---

Figure 4-26 illustrates the results of transversal wave velocity (S-wave) for both control and degraded samples, similar trend was observed as longitudinal wave velocity. Only in the case of w/c ratio 0.45, the wave velocity is decreased after 90 days of immersion, and for w/c ratio 0.30 the velocity slowed down at the end of exposure time. This demonstrates that the S-waves may be more sensitive than P-waves to the changes of mortar microstructure due to the sulfate attack.

The effect of ettringite formation (sulfate attack) on the ultrasonic wave velocity is summarized by (Song and Chen, 2011) and (Chen et al. 2008), the variation of ultrasonic wave velocity is affected by three factors:

- The first factor is continuation of hydration of cementitious materials and this will lead to the decreasing of porosity of the samples due to filling it by hydration products, therefore, the velocity of ultrasonic waves is increased ( this can be seen for control samples)
- The second factor is the nucleation and growth of delayed ettringite, and may fill the pores of mortar samples. Because of this reason as mentioned previously, the porosity of concrete will decrease and it also lead to the increasing of ultrasonic wave velocity (this can be seen with w/c ratios 0.45, 0.375 and 0.30). These two factors may lead to the increase of the average modulus of the materials, thus, increasing ultrasonic wave velocity.
- The third factor is damage evolution, and ultrasonic wave velocity will decreases because the decreasing effective modulus due to the damage. Therefore, variation of the ultrasonic wave velocity depend on the competition between effect caused by the first and second factors and weakened effect produced by the third factor (also this can be seen for w/c ratios 0.375, 0.45 and 0.525).

#### 4. Results and discussion the Degradation Process by Sodium Sulfate Solution

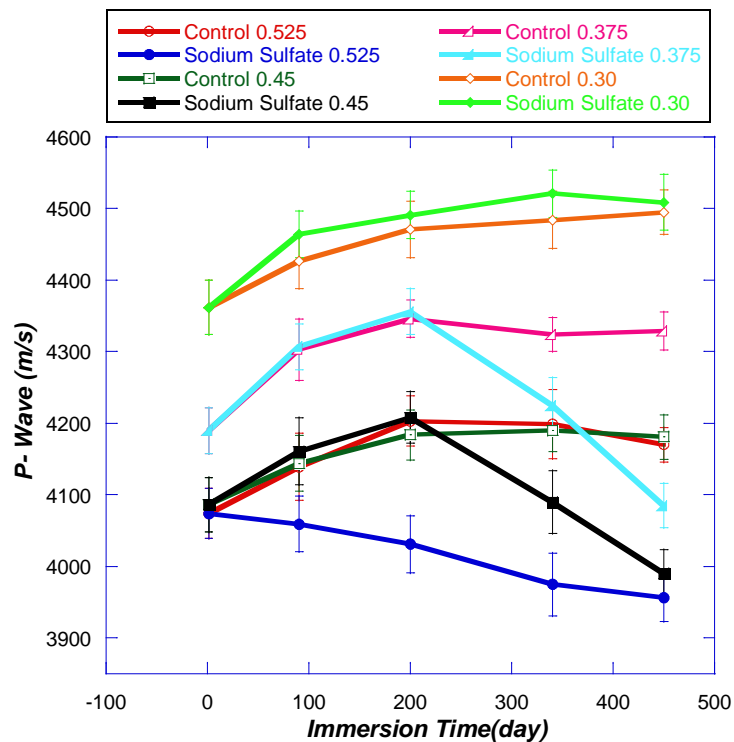


Figure 4-25 Longitudinal wave velocity with time

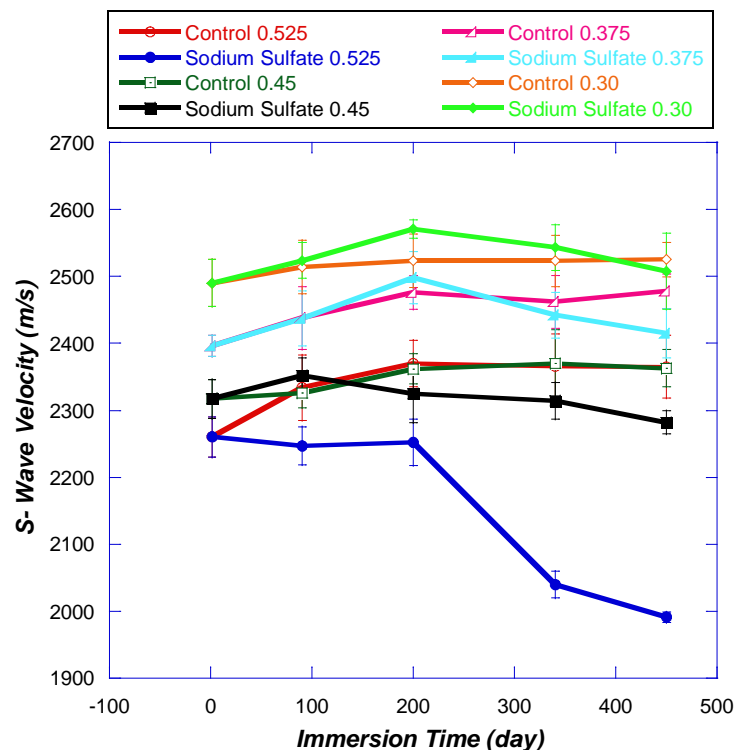


Figure 4-26 Transversal wave velocity with time

### 4.1.7. Ultrasonic Attenuation Profile Area (APA)

As mentioned previously in the introduction that the parameter of attenuation profile area (APA) is estimated by (L Vergara, et al 2001) and used by (Fuente, 2004). It is found that this parameter is successful to estimate the mortar and cement paste porosity and to follow the process of curing and impregnation of these materials. This parameter is used in this chapter to follow the degradation process of mortar and concrete samples due to the external attack by 10% of sodium sulfate solution.

Thus, before presenting the results of the attenuation profile area of ultrasonic waves, the next figures (from 4-27 to 4-34) are presented to illustrate the spectrograms of ultrasonic waves produced by ultrasonic grain noise mode for frequencies 1 and 3.5MHz. The figures illustrate the variation of attenuation of ultrasonic waves with depth due to the attack by sodium sulfate which led to internal variation in the microstructure of mortar samples due to the ingress of sulfate ions and formation of ettringite as mentioned previously.

The spectrograms for each degradation time for sulfate samples estimated by frequency 3.5MHz are presented in the Figures from 4-27 to 4-30. The figures present ; (a) depth-frequency function spectrogram using a contour representation as curves with the same spectrogram value, (b) depth-and frequency spectrogram with color palette show the same values as (a) but using linear colormap correspondence level. It can be seen the variation in ultrasonic pulse penetration with degradation time. For example, in the case of w/c ratio 0.525, the penetration of ultrasonic pulse is decreased with the increasing of immersion time, this demonstrates that with increasing the degradation time, the penetration of sulfate ions increases more and more, and causing formation of ettringite which filled the pores, (this may occur at early immersion age for high w/c ratio as 0.525). Thus, with increasing the time of degradation, the volume of ettringite increases until becomes more than the pores volume, this generates micro-cracks and cracks that gradually increases with time, leading to decreasing the penetration of ultrasonic pulse into the degraded samples (as demonstrated previously with P and S-waves).

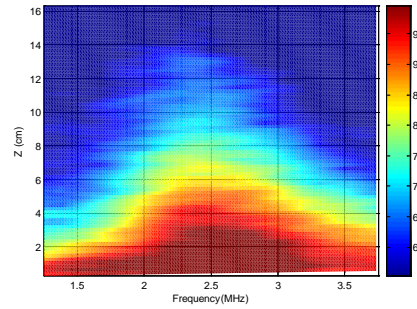
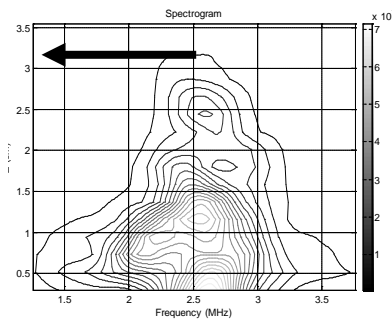
#### 4. Results and discussion the Degradation Process by Sodium Sulfate Solution

---

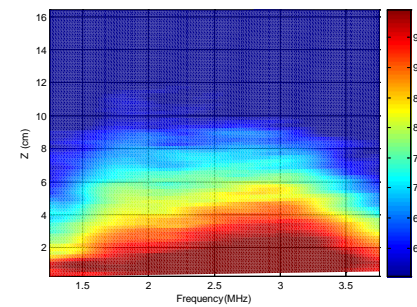
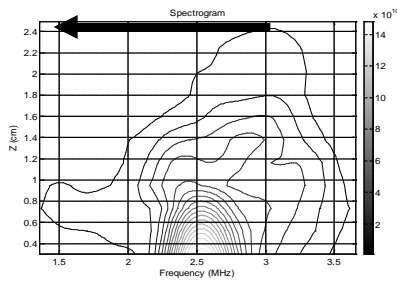
The rate of ultrasonic pulse penetration decreases with increasing the degradation depth. From the figures, it is also observed that the rate of the ultrasonic pulse penetration into the samples degraded by sodium sulfate varies according to the variation of w/c ratio. Thus, when the w/c ratio decreases, the ultrasonic pulse penetration increases, the same trend was observed by (L. Vergara, et al 2003). They found that the penetration of ultrasonic pulse decreases as w/c ratio increases, when they examined and measured the porosity of two mortar samples with w/c ratios 0.40 and 0.50 (non-degraded samples).

The spectrograms for each degradation time for sulfate samples estimated by frequency 1MHz are presented in Figures from 4-31 to 4-34, the same trend as frequency 3.5MHz is observed. On the other hand it can be observed that both of frequencies 1 MHz and 3.5 MHz reveal that, the pulse energy penetrates better around the nominal frequency of inspection and the higher penetration is achieved for immediate lower frequencies due to the attenuation factor and the low-pass filter affect by the examined material. Also, it can be observed that the penetration of ultrasonic pulse for frequency 1MHz is more than the penetration of ultrasonic pulse for frequency 3.5MHz. The high frequency has higher attenuation and lower penetration than the low frequency. However, the perceptual changes in 3.5 MHz reveals more sensitive than 1 MHz. This effect will be discussed in the following section of this chapter.

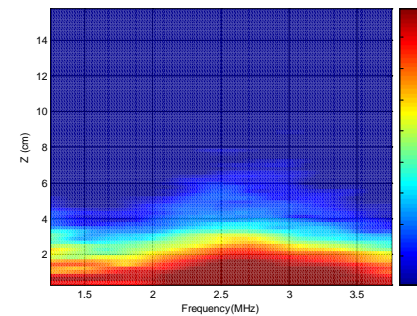
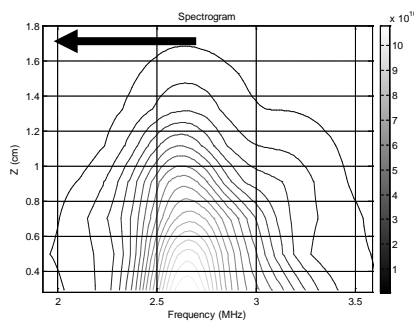
## 4. Results and discussion the Degradation Process by Sodium Sulfate Solution



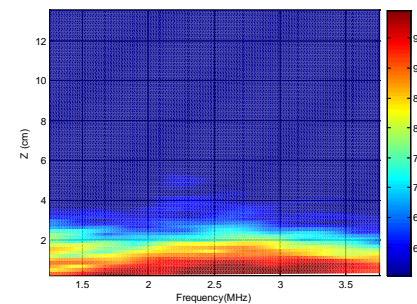
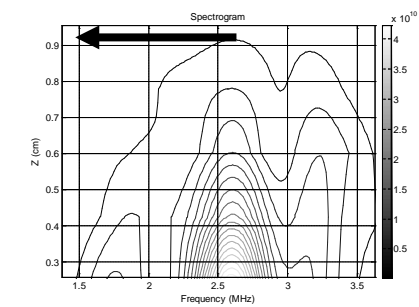
90 days of degradation by sodium sulfate solution



200 days of degradation by sodium sulfate solution



340 days of degradation by sodium sulfate solution



450 days of degradation by sodium sulfate solution

(a)

(b)

**Figure 4-27** (a) Averaged depth–frequency spectrogram (contour), (b) averaged depth- and frequency-dependent spectrogram (pcolor) for each degradation time for  $w/c = 0.525$  mortar degraded by sodium sulfate solution, central frequency 3.5MHz.

## 4. Results and discussion the Degradation Process by Sodium Sulfate Solution

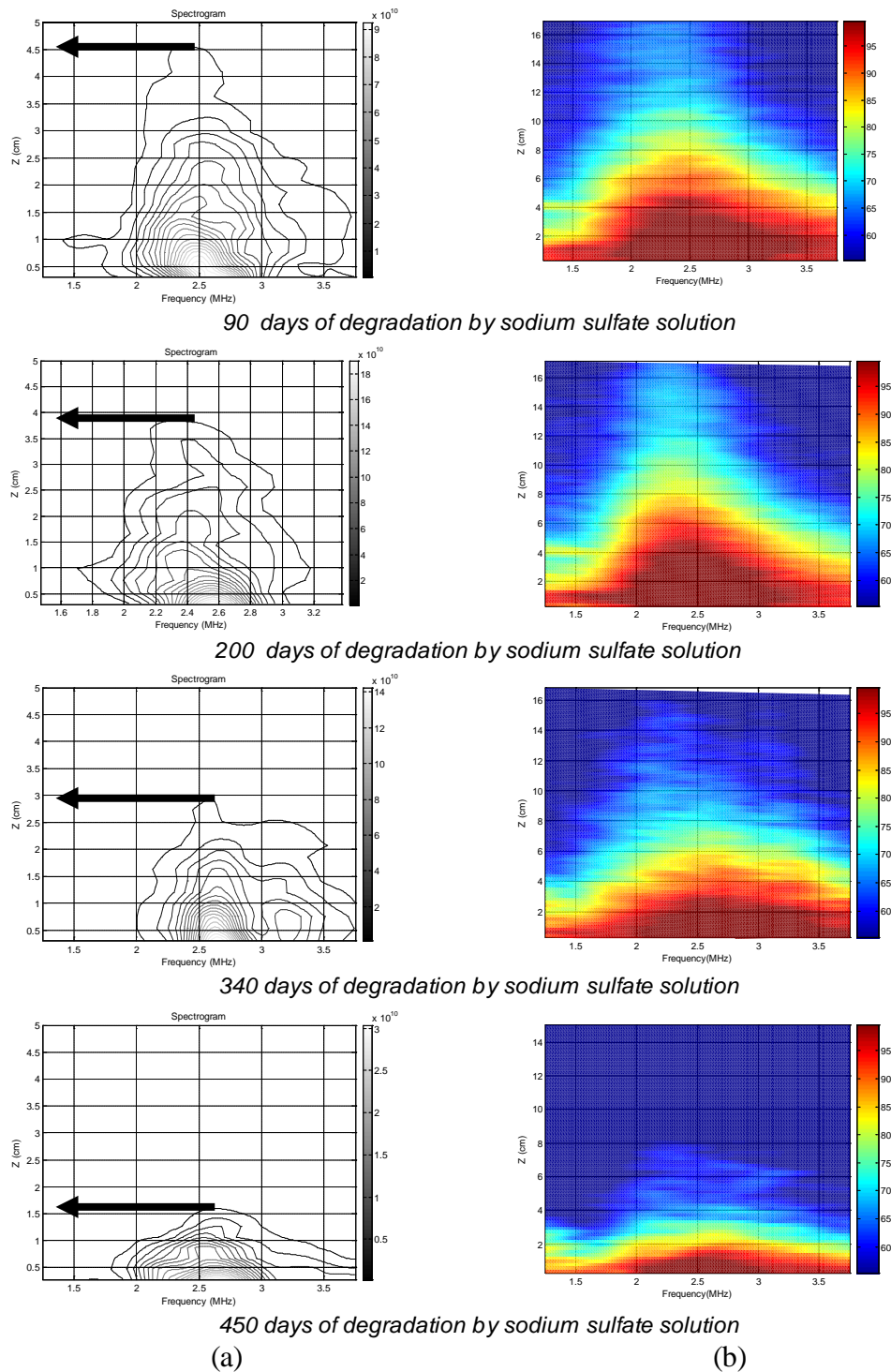


**Figure 4-28** (a) Averaged depth–frequency spectrogram (contour), (b) averaged depth- and frequency-dependent spectrogram (pcolor) for each degradation time for w/c =0.45 mortar degraded by sodium sulfate solution, central frequency 3.5MHz.



## 4. Results and discussion the Degradation Process by Sodium Sulfate Solution

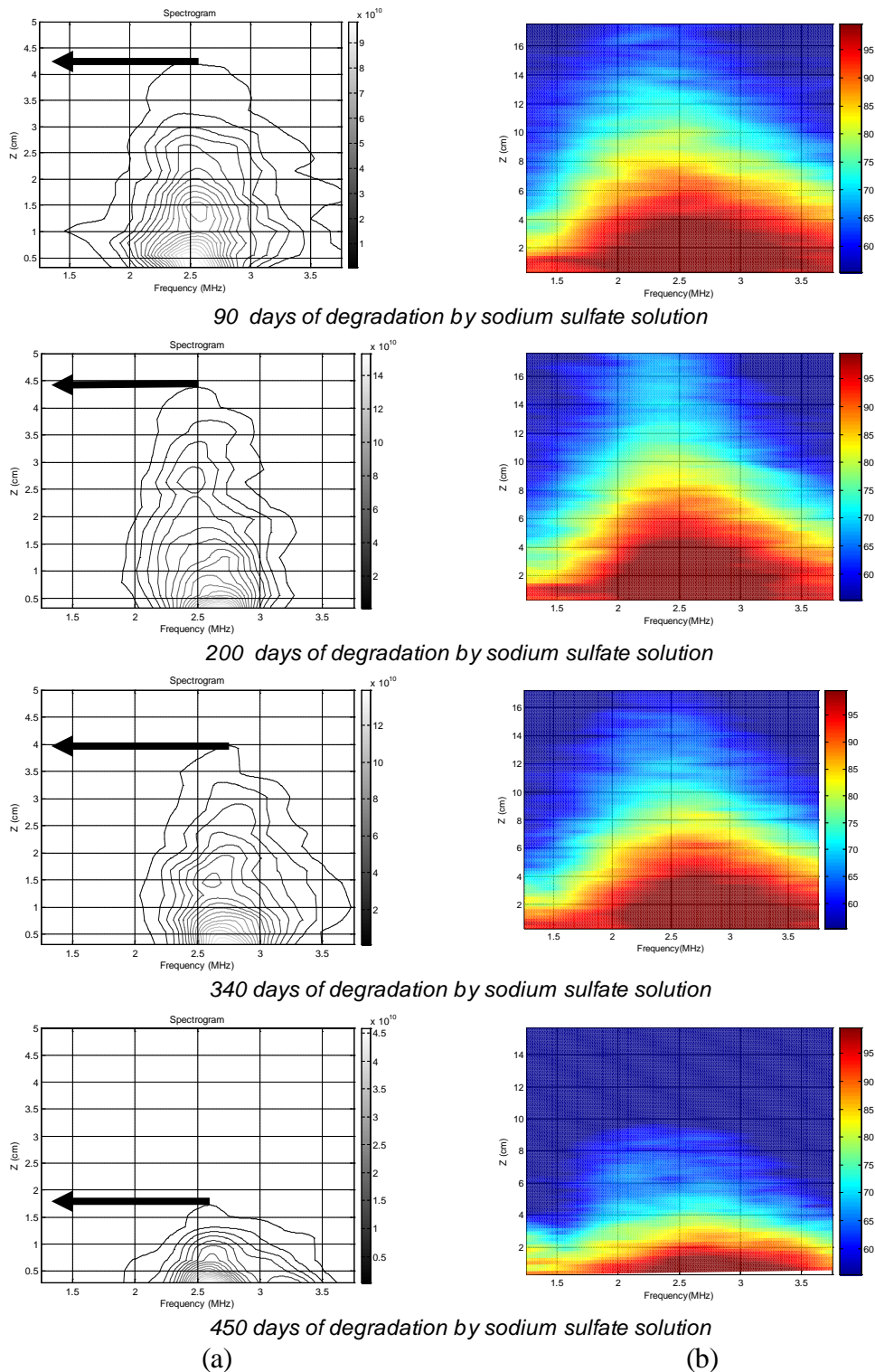


**Figure 4-29** (a) Averaged depth–frequency spectrogram (contour), (b) averaged depth- and frequency-dependent spectrogram (pcolor) for each degradation time for  $w/c = 0.375$  mortar degraded by sodium sulfate solution, central frequency 3.5MHz.



## 4. Results and discussion the Degradation Process by Sodium Sulfate Solution

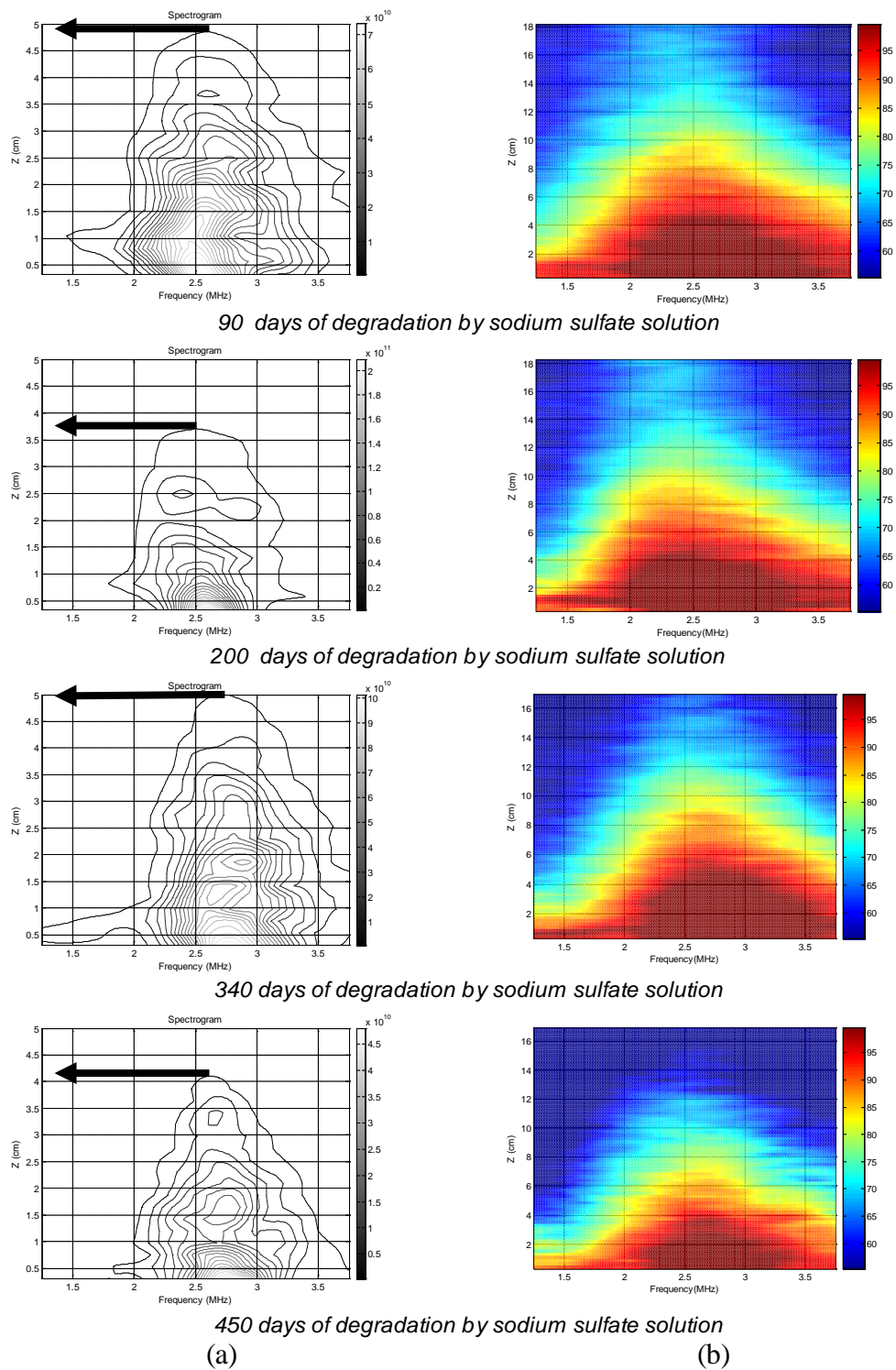


**Figure 4-30** (a) Averaged depth–frequency spectrogram (contour), (b) averaged depth- and frequency-dependent spectrogram (pcolor) for each degradation time for  $w/c = 0.30$  mortar degraded by sodium sulfate solution, central frequency 3.5MHz.

## 4. Results and discussion the Degradation Process by Sodium Sulfate Solution

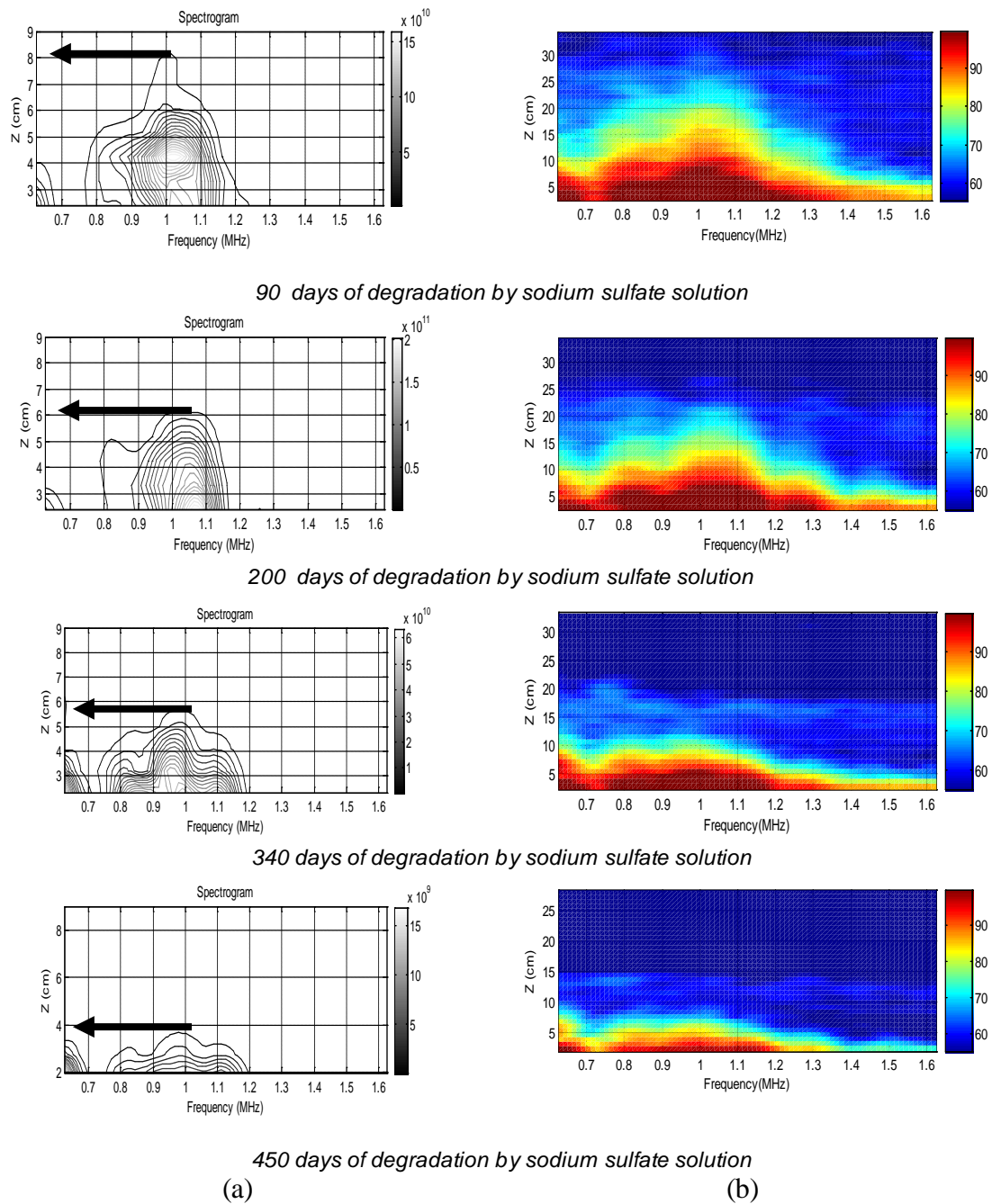


**Figure 4-31** (a) Averaged depth–frequency spectrogram (contour), (b) averaged depth- and frequency-dependent spectrogram (pcolor) for each degradation time for  $w/c = 0.525$  mortar degraded by sodium sulfate solution, central frequency 1 MHz.

## 4. Results and discussion the Degradation Process by Sodium Sulfate Solution

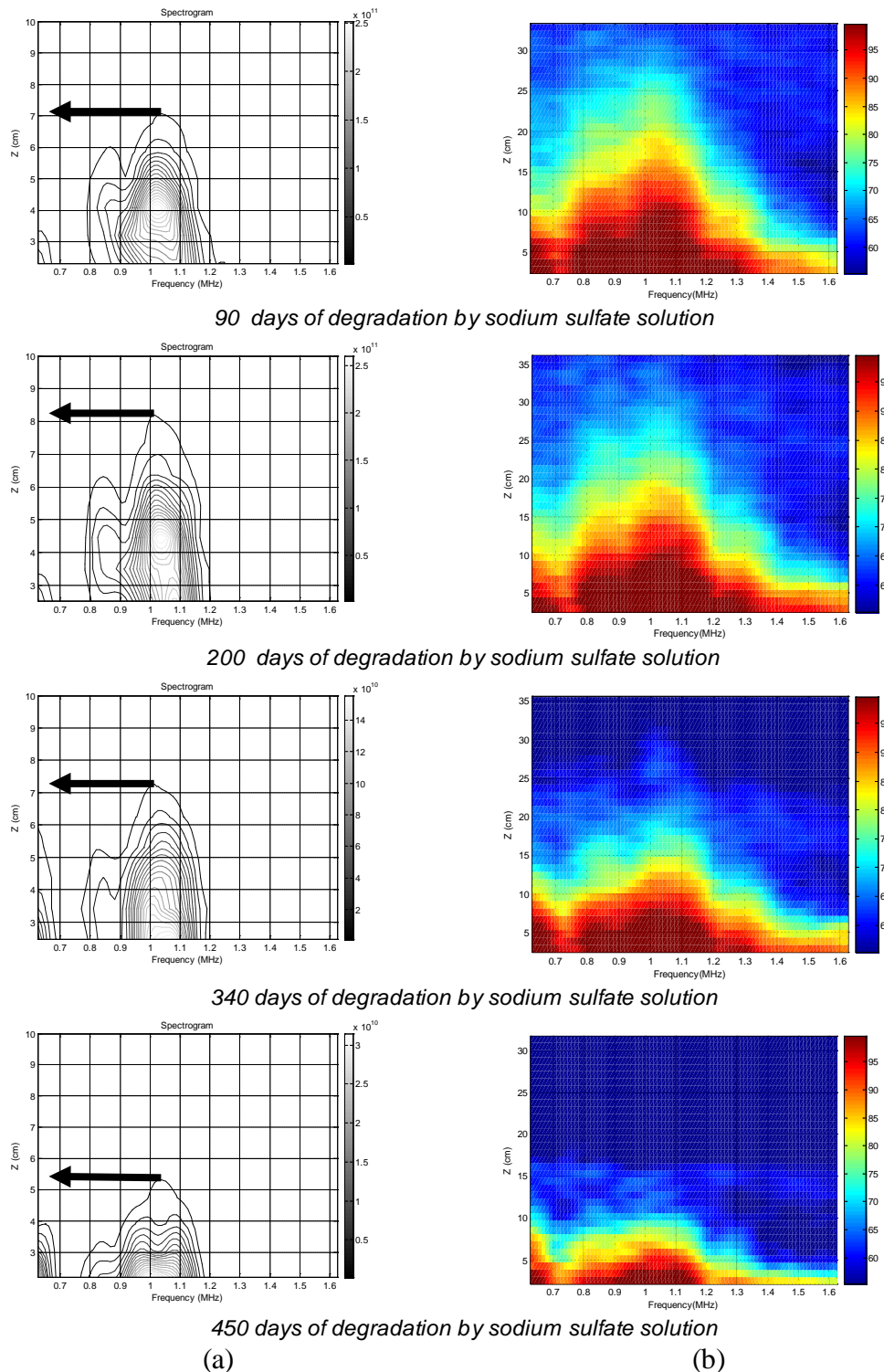


**Figure 4-32** (a) Averaged depth–frequency spectrogram (contour), (b) averaged depth- and frequency-dependent spectrogram (pcolor) for each degradation time for w/c=0.45 mortar degraded by sodium sulfate solution, central frequency 1MHz.

## 4. Results and discussion the Degradation Process by Sodium Sulfate Solution

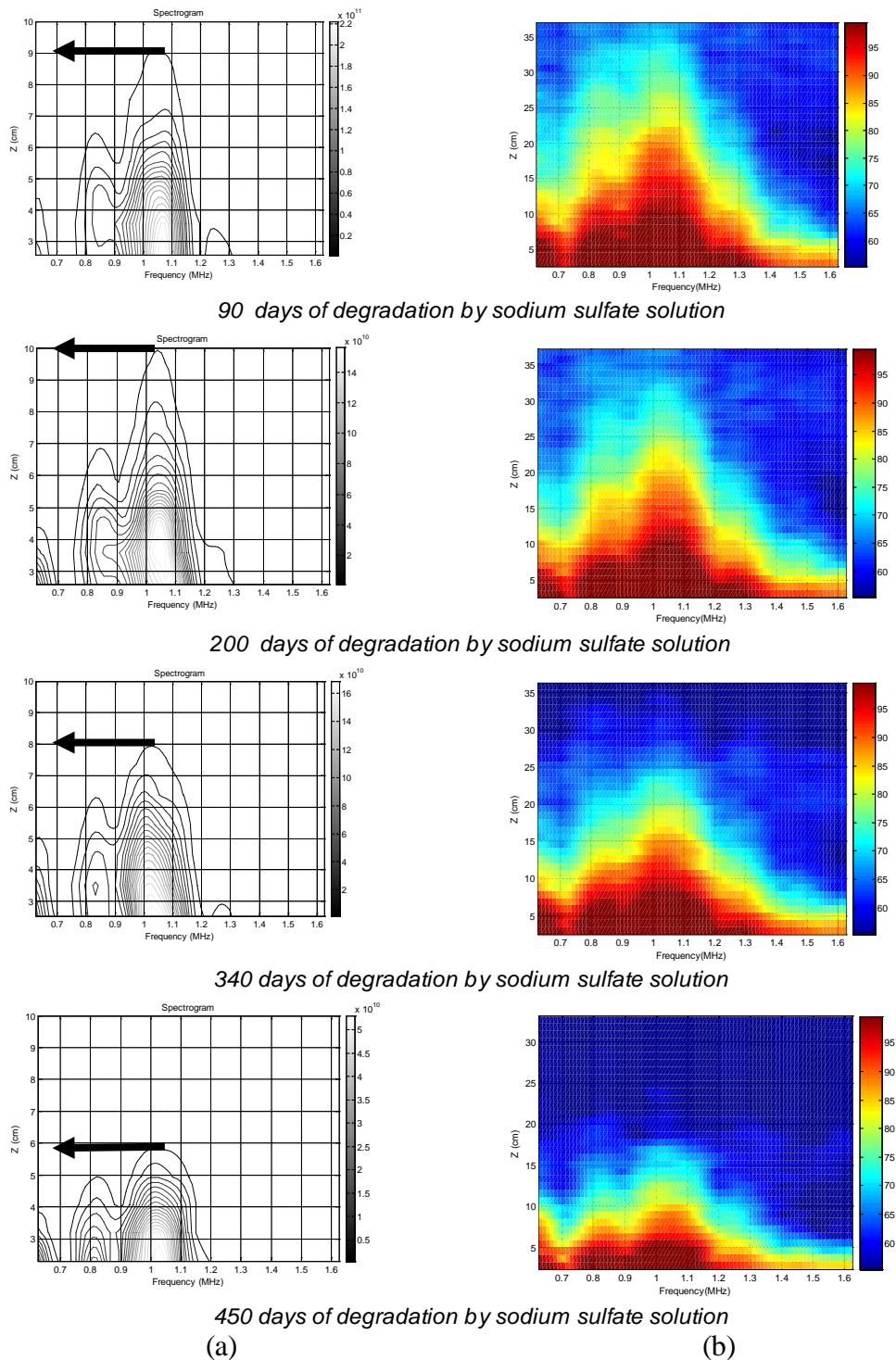


**Figure 4-33** (a) Averaged depth–frequency spectrogram (contour), (b) averaged depth- and frequency-dependent spectrogram (pcolor) for each degradation time for  $w/c = 0.375$  mortar degraded by sodium sulfate solution, central frequency 1MHz.



## 4. Results and discussion the Degradation Process by Sodium Sulfate Solution

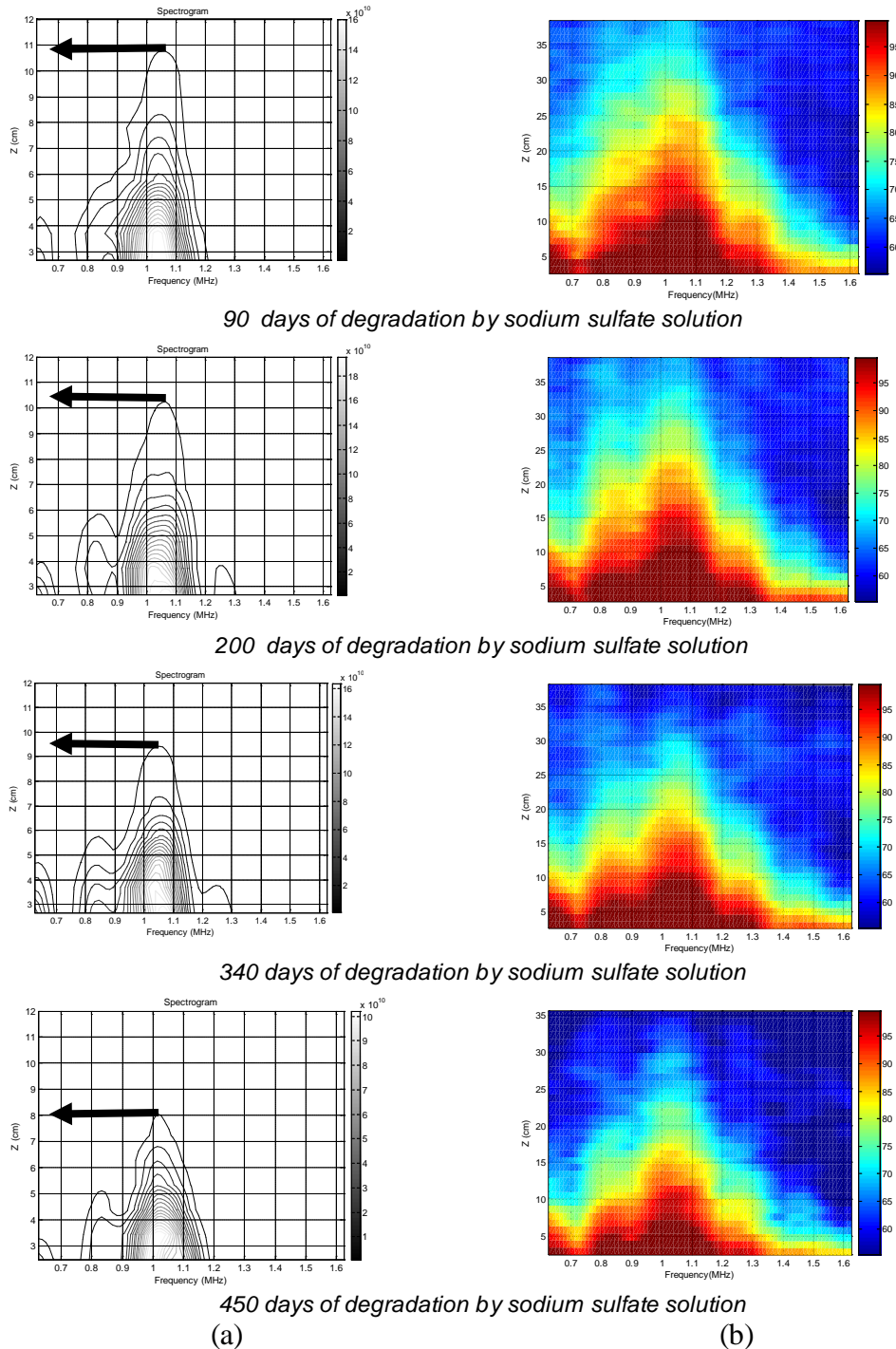


**Figure 4-34** (a) Averaged depth–frequency spectrogram (contour), (b) averaged depth- and frequency-dependent spectrogram (pcolor) for each degradation time for  $w/c=0.30$  mortar degraded by sodium sulfate solution, central frequency 1MHz.

#### 4. Results and discussion the Degradation Process by Sodium Sulfate Solution

---

Figure 4-35 illustrates the results of attenuation profile area (APA) for frequency 1 MHz. The general trend of APA for control samples is a slightly decreasing until the end of exposure time. For sulfate samples, the variation in the values of APA is related to w/c ratio and the time of immersion. For examples, for w/c ratio 0.525, the APA is increased until the end of exposure time, while for w/c ratios 0.45, 0.375 and 0.30, APA is decreased up to more 90 days of immersion, thereafter was increased until the end of exposure time.

Figure 4-36 illustrates the results of attenuation profile area (APA) for frequency 3.5 MHz. For sulfate samples, with water cement ratio 0.525, the APA is decreased up to 90 days, and then it is increased until the end of exposure time by the same trend as APA of 1MHz. For w/c ratios 0.45 and 0.375, the attenuation profile area is decreased up to 200 days of immersion, thereafter; it is increased until the end of exposure time. While for w/c ratio 0.30, APA is remained less than APA of control samples until the end of exposure time.

On the other hand, the percentage of variation for APA 1 and 3.5 MHz can be calculated as follow equation 4.1;

$$\% \text{ variation of APA} = \frac{APA_{Sulfate} - APA_{Control}}{APA_{Control}} * 100 \quad \text{Equation 4. 1}$$

The results of variation of APA for frequencies 1 and 3.5 MHz are presented in Table 4-4 and Table 4-5 and respectively. It is clear that after 450 days of immersion, the percentage of variation of APA decreases as w/c ratio increases for both frequencies 1 and 3.5MHz. For example, for attenuation profile area 1MHz for w/c ratios 0.525, 0.45, 0.375 and 0.30, the percentage of variation are 106%, 104%, 87% and 47% respectively. The same trend is observed for APA 3.5MHz, but the percentage of variation is higher than that of APA 1MHz, (see Table 4-4), for w/c ratios 0.525, 0.45, 0.375 and 0.30 the percentage of variation are 239%, 138%, 101% and -5% respectively, and this confirm as presented in the previous paragraph, the higher

#### 4. Results and discussion the Degradation Process by Sodium Sulfate Solution

---

frequency is the lower penetration. On the other hand, the negative sign indicates that the APA of control samples is higher than the APA of samples degraded by sodium

sulfate. This could be due to that the pores of the degraded samples are filled by ettringite product, which yet did not expanded and cracks are not produced, while control samples have pores more than the pores of degraded samples at the same age of immersion, which may lead to increasing of APA. The negative signs are observed more with APA 3.5MHz, as can be seen in Table 4-5. For w/c ratio 0.525, it is not observed any negative sign, for both w/c ratios 0.45 and 0.375, the negative signs are observed until 200 days, while for w/c ratio 0.30, the negative signs are observed during all exposure time, this almost confirm the results presented in Figure 4-36. Thus, the frequency 3.5MHz could be more sensitive to the microstructure changes due to the sulfate attack than frequency 1MHz as it has a shorter wavelength.

When APA 3.5MHz is compared with APA 1MHz, after 450 days of degradation as can be seen in Table 4-2 and Table 4-3 for the degraded samples, the ratio of (APA 3.5MHz/ APA 1MHz) is decreased with decreasing of w/c ratio, i.e. this ratio was 2.63, 2.15, 1.91 and 1.20 for w/c ratios from 0.525 to 0.30 respectively. When this ratio is compared with the ratio of control samples i.e. the ratio was 1.59, 1.83, 1.77 and 1.85 for w/c ratios from 0.525 to 0.30 respectively, the same trend was not observed.

#### 4. Results and discussion the Degradation Process by Sodium Sulfate Solution

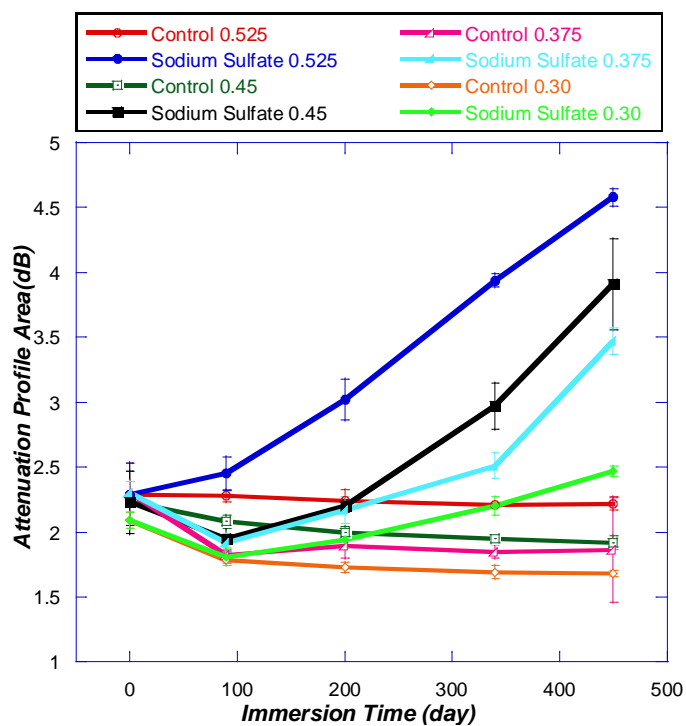


Figure 4-35 Attenuation profile area 1 MHz with time

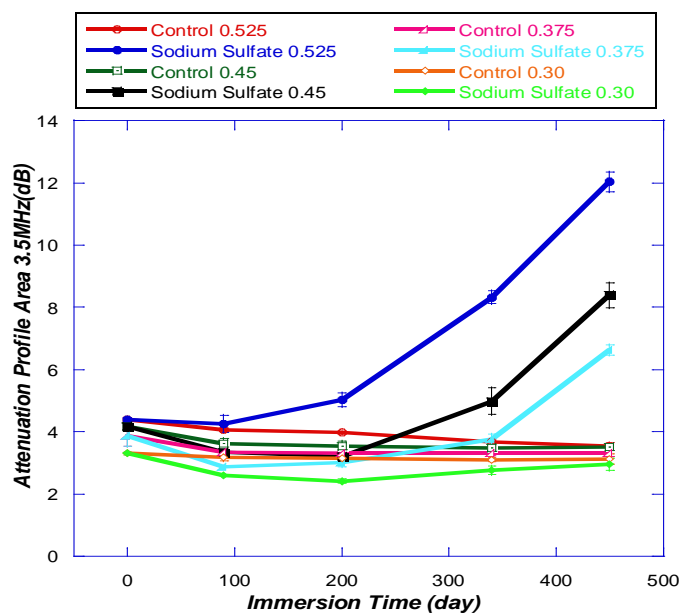


Figure 4-36 Attenuation profile area 3.5 MHz with time



#### 4. Results and discussion the Degradation Process by Sodium Sulfate Solution

**Table 4- 2** Values of attenuation profile area (APA) of frequency 1MHz for control and samples degraded by sodium sulfate solution for 450 days.

Immersion time(day)	w/c = 0.525		w/c = 0.45		w/c = 0.375		w/c = 0.30	
	Co	SS	Co	SS	Co	SS	Co	SS
1	2.29±0.24	2.29±0.24	2.23±0.24	2.23±0.24	2.30±0.09	2.30±0.09	2.09±0.06	2.09±0.06
90	2.28±0.05	2.45±0.13	2.08±0.05	1.95±0.10	1.82±0.04	1.92±0.07	1.78±0.02	1.81±0.07
200	2.24±0.09	3.02±0.16	2.00±0.04	2.20±0.05	1.89±0.09	2.17±0.10	1.73±0.04	1.94±0.06
340	2.21±0.00	3.94±0.05	1.95±0.01	2.97±0.18	1.85±0.05	2.51±0.10	1.69±0.05	2.20±0.07
450	2.22±0.05	4.58±0.07	1.92±0.05	3.91±0.35	1.86±0.04	3.47±0.10	1.68±0.02	2.47±0.04

**Table 4- 3** Values of attenuation profile area (APA) of frequency 3.5MHz for control and samples degraded by sodium sulfate solution for 450 days.

Immersion time(day)	w/c = 0.525		w/c = 0.45		w/c = 0.375		w/c = 0.30	
	Co	SS	Co	SS	Co	SS	Co	SS
1	4.40±0.04	4.40±0.04	4.18±0.09	4.18±0.09	3.86±0.32	3.86±0.32	3.31±0.04	3.31±0.04
90	4.06±0.05	4.25±0.28	3.61±0.17	3.35±0.02	3.34±0.13	2.88±0.00	3.18±0.11	2.60±0.02
200	3.97±0.03	5.02±0.22	3.54±0.17	3.22±0.06	3.33±0.06	3.01±0.13	3.15±0.06	2.42±0.07
340	3.68±0.09	8.33±0.21	3.50±0.10	4.99±0.44	3.33±0.10	3.75±0.18	3.11±0.06	2.77±0.14
450	3.55±0.11	12.03±0.32	3.52±0.08	8.39±0.41	3.31±0.09	6.64±0.17	3.12±0.17	2.97±0.19

**Table 4- 4** % variation of attenuation profile area (APA) of frequency 1MHz due to the degradation process by 10% of sodium sulfate solution

Immersion time(day)	w/c = 0.525	w/c = 0.45	w/c = 0.375	w/c = 0.30
	% variation (±)	% variation (±)	% variation (±)	% variation (±)
1	0	0	0	0
90	7	-6	5	2
200	35	10	15	12
340	78	52	36	30
450	106	104	87	47

**Table 4- 5** % variation of attenuation profile area (APA) of frequency 3.5MHz due to the degradation process by 10% of sodium sulfate solution

Immersion time(day)	w/c = 0.525	w/c = 0.45	w/c = 0.375	w/c = 0.30
	% variation (±)	% variation (±)	% variation (±)	% variation (±)
1	0	0	0	0
90	5	-7	-14	-18
200	26	-9	-10	-23
340	126	43	13	-11
450	239	138	101	-5

### 4.1.8. Ultrasonic Tomography Imaging

Figure 4-37 to Figure 4-40 illustrate the results of Ultrasonic tomography imaging (UTI) for both control and degraded samples until 450 days, and for w/c ratios 0.30, 0.375, 0.45 and 0.525 respectively. The results of two samples are presented for every w/c ratio. The figures show the images of attenuation and velocity of ultrasonic wave realized by UTI technique. Every figure divided into two parts, the left side shows the global attenuation in dB and the right side shows the velocity in km/s for both control and degraded samples. As can be observed at the right of every side it is found a colour bar which permits associating the colours with the values of both velocity and attenuation. For example, colour bar for velocity varies from blue colour which presents the low value of velocity (lower than 4, 2 km/s) to red colour which presents the high value of velocity (higher than 4, 8 km/s); the same can be seen for attenuation.

Figure 4-37 illustrates the maps obtained for w/c ratio 0.30, for control and degraded samples after 90, 200, 340, 450 days of immersion in lime water and sodium sulfate solution. For control samples, almost the change in attenuation is not observed, while for degraded samples the attenuation is decreased until the end of exposure time. On the other hand, it can be seen that ultrasonic wave velocity of the degraded samples is slightly less than ultrasonic wave velocity of control samples. This was confirmed by the plotted mean values of ultrasonic wave velocity, as can be observed in Figure 4-41.

Figure 4-38 illustrates the results of w/c ratio 0.375. For control samples, after 90 days of immersion and until the end of exposure time, both of attenuation and ultrasonic wave velocity almost are not changed. While for the degraded samples, the attenuation of ultrasonic waves is decreased up to 200 days of degradation thereafter, it is increased until the end of exposure time, this is observed clearly at the attacked surfaces of the samples and at the edges of them. Also it can be seen that the velocity of ultrasonic waves is decreased linearly from 90 days until the end of exposure time, as observed on the image (see Figure 4-38). The mean values of ultrasonic wave velocities which are plotted in Figure 4-41 show that the velocity of the degraded samples slightly decreased up to 200 days, thereafter a drop in the decreasing of wave velocity is observed until the

#### 4. Results and discussion the Degradation Process by Sodium Sulfate Solution

---

end of exposure time. For 340 and 450 days, attenuation factor shows an increasing trend in the contour while it is reduced in the core of the samples. The values in the non-edge points can cause errors because the distance would be less than 4 cm of thickness, also because the samples are under degradation process and they show partial disintegration.

Figure 4-39 illustrates the results of UTI for w/c ratio 0.45. A high level of the degradation is observed at 340 days of immersion in sodium sulfate solution., The edges and the sides of the samples are degraded and the attenuation is observed with very high values at the centre of the samples, while after 450 days the samples could be cracked completely, and therefore, ultrasonic waves cannot pass through the material, for this the attenuation is not observed in the images as can be seen in Figure 4-39 . On the other hand, the velocity of the ultrasonic wave is decreased until the end of exposure time, for w/c ratio 0.45. Also, the mean values of the velocity are presented in Figure 4-41. As can be noticed in Table 4-6, the velocity is decreased linearly up to 340 days, after that a drop in the increasing of wave velocity is observed from 340 days until the end of exposure time.

Figure 4-40 illustrates the results of w/c ratio 0.525, it can be seen the expected decreasing in the velocity and the increasing in the attenuation. Ultrasonic wave velocity of the degraded samples is decreased until 340 days of immersion, after that it was difficult to be estimated. This is due to the cracks produced by the effect of ettringite formation as showed previously by SEM examination, thus the samples at 450 days of immersion could be cracked completely.

As can be seen in Table 4-6, for w/c ratio 0.525 the values obtained for velocity at 450 days of immersion are false and do not express the true values of mortar ultrasonic wave velocity. On the other hand, the attenuation also is difficult to be estimated at 340 days of immersion for the same reason presented previously (see Figure 4-40).

#### 4. Results and discussion the Degradation Process by Sodium Sulfate Solution

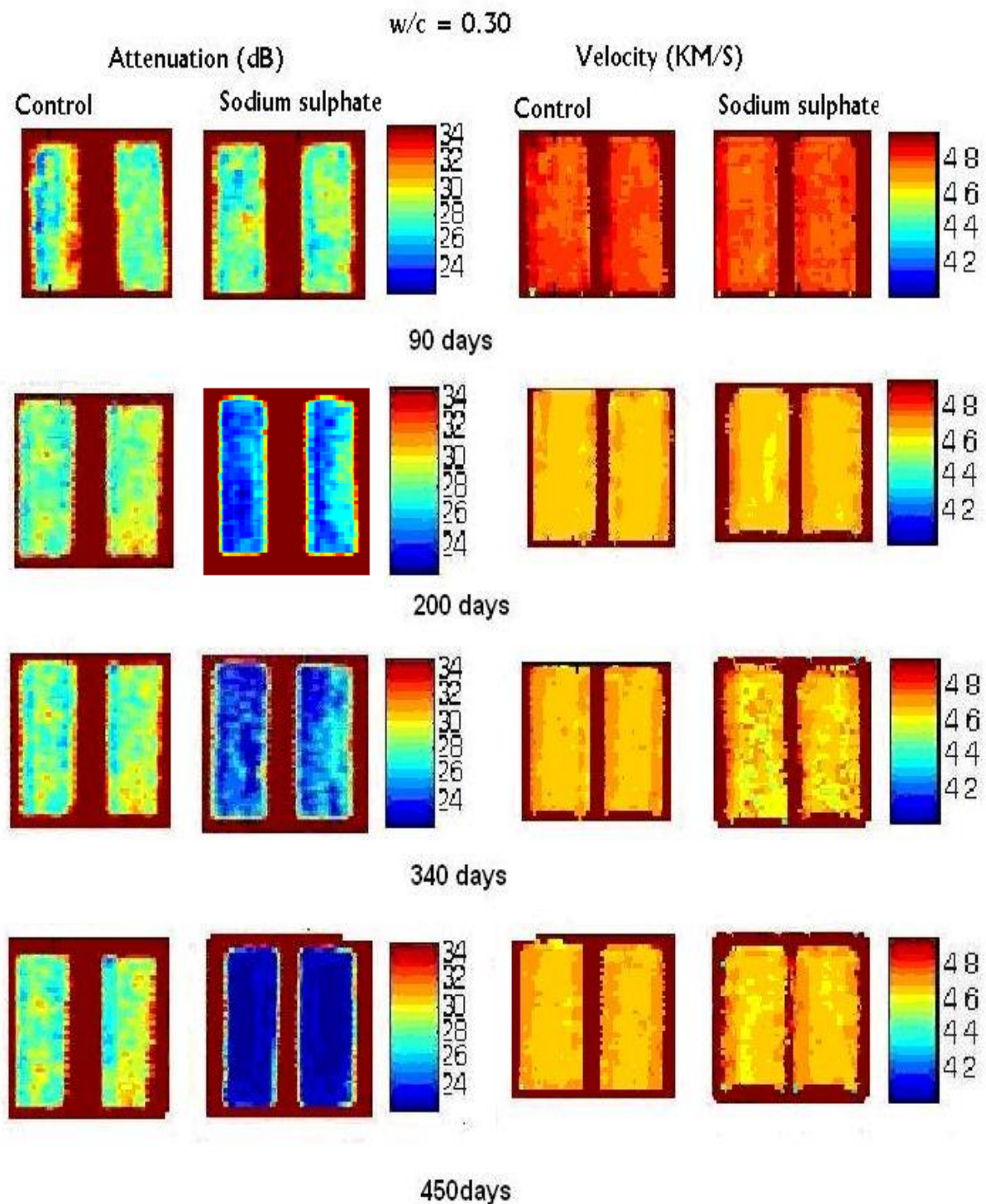


Figure 4-37 Attenuation and velocity of ultrasonic waves for w/c ratio 0.30

#### 4. Results and discussion the Degradation Process by Sodium Sulfate Solution

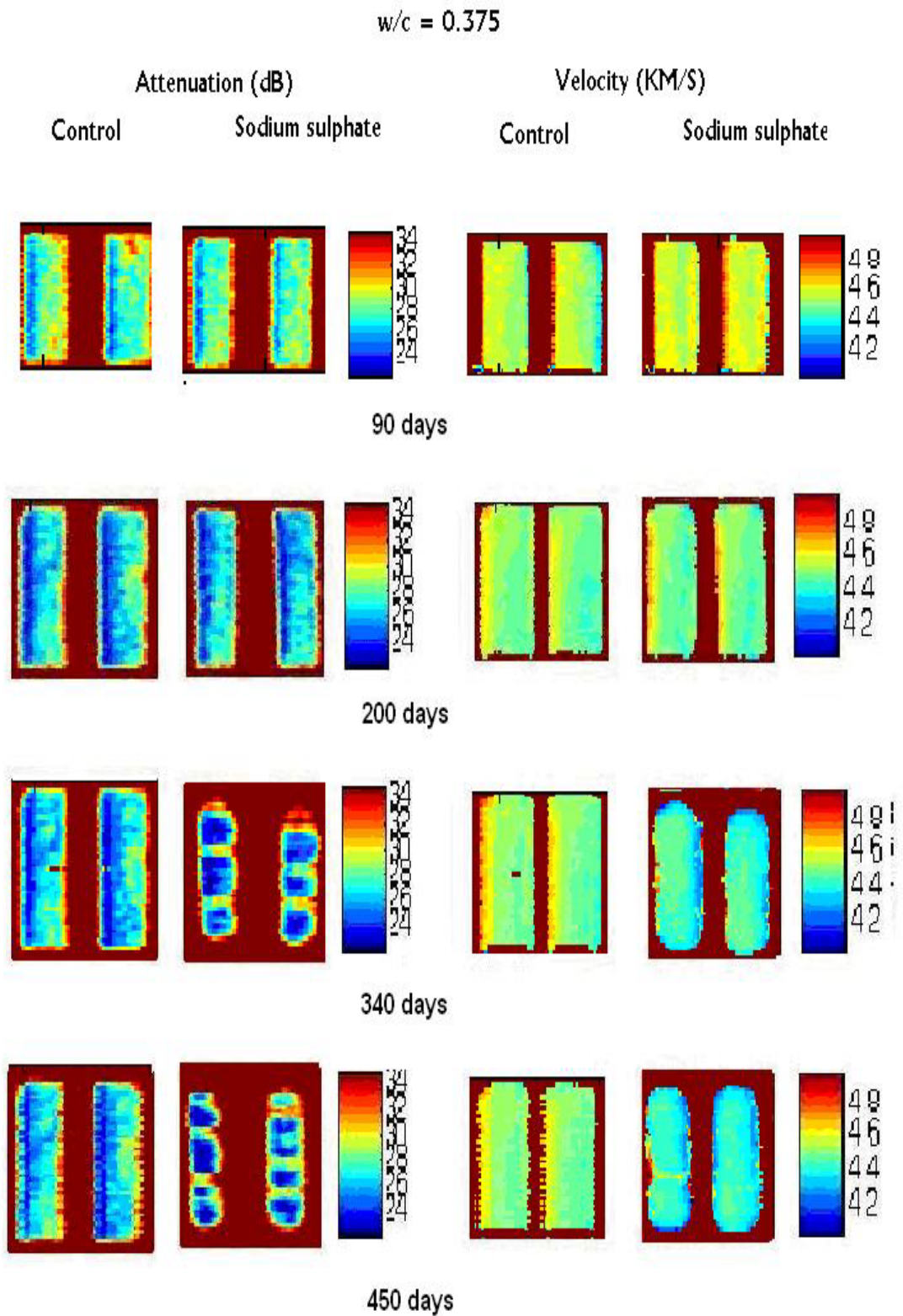


Figure 4-38 Attenuation and velocity of ultrasonic waves for  $w/c$  ratio 0.375



#### 4. Results and discussion the Degradation Process by Sodium Sulfate Solution

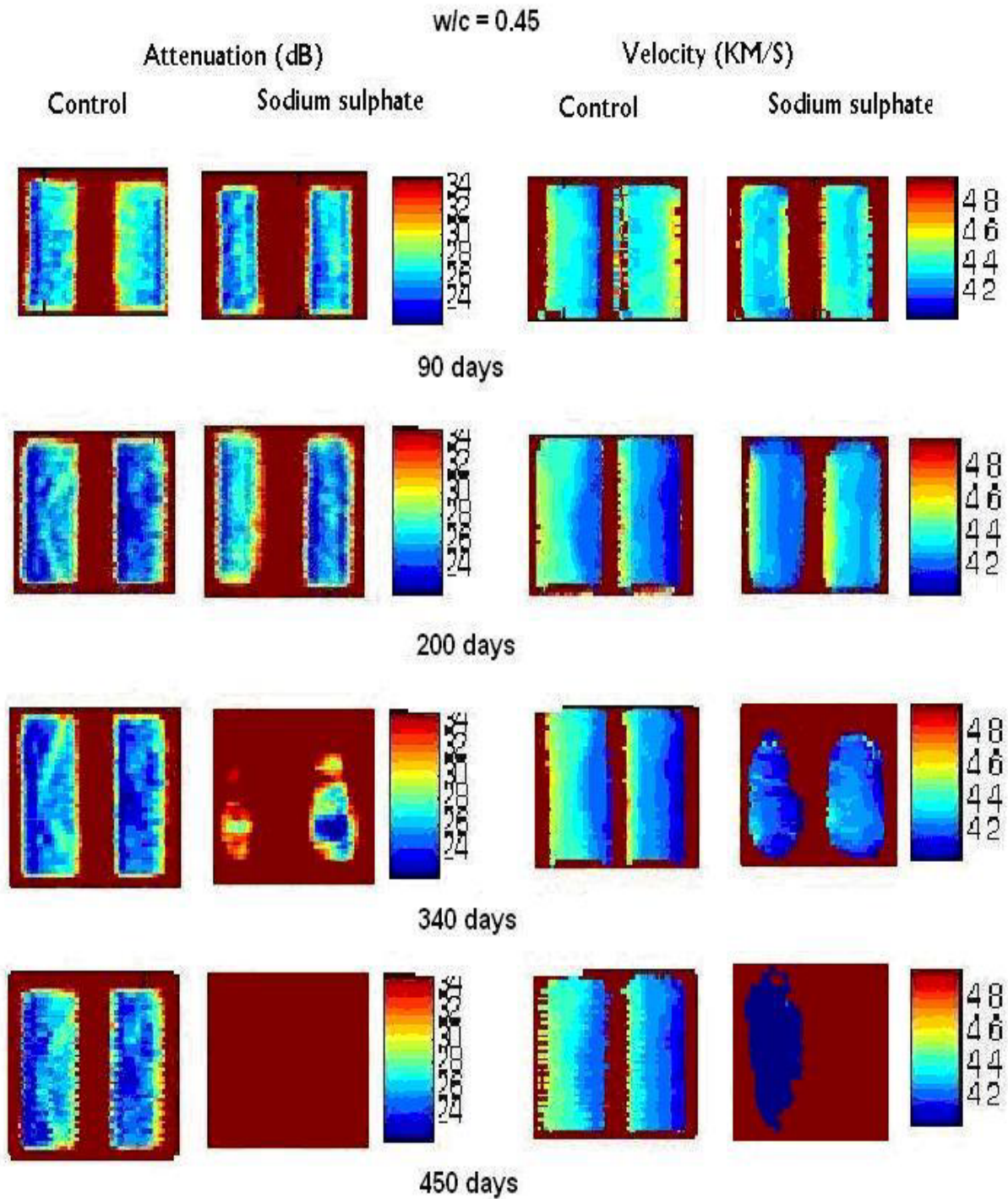
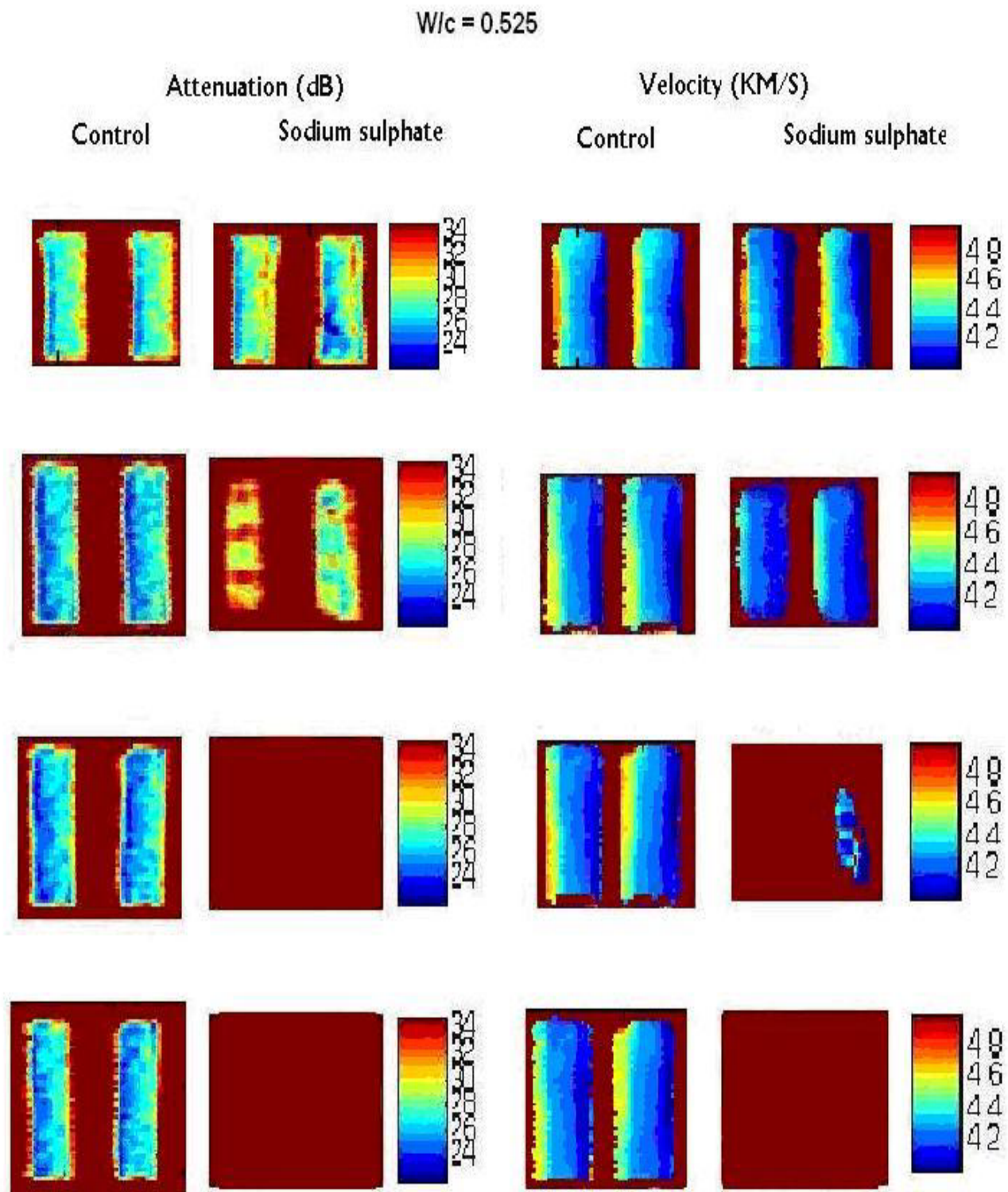


Figure 4-39 Attenuation and velocity of ultrasonic waves for w/c ratio 0.45

#### 4. Results and discussion the Degradation Process by Sodium Sulfate Solution



**Figure 4-40** Attenuation and velocity of ultrasonic waves for w/c ratio 0.525

#### 4. Results and discussion the Degradation Process by Sodium Sulfate Solution

**Table 4-6** Values mean velocity for control and samples degraded by sodium sulfate solution for 450 days.

Immersion time(day)	w/c = 0.30		w/c = 0.375		w/c = 0.45		w/c = 0.525	
	Co	SS	Co	SS	Co	SS	Co	SS
90	4804±8	4792±6	4596±7	4582±3	4384±5	4372±12	4311±13	4285±12
200	4803±10	4791±10	4598±15	4578±3	4445±34	4361±26	4299±22	4231±18
340	4805±8	4779±4	4588±11	4517±18	4443±13	4329±14	4318±10	4111±15
450	4802±6	4794±15	4585±9	4503±4	4422±27	3946±00	4284±13	<b>18.991±00</b>

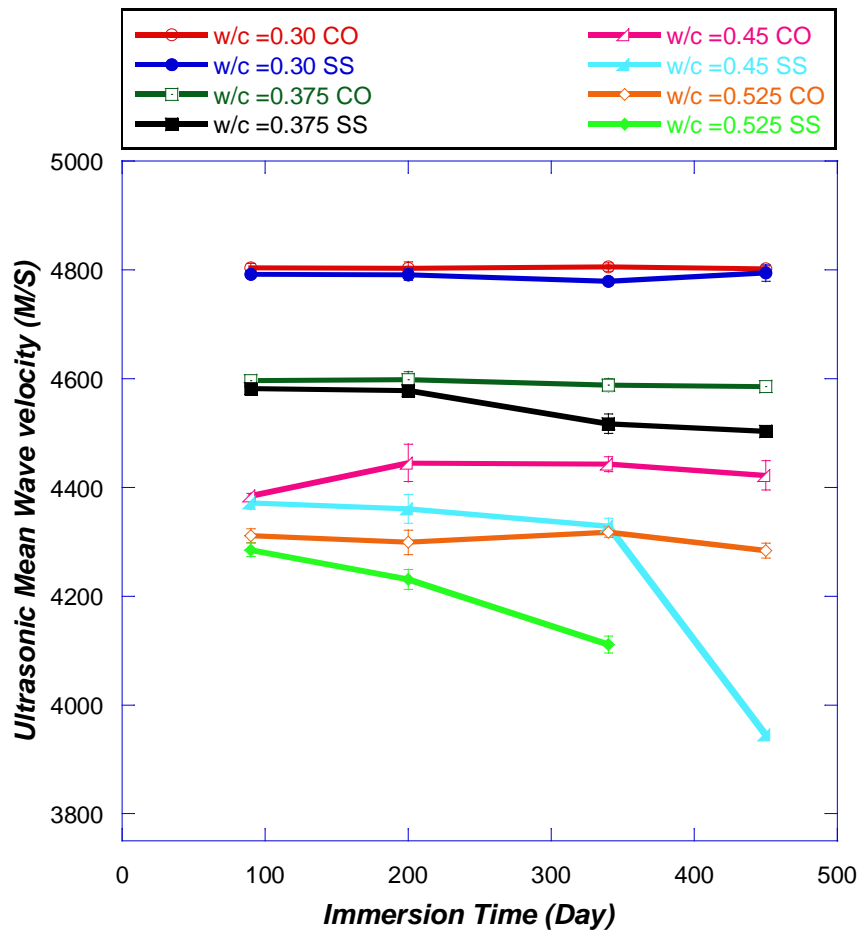


**Figure 4-41** Average of ultrasonic wave velocity obtained by UTI technique for w/c ratios 0.30, 0.375, 0.45 and 0.525, control and samples degraded by sodium sulfate.



### 4.2. Correlation the Measured Parameters for Mortar

#### 4.2.1. Correlation Ultrasonic P and S-Wave Velocity versus Porosity

Figure 4-42 and Figure 4-44 illustrate the variation of P-wave velocity versus porosity for both control and samples degraded by sodium sulfate solution. Ultrasonic wave velocity is affected by both of w/c ratio and porosity, velocity decreases as porosity and w/c ratio increase. The same trend is observed for S-wave velocity as can be seen in Figure 4-43 and Figure 4-45. The decreasing of ultrasonic wave velocity as porosity increases is also observed in a previous study by (Lafhaj et al., 2006).

By using a linear regression performed for both wave velocities (P-waves and S-waves), and to obtain the values of regression coefficient, the present equation is performed;

$$C_{p,s} = a - bx$$

The negative sign in the equation refers to the negative correlation between porosity and ultrasonic wave velocity, (an increasing in porosity causes a decreasing in the wave velocities).

Form Figure 4-8 and Figure 4-25 which illustrate the variation of porosity and P-wave with time respectively, and from the Figure 4-43 which illustrates the correlation curves of the degraded samples, it can be seen that for w/c ratio 0.525, the velocity of P-wave is decreased linearly from the initial immersion time until the end of exposure time. This decreasing in wave velocity is related to the increasing of porosity due to sulfate attack at early immersion age, and the formation of ettringite which filled the pores and caused micro-cracks, and later cracking inside the degraded mortar samples, as mentioned previously in sections 4.1.2, 4.1.4, 4.1.5 and 4.1.6.

For w/c ratios 0.45 and 0.375, when porosity of the degraded samples are compared with porosity of control samples, it is found that the porosity of both w/ c ratios increased at 90 and 200 days respectively. When P-wave velocity of the degraded samples are compared with P-wave velocity of control samples, it is found that the P-wave velocity for both w/c ratios 0.45 and 0.375 is decreased after 200 days of

#### **4. Results and discussion the Degradation Process by Sodium Sulfate Solution**

---

immersion, while for S-wave velocity (see Figure 4-26), the same trend in its variation as porosity is observed. For w/c ratio, 0.45 S-wave velocity is decreased after 90 days of the degradation and for w/c ratio 0.375, it is decreased after 200 days. Thus, as it can be seen that, in the correlation curves (see Figure 4-45) the S-wave velocity has a better correlation with porosity than P-wave velocity. In general, it can be seen that all values of the regression coefficient R are found to be higher than 0.90, which means that the measured variation of ultrasonic wave velocities versus porosity can be described by a linear relationship.

## 4. Results and discussion the Degradation Process by Sodium Sulfate Solution

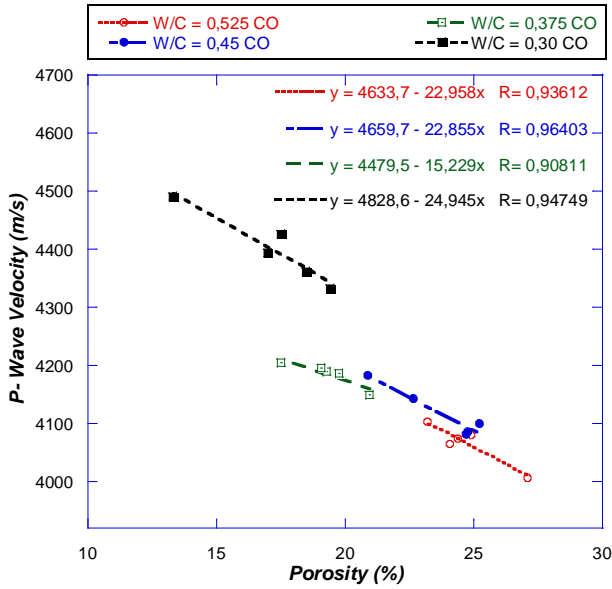


Figure 4-42 Correlation Porosity with P- wave control

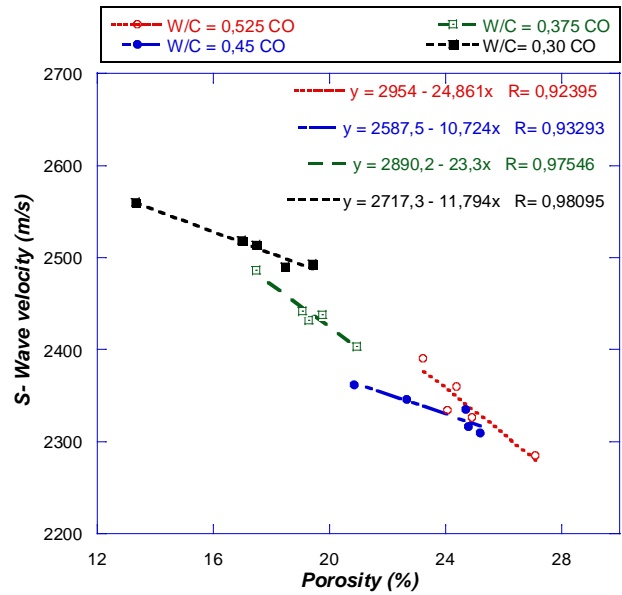


Figure 4-43 Correlation Porosity with S- wave control

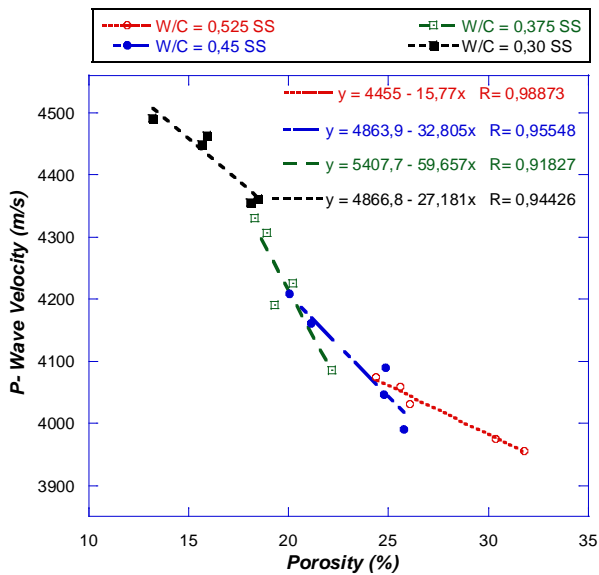


Figure 4-44 Correlation Porosity with P- wave for sodium sulfate samples

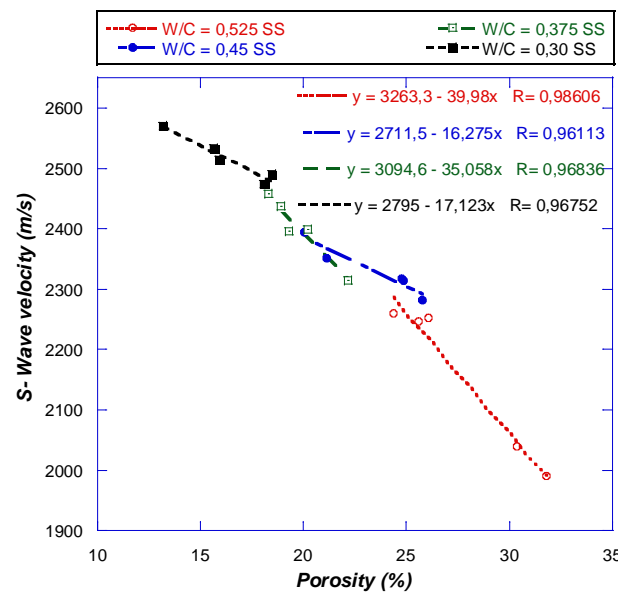


Figure 4-45 Correlation Porosity with S- wave for Sodium sulfate

### 4.2.2. Correlation Attenuation Profile Area versus Porosity

Correlation between porosity and ultrasonic attenuation profile was studied by (Fuente, 2004) to following the curing processes of mortar and cement paste. They concluded that there is a good correlation between the two variables after 28 days of cure time. A continuation to his study, the correlation between the two parameters here will be presented during the degradation process by sulfate attack.

Figures from 4-46 to 4-49 illustrate the correlation of porosity versus attenuation profile area (APA) for both frequencies 1MHz and 3.5MHz, for control and sulfate samples. From the figures, it can be seen that the general trend is increasing of APA with increasing porosity and vice versa. From the Figure 4-8, Figure 4-35 and Figure 4-36 which present the results of open porosity and the results of attenuation profile area for frequencies 1 and 3.5 MHz respectively, and also from the correlation curves for the two parameters, it can be seen that; for both frequencies 1 and 3.5MHz, the same trend is observed for w/c ratio 0.525; APA is increased from the initial immersion time until the end of exposure time. The same behaviour is observed for porosity for the same w/c ratio (0.525). Thus, it is concluded that for the high w/c ratio, the variation of porosity and attenuation profile area due to the degradation process has one step and the increasing of porosity led to increasing of APA.

On the other hand, for the other w/c ratios, the degradation process has a two steps, the first one as mentioned previously, is due to the ingress of sulfate ions and the formation of ettringite which filled the pores, this led to the decrease of porosity of the degraded samples , the rate of porosity decreasing is related to the w/c ratio, as mentioned, the decreasing of porosity due to sulfate attack will continue for a long time as w/c ratio decreases, this can be seen for w/c ratios 0.45, 0.375 and 0.30. It can be considered that at the first step, when the pores were filled completely with ettringite, the degraded samples becomes more homogeneous than control samples which have more porosity for the same w/c ratio. Thus, this may lead to the decreasing of APA at the first degradation step. The second step is deterioration due to the expanding of ettringite crystals which filled the pores, and could be due to the producing micro-cracks and

#### 4. Results and discussion the Degradation Process by Sodium Sulfate Solution

---

cracks inside the samples. Thus, in the degraded samples the increasing of porosity and APA was observed until the end of exposure time.

From the above results, it can be seen that the variation of attenuation profile area is related to the variation of porosity due to sulfate attack. All regression coefficients are more than 0.91 (see table 4.7) and this shows the strong relation between the two parameters. Also, the APA of the frequency 3.5MHz has a better correlation than the APA of the frequency 1MHz. This may demonstrate that the frequency 3.5MHz is more sensitive to the microstructural changes than the frequency 1MHz, because it has a shorter wavelength. For this reason, it can be recommended using a high frequency to estimate the degradation by using the parameter of attenuation profile area of ultrasonic waves (APA).

**Table 4-7** Regression coefficient factors for control and degraded samples for both frequencies 1 and 3.5MHz

<i>w/c ratio</i>	<i>APA of 1MHz</i>		<i>APA of 3.5MHz</i>	
	<i>R<sub>C</sub>*</i>	<i>R<sub>S</sub>*</i>	<i>R<sub>C</sub>*</i>	<i>R<sub>S</sub>*</i>
<b>0.525</b>	0.95	0.98	0.99	0.95
<b>0.45</b>	0.95	0.91	0.98	0.94
<b>0.375</b>	0.91	0.93	0.92	0.95
<b>0.30</b>	0.91	0.91	0.94	0.94

*R<sub>C</sub>\** Regression coefficient of control samples

*R<sub>S</sub>\** Regression coefficient of Sulfate samples

## 4. Results and discussion the Degradation Process by Sodium Sulfate Solution

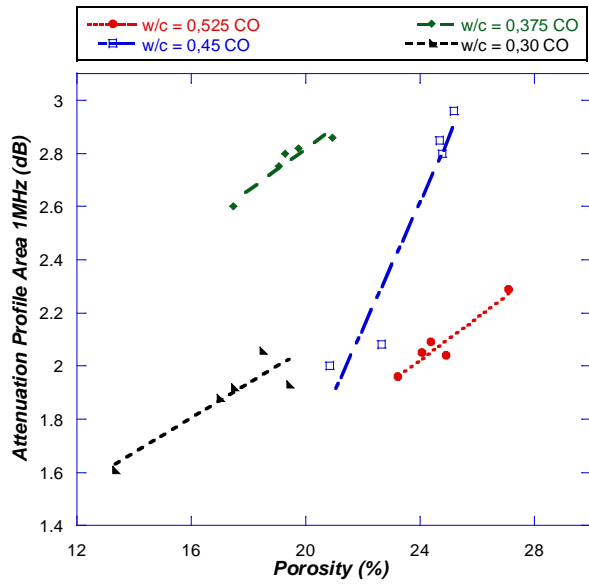


**Figure 4-46** Correlation Porosity with APA 1MHz control

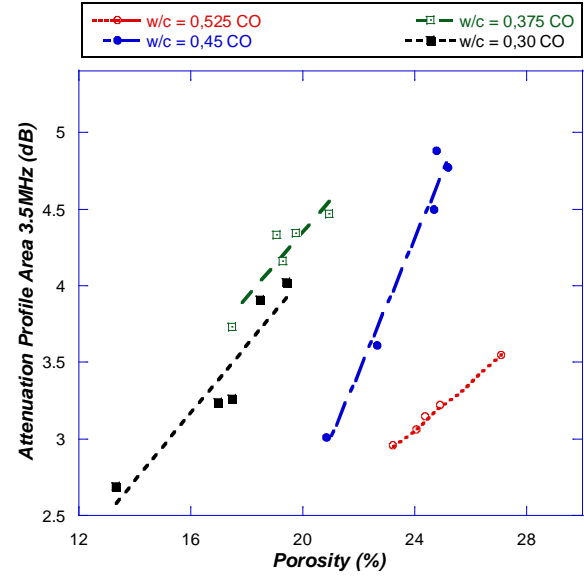


**Figure 4-47** Correlation Porosity with APA 3.5MHz control

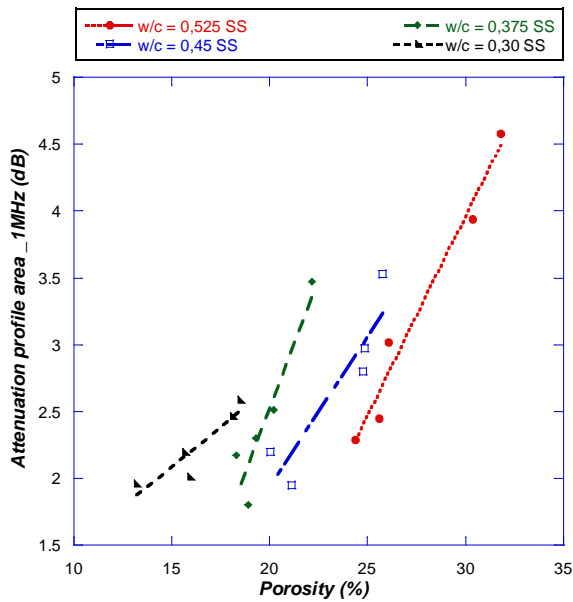


**Figure 4-48** Correlation Porosity with APA 1MHz Sodium sulfate

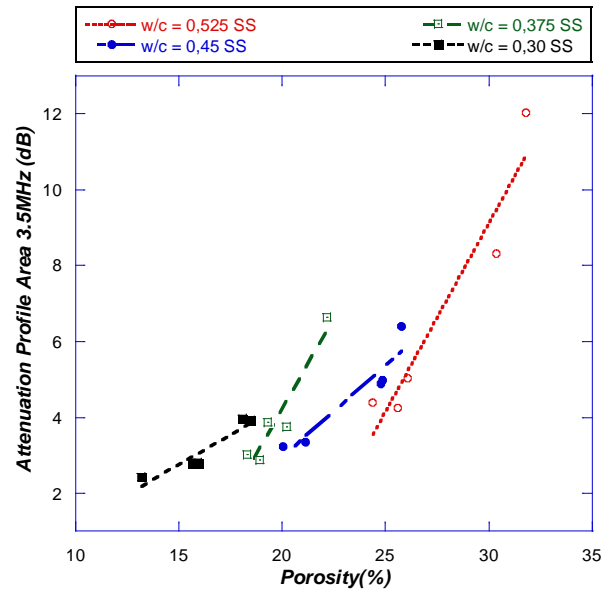


**Figure 4-49** Correlation Porosity with APA 3.5MHz Sodium sulfate

### 4.2.3. Correlation P and S-Wave Velocity versus Compressive and Flexural Strength

Compressive strength might not be the best way to represent the quality of concrete, but because a value for design is needed, it has become acceptable to all engineers that the quality of concrete as cast be determined from the value of its compressive strength. For this, correlation between ultrasonic pulse velocities (P-wave and S-wave) with compressive and flexural strength is needed. To develop such a correlation, velocity reading should be compared with strength measured by an accurate method. But unfortunately, a perfect method does not exist or not yet known. When cubes or cylinders are cast from a mortar or concrete mix or when cores are taken from an existing structure, an assumption is immediately made that these are representative samples. Then, when samples are mechanically crushed, the following three factors at least come into effect (for the same age of concrete). First, sample size; second the non-uniform compression or capping and third the performance of mechanical crushing machine. On the other hand, the ultrasonic pulse velocity values are affected by number of factors, which do not necessary influence the concrete compressive strength in the same way or to the same extend (Gregor et al., 2009).

In this section, the correlation between the ultrasonic wave velocities P and S-waves versus compressive and flexural strength will be presented. In general, it was observed that both of P and S-wave increase with the increasing of strength.

Figures from 4-50 to 4-53 illustrate the correlation curves of compressive strength versus P and S-wave velocity, for both control and degraded samples. For control samples, it can be seen that the wave velocity of both P and S- wave has the same trend of relationship with the compressive strength, increasing of ultrasonic waves as compressive strength increases. As can be seen in the figures, the regression coefficients are not always showing the good correlation between the two parameters, it shows a good correlation with some w/c ratios, while shows a bad correlation with others, this could be due to the reasons mentioned above. In other words, P and S-waves show a

#### 4. Results and discussion the Degradation Process by Sodium Sulfate Solution

---

better correlation coefficient for degraded than the control samples, and also for higher w/c ratios especially 0.525, than the lower w/c ratios.

For degraded samples, from Figure 4-51 and Figure 4-53 which illustrate the correlation curves of compressive strength versus P and S- wave respectively, it is found somehow a good relationship between the two parameters as the regression coefficients show. Thus, for degraded samples, when samples are exposed to sulfate, at early ages of immersion, the crystallization of salts performed ettringite and calcium sulfate may fill the micro-cracks and pores. This will lead to an increase in elastic modulus and therefore, an increasing in both strength and ultrasonic wave velocity. This increasing varies depends on w/c ratio. However, as exposure time goes on, the expansion of ettringite and calcium sulfate results in an increase in micro-cracks. This would lead to decrease in the elastic modulus and so, both strength and wave velocity will decrease. It can be said that when the degradation takes place in the degraded samples, the relationship between the compressive strength and ultrasonic wave velocity will be clear.

In summary, from the previous paragraph, for the correlation between wave velocity and strength, it is found a good relationship between the two parameters when the changes in the microstructure of mortar and concrete are clear, as the case of early ages mortar microstructure development and when the samples are degraded by aggressive elements such as sulfate.

Figures from 4-54 to 4-57 illustrate the correlation curves of P and S-wave versus flexural strength for both control and degraded samples. For control samples (see Figure 4-54 and Figure 4-55), all values of correlation factors are higher than 0.72 which shows a good relationship between the flexural strength and ultrasonic wave velocities (P and S-waves). For degraded samples (see Figure 4-56 and Figure 4-57), it can be seen that the values of regression coefficients are decreasing as w/c ratio decreases, this trend was observed for both P and S-waves for the degraded samples. In general, the results indicate that the ultrasonic wave velocity correlates better with



#### 4. Results and discussion the Degradation Process by Sodium Sulfate Solution

flexural strength than compressive strength. This may show that flexural strength is more sensitive to follow the microstructural changes than compressive strength.

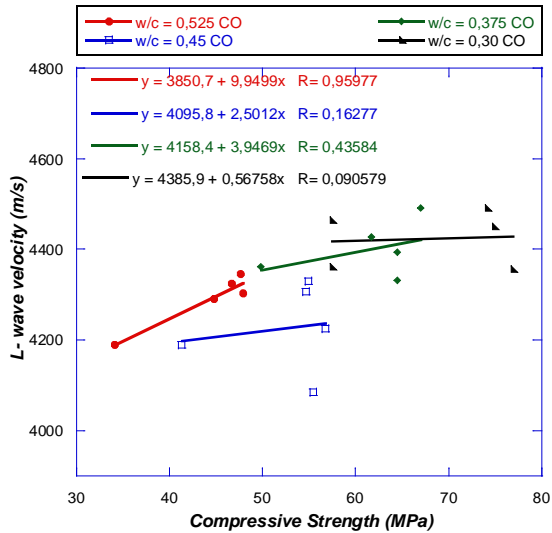


Figure 4-50 Correlation compressive strength with P-wave control

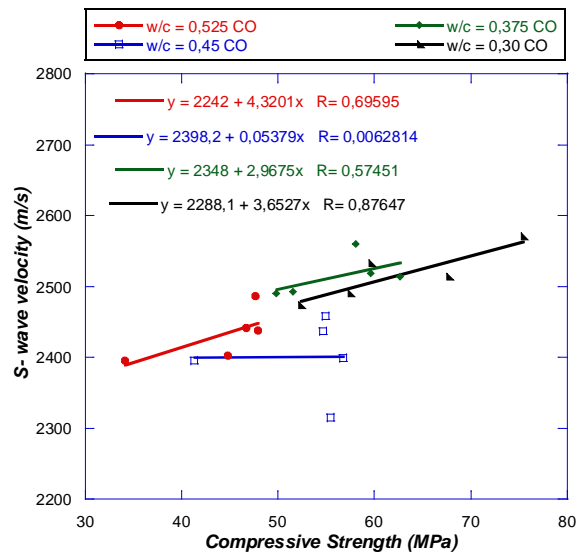


Figure 4-51 Correlation compressive strength with S-wave control

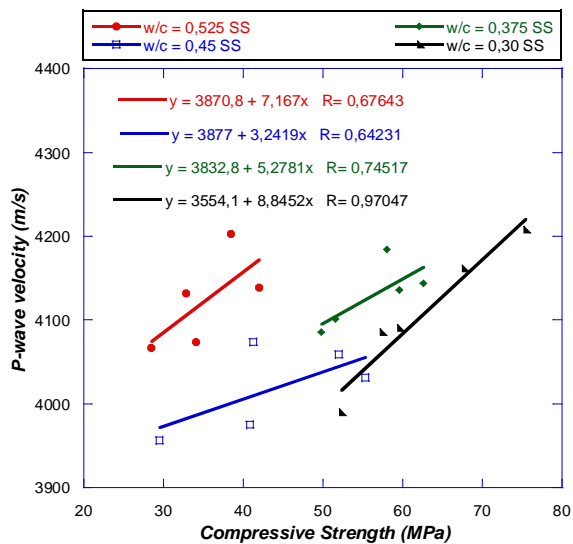


Figure 4-52 Correlation compressive strength with P-wave Sodium sulfate

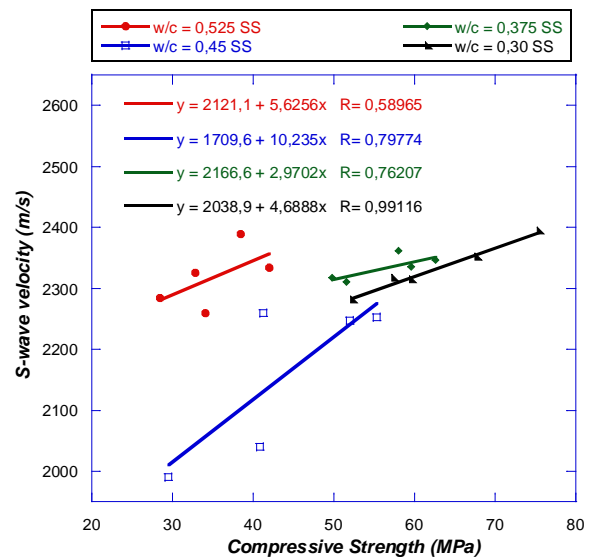
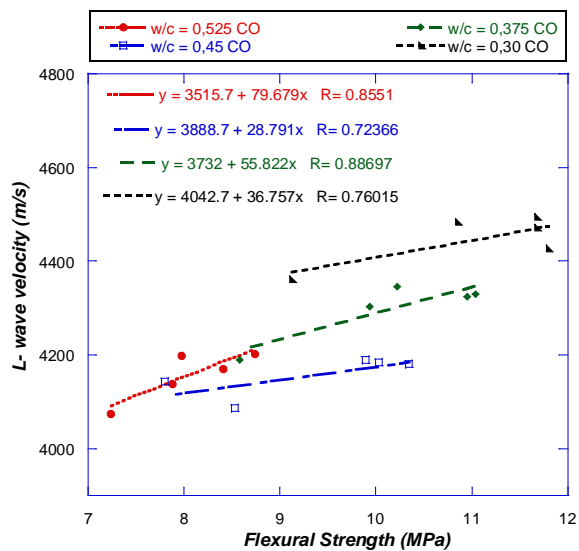
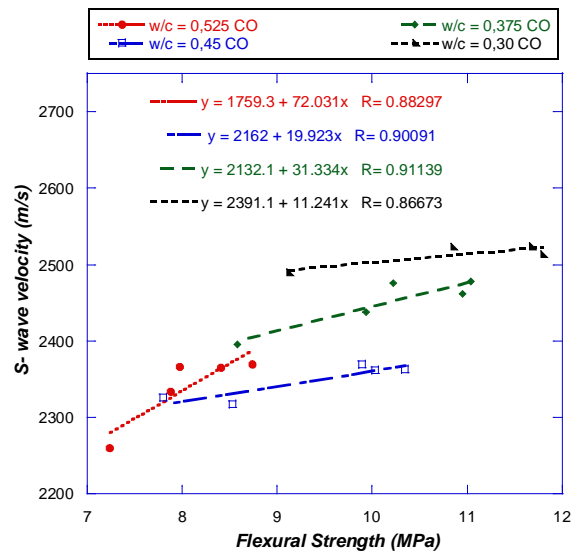


Figure 4-53 Correlation compressive strength with S-wave Sodium sulfate

## 4. Results and discussion the Degradation Process by Sodium Sulfate Solution



**Figure 4-54** Correlation flexural strength with P-wave control



**Figure 4-55** Correlation flexural strength with S-wave control

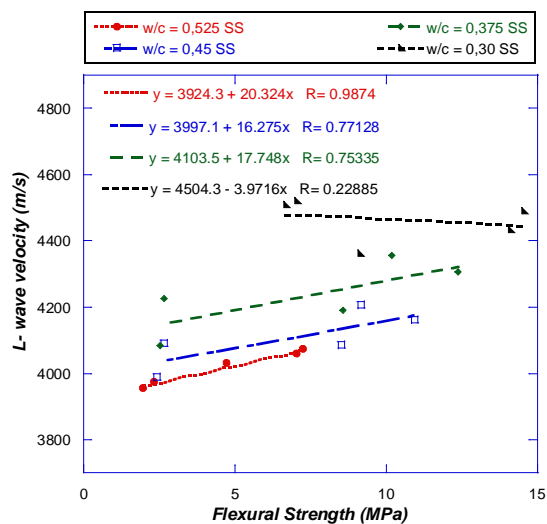


**Figure 4-56** Correlation flexural strength with P-wave Sodium sulfate

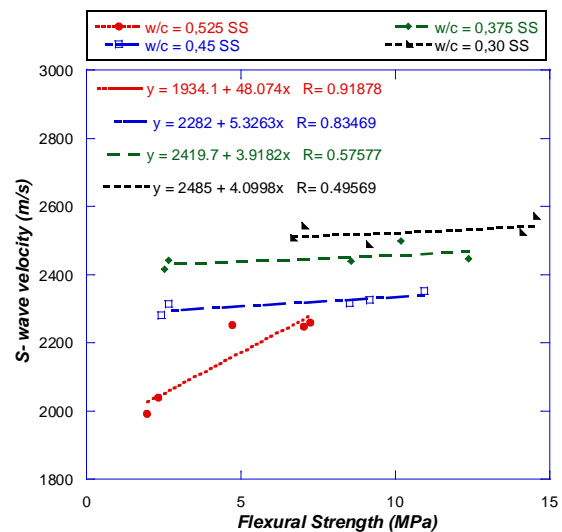


**Figure 4-57** Correlation flexural strength with S-wave Sodium sulfate

### 4.2.4. Correlation Attenuation Profile Area versus Compressive and Flexural Strength

From Figures 4-58 to 4-61 illustrate the correlation of compressive strength with attenuation profile area for frequencies 1MHz and 3.5MHz for control and samples degraded by sodium sulfate solution. It is observed that the attenuation profile area is increasing as compressive strength decreases. For control samples, the same trend is observed as the correlation of strength with ultrasonic wave velocity (as can be seen in Figure 4-58 and Figure 4-59).

For the degraded samples, the compressive strength correlates with APA for both frequencies. This is because of the high level of changing in the microstructure of the degraded samples, due to the formation of ettringite which filled the pores and its increase in the volume with time causes micro-cracks and cracks. This caused a decreasing in the strength of the degraded mortar samples which leads to increasing of the attenuation profile area of ultrasonic waves.

Figures from 4-69 to 4-72 illustrate the correlation curves of flexural strength versus APA of both frequencies 1 and 3.5MHz for both control and degraded samples. It can be seen that for control samples as sulfate samples, the flexural strength has a good relationship with APA, also this trend is observed when flexural is correlated with P and S-waves.

It is known that flexural strength is typically used in Portland cement concrete because it simulates better beam flexural stress as they are subjected to loading. Flexural strength results are sensitive to many factors, including fabricating, curing and loading of the beams. May be for these reasons, flexural strength has a better relationship than compressive strength with the parameters of ultrasonic waves (velocity and attenuation profile area).

## 4. Results and discussion the Degradation Process by Sodium Sulfate Solution

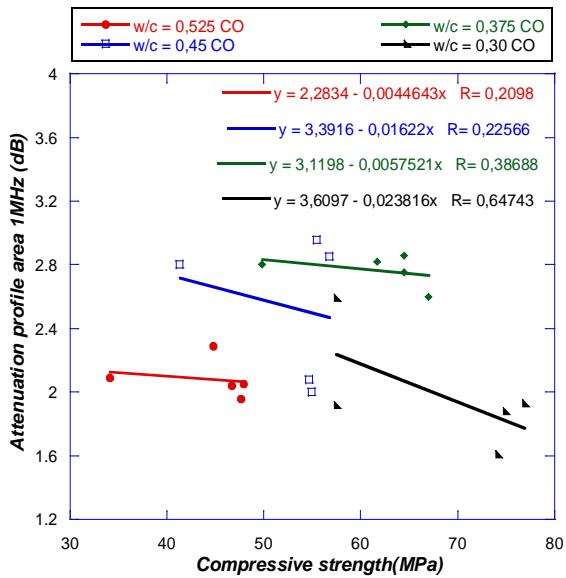


Figure 4-58 Correlation compressive strength APA 1MHz control

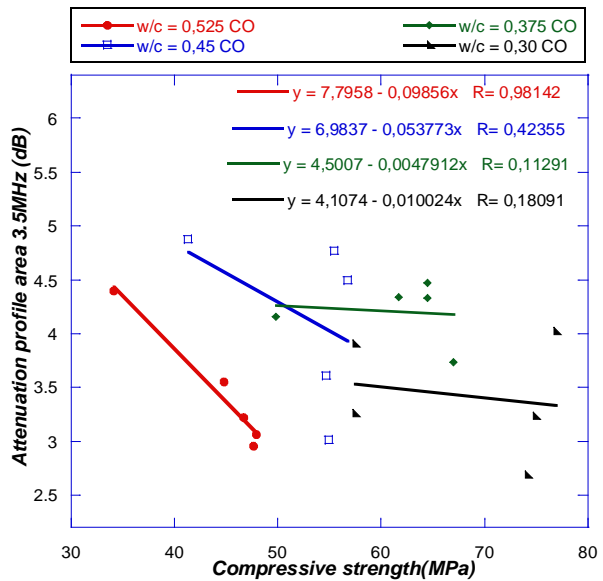


Figure 4-59 Correlation compressive strength with APA 3.5MHz control

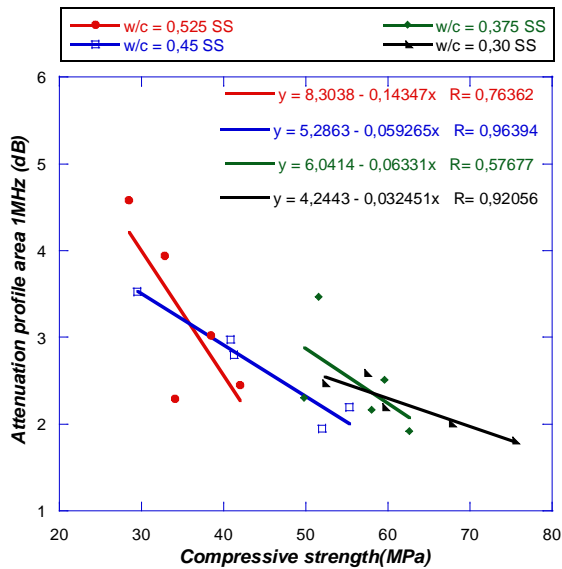


Figure 4-60 Correlation compressive strength with APA 1MHz Sodium sulfate

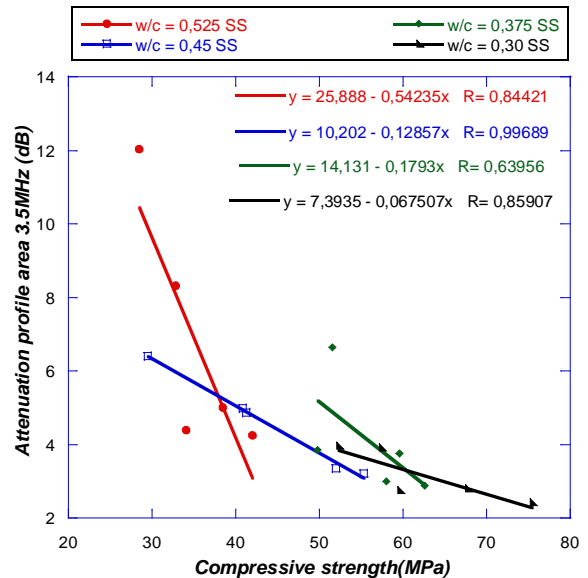
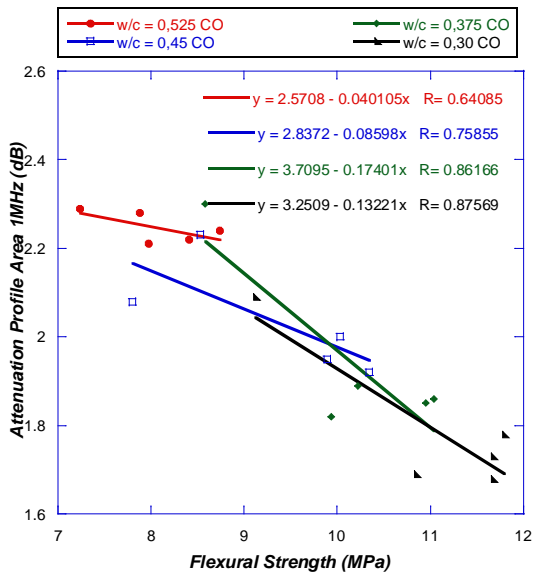
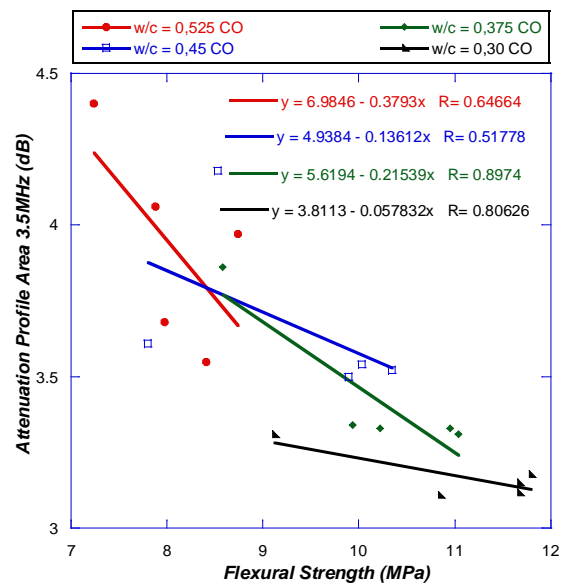


Figure 4-61 Correlation compressive strength with APA 3.5MHz Sodium sulfate

## 4. Results and discussion the Degradation Process by Sodium Sulfate Solution



**Figure 4-62** Correlation Flexural strength with APA 1MHz control



**Figure 4-63** Correlation Flexural strength with APA 3.5MHz control

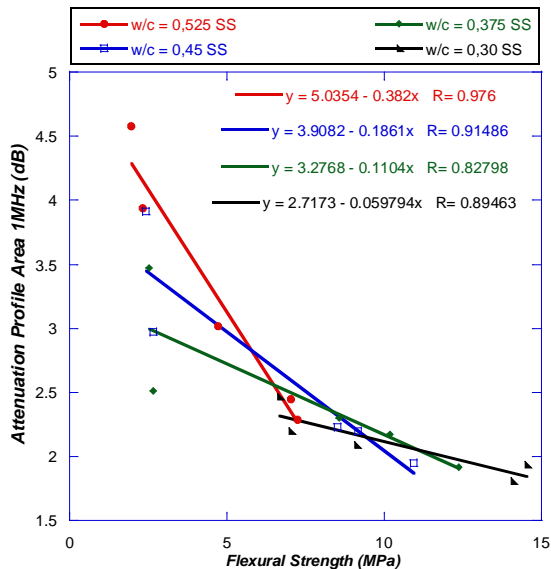


**Figure 4-64** Correlation Flexural strength with APA 1MHz Sodium sulfate

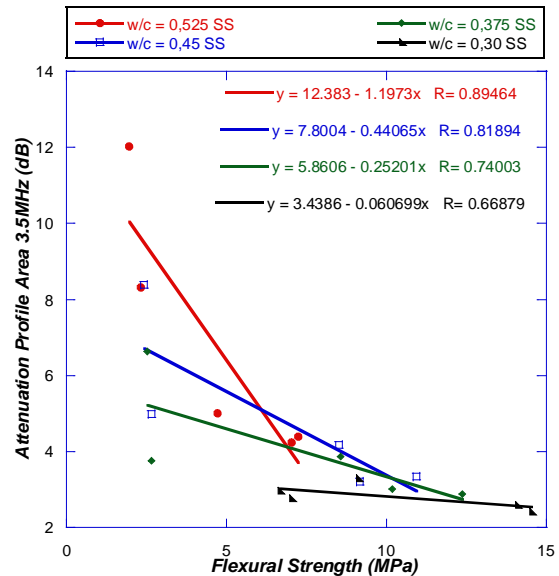


**Figure 4-65** Correlation Flexural strength with APA 3.5MHz Sodium sulfate

### 4.2.5. Correlation P and S-Wave Velocity versus APA

In the previous sections, it was presented the correlation between destructive tests versus the non-destructive tests. In this section it will be presented the correlation between the ultrasonic wave velocities of shear and longitudinal waves obtained by ultrasonic transmission-reception method versus the attenuation profile area of ultrasonic waves for both frequencies 1 and 3.5MHz obtained by ultrasonic grain noise method.

Figures from 4-66 to 4-69 illustrate the correlation of P-wave versus attenuation profile area for both frequencies 1 and 3.5MHz. From the figures, for both control and samples degraded by sodium sulfate, it is found a good negative relationship between the longitudinal wave velocity and attenuation profile area APA. As can be observed the APA decreases with the increasing of P-wave velocity. This was showed previously when both of P-wave velocity and APA was presented with the degradation time (see sections 4.1.6 and 4.1.7). Also as mentioned in sections (4.2.3 and 4.2.4 ) that the degradation by sulfate attack has two steps. The first one is filling the pores by ettringite, and during this stage it is observed increasing of wave velocity and decreasing of APA. The second stage is the degradation which caused the decreasing of velocity and increasing of attenuation profile area. This reflects that both of wave velocity and APA is sensitive to the microstructural changes due to the sulfate attack. The same trend is observed with S-wave when it is correlated with APA (see Figure 4-70 to Figure 4-73).

In general terms, and regarding all the experiments and correlations, it is concluded that the S-wave velocity and the APA 3.5 MHz were showed the best correlation values for degraded samples. Also, the APA 1MHz and P-wave velocity get more apparent fitted curves for control or lower w/c. The flexural strength values show a better correlation with ultrasonic parameters, especially with S-wave as it is expected.

## 4. Results and discussion the Degradation Process by Sodium Sulfate Solution

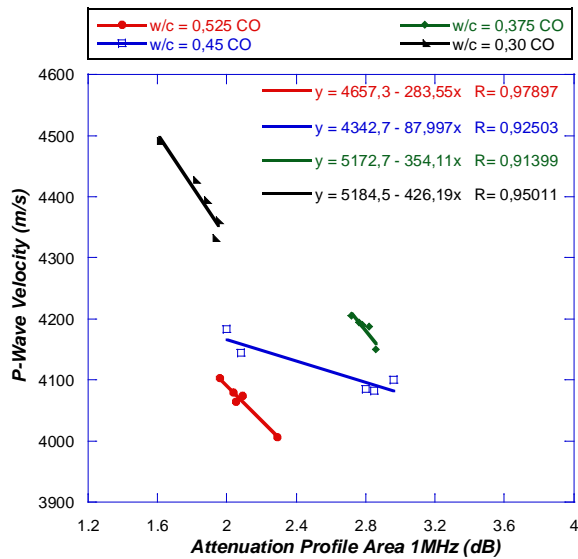


**Figure 4-66** Correlation P-Wave with APA 1MHz control

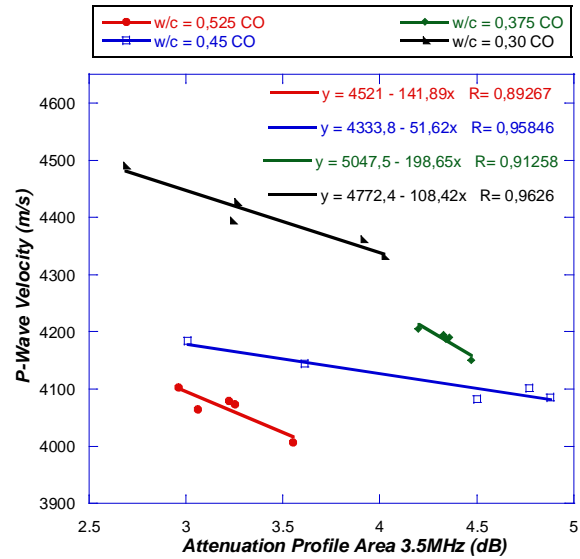


**Figure 4-67** Correlation P-Wave with APA 3.5MHz control

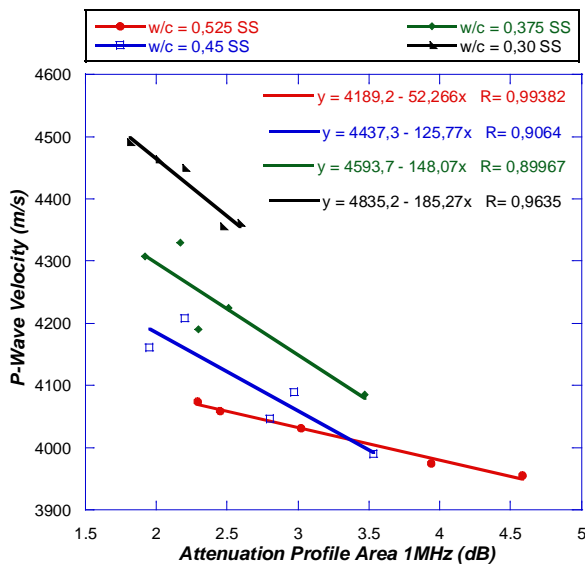


**Figure 4-68** Correlation P-Wave with APA 1MHz Sodium sulfate

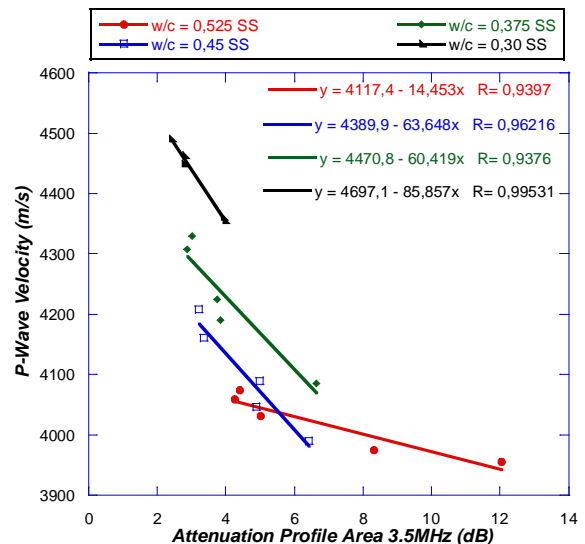


**Figure 4-69** Correlation P-Wave with APA 3.5MHz Sodium sulfate

## 4. Results and discussion the Degradation Process by Sodium Sulfate Solution

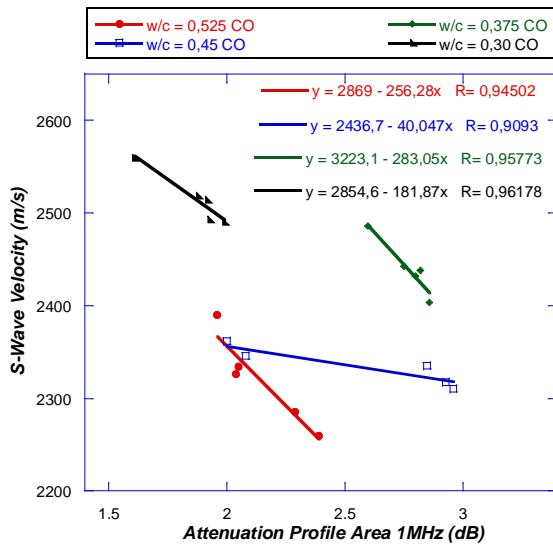


**Figure 4-70** Correlation S-Wave with APA 1MHz control

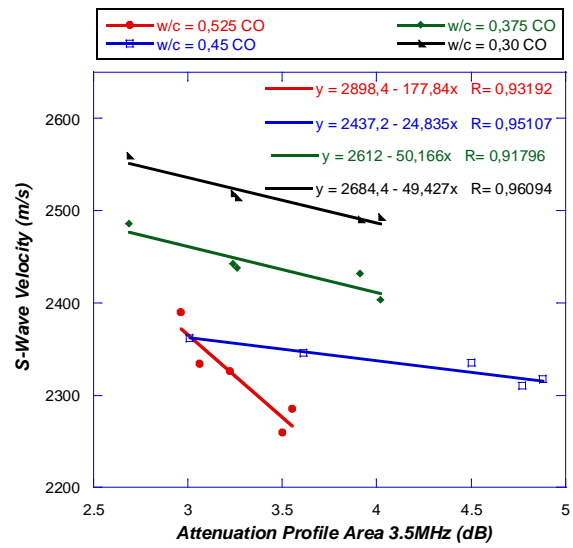


**Figure 4-71** Correlation S-Wave with APA 3.5MHz control

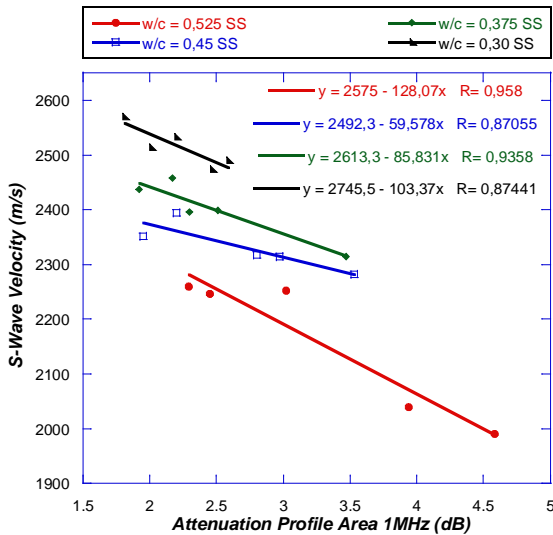


**Figure 4-72** Correlation S-Wave with APA 1MHz Sodium sulfate

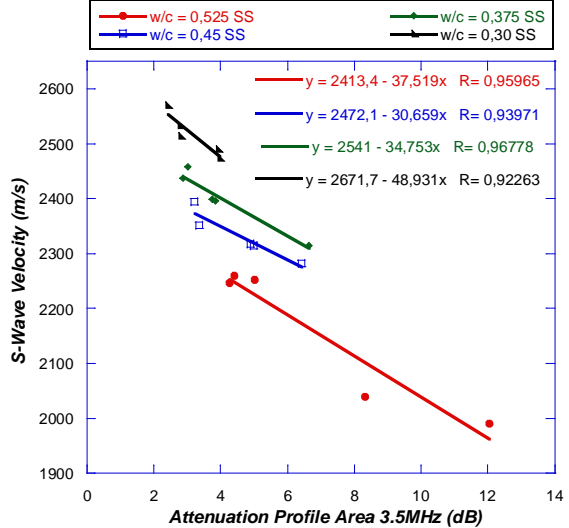


**Figure 4-73** Correlation S-Wave with APA 3.5MHz Sodium sulfate



### 4.3. Analysis and Discussion the Results of Concrete

#### 4.3.1. Scanning Electron Microscopy (SEM)

As mentioned previously that scanning electron microscopy test (SEM) is realized to observe the changes which occur in the microstructure of mortar and concrete samples due to the penetration of aggressive elements. This helps understanding and interpreting the behaviour of ultrasonic waves when interacts with the microstructure of the degraded cement-based materials. Also, it helps understanding and interpreting the result of destructive tests. In this section, the following of microstructural changes and sulfate ion penetration depth are studied, for the two types of precast concrete under investigation, sulfate resistant Portland cement (SRPC) and Portland-limestone cement (PLC).

Figures 4-74 and 4-75 illustrate the SEM results of LPC concrete samples immersed for 220 and 470 days in 10% sodium sulfate solution. The samples are studied from outside surface towards its centre; many points are tested at different distances. Figure 4-74 presents the results of a sample degraded for 220 days, three points are tested, the first point falls at distance of 5.231mm from the surface of the sample, as can be seen in fig (A) deposits of ettringite are filled an air void, fig (B) shows the EDS spectrum which indicates the relative Al, S and Ca peak intensities expected for ettringite. The second point falls at distance of 6.857 mm from the surface (see fig c), it can be observed formation of a network of cracks which produced due to the expansion of ettringite. To follow the penetration of sulfate ion into the sample, the third point is selected at distance of 17.751 mm from the surface, as it can be seen in fig (D), deposited of ettringite fills the pore void and caused distress which lead to cracks produced, fig (F) shows the EDS spectrum indicates the relative Al, S and Ca peak intensities expected for ettringite. From these results, it was found that after 220 days of immersion in sodium sulfate solution, the sulfate ions are penetrated the PLC samples, and ettringite was formed until depth of 17.751 mm or more.

#### 4. Results and discussion the Degradation Process by Sodium Sulfate Solution

---

By the continuation of the process of the degradation, Figure 4-75 (A, B, C, D, E and F) illustrates the SEM results of a sample degraded for 470 days, by the same way, as presented the result of 220 days degraded sample, also different points from the surface to the centre of the samples are studied. Figure 4-75 (A, C, E and F) shows that, deposits of ettringite filled the pores and cavities of the specimen at distances 2.203, 8.718, 21.815 and 23.613 mm, respectively from the attacked surface of the sample. Figure 4-75 (B and D) shows the EDS spectrum analysis which indicates the relative Al, S and Ca peak intensities expected for ettringite. Although the maximum depth studied was 23.613 mm from the attacked surface, but may be the penetration of sulfate ions is higher than this depth.

Figure 4-76 (A and B) illustrates SEM results of SRPC samples degraded for 220 and 470 days, respectively. Figure A shows the results of a point falls at distance of 2.832mm from the attacked surface, and figure B is for a point falls at 2.052mm from the core surface. Both of figures A and B have a pore void, and it is not formed aggressive products inside the pores, as ettringite for example. Also, it is not produced cracks until 470 days of immersion in sodium sulfate solution.

From the presented SEM results for both concrete types (SRPC and PLC), the difference between the degradation level of them due to the attack by sodium sulfate solution are explained. For SRPC samples, no signs of degradation are observed, this is due to; first, the low water-cement ratio used, which reduced the concrete permeability, and second, the low amount of  $C_3A$ . By using Bogue's equations in which the chemical formula present the mass% of each oxide, it is found that the amount of  $C_3A=1.7\%$ ,  $C_2S=16.13\%$  and  $C_3S=76.56\%$ , it can be seen the low amount of  $C_3A$ , on the other hand, the ratio  $C_3S/C_2S$  found to be =4.75 which lead to a high sulfate resistance.

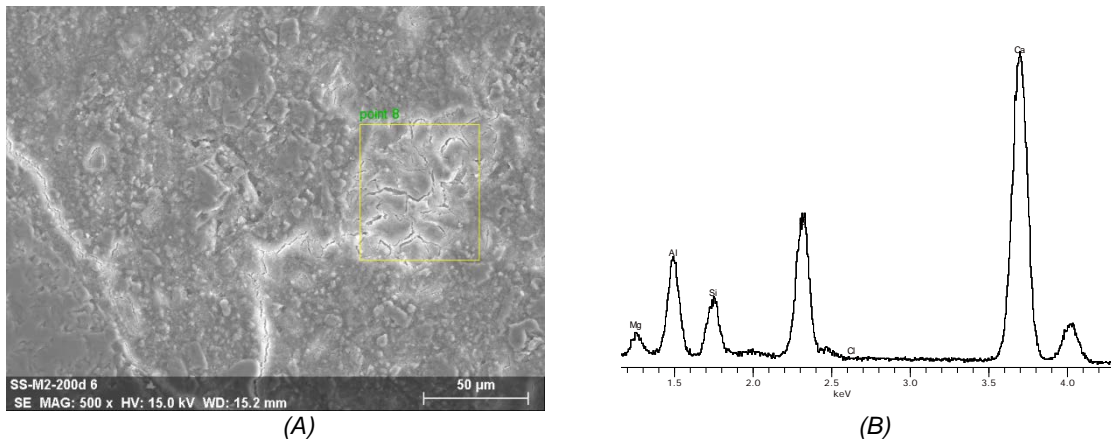
Sahmaran et al (2007) concluded that expansion results at the end of 104 weeks of immersion cement paste in a 5% sodium sulfate solution showed that (SRPC) with high  $C_3S/C_2S$  ratio of 18.3% has a relative poor sulfate resistance. Thus, for limestone Portland cement (LPC) used in this study and also by using using Bogue's equations, it is

#### 4. Results and discussion the Degradation Process by Sodium Sulfate Solution

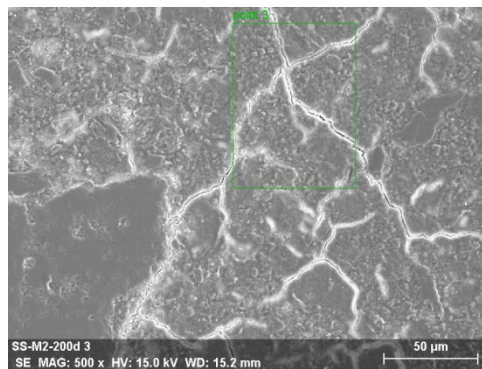
---

found that the amount of  $C_3A=7.1\%$ ,  $C_2S=4.27\%$  and  $C_3S=85.21\%$ , it can be observed a high amount of  $C_3A$ . On the other hand, the ratio  $C_3S/C_2S$  found to be  $=19.96$  which lead to a poor sulfate resistance and causing samples degradation. Based on the microstructural observations LPC concrete samples exposed to sodium sulfate solution. It can be said that ettringite forms in the surface layer, which leads to cracking in this layer and to a lower amount of cracking, in the subsequent layers into which sulfate ions have not ingressed yet. Then, when ettringite is formed in this second layer, it induces cracking in the next non-invaded layer, whereas its own expansion is being restrained by the presence of the third layer and so on (Thansanam and Cohen, 1998).

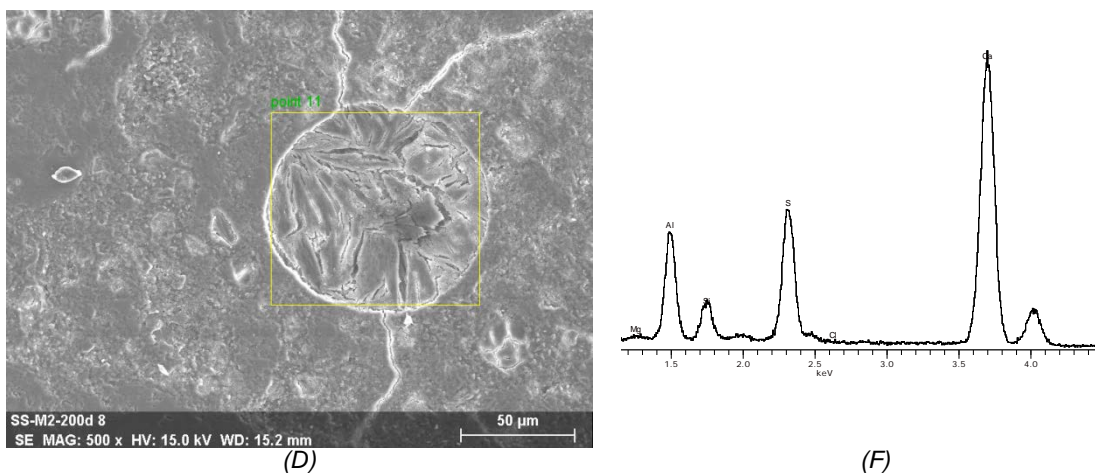
#### 4. Results and discussion the Degradation Process by Sodium Sulfate Solution



(A) ettringite mass deposited in an air void which falls at distance of 5.231mm from the surface of the sample, (B) The EDX spectrum is characteristic for ettringite.



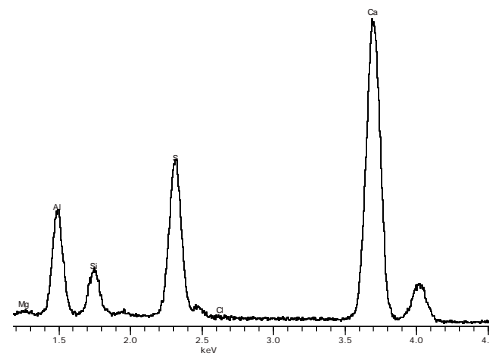
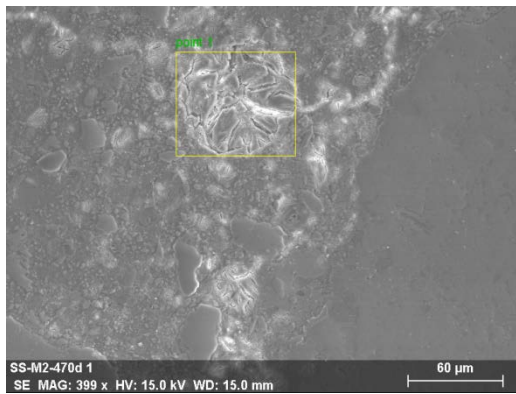
(C) An image illustrate the micro-cracks produced by the effect of ion sulfate penetration for a point falls at distance 6.857mm from the attacked surface



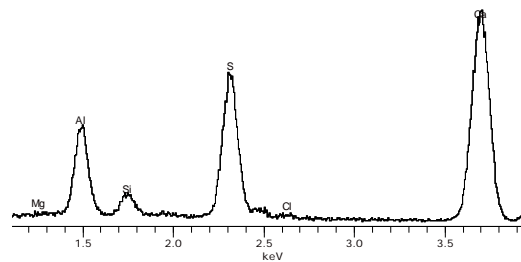
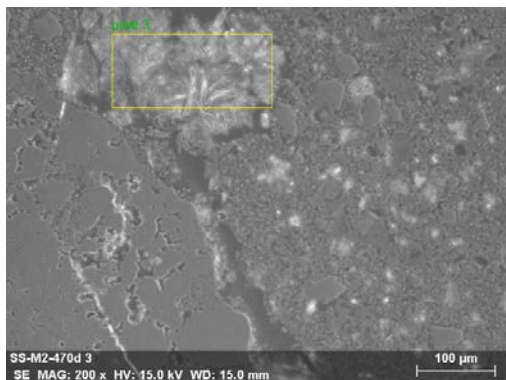
(A) Ettringite mass deposited in an air void which falls at distance of 17.751mm from the surface of the sample, (F) The EDX spectrum is characteristic for ettringite.

**Figure 4-74** Scanning electron micrograph and EDS of CEM II A-L 42.5R concrete specimens exposure to 10% of sodium sulfate solution for 220 days.

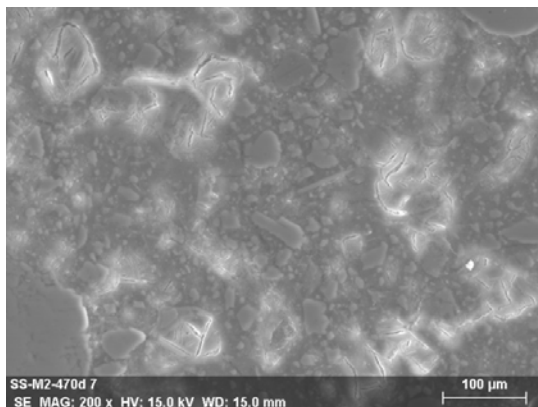
#### 4. Results and discussion the Degradation Process by Sodium Sulfate Solution



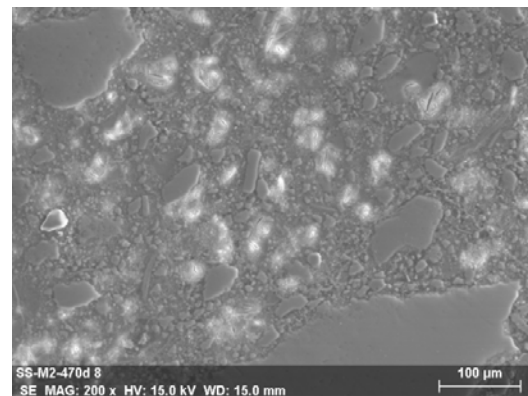
(A) Point (1)- at distance 2.203mm from the sample surface (B)



(C) Point (3)- at distance 8.718 mm from the sample surface (D)



(E) Point (7)-At distance 21.815 mm from the sample surface

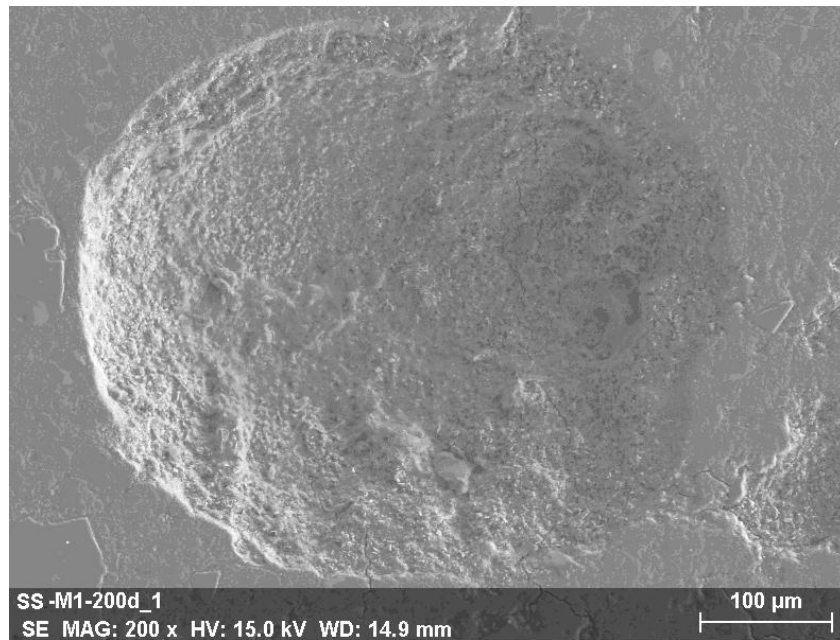


(F) Point (8)- at distance 23.613 mm from the sample surface

**Figure 4-75** Scanning electron micrograph and EDS of CEM II A-L 42.5R concrete specimens exposure to 10% of sodium sulfate solution for 470 days.

#### 4. Results and discussion the Degradation Process by Sodium Sulfate Solution

---



(A) A point falls at distance 2.832mm from the sample surface after 220 days of degradation



(B) A point falls at distance 2.052mm from the sample surface after 470 days of degradation

**Figure 4-76** Scanning electron images for CEM I 42.5R/SR concrete specimens exposure to 10% of sodium sulfate solution for 220 and 470 days.

### 4.3.2. Compressive Strength

The evolution of the compressive strength of concrete specimens placed in sodium sulfate solution is shown in Figure 4-77. It is observed that for control samples for both cement types, the compressive strength is increased slightly until the end of exposure time.

In the case of sulfate samples, for LPC samples, it is observed that at 220 days of immersion the strength of sulfate samples is higher than that of control samples, this increasing in the strength may be due to the ettringite formation inside the pores is in progress, this causes a decrease in porosity and an increase in compressive strength. And after 220 days, a drop in the decreasing of strength is observed until the end of exposure time, this is due to degradation which occurs due to the generation of expansive stresses in the paste component, which develop progressively from the surface. These expansive forces cause a macroscopic expansion of the sample, which at first expands progressively, but at a certain point, when the strength of the unaltered core is unable to withstand the forces from the expanding surface, a progressive mechanical failure of the sample starts with a corresponding rapidly increasing rate of expansion. The formation of cracks around aggregates also opens up the microstructure to penetration of the sulfate solution. For the SRPC degraded samples, the variation in the strength is between increasing and decreasing from the first day until the end of immersion time. This reflects that the samples fabricated by SRPC cement have a good resistance for sulfate ions penetration as showed previously by SEM analysis.



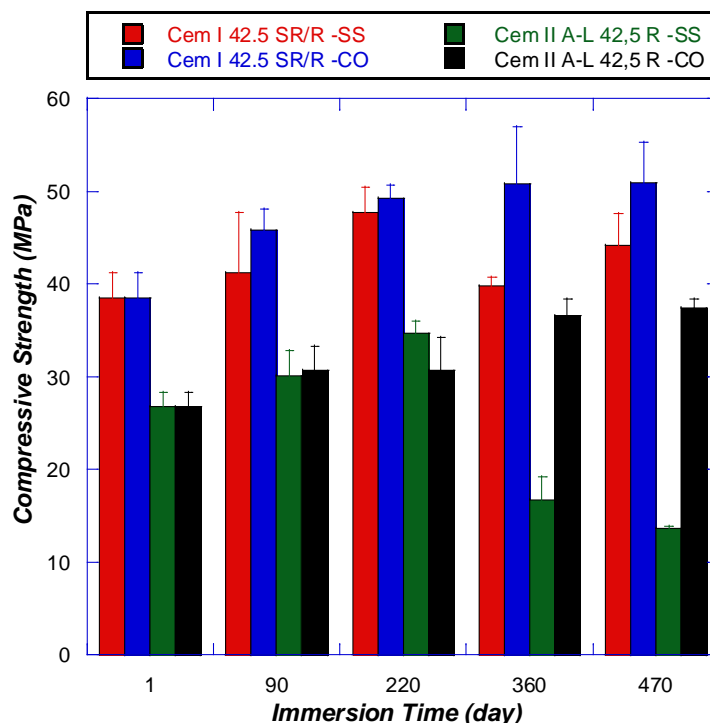


Figure 4-77 Compressive Strength of concrete with time

### 4.3.3. Open Porosity

Figure 4-78 illustrates the results of open porosity for control and samples degraded by sodium sulfate for 470 days. As it can be seen for SRPC samples, when porosity of control samples compared with porosity of degraded samples, almost no/or slightly variation is observed during all the degradation period, and the values of porosity of both of them are similar. This as mentioned previously, due to the low percentage of  $C_3A$  and the low  $C_3S/C_2S$  ratio which led to resistant the penetration of sulfate ions into the samples, for this reasons the degraded SRPC samples tend to have the same trend as control samples.

For LPC samples, it can be seen that the porosity of the degraded samples are decreased than porosity of control samples up to 220 days of immersion, thereafter a drop in the increasing of porosity is observed until the end of exposure time. As showed in SEM



#### 4. Results and discussion the Degradation Process by Sodium Sulfate Solution

results, the surface layers of the sample are filled by ettringite, and may be before 220 days of degradation, the voids of these layers are completely filled with ettringite but cracks do not produced yet, this led to the decreasing of porosity. By a continuation of sulfate ions penetration to the next layers, the rate of penetration may be lower than the surface layers, and on the same time the ettringite is expanded inside the pores and caused cracking in the surface layers which finally led to the increasing of porosity until the end of exposure time. This trend is also observed as explained in details previously in the mortar result sections.

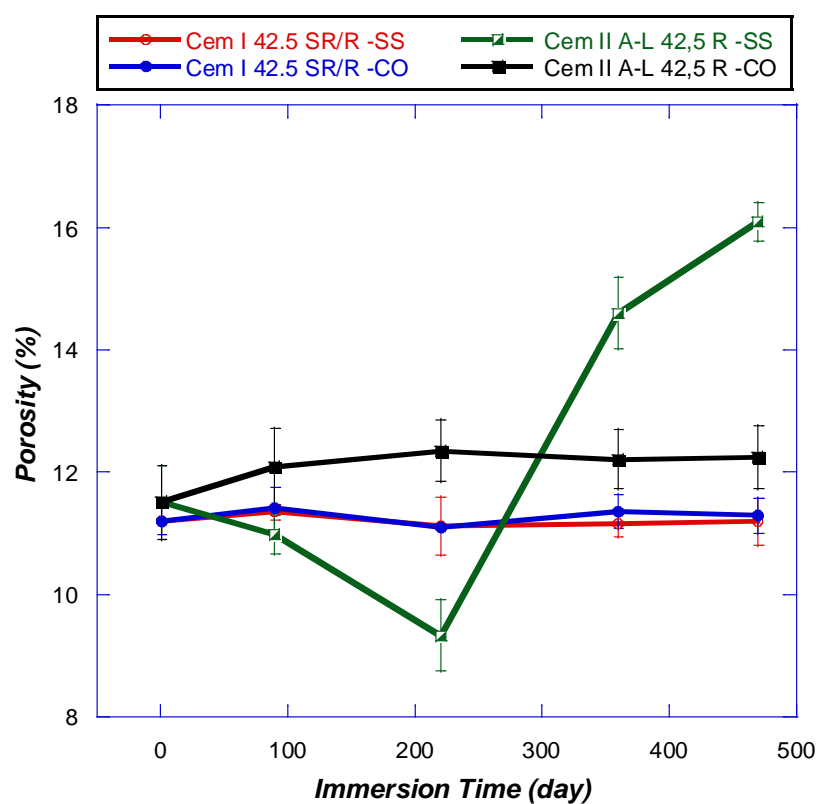


Figure 4-78 Porosity of concrete with time

#### 4.3.4. Ultrasound Longitudinal and Transversal Wave Velocity

Figure 4-79 illustrates the variation of P-wave velocity with time for control and degraded samples. As can be seen for SRPC the variation of P-wave velocity indicates that both of control and the degraded samples almost have the same ultrasonic wave

#### 4. Results and discussion the Degradation Process by Sodium Sulfate Solution

velocity, and the variation of velocity with time shows that the SRPC samples is not affected by the sodium sulfate attack.

On the other hand, for LPC samples when the velocity of ultrasonic waves of control samples compared with that of degraded samples, it can be seen that P-wave velocity of the degraded PLC samples is decreased after 90 days of immersion until the end of exposure time.

For S-wave velocity as can be seen in Figure 4-80 for control samples similar trend is observed as P-wave velocity, the variation of ultrasonic wave velocity from the start until the end of exposure time shows no degradation for SRPC. As can be seen for LPC an increasing in S-wave velocity up to 90 days, after that it is decreased until the end of exposure time. This is due to the ettringite formation as showed by SEM examination. Thus, ultrasonic wave velocity measurements confirmed the results obtained by SEM analysis, which demonstrated that the ettringite is formed only in LPC samples.

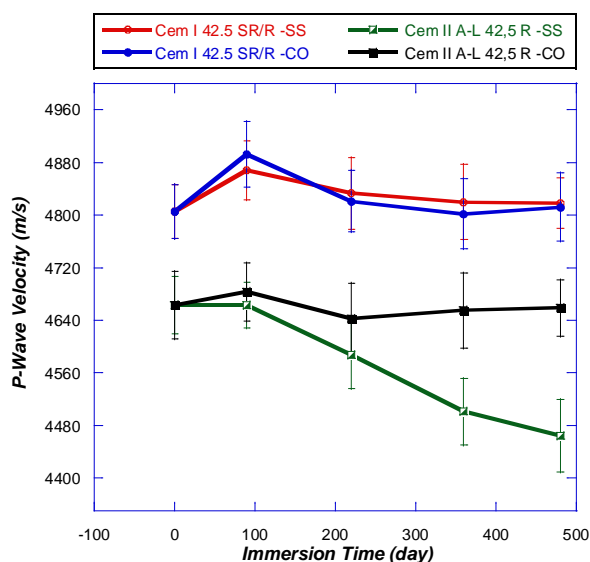


Figure 4-79 P-wave velocity with time

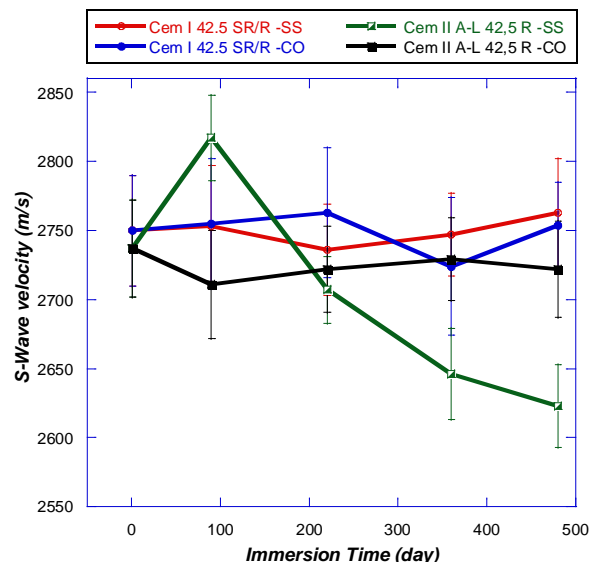


Figure 4-80 S-wave velocity with time

### 4.3.5. Ultrasonic Attenuation Profile Area (APA)

By the effect of the internal variation of the microstructure of concrete due to the degradation by sodium sulfate solution for 90, 220, 360 and 470 days, the variation in the penetration of ultrasonic pulse can be seen in the Figures from 4-81 to 4-84. For LPC degraded samples it can be seen that, for frequency 1MHz (see Figure 4-83) the penetration of ultrasonic pulse increased up to 220 days of immersion thereafter, it was decreased until the end of exposure time. The same trend was observed for frequency 3.5MHz (see Figure 4-84), but is observed that the penetration of ultrasonic pulse for frequency 1MHz is more than the penetration of frequency 3.5MHz. The increasing of penetration of ultrasonic pulse up to 220 days is attributed to the formation of ettringite as observed previously by SEM analysis. And the decreasing of it until the end of exposure time may be attributed to the producing of cracks and micro cracks in the surface layers. It was found by SEM analysis that ettringite was formed at 23.613 mm from the surface, so it is expected that the surface layers were cracked by the effect of expansion of ettringite inside the pores of this layers.

On the other hand for SRPC degraded samples it can be seen that, for frequency 1MHz (Figure 4-81) the penetration of ultrasonic pulse varies between increasing and decreasing from the start to the end of exposure time. The same trend was observed for frequency 3.5MHz (see Figure 4-84).

## 4. Results and discussion the Degradation Process by Sodium Sulfate Solution

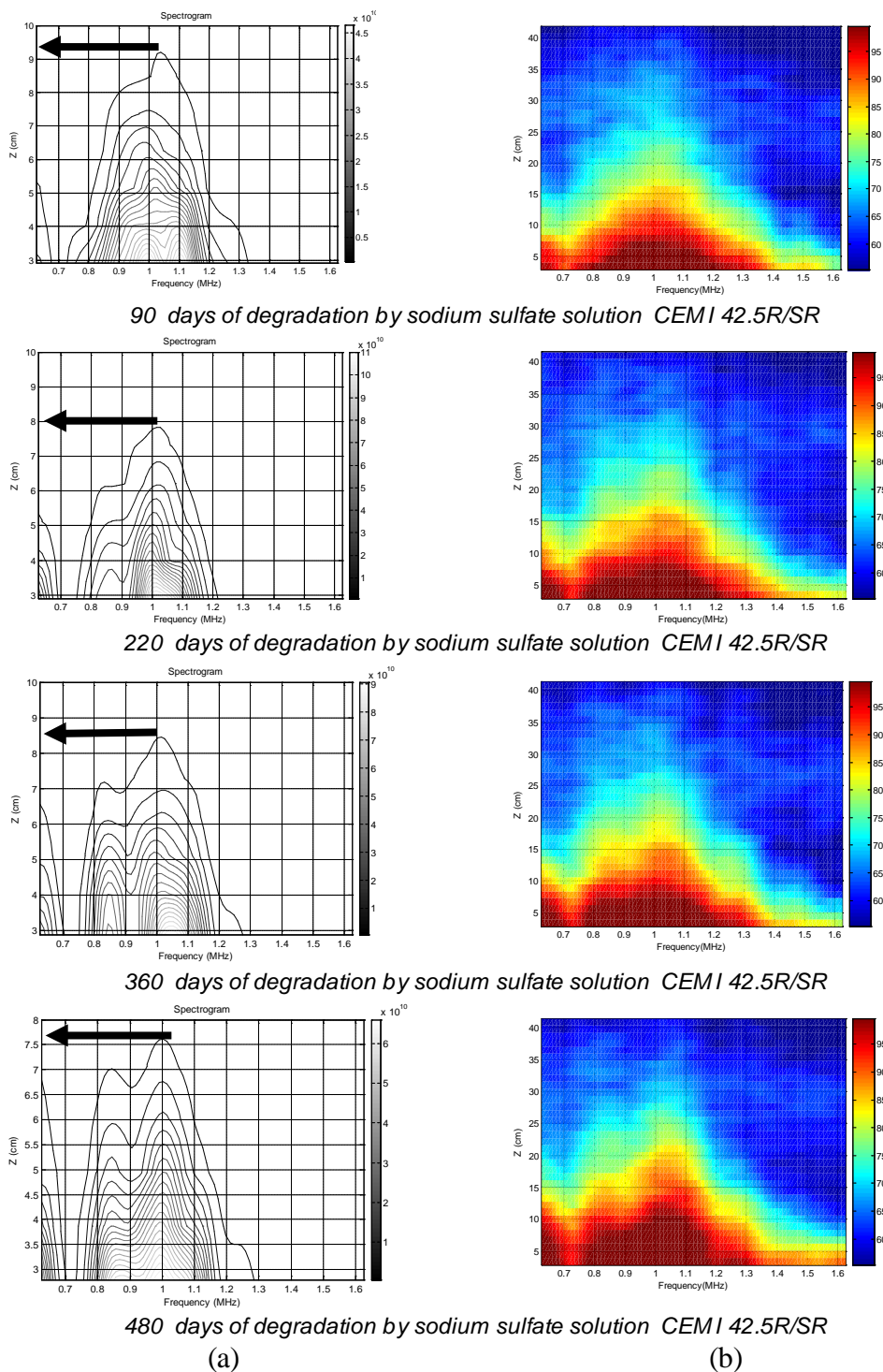
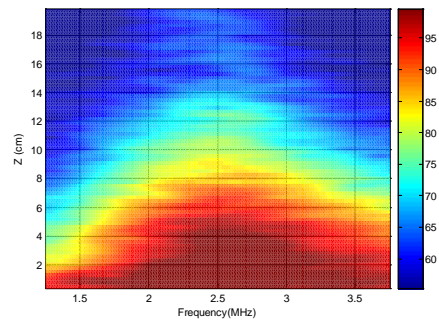
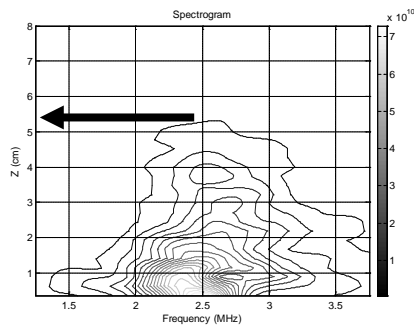
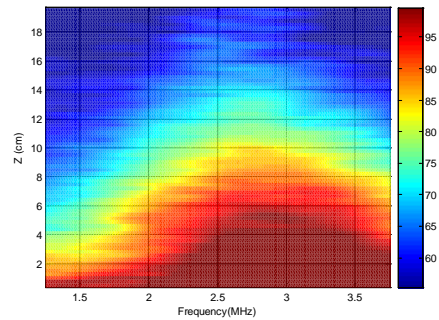
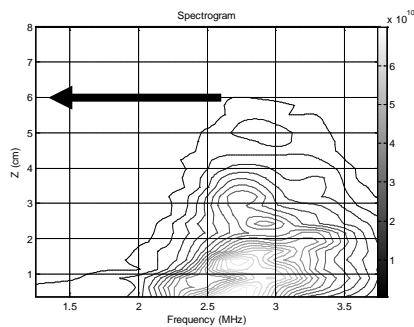


**Figure 4-81** (a) Averaged depth–frequency spectrogram (contour), (b) averaged depth- and frequency-dependent spectrogram (pcolor) for each degradation time for CEMI42.5R/SR degraded by sodium sulfate solution, central frequency 1MHz.

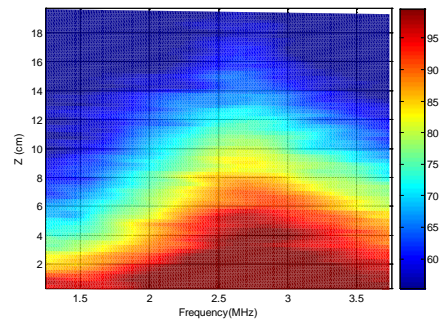
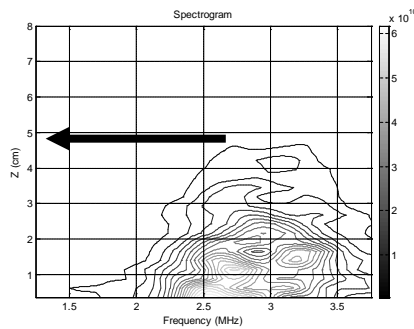
## 4. Results and discussion the Degradation Process by Sodium Sulfate Solution



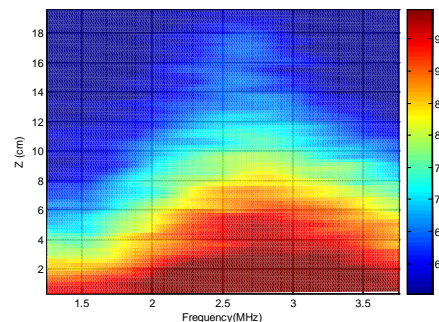
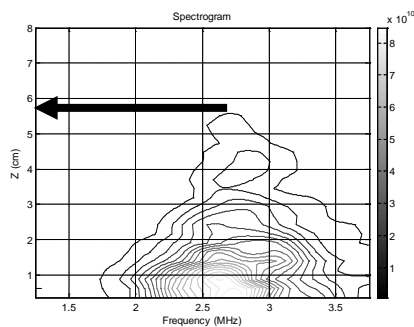
90 days of degradation by sodium sulfate solution CEMI 42.5R/SR



220 days of degradation by sodium sulfate solution CEMI 42.5R/SR



360 days of degradation by sodium sulfate solution CEMI 42.5R/SR



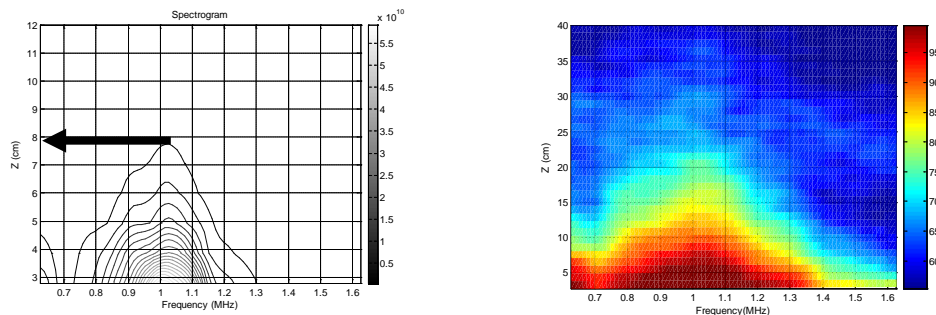
480 days of degradation by sodium sulfate solution CEMI 42.5R/SR

(a)

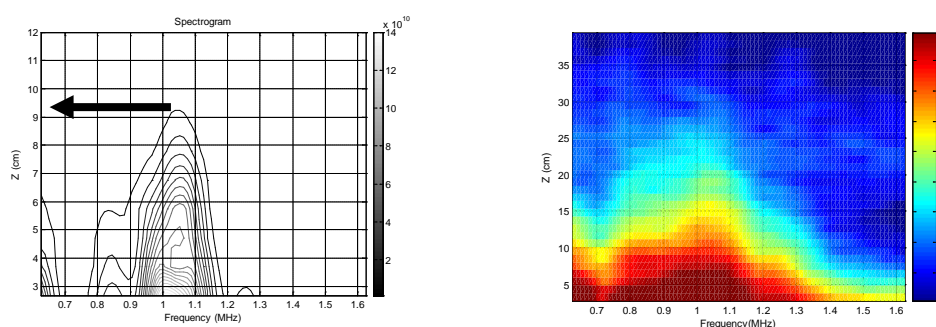
(b)

**Figure 4-82** (a) Averaged depth–frequency spectrogram (contour), (b) averaged depth- and frequency-dependent spectrogram (pcolor) for each degradation time for CEMI42.5R/SR degraded by sodium sulfate solution, central frequency 3.5MHz.

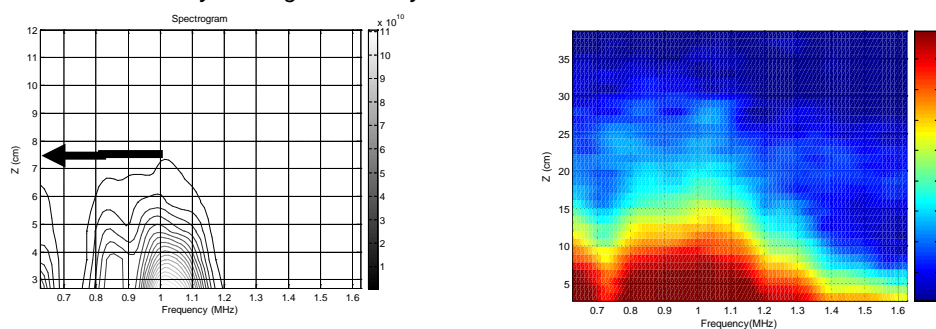
## 4. Results and discussion the Degradation Process by Sodium Sulfate Solution



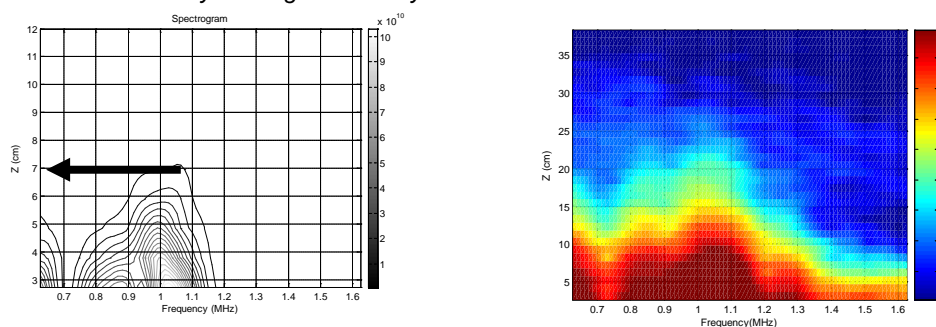
90 days of degradation by sodium sulfate solution CEM II A-L 42.5R



220 days of degradation by sodium sulfate solution CEM II A-L 42.5R



360 days of degradation by sodium sulfate solution CEM II A-L 42.5R



480 days of degradation by sodium sulfate solution CEM II A-L 42.5R

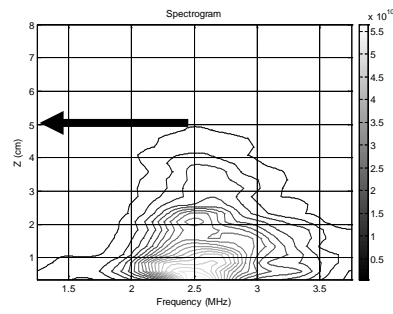
(a)

(b)

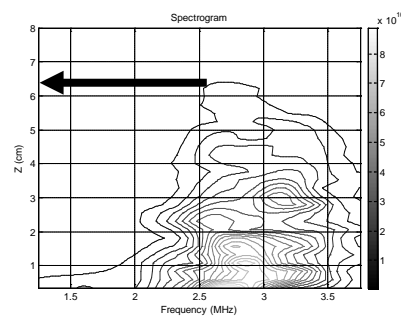
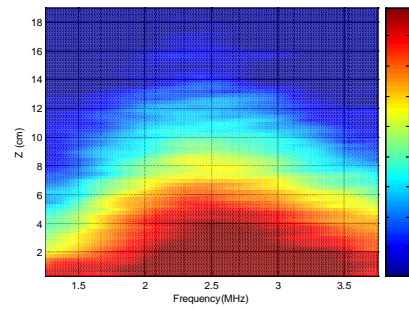
**Figure 4-83** (a) Averaged depth–frequency spectrogram (contour), (b) averaged depth- and frequency-dependent spectrogram (pcolor) for each degradation time for CEM II A-L 42.5R degraded by sodium sulfate solution, central frequency 1MHz.



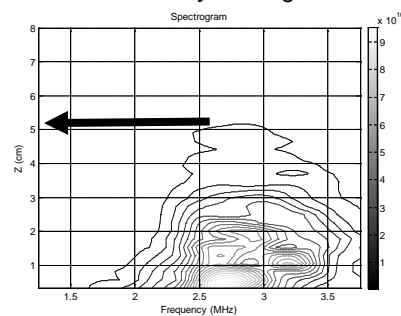
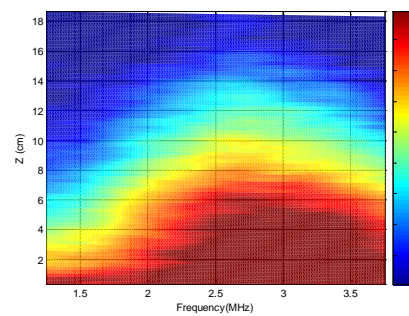
## 4. Results and discussion the Degradation Process by Sodium Sulfate Solution



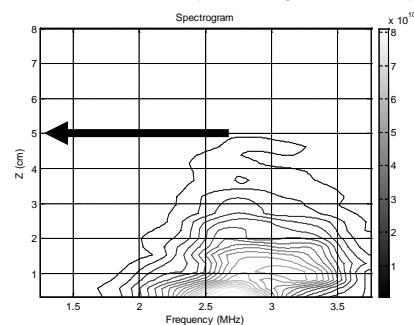
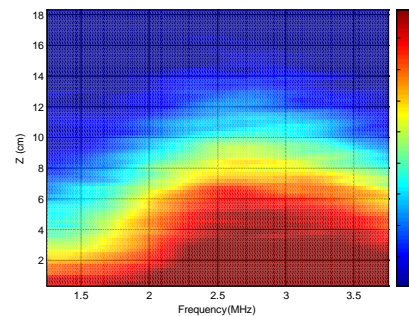
90 days of degradation by sodium sulfate solution CEM II A-L 42.5R



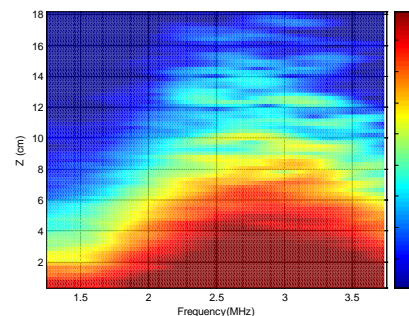
220 days of degradation by sodium sulfate solution CEM II A-L 42.5R



360 days of degradation by sodium sulfate solution CEM II A-L 42.5R



480 days of degradation by sodium sulfate solution CEM II A-L 42.5R



(a)

(b)

**Figure 4-84** (a) Averaged depth–frequency spectrogram (contour), (b) averaged depth- and frequency-dependent spectrogram (pcolor) for each degradation time for CEM II A-L 42.5R degraded by sodium sulfate solution, central frequency 3.5MHz.

#### 4. Results and discussion the Degradation Process by Sodium Sulfate Solution

---

Figure 4-85 and Figure 4-86 illustrate the results of attenuation profile area for both frequencies 1 and 3.5 MHz respectively. For frequency 1MHz, Figure 4-85 presents the results of SRPC and LPC for control and the degraded samples. It can be seen that for SRPC samples a lightly variation of APA is observed as control as degraded samples, and almost both of control and degraded samples have a similar values of APA. This reflects that the samples fabricated by SRPC are not affected by sulfate attack and these results confirmed the results obtained by SEM analysis.

On the other hand for LPC samples, for control samples a lightly/or not variation is observed during all of exposure time. For the samples degraded by sodium sulfate solution it can be observed two steps of degradation, the first step is a decreasing of the attenuation profile area up to 220 days of immersion and this decreasing as demonstrated previously due to filling the pores by ettringite products. The second step, by the expansion of ettringite inside the pores and producing cracks and micro cracks, this caused an increasing in APA from 220 days until the end of exposure time as can be seen in the figure.

For frequency 3.5MHz, Figure 4-86 presents the results of SRPC and LPC for control and the degraded samples. For both SRPC samples (control and degraded) and the control samples of LPC the same trend as 1MHz is observed. On the other hand for the degraded samples of LPC, also two steps of degradation are observed. The first step is from the start up to 90 days of immersion, the second one is from 90 days until the end of exposure time. It can be seen that for 3.5MHz the decreasing of APA was up to 90 days while for 1MHz the decreasing of APA was up to 220 days, this reflects that the frequency 3.5MHz is more sensitive to the microstructural changes due to the degradation process; also this was observed in the section results of mortar.



#### 4. Results and discussion the Degradation Process by Sodium Sulfate Solution

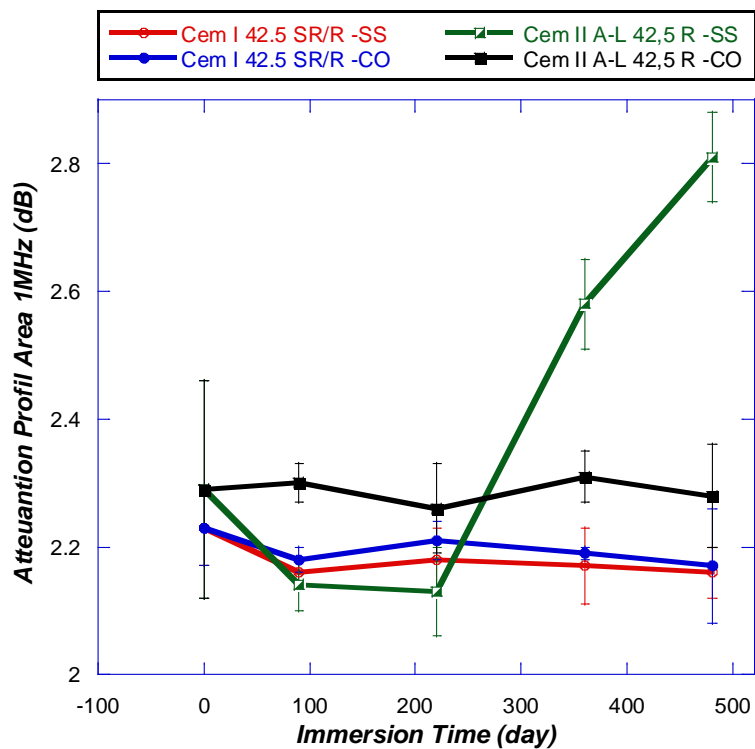


Figure 4-85 Attenuation profile area 1MHz with time

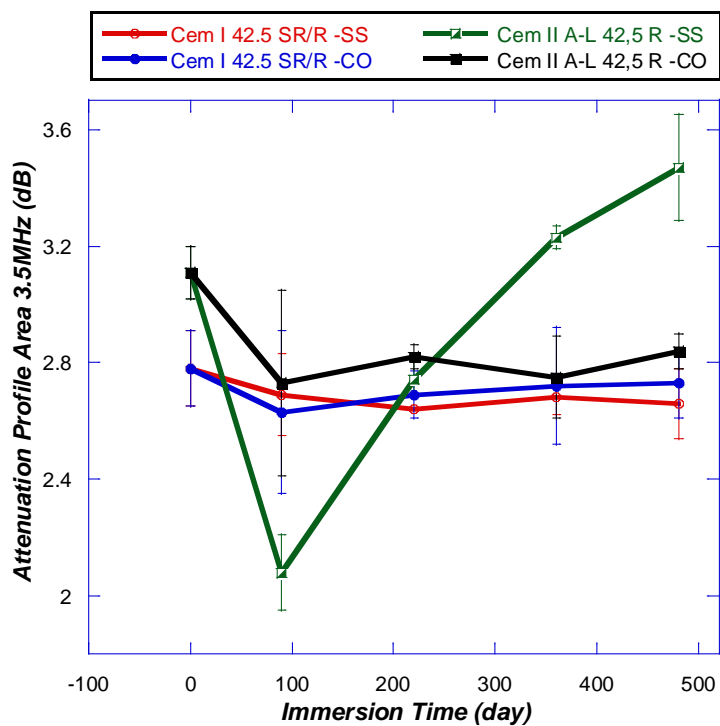


Figure 4-86 Attenuation profile area 3.5MHz with time

### 4.3.6. Ultrasonic Tomography Imaging

Figures from 4-87 to 4-88 illustrate the results of ultrasonic tomography imaging test for both control and samples degraded by sodium sulfate solution for 90,220,370 and 480 days. The figures show the images of both velocity and attenuation of ultrasonic waves in the direction of sample axis (axial) and in the direction perpendicular to the sample axis (radial). As can be seen in the figures, for control samples of LPC and for the control and degraded samples of SRPC, the images show a slightly/or no variation on ultrasonic wave velocity. This was confirmed in Figure 4-91 when ultrasonic mean wave velocity is plotted with degradation time. Also the values of ultrasonic mean velocity are presented in the Tables from 4-7 to 4-11 for both control and degraded samples. Thus, it can be seen for the control samples of LPC, the velocity of ultrasonic waves varies between 4915 - 4950 m/s for axial direction and between 4920-4907 m/s for radial direction. Also is observed for control SRPC samples the mean velocity varies between 5043-5062 m/s for axial and between 5031-5020 for radial direction. The presented results of control samples show that;

- the velocity of ultrasonic waves for SRPC is higher than the velocity of LPC, the same trend is observed previously for longitudinal and shear wave velocity (see section 4.3.4)
- Ultrasonic wave velocities for both axial and radial directions are somewhat equivalent for both cement types, as can be seen in Figure 4-92.

For the degraded samples of LPC, from the images of velocity presented in the Figures from 4-87 to 4-88 it can be estimated the velocity only until 220 days of immersion for the radial direction, after that it was difficult to be estimated from 220 days until the end of exposure time. This is due to the cracks produced by ettringite formation, as can be seen in the Table 4-9 the values of ultrasonic mean velocity for both immersion times 370 and 480 days are **7378** and **8618** respectively. It is clear that these values are incorrect and do not reflect the real values of the degraded samples at these times, because the rate of ultrasonic wave velocity for control LPC samples is between 4915 and 4956m/s as demonstrated previously. And the values of wave velocity of the

#### 4. Results and discussion the Degradation Process by Sodium Sulfate Solution

---

degraded samples must be in the same range of these values depending on the degradation level.

It is known that the diameter of the examined samples is approximately 75 mm and its length is approximately 150mm as showed in chapter 3 (section 3.2.2.). From SEM analysis it is observed that ettringite was formed at approximately 20mm from the surface, which means that the degraded depth around the samples is approximately 20mm, also this means that the path length of ultrasonic pulse has 40 mm degraded distance or more from the whole path length (for radial direction), on the other hand the contact between the sender and receiver transducers is not direct, all this may be affected on ultrasonic sending pules by sender transducer to be received by receiver transducers. For this reason the measurement in the axial direction is realized to minimize the degraded distance on the path way of ultrasonic pulse as possible, also the two faces of the sample were covered by an epoxy resin layer (see Figure 4-93) to prevent the degradation from the sample face direction. Thus, when a beam of ultrasonic waves is sending from the transducer, part of it goes on the degraded path way (cracked zone), another part travel on a non-degraded zone (non-attacked by sodium sulfate or filled by ettringite but yet it is not cracked).

Figure 4-91 illustrates the results obtained from axial measurement as described above for a degraded LPC sample, it can be observed in the figure that, the ultrasonic wave velocity increases slightly up to 220 days, thereafter it was decreased until the end of exposure time, and this is due to the degradation by sodium sulfate as explained previously.

#### 4. Results and discussion the Degradation Process by Sodium Sulfate Solution

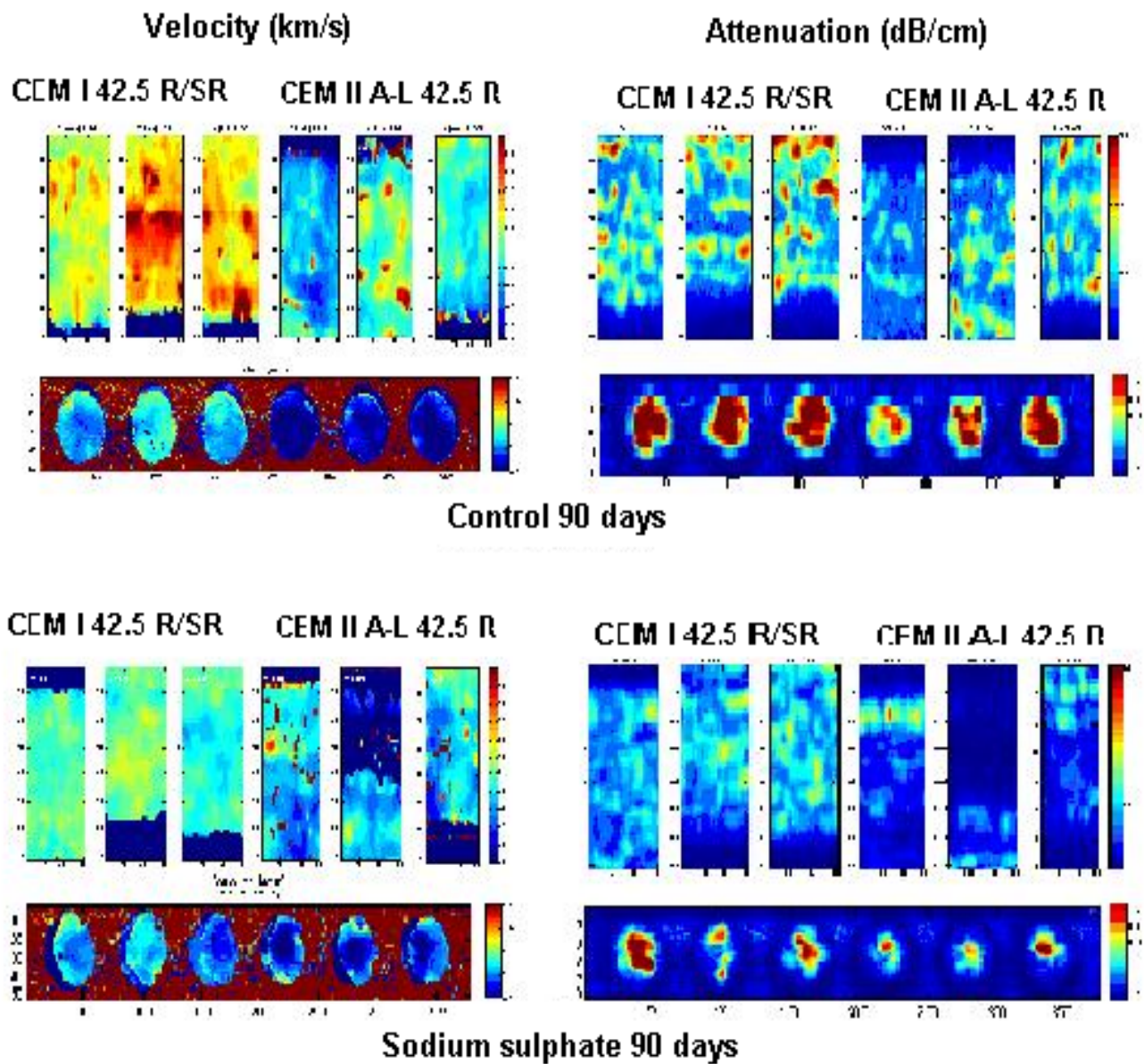


Figure 4-87 Ultrasonic tomography for sodium sulfate and control samples for 90 days of immersion time

#### 4. Results and discussion the Degradation Process by Sodium Sulfate Solution

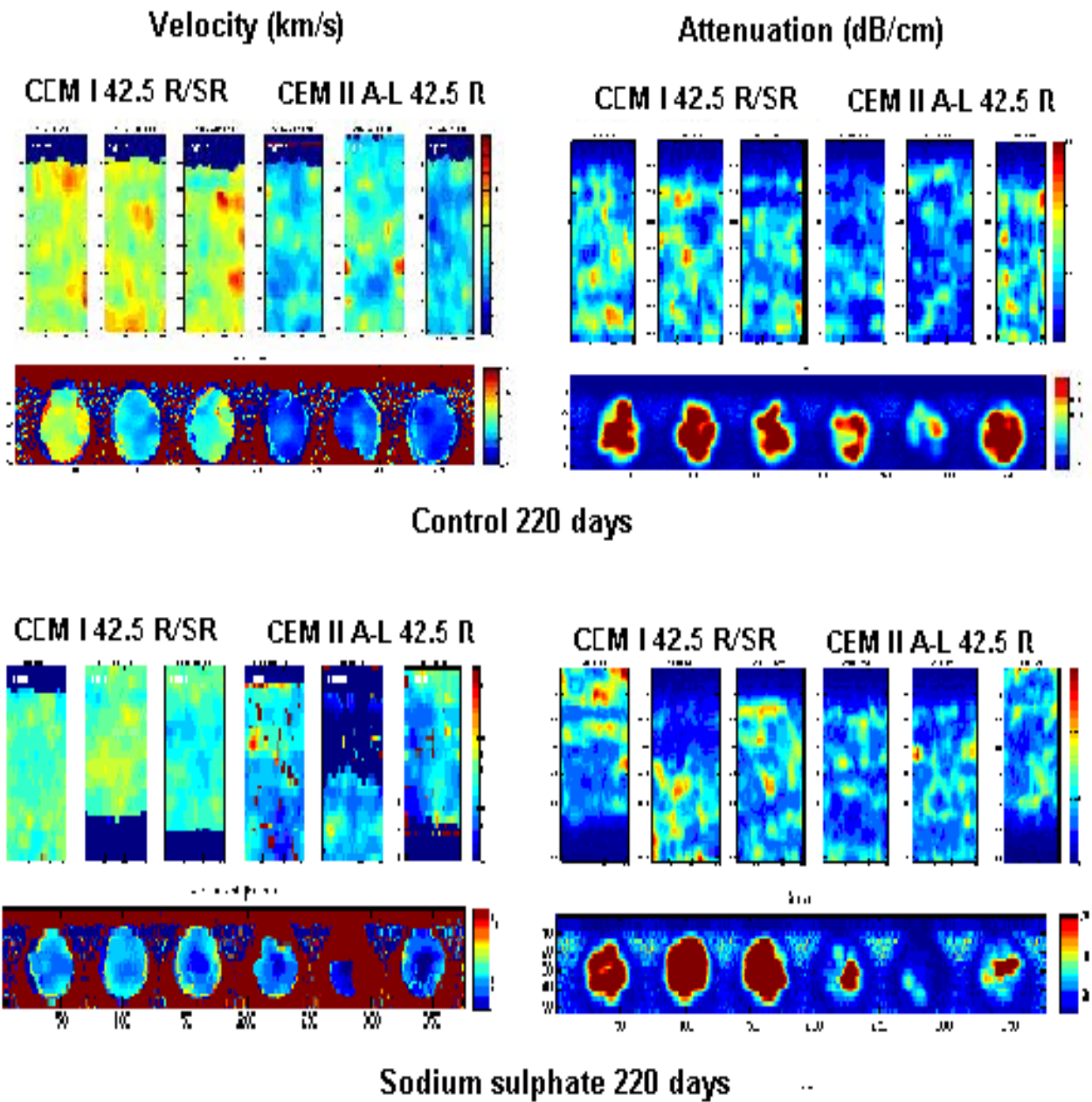


Figure 4-88 Ultrasonic tomography for sodium sulfate and control samples for 220 days of immersion time

#### 4. Results and discussion the Degradation Process by Sodium Sulfate Solution

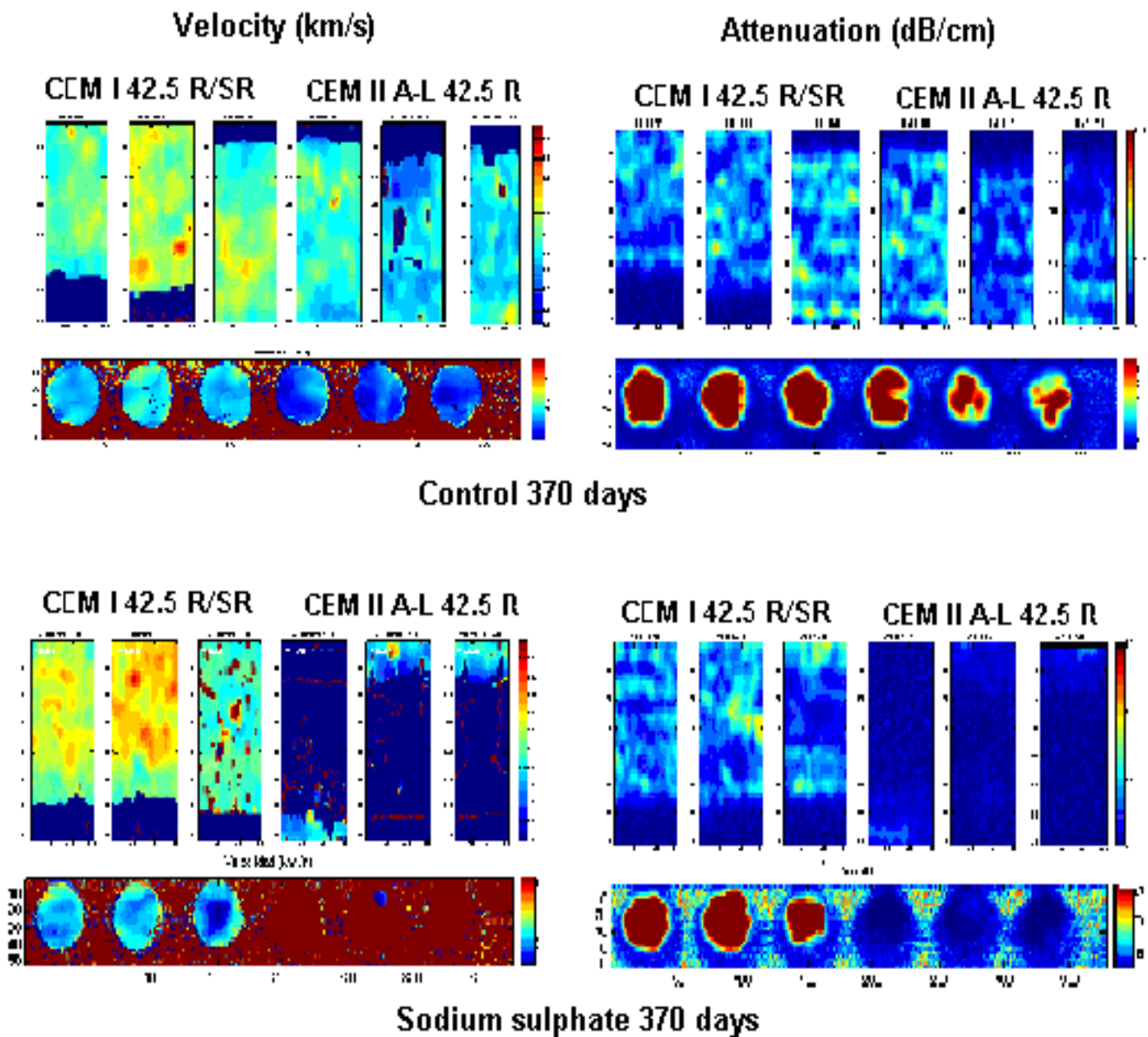


Figure 4-89 Ultrasonic tomography for sodium sulfate and control samples for 370 days of immersion time



#### 4. Results and discussion the Degradation Process by Sodium Sulfate Solution

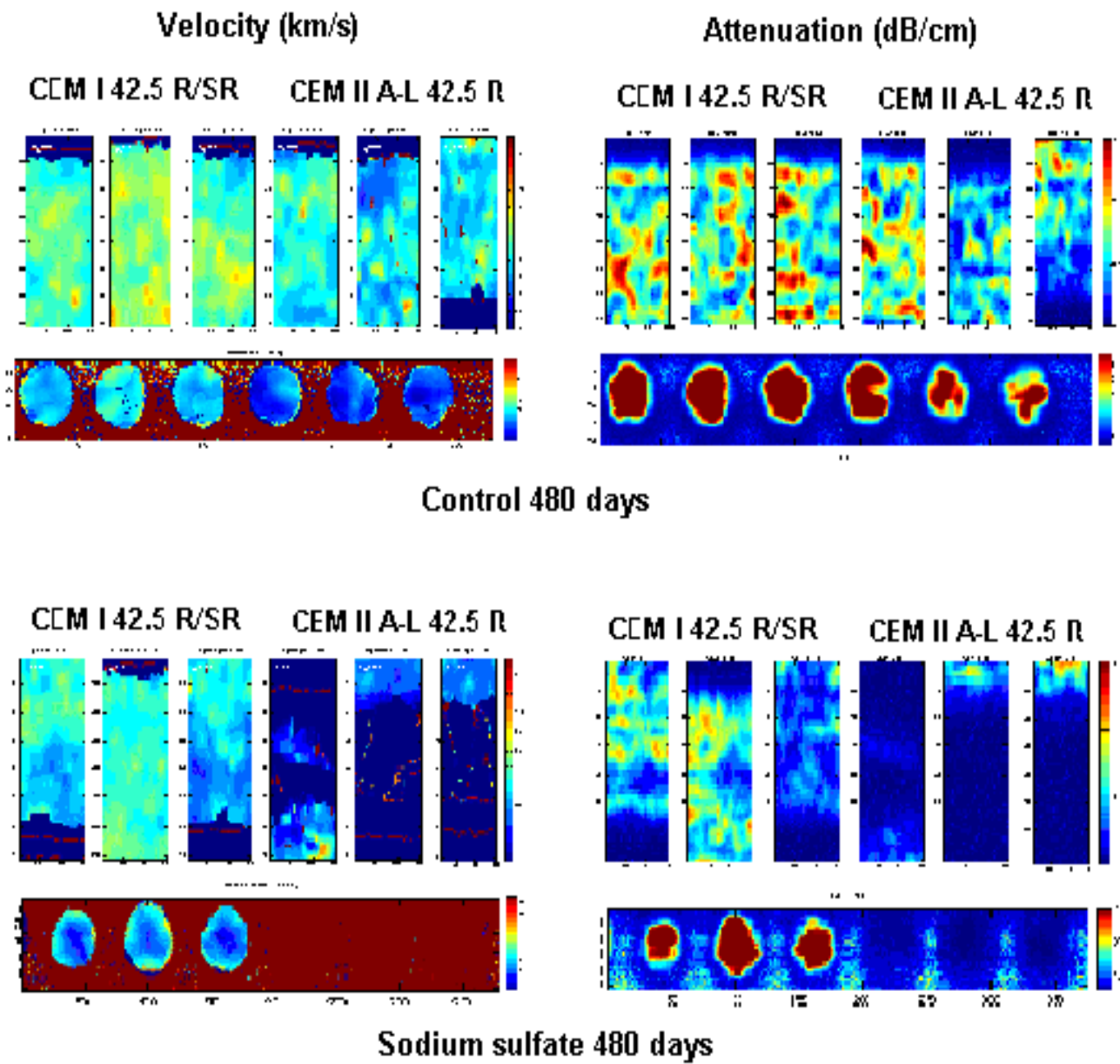
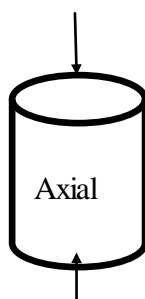


Figure 4-90 Ultrasonic tomography for sodium sulfate and control samples for 480 days of immersion time

#### 4. Results and discussion the Degradation Process by Sodium Sulfate Solution

**Table 4- 8** Ultrasonic mean velocity of the degraded samples in the direction of sample axis (Axial)

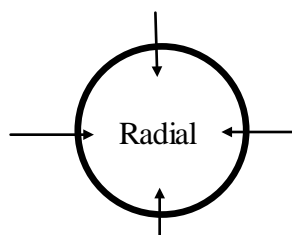
<i>Degradation time (day)</i>	<i>SRPC</i>		<i>LPC</i>	
	<i>V<sub>m</sub>(m/s)</i>	<i>S.D*</i>	<i>V<sub>m</sub>(m/s)</i>	<i>S.D*</i>
<b>90</b>	4988	40	4845	10
<b>220</b>	5063	51	4861	20
<b>370</b>	5078	78	4838	26
<b>480</b>	5097	66	4756	28



\* Standard deviation

**Table 4- 9** Ultrasonic mean velocity of the degraded samples in the direction perpendicular to the sample axis (Radial)

<i>Degradation time (day)</i>	<i>SRPC</i>		<i>LPC</i>	
	<i>V<sub>m</sub>(m/s)</i>	<i>S.D</i>	<i>V<sub>m</sub>(m/s)</i>	<i>S.D</i>
<b>90</b>	4993	75	4845	32
<b>220</b>	4982	40	4879	40
<b>370</b>	4978	83	<b>7378*</b>	<b>2183*</b>
<b>480</b>	4951	95	<b>8618*</b>	<b>309*</b>



\*Incorrect values



#### 4. Results and discussion the Degradation Process by Sodium Sulfate Solution

**Table 4-10** Ultrasonic mean velocity of the control samples in the direction of sample axis (Axial)

<i>Degradation time (day)</i>	<i>SRPC</i>		<i>LPC</i>	
	<i>V<sub>m</sub>(m/s)</i>	<i>S.D</i>	<i>V<sub>m</sub>(m/s)</i>	<i>S.D</i>
<b>90</b>	5043	51	4915	25
<b>220</b>	5037	16	4956	26
<b>370</b>	5044	16	4939	30
<b>480</b>	5062	33	4956	14

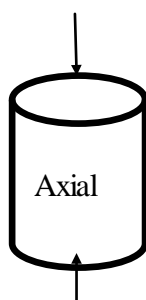
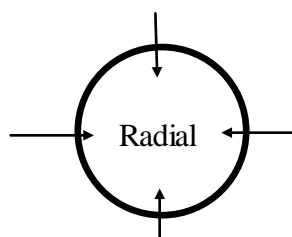


**Table 4-11** Ultrasonic mean velocity of the control samples in the direction perpendicular to the sample axis (Radial)

<i>Degradation time (day)</i>	<i>SRPC</i>		<i>LPC</i>	
	<i>V<sub>m</sub>(m/s)</i>	<i>S.D</i>	<i>V<sub>m</sub>(m/s)</i>	<i>S.D</i>
<b>90</b>	5031	29	4920	116
<b>220</b>	5038	27	4906	29
<b>370</b>	5042	44	4916	27
<b>480</b>	5020	40	4907	29



#### 4. Results and discussion the Degradation Process by Sodium Sulfate Solution

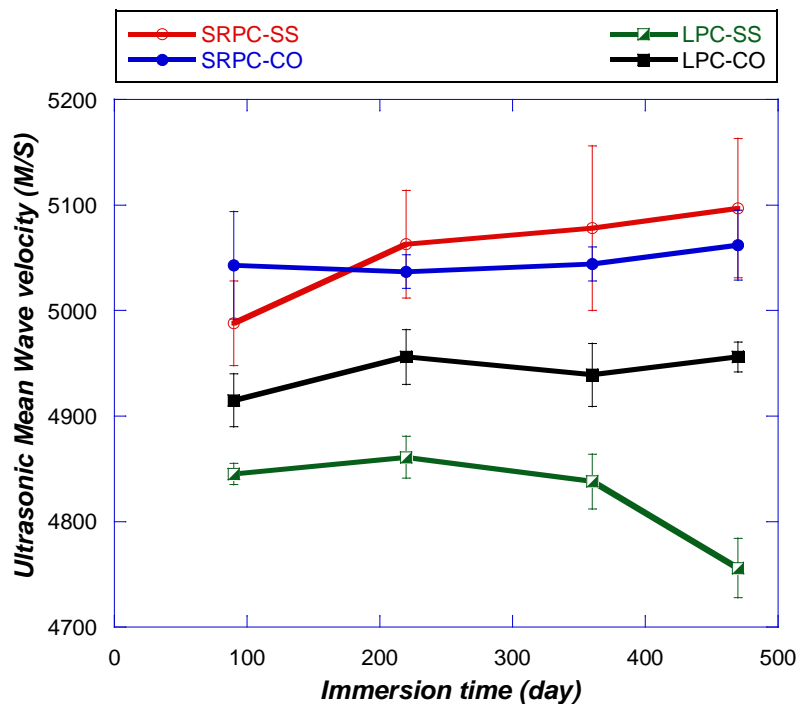


Figure 4-91 Variation of ultrasonic mean velocity with time

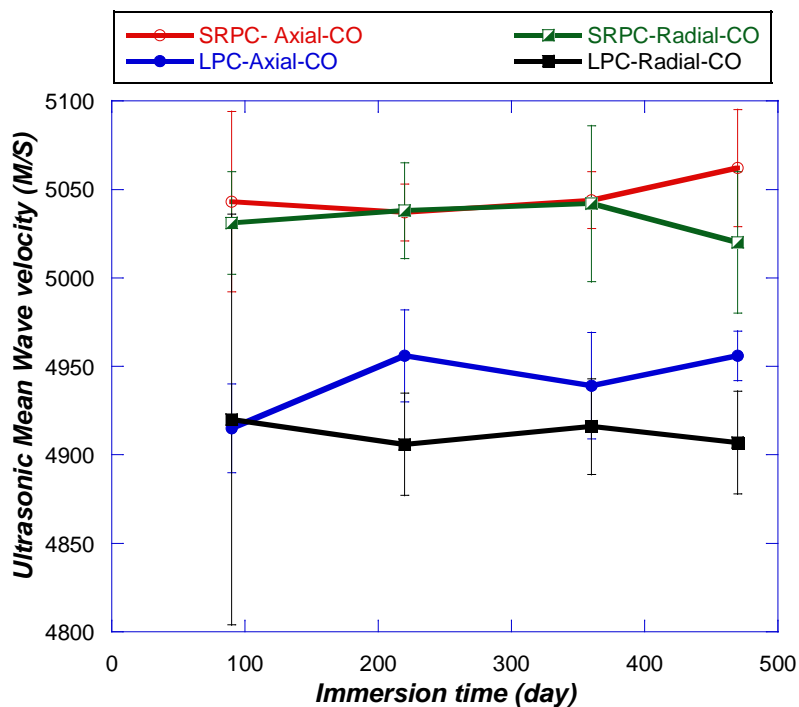
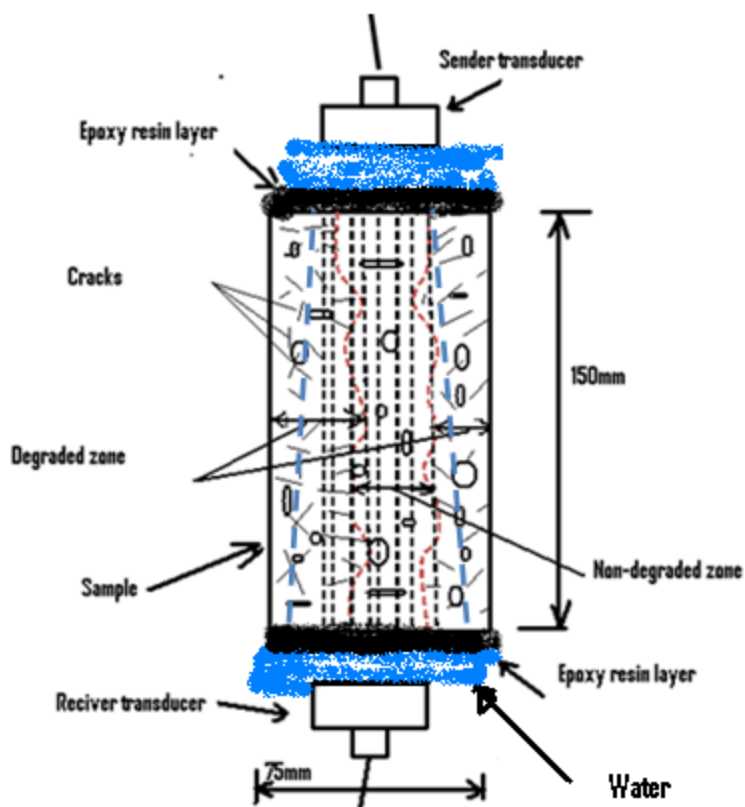
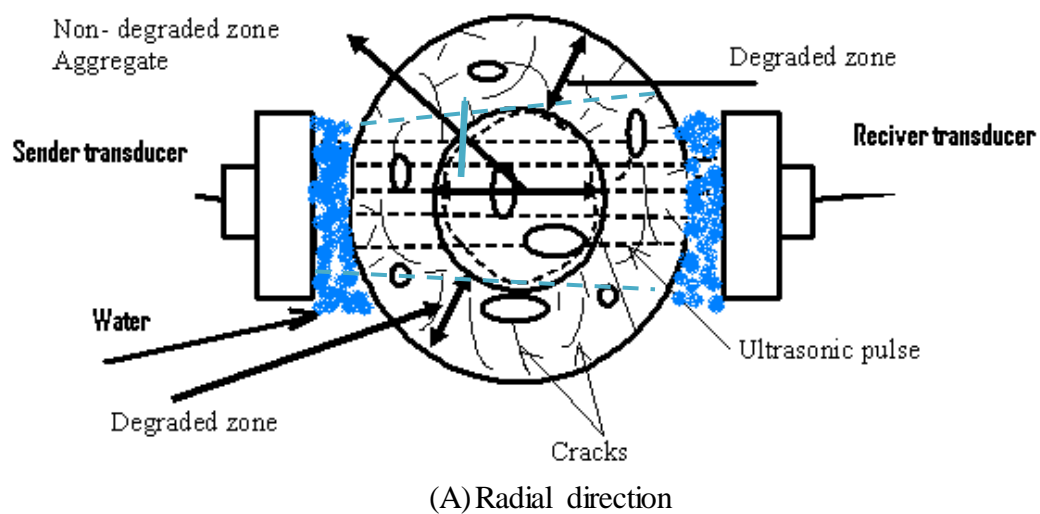


Figure 4-92 Comparison between ultrasonic mean velocity axial and radial

#### 4. Results and discussion the Degradation Process by Sodium Sulfate Solution



**Figure 4-93** Scheme of a sample degraded by sodium sulfate solution and the effect of the degraded path way on the ultrasonic pulse

### 4.4. Correlation the Measured Parameters for Concrete

#### 4.4.1. Correlation Ultrasonic P and S-Wave Velocity versus Porosity

Figures 4-94 and 4-95 illustrate the relationship between P and S-wave velocity versus porosity for both control and degraded samples. From the figures, it is found good relationship between ultrasonic wave velocity and porosity for LPC degraded samples ( $R=0.80$  for P-wave and  $R=0.73$  for S-wave).

As showed in mortar section (section 4.2.1) which presents the relationship between the same parameters, it is found that the relationship between the ultrasonic wave velocity and porosity for mortar is stronger than concrete (All regression coefficient R values for mortar are more than 0.90). This may be because the mortar is more homogeneous than concrete, also the concrete under study has a low w/c ratio (0.30), and this limits the microstructural changes.

On the other hand, for LPC control samples and for degraded and control samples of SRPC, all R values of P-wave are more than 0.71 and for S-wave are more than 0.50. As showed previously in the Figure 4-79 which present P-wave velocity results and Figure 4-80 which present S-wave velocity results, also from Figure 4-78 which shows porosity results, it is observed that the porosity almost does not change during the investigation period, and the ultrasonic wave velocities varies slightly between increasing and decreasing during the immersion time. Thus, it can be said that for porosity, the porosity estimation is for the whole sample. While for ultrasonic wave velocity, the measurement depends on the path way of ultrasonic pulse which may change from time test to another which causes an increasing or a decreasing of wave velocity, especially with heterogeneous materials as concrete under study which has a very low porosity ratio.

In resume, from the previous result, it could be said that two cases are found when the relation between porosity and ultrasonic wave velocity is studied;

#### 4. Results and discussion the Degradation Process by Sodium Sulfate Solution

- The first case is when microstructural changes of concrete occurs, this will be found in the stage of hydration process until been completed and when the concrete is degraded by aggressive element such as sodium sulfate. Thus, for both cases, the variation of porosity is high and will affect on the velocity of ultrasonic waves. This is observed in the case of LPC degraded samples and the relationship between them will be linear.
- The second case when the concrete microstructure non-changes, this occurs when the hydration process is completed, and before starting of the degradation process by aggressive elements, when concrete is put on service. In this case, the variation of porosity is very small and the behaviour of ultrasonic waves will depend more on the amount of aggregate in concrete, which causes increasing or decreasing of ultrasonic wave velocity. Thus, for this case, when porosity results are plotted versus ultrasonic wave velocity results and by the linear fitting curve for these results, the coefficient regression values may refers to that the relationship between them is not good. This is observed for LPC control samples and SRPC samples in Figure 4-95. Also it is observed that the degraded samples show a better correlation that the control, especially for the LPC that performs stronger degradation process. On the other hand, P-wave velocity shows also better correlation with the porosity that S-wave (see Figures 4-94 and 4-95).

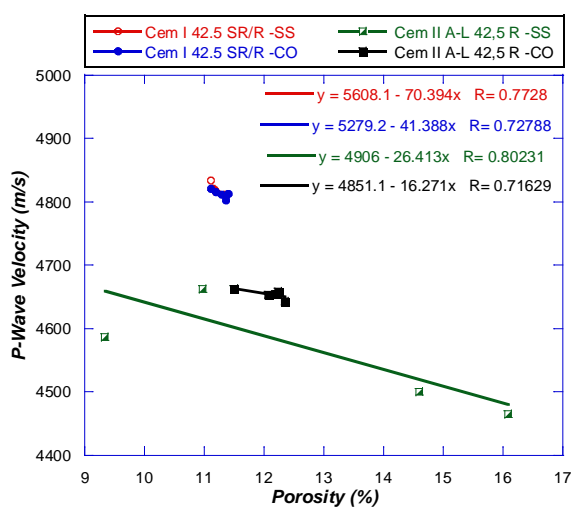


**Figure 4-94** Correlation Porosity with P-wave control and sodium sulfate

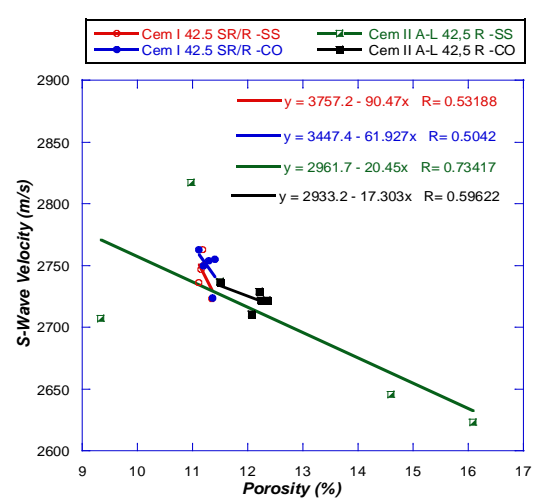


**Figure 4-95** Correlation Porosity with S-wave control and sodium sulfate

### 4.4.2. Correlation Attenuation Profile Area versus Porosity

Figures 4-96 and 4-97 illustrate the relationship between attenuation profile area versus porosity for both frequencies 1 and 3.5MHz. As showed in mortar section, it is found a positive relationship between porosity and APA (increasing of porosity leads to increasing of APA). In the figures, it can be seen that, for LPC degraded samples the value of R is more than 0.97 for the frequency 1MHz and more than 0.71 for the frequency 3.5MHz, which demonstrates the good relationship between the two parameters. On the other hand, based on the presented results in the previous section (4.4.1), it is expected the same trend of relationship of porosity with APA which is similar to its relationship with ultrasonic wave velocity. This can be seen in the figures for the tested samples; and this may be due to the same reasons that mentioned in the previous section. As the previous correlation of the degraded LPC samples, it is observed a stronger variation in the parameters due to the most evidence degradation process that have been take place on it.

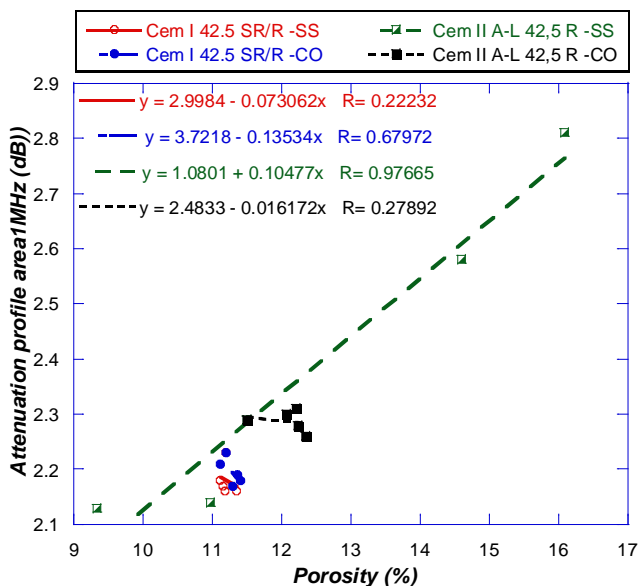


**Figure 4-96** Correlation Porosity with APA 1MHz control and sodium sulfate

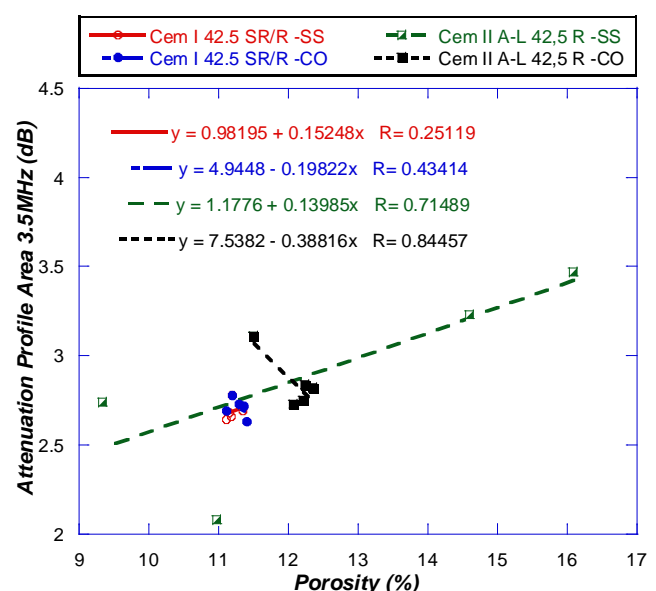


**Figure 4-97** Correlation Porosity with APA 3.5MHz control and sodium sulfate

## 4. Results and discussion the Degradation Process by Sodium Sulfate Solution

### 4.4.3. Correlation P and S-wave Velocity versus Compressive Strength

Figures 4-98 and 4-99 illustrate the relationship between ultrasonic wave velocity and compressive strength for both control and degraded samples. For the LPC samples, it can be seen the same trend as observed previously in the sections (4.4.1 and 4.4.2), it is found a good positive relationship between compressive and ultrasonic wave velocity (in the case of degradation or in the period of hydration). The relationship between the two parameters was explained and detailed in section (4.2.3) for mortar samples, as mentioned in this section, ultrasonic pulse velocity values are affected by number of factors, which do not necessary influence the concrete compressive strength in the same way or to the same extend. For this reason, it can be observed, for the control LPC samples and for SRPC samples, that the values of (R) are small.

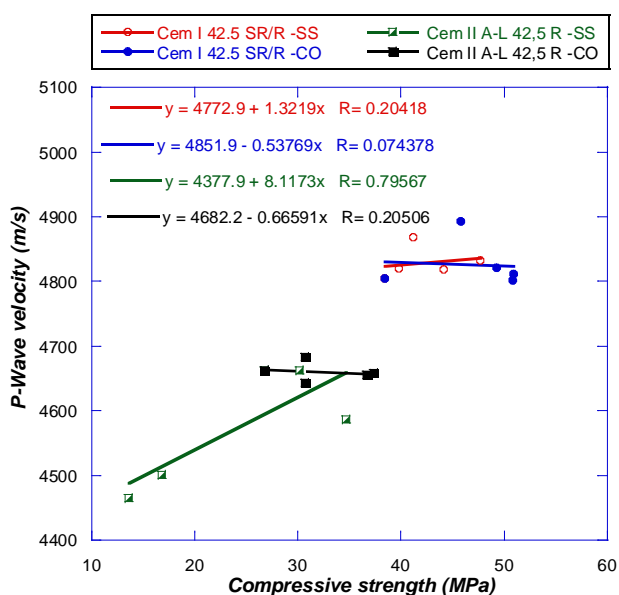


**Figure 4-98** Correlation compressive strength with P-wave control and sodium sulfate

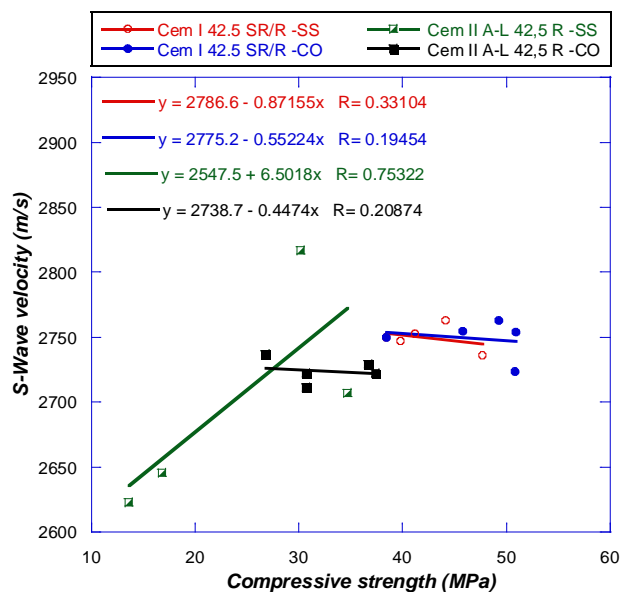


**Figure 4-99** Correlation compressive strength with S-wave control and sodium sulfate

## 4. Results and discussion the Degradation Process by Sodium Sulfate Solution

### 4.4.4. Correlation Attenuation profile Area versus Compressive Strength

Figures 4-100 and 4-101 show the relationship between Attenuation profile area and compressive strength. As can be seen in the figures that attenuation profile area increases with the increasing of compressive strength, when the sulfate ions penetrates the concrete samples and forms ettringite, which with time is expanded and leads to increasing of porosity. This changing in the microstructure causes increasing of APA of ultrasonic waves and decreasing of compressive strength. It can be observed in the figures, for LPC degraded samples, that the values of R are 0.52 for the frequency 1MHz and 0.75 for the frequency 3.5MHz.

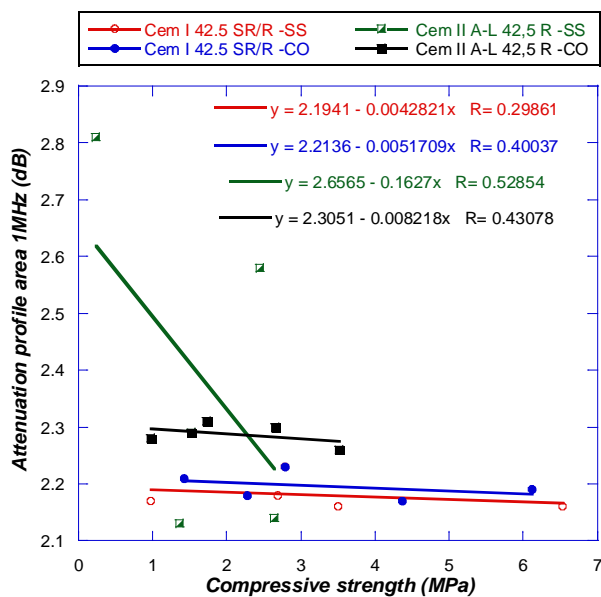


**Figure 4-100** Correlation compressive strength with APA 1MHz control and sodium sulfate

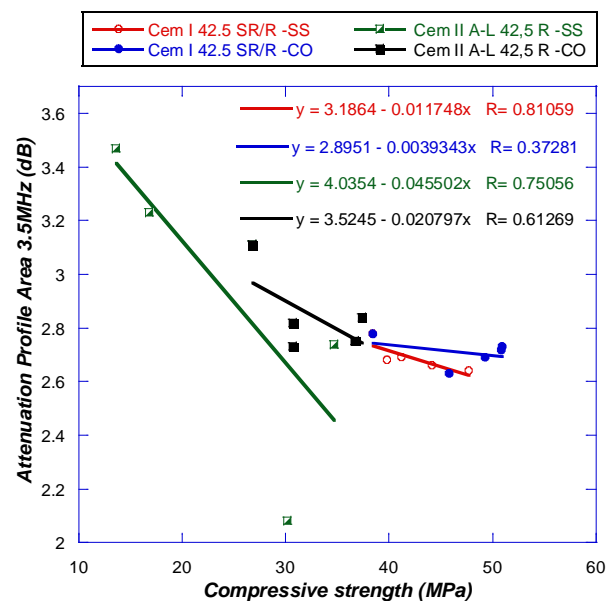


**Figure 4-101** Correlation compressive strength with APA 3.5MHz control and sodium sulfate



4.4.5. Correlation P- Wave and S-wave versus APA

Figures from 4-102 to 4-105 illustrate the relationship between the non-destructive test parameters and each other. The relationship between ultrasonic wave velocities versus attenuation profile area for frequencies 1 and 3.5MHz is plotted in the figures, it can be seen for LPC degraded samples that, ultrasonic wave velocity increases with the decreasing of APA, this trend is the same for both P and S-wave velocity. All coefficient regressions are more than 0.72 for P-wave and more than 0.84 for S-wave which shows the good relationship between these parameters.

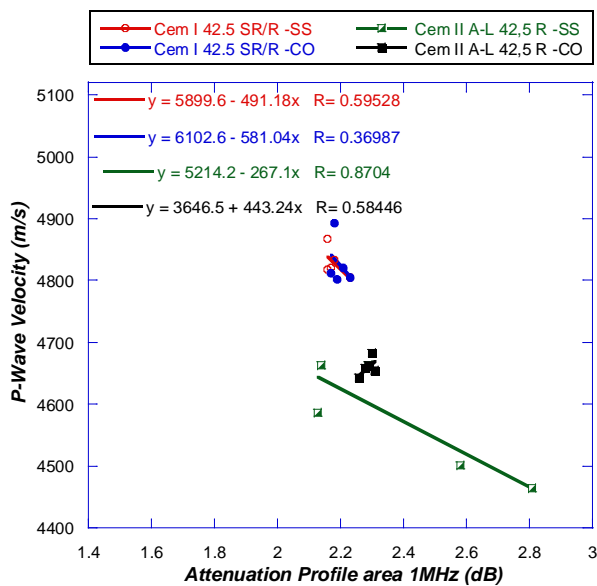


Figure 4-102 Correlation P-wave with APA 1MHz control and sodium sulfate

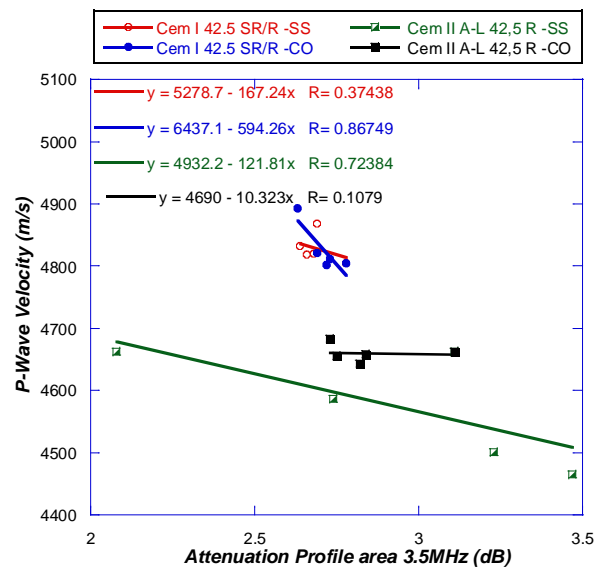
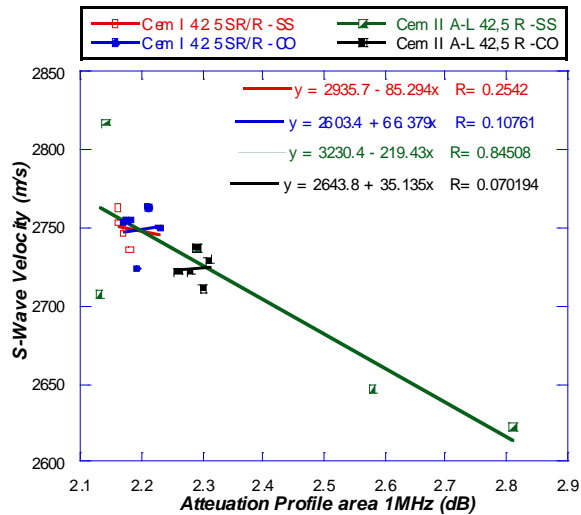
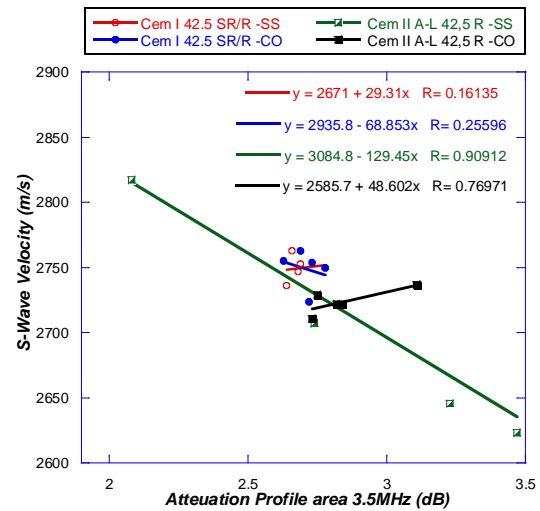


Figure 4-103 Correlation P-wave with APA 3.5MHz control and sodium sulfate

#### 4. Results and discussion the Degradation Process by Sodium Sulfate Solution



**Figure 4-104** Correlation S-wave with APA 1MHz control and sodium sulfate



**Figure 4-105** Correlation S-wave with APA 3.5MHz for control and sodium sulfate

From the presented results of the samples degraded by sodium sulfate solution, it is found that, both of destructive and non-destructive parameters showed two stages of degradation, due to the formation of ettringite in the first stage which led to filling the pores and thereafter caused increasing of strength, ultrasonic wave velocity and decreasing of porosity and attenuation profile area. The behaviour of these parameters was changed to be the contrast in the second stage, when ettringite was expanded and caused producing micro-cracks and cracks as explained previously. Only for w/c ratio 0.525, sometimes one stage is observed due to its high porosity level which facilitated the penetration of sulfate ions to penetrate the samples at early immersion time. As a summary of the conclusions obtained in this chapter are;

- The S-waves velocity correlates better with mortar porosity than P-wave velocity, the contrast is observed for concrete porosity. (P-wave velocity has a better correlation with porosity than S-wave velocity).
- When the degraded samples are examined using the frequencies 1 and 3.5MHz, it is found that, the frequency 3.5MHz has a lower penetration depth than the

#### 4. Results and discussion the Degradation Process by Sodium Sulfate Solution

---

frequency 1MHz. On the other hand it is concluded that the high frequency is more sensitive to the changing in the microstructure of cement-based materials, because it has a shorter wavelength than the low frequency.

- It is found a good relationship between ultrasonic wave velocities (P and S-waves) and both of Porosity and strength, the relationship between them is linear. Also similar behaviour is observed when APA was correlated with porosity and strength.
- From the correlation between ultrasonic wave velocity and strength, it is found a good relationship between the two parameters when the changes in the microstructure of mortar and concrete are clear, as in the case of early ages mortar microstructure development and when the samples are degraded by sodium sulfate, this is observed for both mortar and concrete samples.
- As destructive test, flexural strength is considered more accurate than compressive strength and it has a good relationship with ultrasonic parameters; it is known that flexural strength is typically used in Portland cement concrete because it simulates better, beam flexural stress as they are subjected to loading. On the other hand flexural strength results are sensitive to many factors, including fabricating, curing and loading of the beams. May be for these reasons, flexural strength has a better relationship than compressive strength with the parameters of ultrasonic waves (velocity and attenuation profile area).
- It is found a good relationship between APA and ultrasonic wave velocity.
- The correlation between the parameters of mortar is better than the correlation between the parameters of concrete, this is may be because mortar is less heterogeneous than concrete.
- One objective was to find a general non-destructive procedure to analyse and follow the degradation process due to sulphate attack. From the previous presented results of Chapter 4, it can be found some general trends that there are useful to establish a general procedure to be applied in the real cases of mortar and concrete structure inspections. As can be seen in the figures from 4-106 to 4-108. On the left hand side of the figures show global regression for each case and the left hand side shows the 10% error interval. Almost all experimental data

#### **4. Results and discussion the Degradation Process by Sodium Sulfate Solution**

---

were within the interval; therefore the ultrasonic parameter can be used to estimate the porosity with an equivalent standard error for the destructive parameter. In those cases, it is possible to use the ultrasonic testing instead of the destructive tests.

#### 4. Results and discussion the Degradation Process by Sodium Sulfate Solution

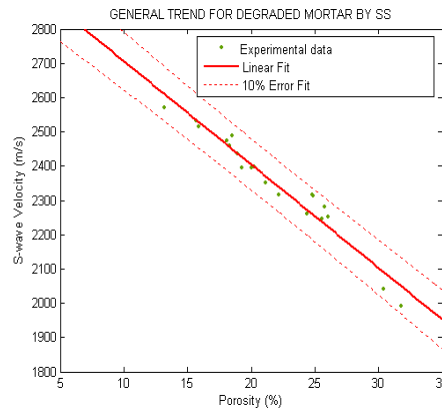
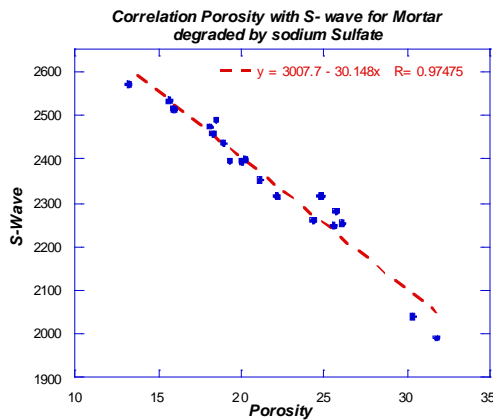


**Figure 4-106** General trend for estimation porosity using S-wave velocity of mortar degraded by SS

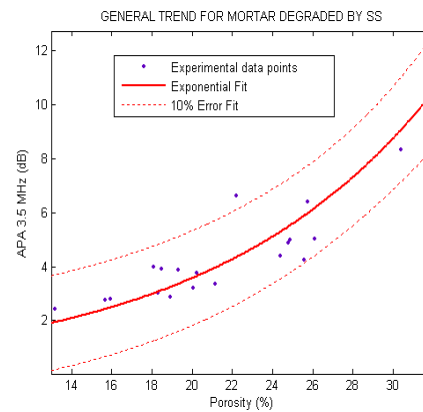
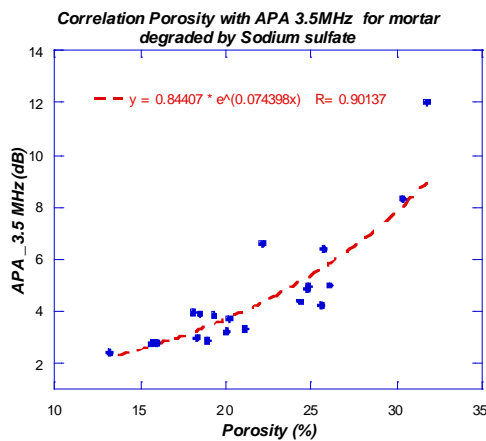


**Figure 4-107** General trend for estimation Porosity using APA 3.5MHz of mortar degraded by SS

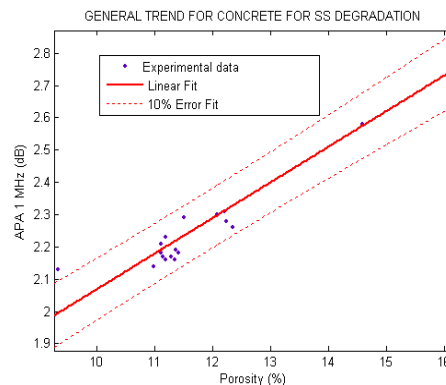
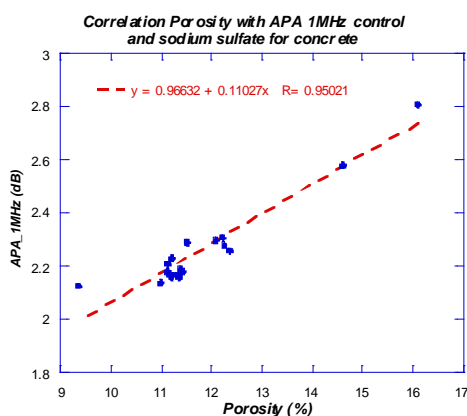


**Figure 4-108** General trend for estimation Porosity using APA 1MHz of control and concrete degraded by SS

#### 4. Results and discussion the Degradation Process by Sodium Sulfate Solution

---

# CHAPTER 5

**Results and Discussion the Degradation  
process by Ammonium Nitrate**

---





# 5 Results and Discussion the Degradation Process Ammonium Nitrate

In this chapter, the results of mortar samples and precast concrete cores degraded by ammonium nitrate solutions (4mol/L), which accelerates the degradation kinetics at least by a factor 300, are presented. So, by using this aggressive solution, it was easy to obtain an accelerated process and a high degradation level in a short time due to the decalcification process. Samples were immersed into the solution for 1, 20, 35 and 50 days for mortar samples, and for 1, 49, 96, 190 and 290 days for precast concrete samples.

To follow and estimate the degradation process, a conjunction of non-destructive and destructive tests were performed. The non-destructive techniques used in this chapter are; (a) Ultrasonic grain noise (to obtain the parameter of attenuation profile area APA, using frequencies 1 and 3.5MHz), (b) Ultrasonic through-transmission (to obtain ultrasonic longitudinal wave velocity by using frequency of 1MHz and ultrasonic shear wave velocity by using frequency of 500KHz). The destructive techniques are compressive strength test, flexural strength (only for mortar samples) and open porosity test. Finally, the correlations between non-destructive and destructive parameters were presented and discussed the obtained trends.

## 5.1. Analysis and Discussion the Results of Mortar

### 5.1.1. Compressive and Flexural Strength

Figure 5-1 presents the results of compressive and flexural strength, respectively, for control and samples degraded by ammonium nitrate solution for 1, 20, 35 and 50 days. In the left side of Figure 5-1, we can see that for control samples, the strength is increasing slowly until the end of exposure time and this is because the hydration process is in progress and this causes an evolution in the strength. The compressive strength of  $w/c=0.55$  is lower than  $w/c=0.40$ . It has been shown that the  $w/c$  ratio of

## 5. Results and Discussion of Degradation Process by Ammonium Nitrate

---

cementitious materials is the major factor in controlling compressive strength, when w/c ratio increases the compressive strength decreases (Neville, 1995). This is explained by the fact that the quantities of water excess of that required to hydrate the cement forms capillary pores within the matrix. The greater the proportion of capillary pores, the weaker is the material.

For ammonium nitrate samples, the drop in the strength for both w/c ratios, with degradation time, can be observed. This drop in strength is because ammonium nitrate solution is very corrosive to cementations materials and leads to dissolution of cement-based materials. The reaction products are calcium nitrate and ammonia, both of which are easily dissolved in water (Schneider and Chen, 2005). The consequence is a progressive leaching of portlandite and C-S-H, leaching of concrete means that the ammonium nitrate neutralizes the hardened cement paste and dissolves the calcium hydroxide and other hydration products in the concrete, which cause a decrease of the mechanical properties of mortar samples, such as compressive and flexural strength. The same trend was observed in the case of flexural strength as can be seen in the right side of Figure 5-1.

Figure 5-2 represents the compressive and flexural strength losses for degraded samples. It can be seen that the strength loss is increasing by the increase of both immersion time and w/c ratios. For example, as can be seen in Table 5-1 and in the left side of Figure 5-2, after 20, 35 and 55 days of immersion in ammonium nitrate, compressive strength loss for w/c 0.55 was about 58%, 71% and 83% respectively, while in the case of w/c 0.40 it was about 39%, 56% and 59% respectively. This increase slowed down as the leaching process advanced, and this is related to the consumption of portlandite and the leaching of C-S-H. On the other hand, the same trend was observed for flexural strength. Also, it can be observed that, the loss of strength is related to w/c ratio, as can be seen in Figure 5-2, Table 5-1 and Table 5-2 the strength losses of w/c ratio 0.55 is higher than the strength losses of w/c ratio 0.40 (for both compressive and flexural strength).

## 5. Results and Discussion of Degradation Process by Ammonium Nitrate

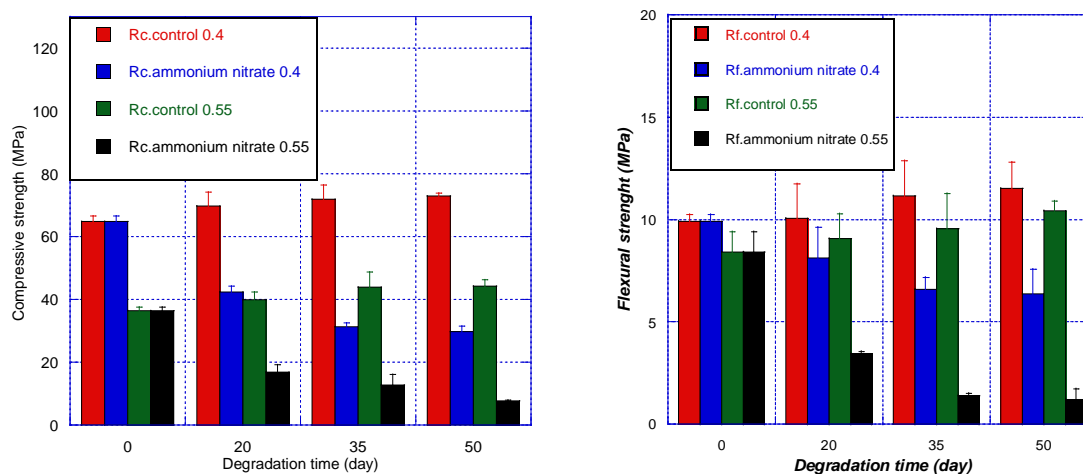


**Figure 5-1** Compressive and flexural strength of mortar samples submerged in 4 moles of ammonium nitrate

**Table 5- 1** Compressive strength and compressive strength loss for control and ammonium nitrate samples

Compressive strength (MPa) w/c= 0.40			Compressive strength (MPa) w/c= 0.55		
Control	Ammonium nitrate	Loss (%)	Control	Ammonium nitrate	Loss (%)
64.83	64.83	0.0	36.35	36.35	0.0
69.77	42.41	39	39.88	16.80	58
71.88	31.32	56	43.91	12.74	71
72.95	29.77	59	44.21	7.69	83

**Table 5- 2** Flexural strength and Flexural strength loss for control and ammonium nitrate samples

Flexural strength(MPa) w/c= 0.40			Flexural strength(MPa) w/c= 0.55		
Control	Ammonium nitrate	Loss (%)	Control	Ammonium nitrate	Loss (%)
9.93	9.93	0.0	8.40	8.4	0.0
10.04	8.12	19	9.08	3.44	62
11.17	6.57	41	9.55	1.41	85
11.51	6,37	45	10.40	1.21	88

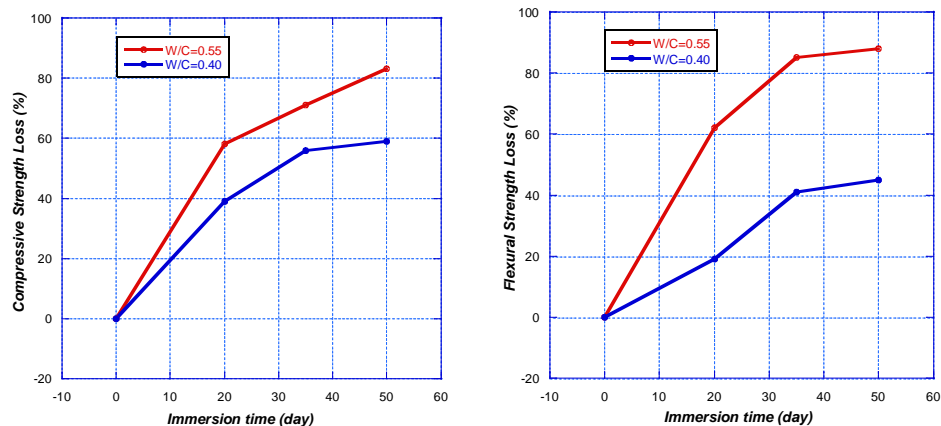
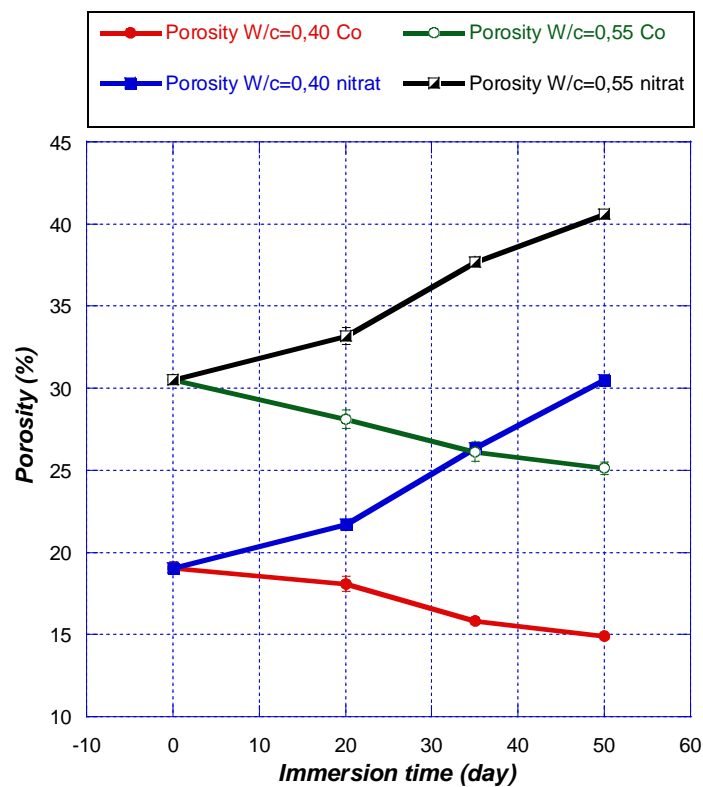


Figure 5-2 Compressive and flexural Strength loss of mortar samples

### 5.1.2. Open Porosity

Figure 5-3 illustrates the results of open porosity for both control and ammonium nitrate samples. In that figure, it can be observed that for control samples, the porosity is decreasing slowly until the end of exposure time, because the hydration process is in progress and this causes the filling of the pores by the hydration products. For ammonium nitrate samples, it can be seen that there is an increasing in the porosity for both w/c ratios and this increasing slows down as the leaching process advances.

The increasing in porosity of ammonium nitrate samples compared with the porosity of control samples is due to the chemical attack by ammonium nitrate, which induces total leaching of portlandite and progressive decalcification of C-S-H. Several studies have shown that leaching process for mortar or for cement paste tends to increase its porosity and to reduce its mechanical strength (Carde et al., 1996; Gérard, 1996; Le Bellego et al., 2000). The leaching process causes some changes in mortar microstructure that can be divided into several steps. First, the leaching process of portlandite leads to an increase in the size volume of capillary porosity. Second, leaching of C-S-H increases micro-porosity and could lead to microstructural changes in the C-S-H structure (Hernández et al., 2006)



**Figure 5-3** Porosity of mortar submerged in 4 moles of ammonium nitrate and control

### 5.1.3. Ultrasonic Longitudinal and Transversal Wave Velocity

Figures 5-4 and 5-5 illustrate the results of ultrasonic longitudinal and transversal wave velocities for mortar samples immersed in ammonium nitrate solution for 1, 20, 35 and 50 days. A significant decrease for both velocities with the time of degradation was observed. The decrease of velocity can be explained by the fact that, as mentioned in the previous paragraph, when mortar samples are subjected to ammonium nitrate, which induce leaching of portlandite and the progressive of decalcification of C-S-H, result an increasing in porosity which causes a faster decreasing in young's modulus than density of mortar samples and then decreasing in the velocity of ultrasonic waves. The same trend was observed in the case of transversal wave velocities, as can be seen in the figure 5.5, a decreasing in the wave velocity with the increasing of the degradation time.

## 5. Results and Discussion of Degradation Process by Ammonium Nitrate

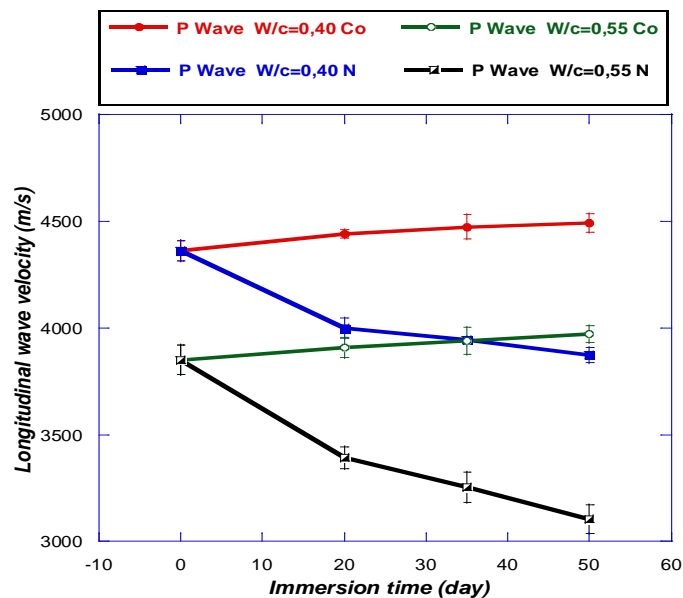


Figure 5-4 Longitudinal wave velocity with time for ammonium nitrate and control samples

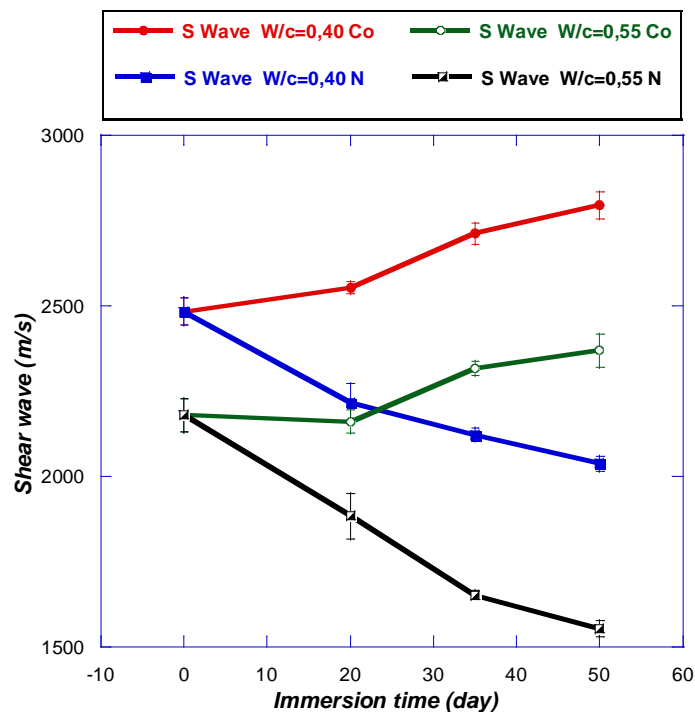


Figure 5-5 Shear wave velocity with time for ammonium nitrate and control samples

### 5.1.4. Ultrasonic Attenuation Profile Area (APA) 1 and 3.5 MHz

“When an ultrasonic pulse propagates inside a material, it suffers some variation related to the properties of the specimen. Of particular significance is the attenuation experienced by the pulse, which is, in general, frequency dependent. The attenuation will also be depth dependent if the material changes its properties with depth” (L vergara et al., 2003)

Thus, before presenting the results of the attenuation profile area of ultrasonic waves, and by the same way as presented previously in chapter 4, the next figures from 5-6 to 5-9 will be presented to illustrate the variation of attenuation with depth, due to the internal variation in the microstructure of mortar samples degraded by ammonium nitrate solution for 1, 20, 35 and 50 days. The figures present only the results of the degraded samples, for the two w/c ratios 0.40 and 0.55, for both frequencies 1 and 3.5MHz. From the figures, it is observed that the general trend is decreasing in the penetration of ultrasonic pulse with the increasing of immersion time in ammonium nitrate solution, also it is observed that the penetration depth of ultrasonic pulse is higher in the case of w/c=0.40 than w/c =0.55. The amount of leached calcium increases with w/c ratio, and a higher w/c values are corresponding to a higher porosity which leads to a higher degradation depth and a low penetration for ultrasound pulse. On the other hand, a sharp drop in the decreasing of ultrasonic pulse penetration was observed from 1 to 20 days of degradation time for both w/c ratios, thereafter, from 20 to 50 days of degradation the decrease was continued slowly. A sharp drop also was observed for the same period, when the degraded depth was calculated by using Phenolphthalein, as observed in Table 5-5. This drop may be due to the fact that chemical degradation is initiated by the loss of chemical equilibrium between solid skelton and acid interstitial solution at the boundaries of sample in contact with aggressive solution. One can see that during the first stage, the PH value of the solution increases very quickly to reach about 9 after a few days. Then, the increase in PH value becomes slower and progressively reaches a quasi-stationary value. The quick increase of PH value may correspond to the fast dissolution of portlandite (Xie, et al., 2008).

## 5. Results and Discussion of Degradation Process by Ammonium Nitrate

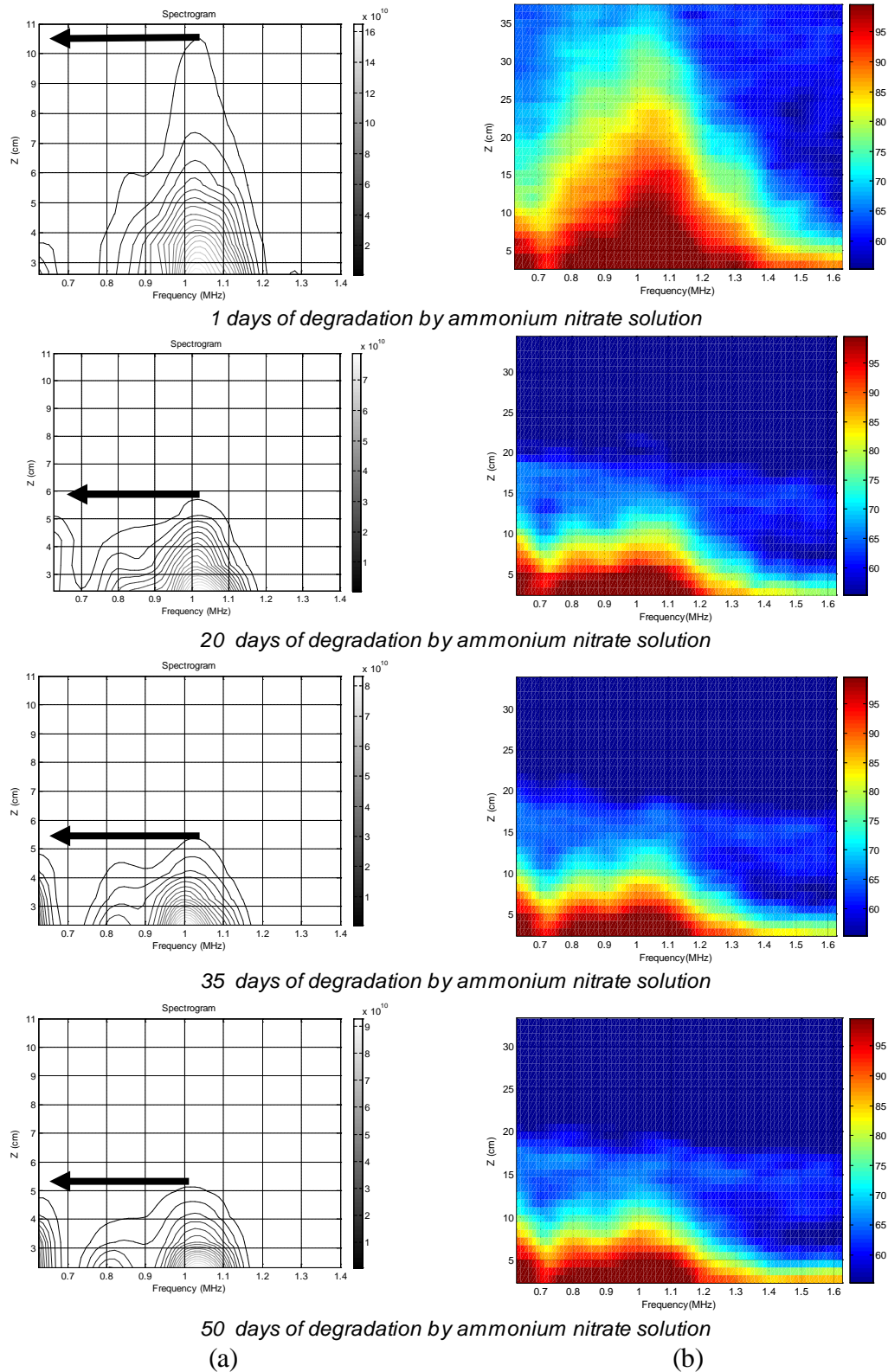


**Figure 5-6** (a) Averaged depth–frequency spectrogram (contour), (b) averaged depth- and frequency-dependent spectrogram (pcolor) for each degradation time for w/c =0.40 mortar degraded by ammonium nitrate solution, central frequency 1MHz.



## 5. Results and Discussion of Degradation Process by Ammonium Nitrate

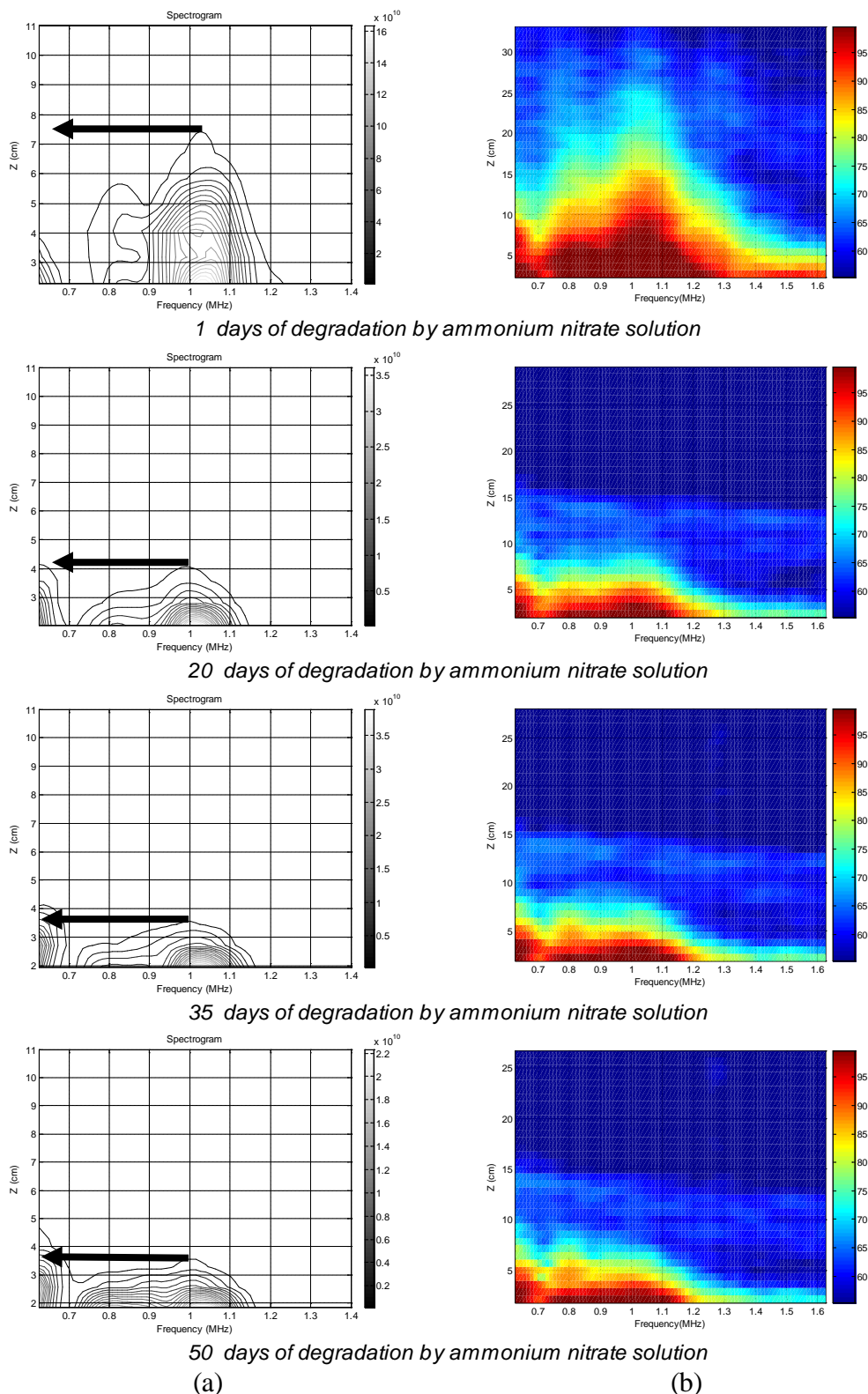


**Figure 5-7** (a) Averaged depth–frequency spectrogram (contour), (b) averaged depth– and frequency–dependent spectrogram (pcolor) for each degradation time for  $w/c = 0.55$  mortar degraded by ammonium nitrate solution, central frequency 1MHz.

## 5. Results and Discussion of Degradation Process by Ammonium Nitrate

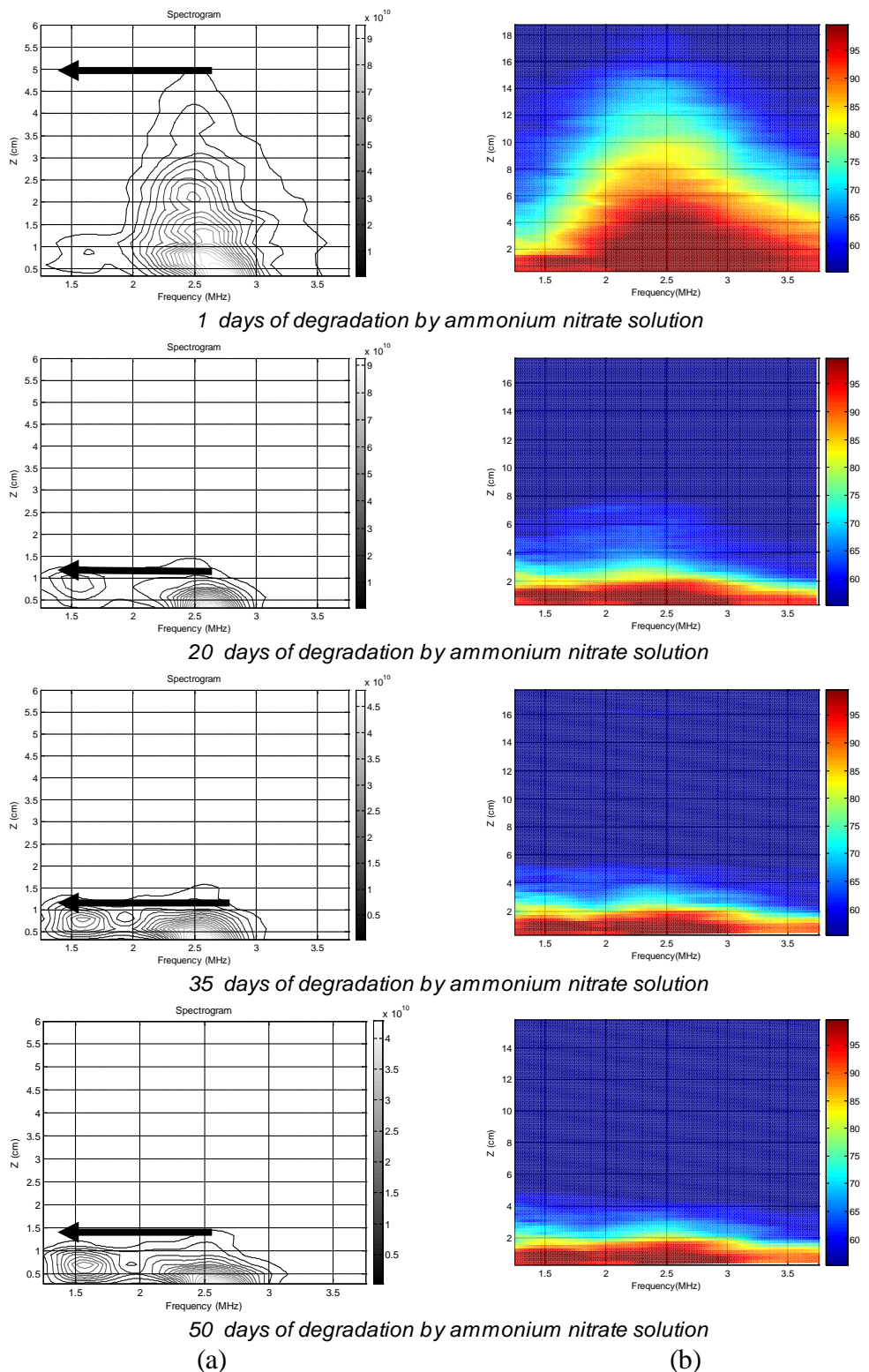


**Figure 5-8** (a) Averaged depth–frequency spectrogram (contour), (b) averaged depth- and frequency-dependent spectrogram (pcolor) for each degradation time for w/c =0.40 mortars degraded by ammonium nitrate solution, central frequency 3.5MHz.

## 5. Results and Discussion of Degradation Process by Ammonium Nitrate

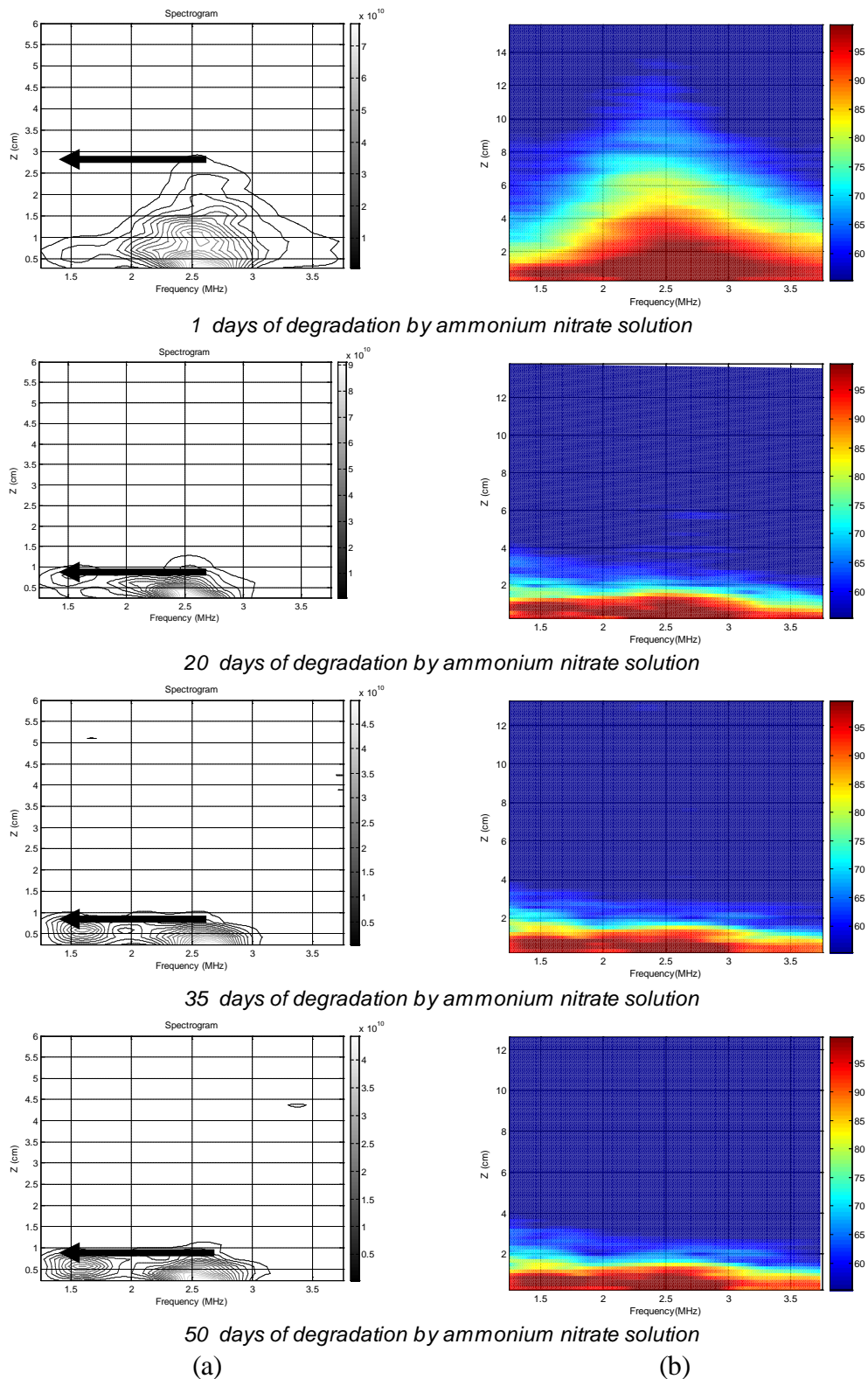


**Figure 5-9** (a) Averaged depth–frequency spectrogram (contour), (b) averaged depth– and frequency–dependent spectrogram (pcolor) for each degradation time for  $w/c = 0.55$  mortar degraded by ammonium nitrate solution, central frequency 3.5MHz.

## 5. Results and Discussion of Degradation Process by Ammonium Nitrate

---

Figures 5-10 and 5-11 illustrate the results of attenuation profile area for both frequencies 1 and 3.5 MHz respectively. In Figure 5-10, attenuation profile area (APA) for samples degraded by ammonium nitrate was increased with increasing the degradation time for both w/c ratios 0.40 and 0.55. It is observed that the high w/c ratio has attenuation higher than the low w/c ratio. On the other hand, in the case of control samples, it can be seen that the parameter APA was decreased slowly with time. This is due to the fact that the hydration process is completing with the time, and therefore, the porosity is decreasing because the pores were filled by the hydration products and finally results a decrease of APA.

In Figure 5-10, it is found a drop in the increasing of the (APA) after 20 days. For example, in the case of 1MHz, for w/c ratio 0.40, the attenuation profile area was increased by 76.71 % after 20 days of degradation to reach to 84.02% at the end of immersion time (an increment of 7.31% from 20 to 55 days of degradation), the same trend was observed in the case of w/c ratio 0.55 that was increased by 51.76% after 20 days to reach to 74% at the end of immersion time (an increment of 22.24 % from 20 to 55 days of degradation), see Table 5-3. On the other hand, as seen in Table 5-5, which present the thickness depth of the degraded samples using phenolphthalein test, the same trend is observed, i.e. a drop in the increased degraded layer. This reflects the increasing in the attenuation profile area of ultrasonic waves that is caused by the effect of the increasing in the degraded zone which in turn is caused by the leaching process of portlandite.

In Figure 5-11, which presents the results of attenuation profile area for frequency 3.5MHz, the same trend was observed as in the case of 1MHz. For w/c ratio 0.40, the attenuation profile area was increased by 159.34 % after 20 days of degradation to reach to 178.61% at the end of immersion time (an increment of 19.25% from 20 to 55 days of degradation) and in the case of w/c ratio 0.55, it was increased by 87.64% after 20 days to reach to 138% at the end of immersion time (an increment of 50.36 % from 20 to 55 days of degradation) see Table 5-4.

## 5. Results and Discussion of Degradation Process by Ammonium Nitrate

From the previous results, as seen for both frequencies, the same trend was observed. However, in the case of frequency 3.5MHz, the increasing in (APA) is higher than frequency 1MHz. For example, for the degraded samples, in the case of frequency 1MHz, for w/c ratio 0.4; the parameter of attenuation profile area (APA) was increased from 2.19 to 4.03 dB and for w/c ratio 0.55, it was increased from 2.84 to 4.95dB, while in the case of 3.5MHz, it was increased from 3.74 to 10.38 dB with w/c ratio 0.40 and from 5.42 to 12.90 dB for w/c ratio 0.55. As we can see, the value of (APA) of frequency 3.5MHz is 2.58 times for w/c ratio 0.4 and 2.61 times for w/c ratio 0.55 (at 50 days of degradation time).

From the results of (APA) for both frequencies, it is concluded that;

- This parameter is sensitive to estimate the degradation and it increases by the increasing of the degraded depth.
- The (APA) is sensitive to the changes of microstructure of the degraded mortar and it increases by the increasing both of w/c ratio and frequency.
- The frequency of 3.5MHz is more sensitive to the microstructure changes than the frequency 1MHz.

**Table 5-3** Attenuation profile area (APA) for frequency 1MHz for control and ammonium nitrate samples

Attenuation profile Area (dB) For frequency 1MHz								
Immersion time	W/C = 0.40				W/C = 0.55			
	Control	S.D	NH4NO3	S.D	Control	S.D	NH4NO3	S.D
1	2.19	±0.03	2.19	±0.03	2.84	±0.17	2.84	±0.17
20	2.05	±0.05	3.87	±0.03	2.51	±0.08	4.31	±0.02
35	1.99	±0.07	3.92	±0.05	2.41	±0.09	4.71	±0.19
50	1.93	±0.03	4.03	±0.03	2.35	±0.05	4.95	±0.07

## 5. Results and Discussion of Degradation Process by Ammonium Nitrate

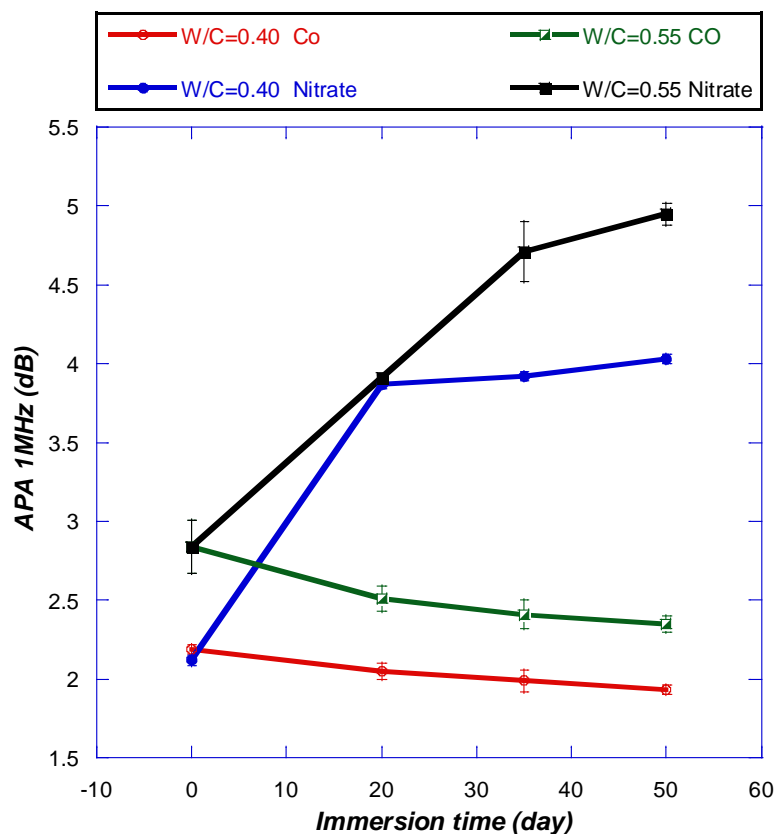


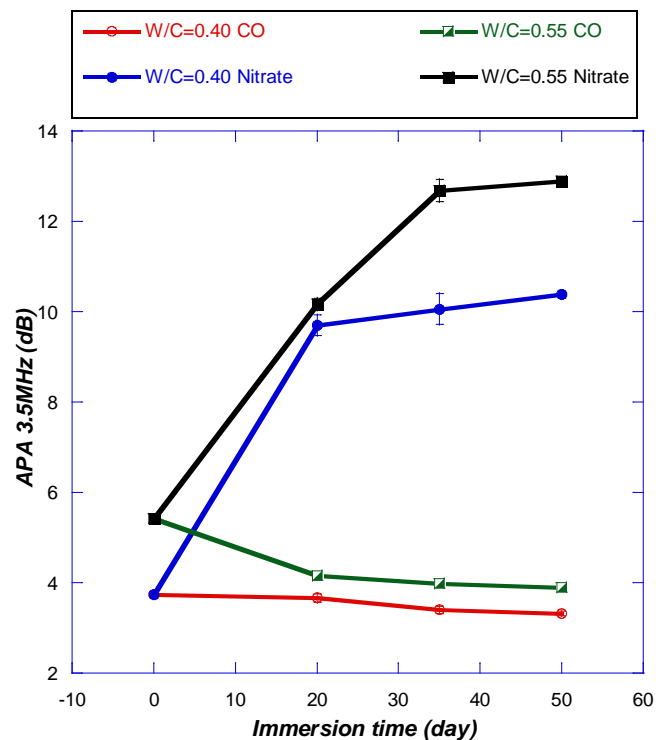
**Figure 5-10** Attenuation profile area 1 MHz with time for ammonium nitrate and control samples

**Table 5-4** Attenuation profile area (APA) for frequency 3.5MHz for control and ammonium nitrate samples

Attenuation profile Area (dB) for frequency 3.5MHz								
Immersion time	W/C = 0.40				W/C = 0.55			
	Control	S.D	NH4NO3	S.D	Control	S.D	NH4NO3	S.D
1	3.74	±0.06	3.74	±0.06	5.42	±0.08	5.42	±0.02
20	3.66	±0.09	9.70	±0.2	4.15	±0.06	10.17	±0.12
35	3.40	±0.07	10.05	±0.3	3.99	±0.06	12.69	±0.25
50	3.35	±0.05	10.38	±0.08	3.89	±0.05	12.90	±0.03











## 5. Results and Discussion of Degradation Process by Ammonium Nitrate



**Figure 5-11** Attenuation profile area 3.5 MHz with time for ammonium nitrate and control samples

**Table 5-5** The thickness depth of the degraded samples estimated by Phenolphthalein

Degradation time (day)	Degraded thickness (mm)	w/c=.40	Degraded thickness (mm)	w/c=.55
1	0.0		0.0	
20	4±1		6±2	
35	6±1		11±1	
50	7±1		16±2	

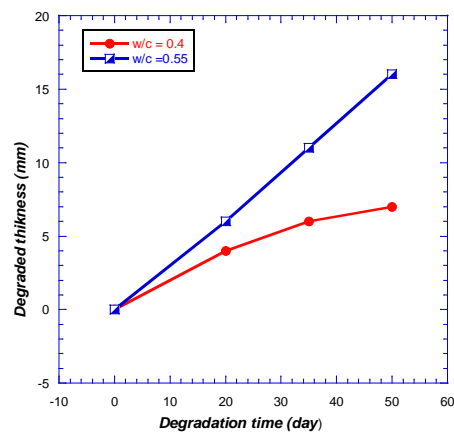


**Figure 5-12** Evolution of the degraded thickness with time

## 5.2. Correlation the Measured Parameters for Mortar

### 5.2.1. Correlation Ultrasonic P and S-wave Velocity versus Porosity

Figures 5-13 and 5-14 illustrate the correlation of porosity versus both longitudinal and transversal ultrasonic wave velocities. For the samples degraded by ammonium nitrate, the velocity of both waves decrease as porosity increases. It is found a good relationship between the two parameters (porosity and wave velocity). As declared previously, the degraded thickness was increased with the degradation time. The evolution of the degraded thickness can be explained by the decalcification of portlandite which leads to micro porosity and by decalcification of C-S-H hydrates which leads to macro porosity. This decalcification affects the hydraulic properties of mortar, mainly porosity and as elastic moduli depends on it; this induces the relationship between porosity and ultrasonic wave velocity (Lafhaj and Goueygou, 2009). All values of the regression coefficient R are found to be higher than 0.85. For the samples degraded by ammonium nitrate, porosity has a better correlation with shear wave velocity than longitudinal wave velocity, as can be seen in the figures.



## 5. Results and Discussion of Degradation Process by Ammonium Nitrate

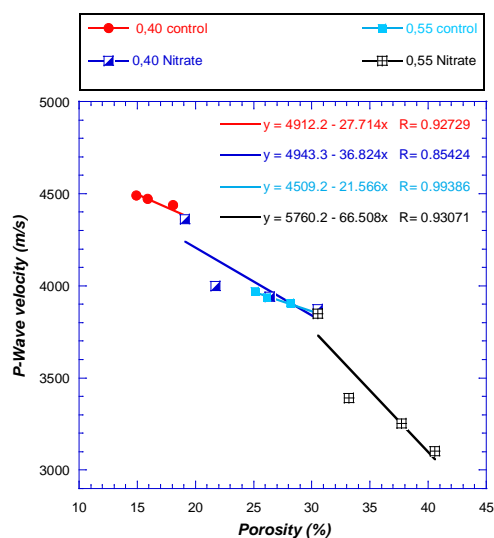


**Figure 5-13** Correlation Porosity with P- wave velocity for ammonium nitrate and control samples

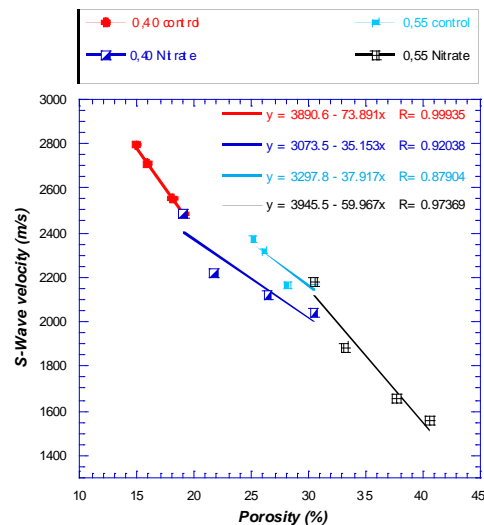


**Figure 5-14** Correlation Porosity with S- wave velocity for ammonium nitrate and control samples

### 5.2.2. Correlation Ultrasonic Attenuation Profile Area versus Porosity

Figure 5-15 and Figure 5-16 show the correlation of ultrasonic attenuation profile area (APA) versus porosity for both frequencies 1 and 3.5MHz. It is known that the hydration process is completing approximately at 90 curing days, the old of the control samples is 78 days (28 days of cure plus 50 days of degradation). For control samples, both of porosity and (APA) decrease with time because the hydration process is in progress (before 90 days of hydration). For ammonium nitrate samples, it is observed that when the porosity is increasing, the attenuation profile area increases. From the figures, it is found a strong relationship between the two parameters, all values of the regression coefficient R are found to be higher than 0.94. This reflects a good correlation between porosity and attenuation profile area.

From the correlation porosity versus attenuation profile area and ultrasonic wave velocity, it is concluded that;

- The porosity has a better correlation with attenuation profile area for the frequency 3.5MHz than the attenuation profile area for the frequency 1MHz.

## 5. Results and Discussion of Degradation Process by Ammonium Nitrate

- The porosity has a better correlation with attenuation profile area than ultrasonic wave velocity.

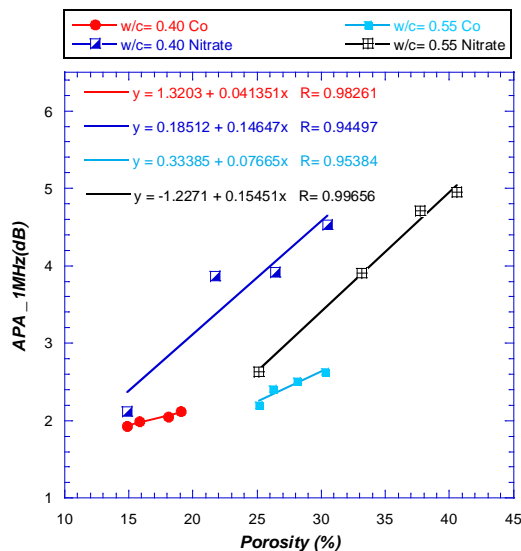


**Figure 5-15** Correlation Porosity with APA 1MHz for ammonium nitrate and control samples

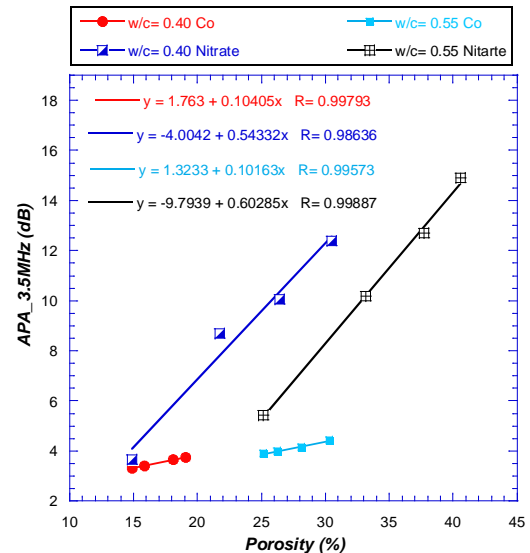


**Figure 5-16** Correlation Porosity with APA 3.5MHz for ammonium nitrate and control samples

### 5.2.3. Correlation P and S-wave Velocity versus Compressive and Flexural Strength

As seen in chapter 4 (section 4.2.3), the correlation between flexural and compressive strength versus shear and longitudinal waves is found when the changes in the microstructure of mortar and concrete are clear and notable, as the case of early ages concrete and mortar microstructure development and the degraded by aggressive elements. On the other hand, the ultrasonic pulse velocity values are affected by number of factors, which do not necessary influence the concrete compressive and flexural strength in the same way or to the same extend.

The correlation of compressive and flexural strength versus longitudinal and shear wave velocity is illustrated in the Figures from 5-17 to 5-20. It can be seen a good relationship for both control and ammonium nitrate samples. For control samples, as

## 5. Results and Discussion of Degradation Process by Ammonium Nitrate

---

mentioned in the previous section (5.2.2), our samples are 78 days old (early ages mortar microstructure development), so the variation is notable for both strength (flexural and compressive) and for wave velocity (longitudinal and shear), the strength is decreasing as the wave velocity increases. The regression coefficient  $R$  is higher than 0.86 for flexural strength and higher than 0.87 for compressive strength (see the figures). For ammonium nitrate samples, the relation between the strength and ultrasonic wave velocity can be seen. As mentioned previously in section 5.1.1 and 5.1.3, leaching of portlandite and decalcification of C-S-H, cause a decrease in the strength and an increasing in porosity, which finally leads to a decreasing in the wave velocity. From the figures it can be observed that, the regression coefficient  $R$  is higher than 0.95 for flexural strength and higher than 0.96 for compressive strength, which means that the relationship between the strength and ultrasonic wave velocity is good at early age and degraded samples.

From the correlation strength versus ultrasonic wave velocity, it is concluded that;

- It is not always found a good relationship between the strength and the wave velocity, because the ultrasonic pulse velocity values are affected by number of factors, which do not necessary influence the concrete compressive and flexural strength in the same way or to the same extend.
  
- Correlation strength with wave velocity is acceptable for early ages and degraded cementitious materials, because the changes in the microstructure are clear and notable.

## 5. Results and Discussion of Degradation Process by Ammonium Nitrate

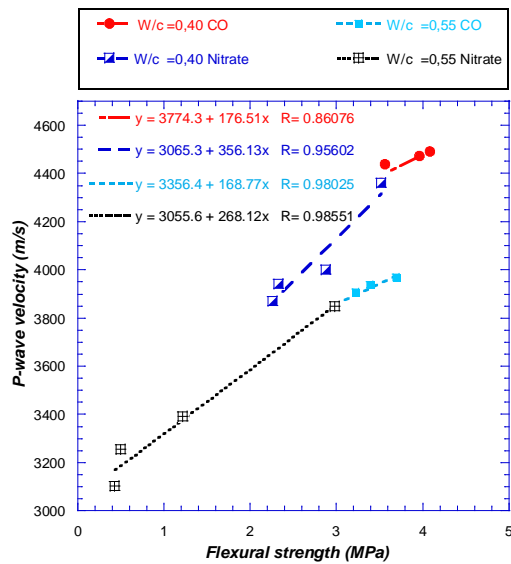


**Figure 5-17** Correlation flexural strength with P-wave velocity for ammonium nitrate and control samples

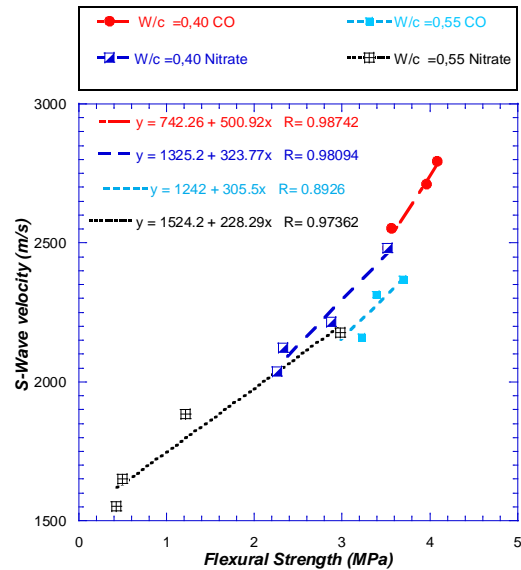


**Figure 5-18** Correlation flexural strength with S-wave velocity for ammonium nitrate and control samples

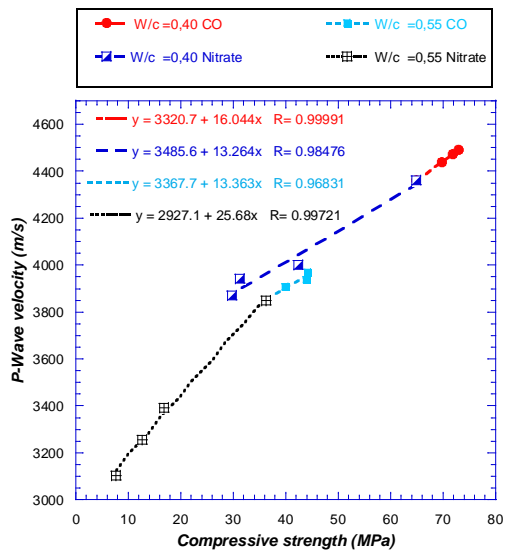


**Figure 5-19** Correlation compressive strength with P-wave velocity for ammonium nitrate and control samples

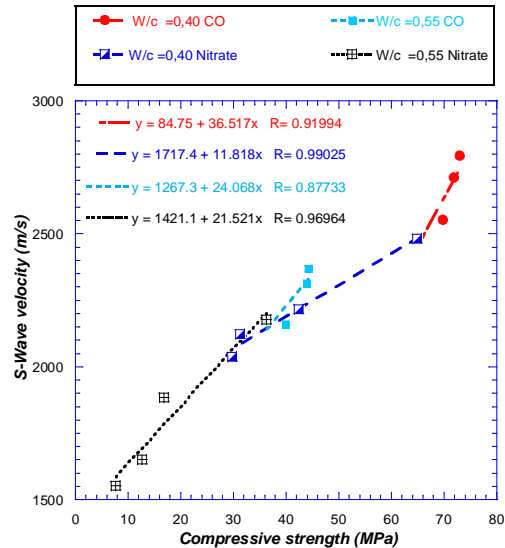


**Figure 5-20** Correlation compressive strength with S-wave velocity for ammonium nitrate and control samples

5.2.4. Correlation Attenuation Profile Area versus Compressive and Flexural Strength

From Figure 5-21 to Figure 5-24, the correlation of strength (flexural and compressive) versus APA (1 and 3.5MHz) is illustrated. From the figures and the results presented in sections 5.1.1 and 5.1.4 it can be observed that, APA of the degraded samples increases as the strength decreases. The contrast behaviour can be seen for the control samples, this shows the negative relationship between the strength and the APA, i.e. when one decreases the other is increasing and vice versa. From the figures, it is observed that all values of regression coefficient R are higher than 0.91 and this demonstrate the good relationship between the strength and the APA, when a high degradation level is found.

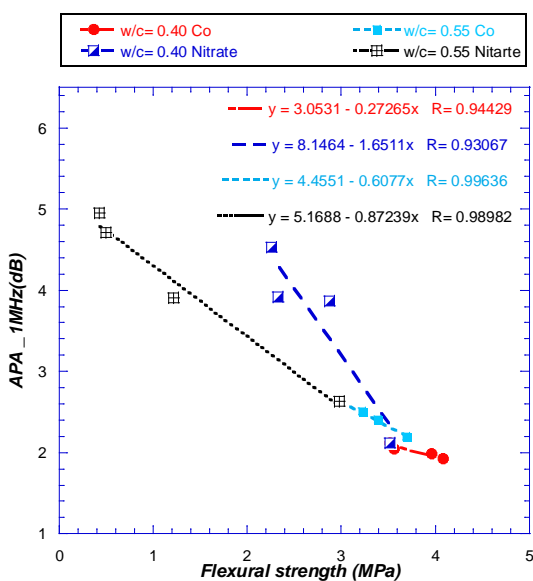


Figure 5-21 Correlation flexural strength with APA 1MHz for ammonium nitrate and control samples

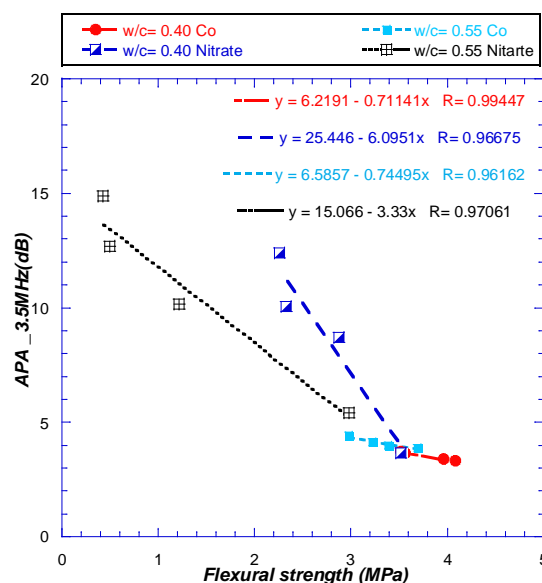
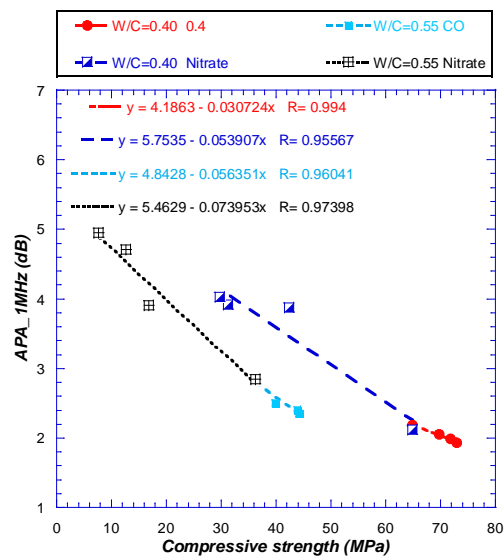
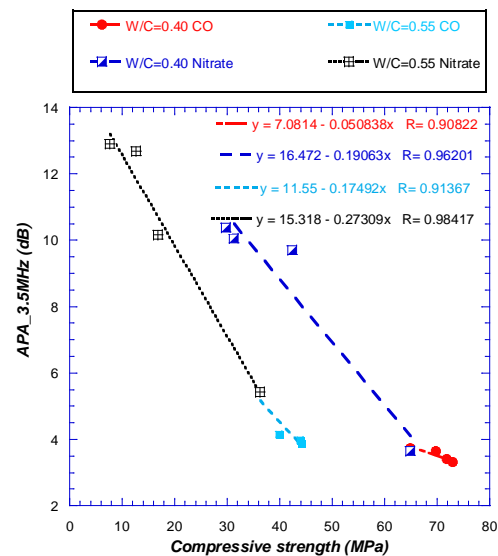


Figure 5-22 Correlation flexural strength with APA 3.5MHz for ammonium nitrate and control samples

## 5. Results and Discussion of Degradation Process by Ammonium Nitrate



**Figure 5-23** Correlation compressive strength with APA 1MHz for ammonium nitrate and control samples



**Figure 5-24** Correlation compressive strength with APA 3.5MHz for ammonium nitrate and control samples

### 5.2.5. Correlation P and S-wave versus APA

From Figure 5-25 to 5-28, the correlation curves between longitudinal and transversal wave velocities versus attenuation profile area for frequencies 1 and 3.5 MHz is illustrated, for both control and ammonium nitrate samples. The figures show the negative relationship between wave velocity and APA, i.e. APA decreases as wave velocity increases. The correlation factor for the samples degraded by ammonium nitrate is higher than 0.95.

From the correlation curves of APA versus flexural strength, compressive strength, p-wave velocity and S-wave velocity, it is concluded that;

- Attenuation profile area has a good relationship with compressive and flexural strength.
- Attenuation profile area has a good relationship with ultrasonic wave velocities (P and S-wave), which is higher than its correlation with the compressive and flexural strength

## 5. Results and Discussion of Degradation Process by Ammonium Nitrate

- The relationship between the attenuation profile areas of ultrasonic wave is negative with compressive strength, flexural strength, longitudinal and shear wave velocity and it is positive with porosity.

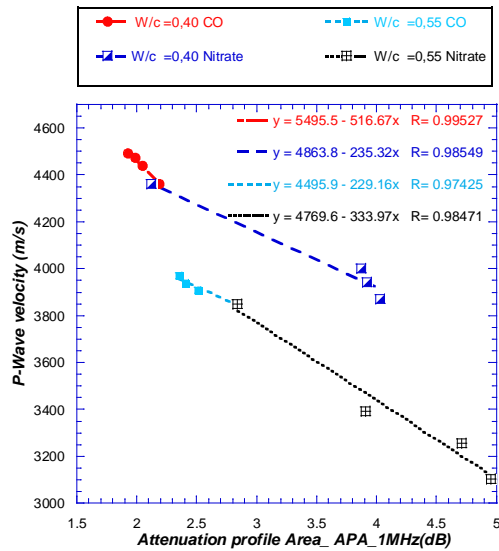


Figure 5-25 Correlation P-Wave with APA 1MHz.

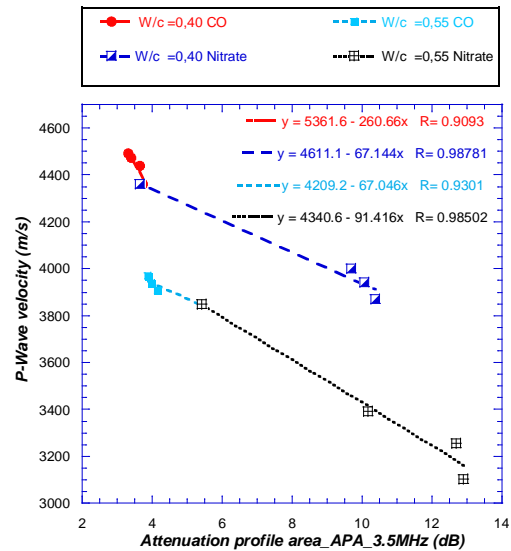


Figure 5-26 Correlation P-Wave with APA 3.5MHz.

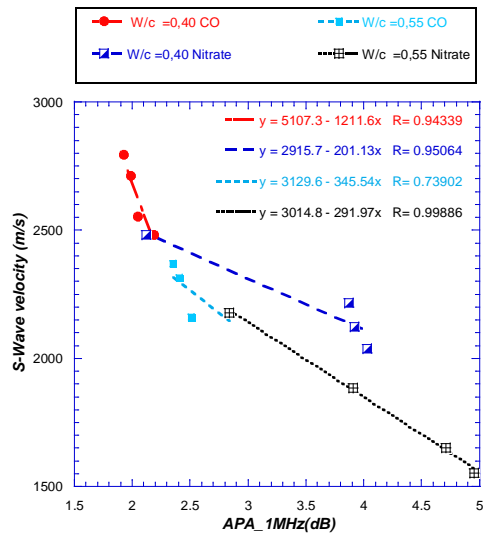


Figure 5-27 Correlation S-Wave with APA 1MHz.

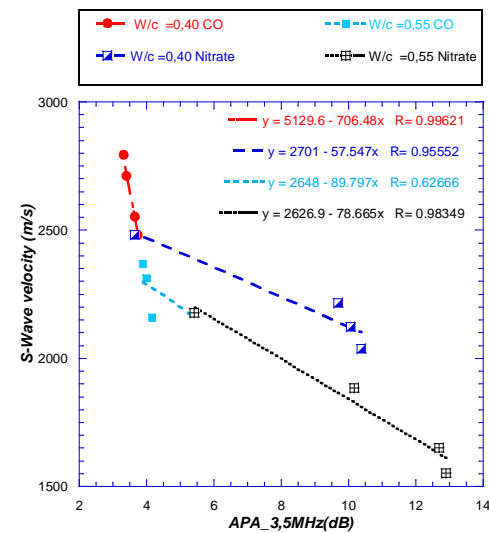


Figure 5-28 Correlation S-Wave with APA 3.5MHz

### 5.3. Analysis and Discussion the Results of Concrete

As mentioned previously that water to cement ratio plays an important role in the penetration of aggressive element into the cementitious materials. So, it has been recognized to use a low w/c ratio for obtaining a good concrete with a high durability and to avoid the deterioration by such aggressive elements as possible. The concrete used in this study, as mentioned in (chapter 1), is a concrete in service (real case study) and it has a low w/c ratio (0.30). Thus, it was expected that the deterioration process will be very slow and needs many years to deteriorate. For this reason, the solution of ammonium nitrate is used to obtain an accelerate deterioration process for this type of concrete, to see the capability of the techniques presented in (chapter 3) to estimate the degradation process of the investigated precast concrete cores degraded by 4 mol of ammonium nitrate solution.

#### 5.3.1. Compressive Strength

The results of the compressive strength tests of investigated precast concrete cores for both control and samples degraded by ammonium nitrate are presented in Table 5-6 and Figure 5-29 (A) for both control and degraded samples. It can be observed that the compressive strength of SRPC concrete is higher than the PLC concrete samples. This is because the samples fabricated by cement I 42.4 R/SR have a cement content higher than the samples fabricated by cement II A-L 42.5R (see table 3.5, chapter 3)

The compressive strength for control samples tends to increase with time. On the other hand, the compressive strength of the degraded samples decreases slightly until the end of exposure time. As cementitious materials are based on calcium and silica oxides, its hydration products consist mainly of calcium-hydrate, Ca-Al-hydrate and Ca-Si-hydrate. The leaching effect is essential a decalcifying effect, i.e.  $\text{Ca}^{2+}$  ion are dissolved and  $\text{NO}_3^-$  ions penetrate into concrete. This causes a loss of the mechanical strength of concrete, the same trend was observed for the two types of precast concrete samples.



## 5. Results and Discussion of Degradation Process by Ammonium Nitrate

Figure 5-29 (B) presents the loss in the strength for the two types of precast concrete degraded by ammonium nitrate solution, as can be seen, the loss of strength increases with the increasing of degradation time.

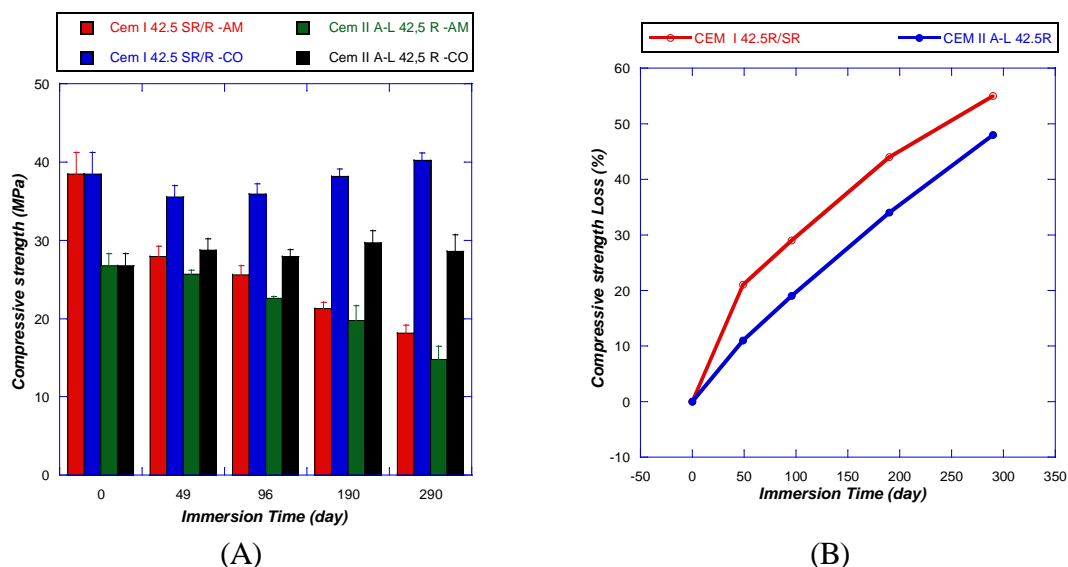


**Figure 5-29** (A) The compressive strength of the precast concrete cores degraded by 4 moles of ammonium nitrate solution and control samples; (B) The loss in the strength due to the degradation process

**Table 5-6** Compressive strength and compressive strength loss for control and ammonium nitrate samples

Time(day)	Compressive strength (MPa) CEM I 42.5R/SR			Compressive strength (MPa) CEM II A-L 42.5R		
	Control	Ammonium nitrate	Loss (%)	Control	Ammonium nitrate	Loss (%)
	1	38.44±2.79	38.44±2.77	0	26.77±1.52	26.77±1.52
49	35.51±1.50	27.94±1.28	21	28.70±1.46	25.68±0.50	11
96	35.88±1.30	25.62±1.17	29	27.93±0.91	22.58±0.23	19
190	38.14±1.00	21.29±0.77	44	29.71±1.54	19.74±1.91	34
290	40.18±1.02	18.13±1.02	55	28.60±2.10	14.79±1.70	48

### 5.3.2. Open Porosity

Figure 5-30 and Table 5-7 displays the results of porosity of precast concrete for control and degraded samples. It is observed that the porosity of control samples for both cement types do not change with time and the difference between the porosity values for both cement types is very small. It is known that porosity is related to the w/c ratio, while for degraded samples, the porosity increases linearly until the end of immersion time. Also, it is clear from the figure that the porosity of samples fabricated by CEM II A-L 42.5 R is a little bit higher than the porosity of samples fabricated by CEM I 42.4 R/SR, but the difference between the two porosity values for the degraded samples is small, (see Table 5-7 ) and this is due to the low w/c ratio of the samples. This increasing in porosity is due to the evolution of the degraded zone by the leaching of ions. The leaching of ions (mainly calcium and hydroxide) from the pore solution to the external environment is responsible for the dissolution of these hydrates. The consequences of ionic leaching are representing the increase of the porosity with the degradation time.

**Table 5-7** Porosity variation of control and ammonium nitrate samples

Time (day)	Porosity (%) - CEM I 42.5R/SR		Porosity (%) - CEM II A-L 42.5R	
	Control	Ammonium nitrate	Control	Ammonium nitrate
1	11.37±0.22	11.37±0.22	12.75±0.60	12.75±0.60
49	11.99±0.35	11.90±0.38	12.87±0.43	13.27±0.43
96	12.06±0.04	12.65±0.14	12.91±0.32	14.07±0.14
190	12.16±0.28	14.28±0.35	13.00±0.29	15.87±0.21
290	11.93±0.29	15.23±0.23	12.80±0.50	16.65±0.12

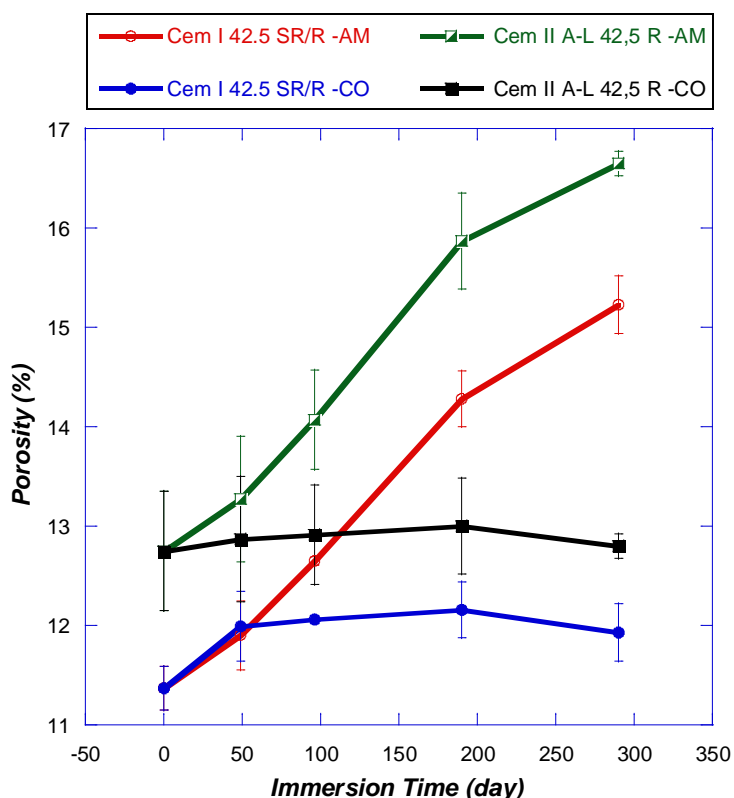


**Figure 5-30** Open porosity of precast concrete cores degraded by ammonium nitrate and control samples

### 5.3.3. Ultrasonic Longitudinal and Transversal Wave Velocity

Figure 5-31 (A and B), Table 5-8 and Table 5-9 present the result of ultrasonic longitudinal and shear wave velocity for control and degraded samples. The same trend was observed in the figure for both P and S-wave. For control samples, the velocity of ultrasonic waves varies up and down from the initial time to the end of experimental time; this variation is perhaps due to the variation of the place of measured points every measure time. As mentioned previously, the concrete is heterogeneous material, thus one time, most of the pathway of ultrasonic wave contains sand which causes an increasing in the wave velocity for that measured points. In the other time, most of the pathway contains limestone aggregate which has a lower wave velocity than sand. For ammonium nitrate samples, the general trend is decreasing in the wave velocity from the initial time until the end of exposure time, for both waves longitudinal and shear.

## 5. Results and Discussion of Degradation Process by Ammonium Nitrate

---

From the first day of the degradation process up to 96 days, the variation in the ultrasonic wave velocity is very small (almost, no variation). Then, it can be observed that the wave velocity decreases slowly until 290 days of the degradation time (see Table 5-8 and Table 5-9). The slow variation in the ultrasonic wave velocity during all deterioration time is because the concrete under studying is a very strong concrete. This is due to the low w/c ratio and the high compaction process by using additives and a mechanical vibration which lead to obtaining a concrete with a very low porosity. Thus, it was difficult for NO<sub>3</sub> ions to penetrate the concrete therefore, the process of decalcification of calcium and dissolution of C-S-H was advanced slowly. On the other hand, in Figure 5-32 which illustrates the degradation depth for a sample degraded by ammonium nitrate for 290 days, the pathway of ultrasonic wave may has aggregate which is not affected by the degradation process. As it is known that the degradation affects the cement paste, one possible explanation is that the variation in the velocity of the ultrasonic wave depends on the degraded volume of cement paste inside the sample.

From the analysis of the results of ultrasonic longitudinal and shear wave velocity, it is clear that the rate of decreasing in the wave velocity depends not only on the degradation depth, but also depends on the volume of degraded cement paste in the sample. It is known that the aggregate volume in the concrete mixture is the most, for this, it is expected that the decrease in the ultrasonic wave velocity will continue by slow rate.

## 5. Results and Discussion of Degradation Process by Ammonium Nitrate

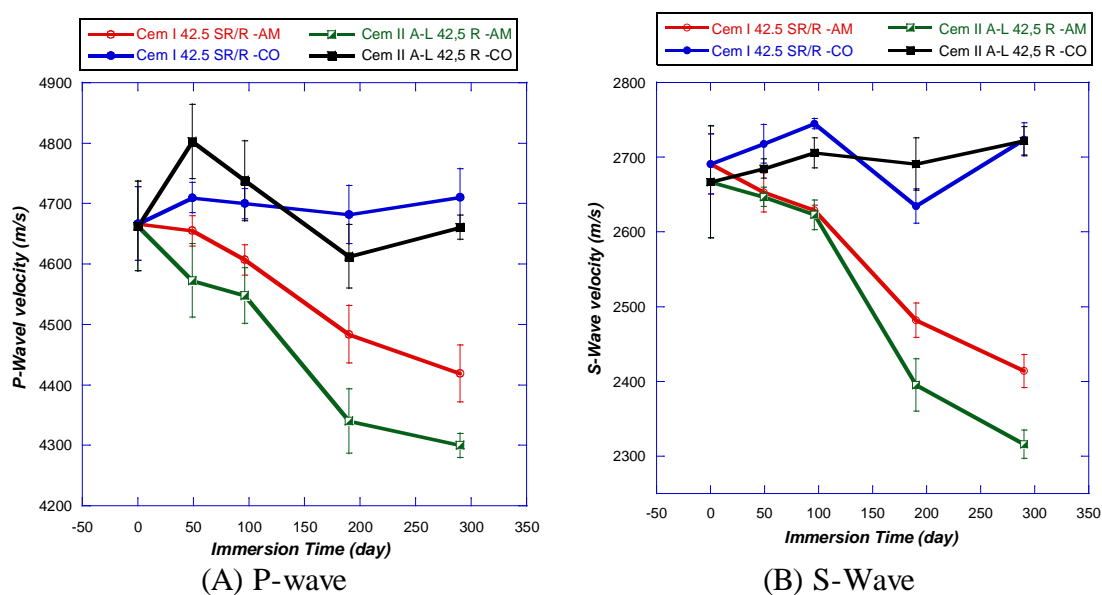


**Figure 5-31** P and S-wave velocity of the precast concrete cores for samples degraded by 4 moles of ammonium nitrate solution and control samples

**Table 5-8** P-wave Velocity Variation of control and ammonium nitrate samples

Time (day)	P-wave (m/s)-CEM I 42.5R/SR		P-wave (m/s)-CEM II A-L 42.5R	
	Control	Ammonium nitrate	Control	Ammonium nitrate
1	4667±61	4667±61	4663±74	4663±74
49	4710±25	4655±21	4803±61	4573±61
96	4700±25	4607±48	4738±66	4540±46
190	4682±48	4484±48	4613±53	4340±50
290	4711±47	4419±42	4661±20	4300±19

**Table 5-9** Variation of S-wave velocity for control and ammonium nitrate samples

Time (day)	S-wave (m/s)-CEM I 42.5R/SR		S-wave (m/s)-CEM II A-L 42.5R	
	Control	Ammonium nitrate	Control	Ammonium nitrate
1	2691±40	2691±40	2667±71	2667±71
49	2718±26	2653±20	2685±13	2647±18
96	2748±07	2629±09	2706±20	2623±22
190	2635±23	2482±18	2691±35	3395±30
290	2724±22	2414±23	2722±19	3316±12

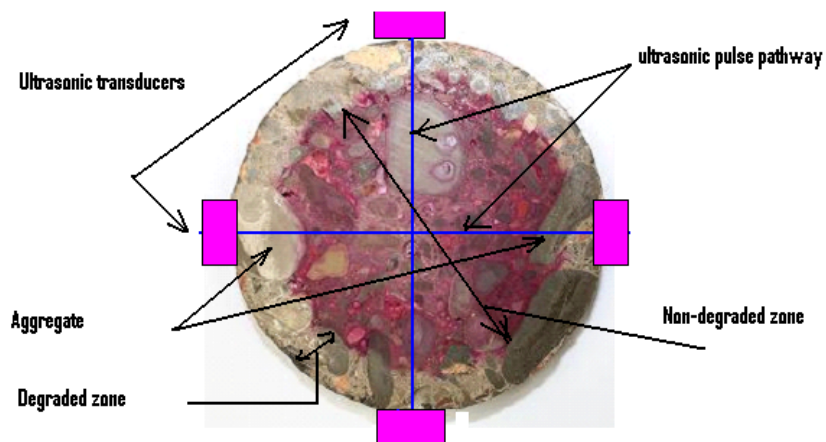


**Figure 5-32** Degradation depth for a sample degraded for 290 days

### 5.3.4. Ultrasonic Attenuation Profile Area (APA)

Figures from 5-33 to 5-36 illustrate the variation of attenuation of ultrasonic waves with time for the degraded samples. By the effect of the internal variation of the microstructure of concrete due to the degradation by ammonium nitrate solution for 49, 96, 190 and 290 days, the variation in the penetration of ultrasonic pulse can be seen. The same trend was observed for both SRPC and LPC samples, a decreasing of ultrasonic pulse linearly with time. But the penetration depth of SRPC samples is slightly less than LPC samples. Also it is observed that the frequency 3.5 MHz has a penetration depth less than frequency 1MHz.

## 5. Results and Discussion of Degradation Process by Ammonium Nitrate

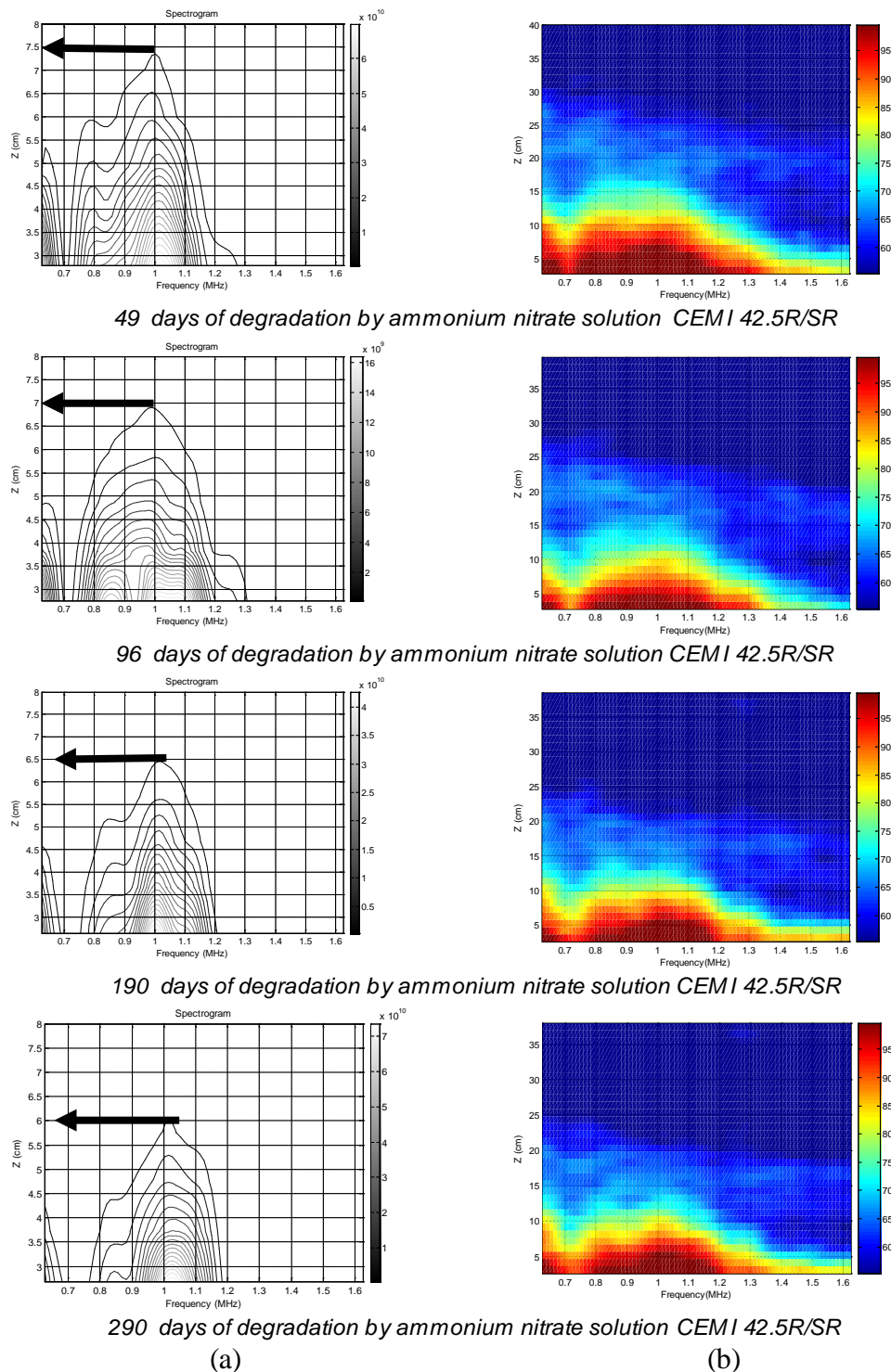


**Figure 5-33** (a) Averaged depth–frequency spectrogram (contour), (b) averaged depth- and frequency-dependent spectrogram (pcolor) for each degradation time for CEMI42.5R/SR degraded by ammonium nitrate solution, central frequency 1MHz.

## 5. Results and Discussion of Degradation Process by Ammonium Nitrate

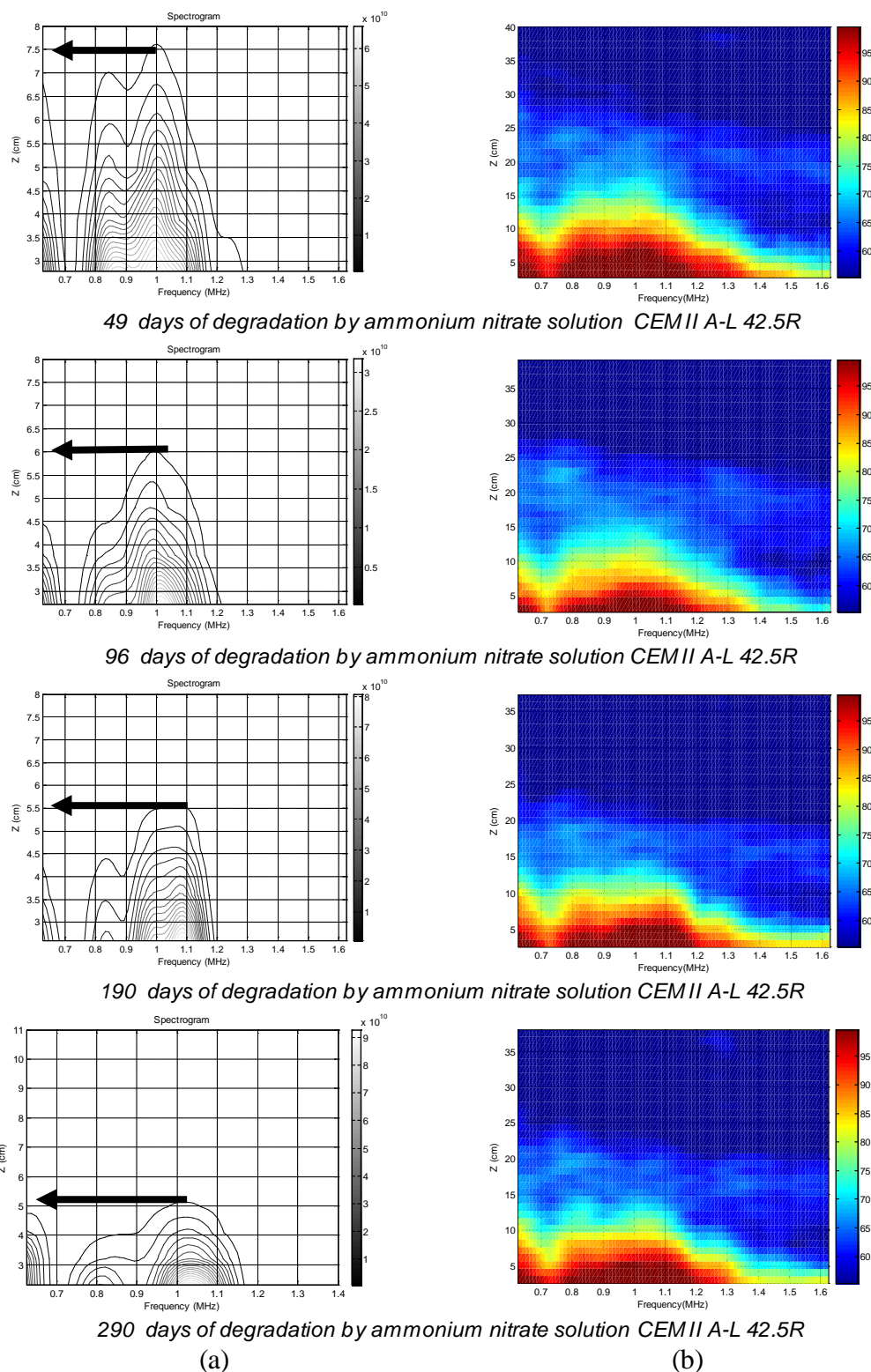


**Figure 5-34** (a) Averaged depth–frequency spectrogram (contour), (b) averaged depth- and frequency-dependent spectrogram (pcolor) for each degradation time for CEM II A-L 42.5R degraded by ammonium nitrate solution, central frequency 1MHz.



## 5. Results and Discussion of Degradation Process by Ammonium Nitrate

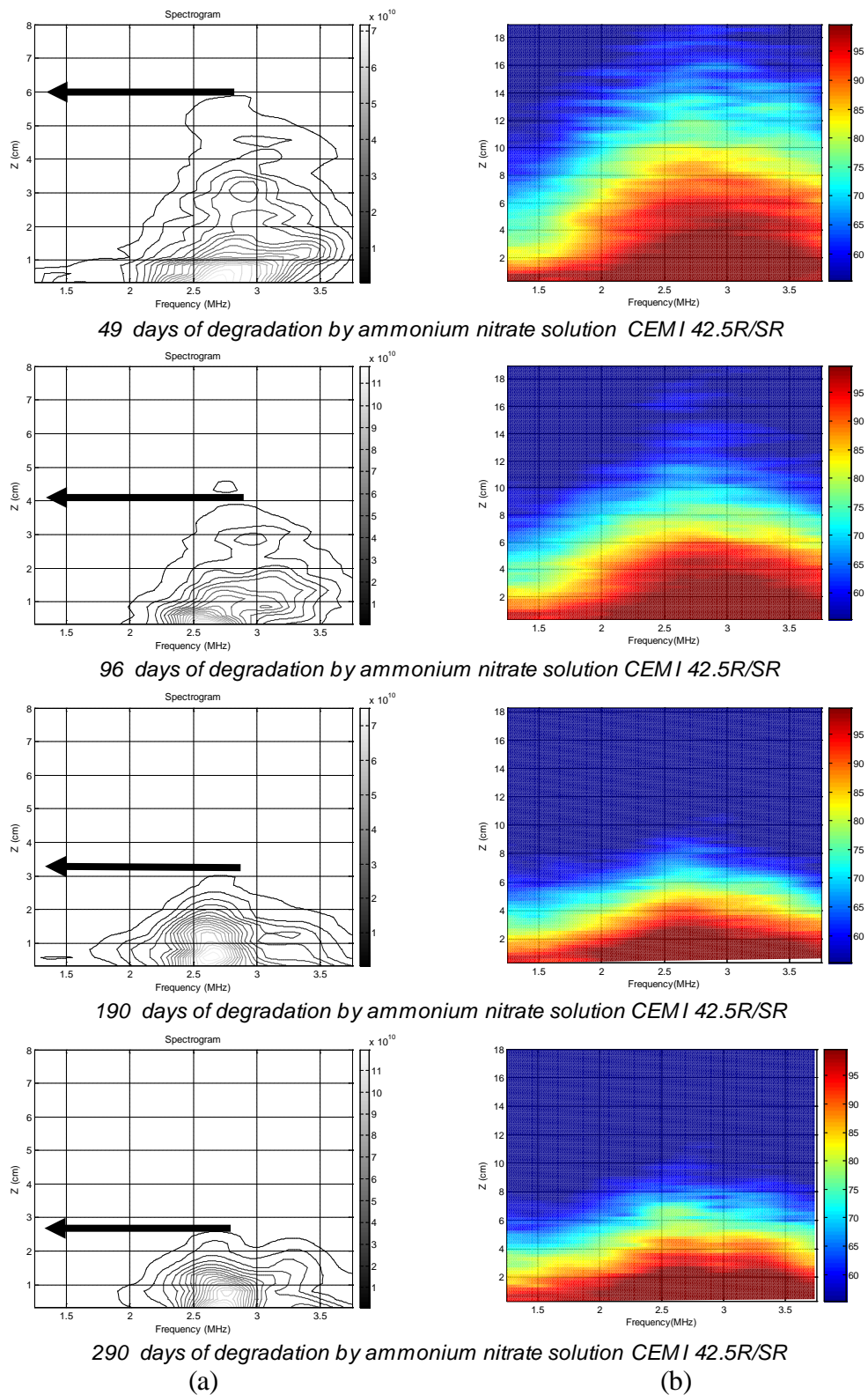


**Figure 5-35** (a) Averaged depth–frequency spectrogram (contour), (b) averaged depth- and frequency-dependent spectrogram (pcolor) for each degradation time for CEMI42.5R/SR degraded by ammonium nitrate solution, central frequency 3.5MHz.

## 5. Results and Discussion of Degradation Process by Ammonium Nitrate

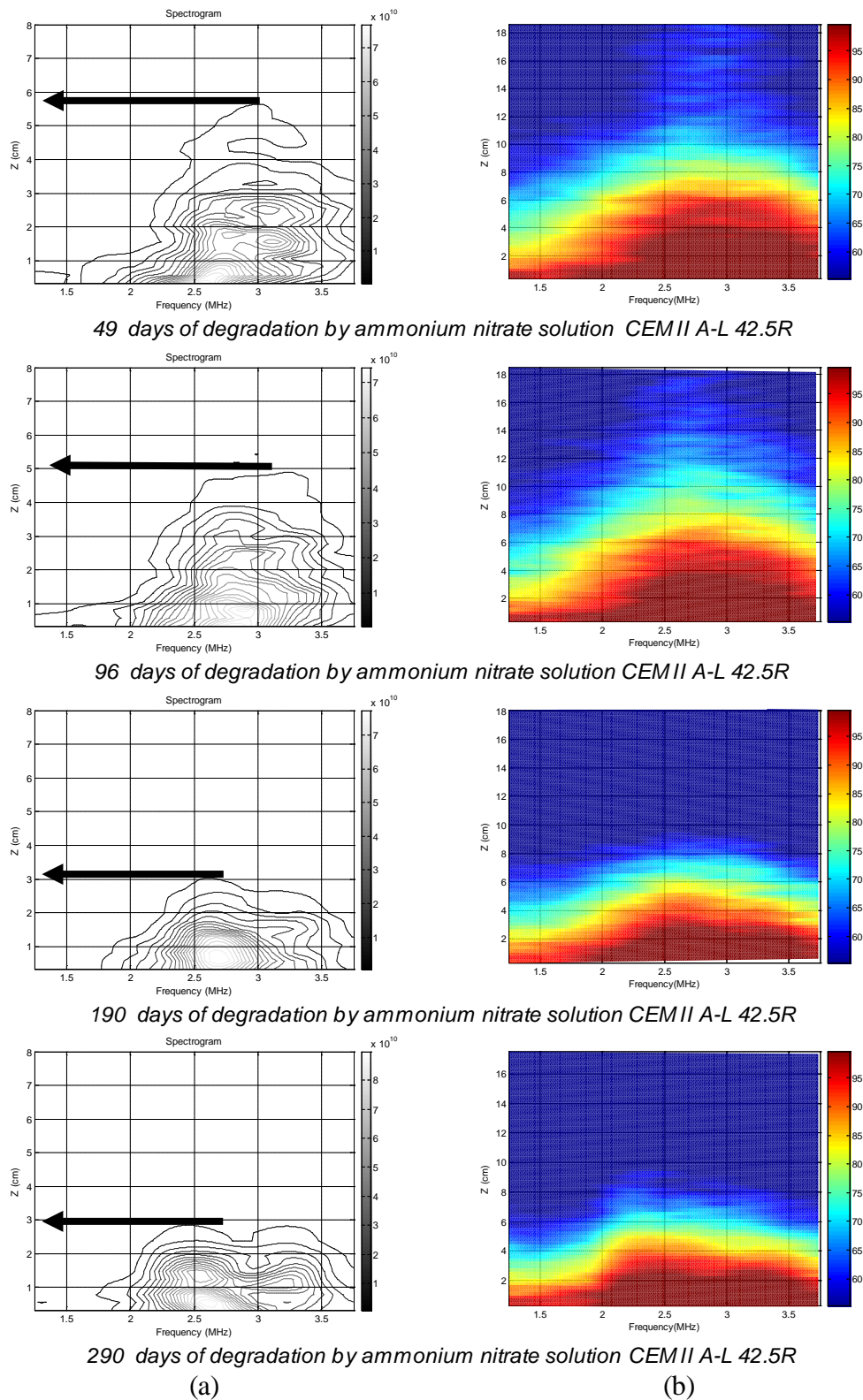


**Figure 5-36** (a) Averaged depth–frequency spectrogram (contour), (b) averaged depth- and frequency-dependent spectrogram (pcolor) for each degradation time for CEM II A-L 42.5R degraded by ammonium nitrate solution, central frequency 3.5MHz.

## 5. Results and Discussion of Degradation Process by Ammonium Nitrate

Figure 5-37 (A and B) illustrates the results of APA for both frequencies 1 and 3.5MHz for control and degraded samples. For control samples, for both concrete types and for both frequencies, the variation of the attenuation profile area is very small (almost, no variation), which is normal because of there is no degradation.

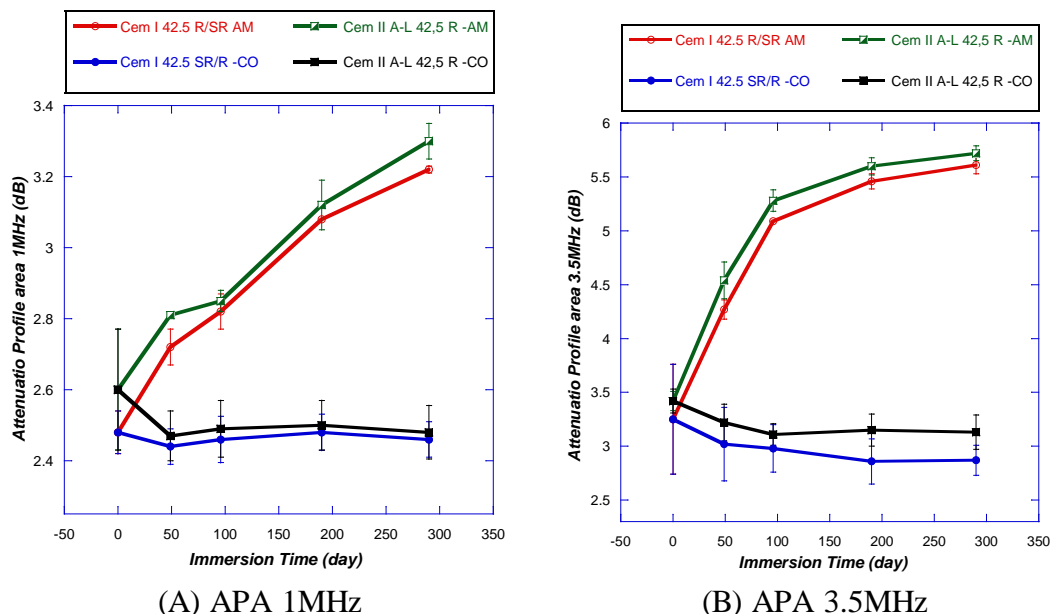
For the samples degraded by ammonium nitrate, an increasing in the APA from the start until the end of degradation time can be observed, and the CEM II A-L 42.5R has attenuation higher than the CEM I 42.5 R/SR because the contain of CEM I 42.4 R/SR is more than the contain of CEM II A-L 42.5R in the samples, as mentioned previously. The rate of the increasing depends on the degradation depth due to the leaching process of calcium.

Table 5-10 and Table 5-11 present the values of APA for both frequencies and for both concrete types. When these values are compared with the values obtained for mortar samples, which was presented previously in Table 5-3and Table 5-4, the capacity and the sensibility of this parameter can be seen in order to estimate the degradation level, and how APA can follow the changes of the microstructure of cementitious materials in all levels of the degradation (a high degradation level, as in the case of mortar samples, and a low degradation level, as in the case of precast concrete samples).

**Table 5- 10** APA 1MHz for control and ammonium nitrate samples

Time (day)	APA 1 MHz (dB)-CEM I 42.5R/SR		APA 1 MHz (dB)-CEM II A-L 42.5R	
	Control	Ammonium nitrate	Control	Ammonium nitrate
1	2.48±0.06	2.48±0.06	2.60±0.17	2.60±0.17
49	2.44±0.05	2.72±0.05	2.47±0.07	2.81±0.00
96	2.46±0.07	2.82±0.05	2.49±0.08	2.85±0.03
190	2.48±0.05	3.08±0.00	2.50±0.07	3.12±0.07
290	2.46±0.04	3.22±0.10	2.48±0.08	3.30±0.05

## 5. Results and Discussion of Degradation Process by Ammonium Nitrate



**Figure 5-37** Attenuation profile area for frequencies (1 and 3.5MHz) of the precast concrete cores for samples degraded by 4 moles of ammonium nitrate solution and control samples

**Table 5- 11** APA 3.5 MHz for control and ammonium nitrate samples

Time (day)	APA 3.5 MHz (dB)-CEM I 42.5R/SR		APA 3.5 MHz (dB)-CEM II A-L 42.5R	
	Control	Ammonium nitrate	Control	Ammonium nitrate
1	3.25±0.51	3.25±0.51	3.42±0.11	3.42±0.11
49	3.02±0.34	4.27±0.21	3.22±0.17	4.54±0.17
96	2.98±0.22	5.09±0.48	3.11±0.10	5.28±0.10
190	2.86±0.21	5.46±0.48	3.15±0.15	5.60±0.08
290	2.87±0.14	5.61±0.42	3.13±0.16	5.72±0.07

### 5.4. Correlation the Measured Parameters for Concrete

#### 5.4.1. Correlation Ultrasonic P and S-Wave Velocity versus Porosity

Figure 5-38 and Figure 5-39 illustrate the correlation curves of porosity versus longitudinal and shear wave, respectively, for the samples degraded by ammonium

## 5. Results and Discussion of Degradation Process by Ammonium Nitrate

nitrate. From the curves, it is clear that with the increasing of porosity values due to the degradation process, the ultrasonic wave velocities (P and S-waves) decrease. All values of regression coefficient R are higher than 0.98, which confirms the strong relation between porosity and ultrasonic wave velocities.

Similar results were obtained in the first section of this chapter (results of mortar samples), and it was found a high correlation between the two parameters, as in the case of concrete samples. The relationship between porosity and ultrasonic wave velocity was studied for cement paste as a homogeneous material (Fethi et al., 2009), for mortar as a more homogeneous material than concrete (Lafhaj et al., 2006; Lafhaj and Goueygou, 2009) and in this study, for concrete as a heterogeneous material. In all previous studies, it was found a strong relationship between porosity and ultrasonic wave velocity and this relation is linear. Thus, it is concluded that;

- The using of ultrasonic wave velocity is successful to estimate the porosity and to follow the degradation of cement paste, mortar and concrete when they are subjected to aggressive environments.
- Ultrasonic P-wave velocity somehow correlates better with porosity than S-wave velocity

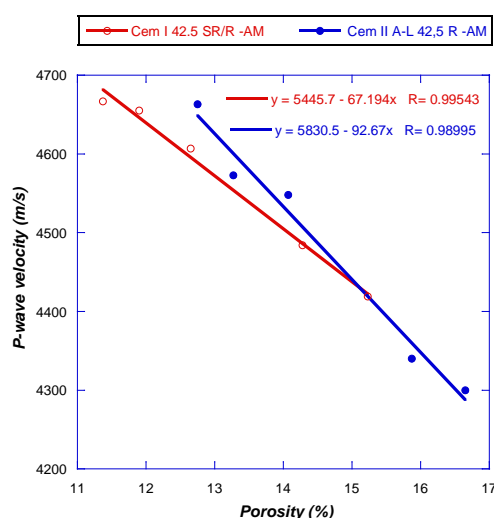


**Figure 5-38** Correlation Porosity with P- wave for ammonium nitrate samples

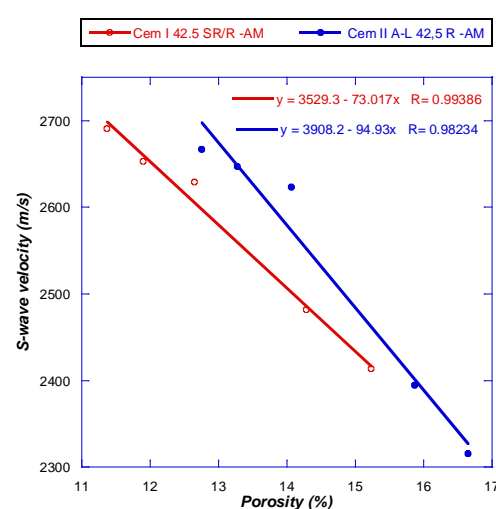


**Figure 5-39** Correlation Porosity with S- wave for ammonium nitrate samples

### 5.4.2. Correlation Attenuation Profile Area versus Porosity

Figures 5-40 and 5-41 illustrate the correlation curve of porosity versus the parameter of attenuation profile area (APA) for frequencies 1 and 3.5 MHz respectively. As mentioned previously in the section of mortar samples, the attenuation profile area increases by the increasing of porosity which increases due to the increasing of the degraded layer in the sample.

From the figures, similar result were obtained for the precast concrete samples, the APA increases linearly with porosity and all the coefficients regression R are higher than 0.85. When the correlation both of attenuation profile area and ultrasonic wave velocity versus porosity is compared, it can be observed that porosity correlates better with ultrasonic wave velocity. As mentioned previously in chapter 4, the APA was found to be successful to follow the cure process of cement-based materials, such as cement paste and mortar, and to estimate its porosity (L Vergara, et al 2001 and Fuente, 2004). By using this parameter in this study to follow the degradation of mortar and precast concrete samples, it was found that this parameter has a good correlation with porosity and it is successful to estimate and to follow the degradation process.

## 5. Results and Discussion of Degradation Process by Ammonium Nitrate

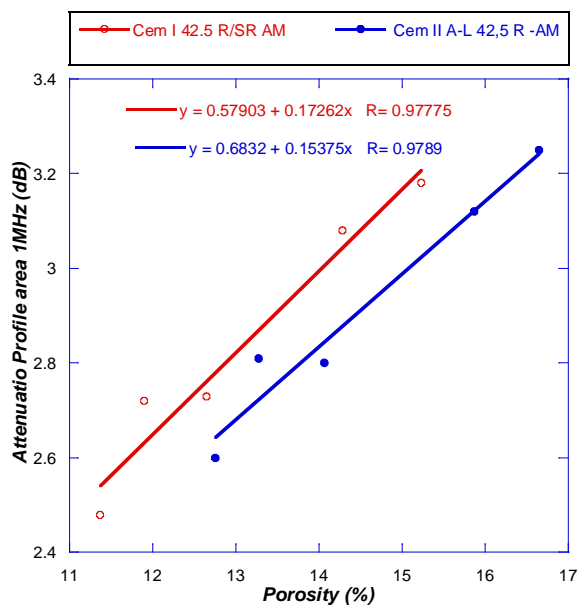


**Figure 5-40** Correlation Porosity with APA 1MHz for ammonium nitrate samples

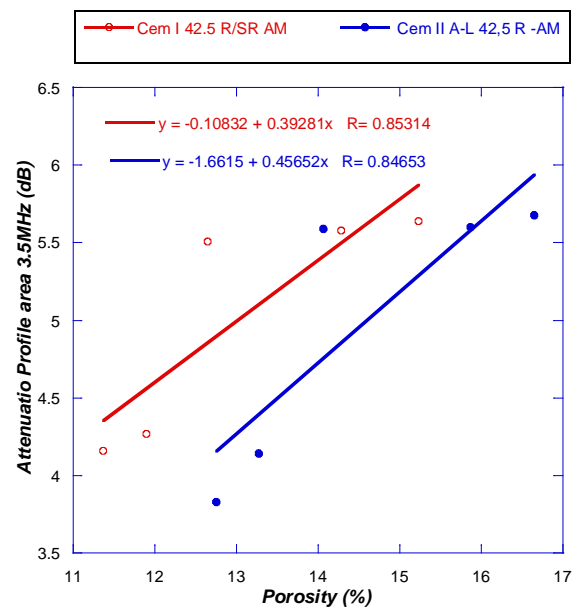


**Figure 5-41** Correlation Porosity with APA 3.5MHz for ammonium nitrate samples

### 5.4.3. Correlation P and S-Wave Velocity versus Compressive Strength

Figure 5-42 and Figure 5-43 illustrate the correlation curves of compressive strength versus longitudinal and shear wave velocity, respectively, for precast concrete samples degraded by ammonium nitrate solution. Ultrasonic wave velocity is related to the mechanical properties of the investigated material and more directly to the modulus of elasticity (G. Rüstem et al., 2006). As mentioned previously, the degradation of mortar and concrete by ammonium nitrate solution leads to decalcification of calcium and dissolution of C-S-H, which leads to a decreasing of the mechanical strength of the degraded material. Thus, the variation of ultrasonic wave velocity is affected by the variation of strength. As it can be seen in the figures, both of P and S-wave velocity decrease with decreasing of compressive strength of the degraded samples, and the regression coefficient R was found to be higher than 0.86, which shows the good relationship between ultrasonic wave velocity and concrete strength.

The correlation of compressive strength of cement paste versus ultrasonic wave velocity was studied by (Fuente, 2004), for 7, 28 and 90 days of curing. He found a good



## 5. Results and Discussion of Degradation Process by Ammonium Nitrate

correlation between the two parameters (R higher 0.96) and the relationship between ultrasonic wave velocity and strength was linear.

The correlation of compressive strength of mortar with ultrasonic wave velocity was studied by (G. Rüstem et al., 2006). Mortar with mineral admixture (silica fume, fly ash and blast furnace slag), for curing periods 7, 28 and 90 days were studied. The authors found a good correlation between the strength and wave velocity (R higher 0.94), and the relationship between the two parameters was exponential and linear.

The previous studies showed the correlation of compressive strength with ultrasonic wave velocity for both cement paste and mortar in the curing period. Thus, after studying the degradation process of mortar and precast concrete, it can be concluded that;

- It is found a good relationship between compressive strength and ultrasonic wave velocity during the curing period of cement-based materials and during the degradation process.

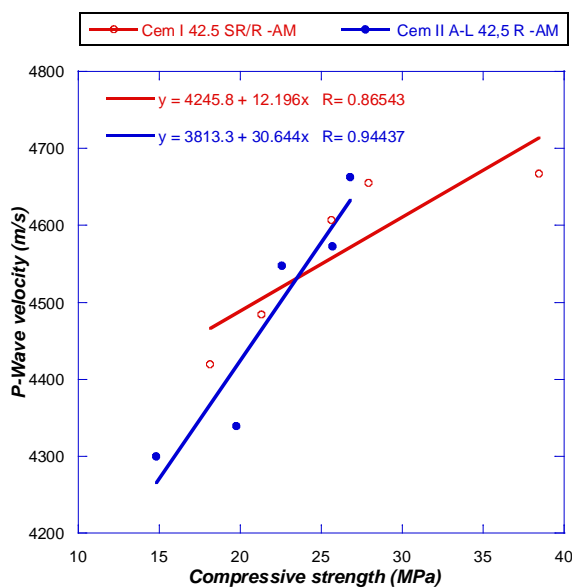


**Figure 5-42** Correlation compressive strength with P-wave for ammonium nitrate samples

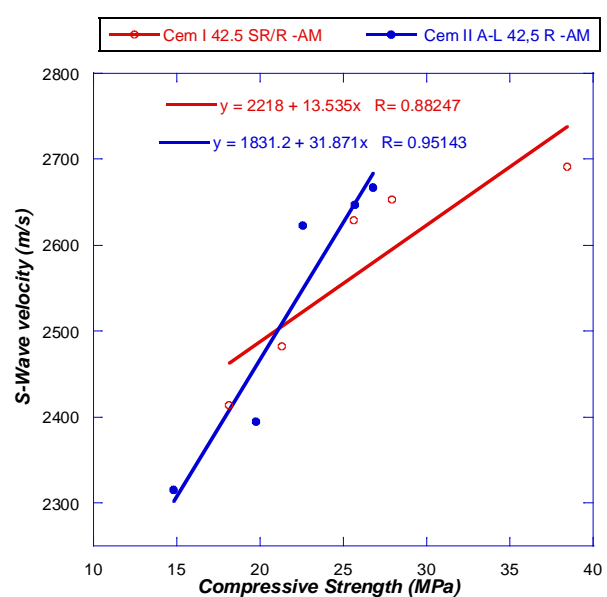


**Figure 5-43** Correlation compressive strength with S-wave for ammonium nitrate samples



### 5.4.4. Correlation Attenuation Profile Area versus Compressive Strength

Figures 5-44 and 5-45 illustrate the correlation curves of compressive strength versus attenuation profile area (APA 1 and 3.5 MHz). A negative relation between compressive strength and attenuation profile area is observed in the figures, APA increases with the decreasing of compressive strength due to the degradation process.

Correlation of the compressive strength versus attenuation profile area was studied by (Fuente, 2004), for cement paste (7, 28 and 90 days of curing), they found that APA decreased with the increasing of compressive strength and the regression coefficient was found to be higher than 0.90, which shows the good correlation between the two parameters. By the same way, as the correlation of compressive strength versus P and S-way was presented, it is concluded that;

- For the degraded cement-based materials, the attenuation profile area of ultrasonic waves has a good correlation with the compressive strength.

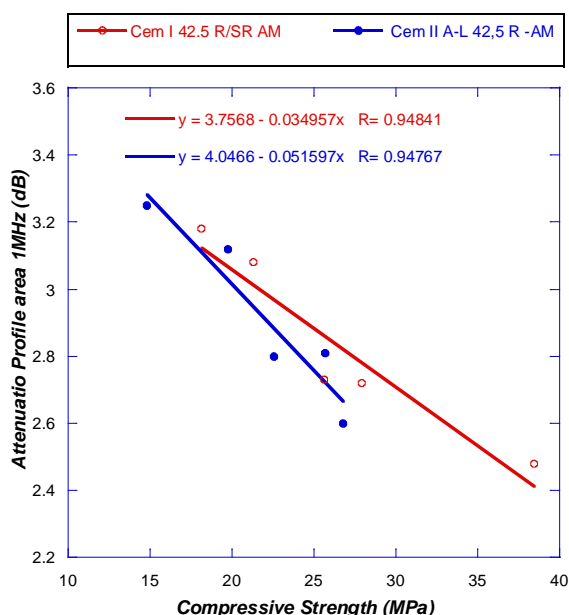


**Figure 5-44** Correlation compressive strength with APA 1MHz for ammonium nitrate samples

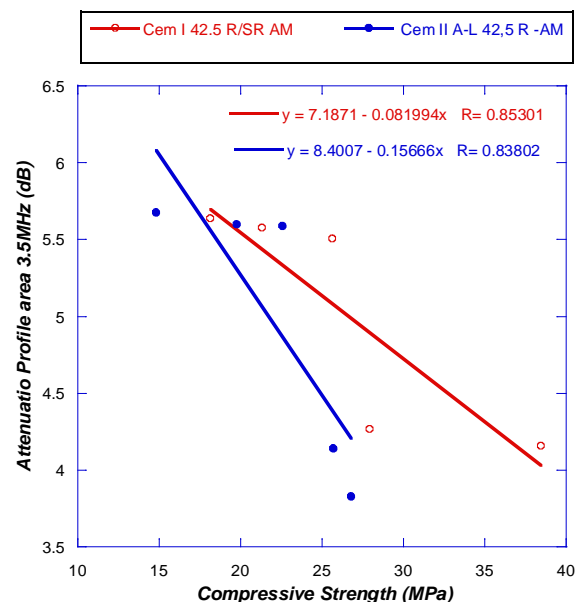


**Figure 5-45** Correlation compressive strength with APA 3.5MHz for ammonium nitrate samples

### 5.4.5. Correlation P and S-waves versus APA

Figures from 5-46 to 5-49 illustrate the correlation curves of longitudinal and shear wave velocity versus attenuation profile area (APA 1 and 3.5MHz), for ammonium nitrate samples. A negative relationship between wave velocity and APA is observed in the figures, APA decreases as wave velocity increases. The correlation factor for both P and S-wave with APA 1MHz is higher than 0.96, and for APA 3.5MHz is higher than 0.73, which reflects that the ultrasonic wave velocity has a better correlation with APA 1MHz than with APA 3.5MHz, this it is not observed in the case of mortar. But, the correlation factor shows the good relationship between the ultrasonic wave velocity (longitudinal and shear wave) and attenuation profile area of ultrasonic wave.

## 5. Results and Discussion of Degradation Process by Ammonium Nitrate

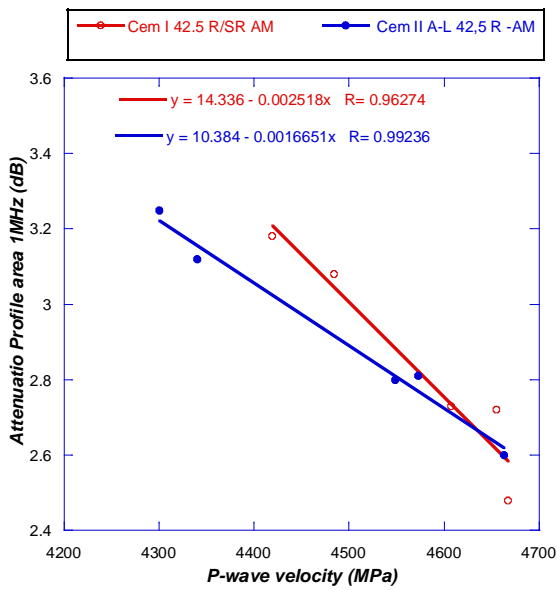


**Figure 5-46** Correlation P-wave with APA 1MHz for ammonium nitrate samples

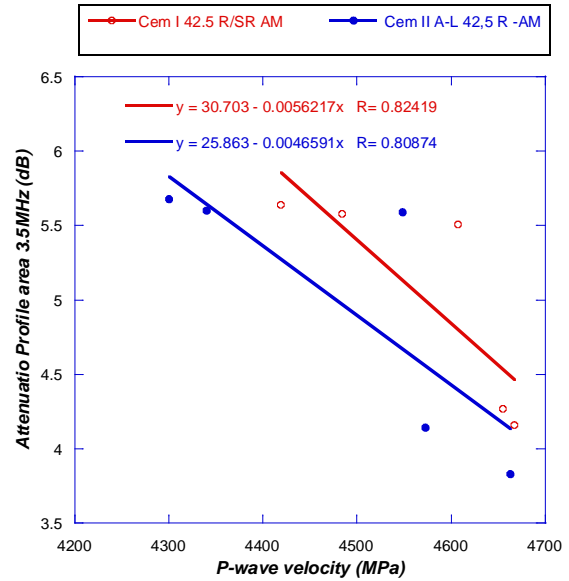


**Figure 5-47** Correlation P-wave with APA 3.5MHz for ammonium nitrate samples

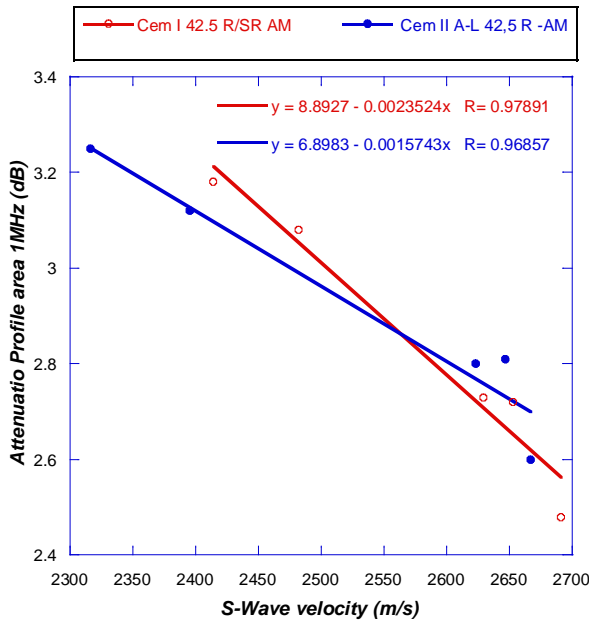


**Figure 5-48** Correlation S-wave with APA 1MHz for ammonium nitrate samples

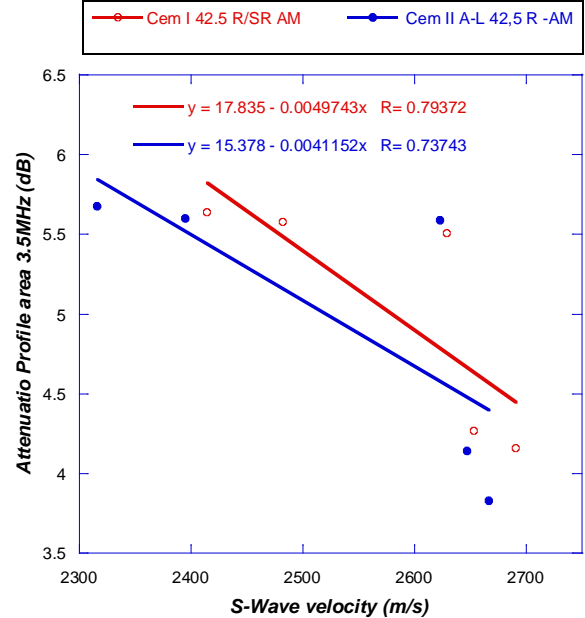


**Figure 5-49** Correlation S-wave with APA 3.5MHz for ammonium nitrate samples

## 5. Results and Discussion of Degradation Process by Ammonium Nitrate

---

As a summary of the conclusions obtained in this chapter are;

- Attenuation profile area (APA) is sensitive to estimate the degradation and it increases by the increasing of the degraded depth.
- The (APA) is sensitive to the changes of microstructure of the degraded mortar and it increases by the increasing both of w/c ratio and frequency.
- The frequency of 3.5MHz is more sensitive to the microstructure changes than the frequency 1MHz.
- Shear wave velocity has a better correlation with Porosity than longitudinal wave velocity for mortar samples and the contrast is observed for concrete samples. This trend also is found for the samples degraded by sodium sulfate.
- The porosity has a better correlation with attenuation profile area for the frequency 3.5MHz than the attenuation profile area for the frequency 1MHz. also it has a better correlation with attenuation profile area than ultrasonic wave velocity.
- It is not always found a good relationship between the strength and the wave velocity, because the ultrasonic pulse velocity values are affected by number of factors, which do not necessary influence the concrete compressive and flexural strength in the same way or to the same extend.
- Correlation of ultrasonic parameters with strength is good and acceptable for early ages and degraded cementitious materials, because the changes in the microstructure are clear and notable.

## 5. Results and Discussion of Degradation Process by Ammonium Nitrate

---

- Attenuation profile area has a good relationship with compressive and flexural strength.
- Attenuation profile area has a good relationship with ultrasonic wave velocities (P and S-wave), which is higher than its correlation with the compressive and flexural strength.
- The relationship between the attenuation profile areas of ultrasonic wave is negative with compressive strength, flexural strength, longitudinal and shear wave velocity and it is positive with porosity.

From the above presented conclusions, it can be said that, the using of ultrasonic wave velocity and attenuation profile area are successful to estimate the porosity and to follow the degradation of cement paste, mortar and concrete when they are subjected to aggressive environments and at early age stage.

One objective was to find a general non-destructive procedure to analyse and follow the decalcification process due to ammonium nitrate. From the previous presented results of Chapter 5, it can be found some general trends that there are useful to establish a general procedure to be applied in the real cases of mortar and concrete structure inspections. As can be seen in the figures from 5-50 to 5-51. On the left hand side of the figures show global regression for each case and the left hand side shows the 10% error interval. Almost all experimental data were within the interval; therefore the ultrasonic parameter can be used to estimate the compressive strength with an equivalent standard error for the destructive parameter. In those cases, it is possible to use the ultrasonic testing instead of the destructive tests

## 5. Results and Discussion of Degradation Process by Ammonium Nitrate

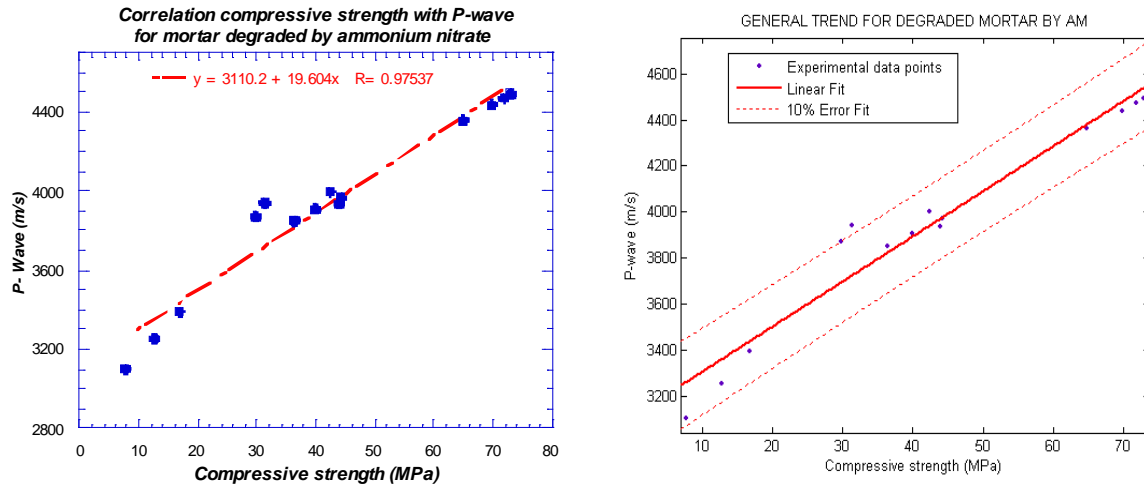


**Figure 5-50** General trend for estimation compressive strength using P-wave velocity of mortar degraded by AM

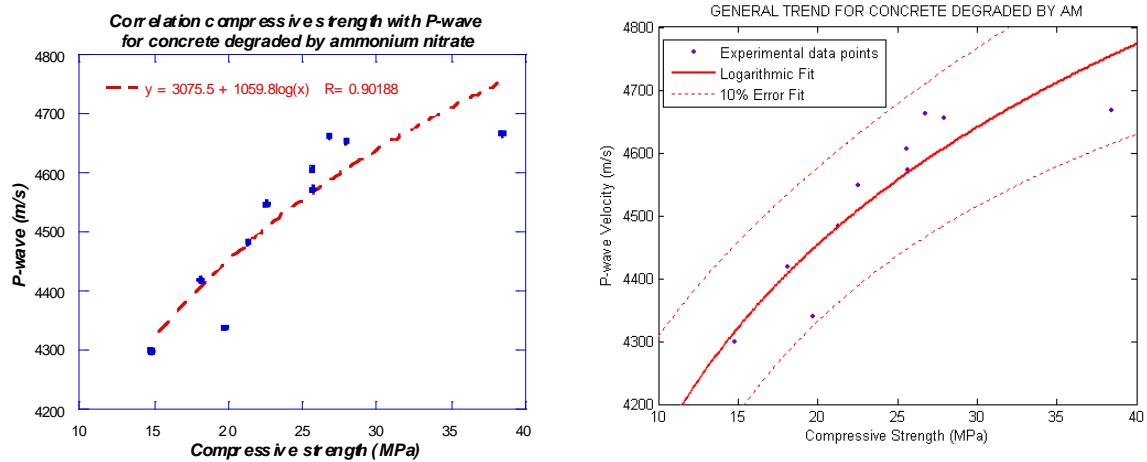


**Figure 5-51** General trend for estimation of compressive strength using P-wave for concrete degraded by AM

# **CHAPTER 6**

**Conclusions and Future Work**

---





## 6 Conclusions

In this work it was studied and analysed the degradation process for mortar and precast concrete samples degraded by sodium sulfate and ammonium nitrate solutions. It was realized several techniques varies between destructive and non- destructive to enhance the objective of this work. Finally from the analysis results of the present work it can be concluded that;

Respecting to the degradation by sulfate attack, ultrasonic wave velocity of longitudinal and shear waves are found successful to follow the two steps of degradation observed for mortar and precast concrete. In the first step the nucleation and growth of delayed ettringite is observed, and the pores were filled by it. Result the porosity of concrete and mortar samples was decreased and led to the increasing of ultrasonic wave velocity in this step. This can be seen with w/c ratios 0.45, 0.375 and 0.30 and for LPC precast concrete degraded samples. In the second step where the damage evolution due to the expansion of ettringite is observed, ultrasonic wave velocity was decreased due to the increasing of porosity. This can be seen for w/c ratios 0.375, 0.45 and 0.525 for mortar and also for LPC degraded samples. On the other hand, when the degradation process by ammonium nitrate is studied, also ultrasonic wave velocity found to be successful to follow the degradation of cement-based materials.

The using of ultrasonic wave velocity is successful to estimate the porosity and to follow the degradation of cement paste, mortar and concrete, when they are subjected to Sulfate attack. In other words, ultrasonic wave velocity (P and S-wave) has a good relationship with porosity for both control and degraded samples, and for mortar and precast concrete, the relationship between wave velocity and porosity found to be linear, a linear relationship between the two parameters is reported by (Lafhaj and Marc, 2009; Fethi et al., 2009; Panzera et al., 2008). Also, it is concluded that, ultrasonic wave velocity correlates better with porosity of mortar samples than porosity of concrete samples. On the other hand, The S-waves velocity correlates better with

mortar porosity than P-wave velocity, the contrast is observed for concrete porosity. (P-wave velocity has a better correlation with porosity than S-wave velocity).

It is found a good linear relationship between ultrasonic wave velocity and strength (compressive and flexural) when the changes in the microstructure of mortar and concrete are clear, as the case of early ages mortar microstructure development and when the samples are degraded by aggressive elements such as sulfate and ammonium nitrate. Panzera et al (2011) cited several studies which correlated the two parameters, some of these studies concluded that it is found a linear relationship between ultrasonic wave velocity and strength of cement based materials such as the studies of (Rajagopalan et al., 1973; Fuente, 2004), other studies found an exponential relationship between velocity and strength as (Demirboga et al., 2004; Trtnik et al., 2009). G. Rüstem et al., (2006) found linear and exponential relationship between the two parameters. On the other hand some studies did not find good relationship between velocity and strength such as the studies of (Popovics and Rose, 1994; Qasrawi, 2000; Turgut and Kucuk, 2006; Panzera et al, 2008). Based on these studies and from the results analysis of this work it can be concluded that; it is found a good correlation between ultrasonic wave velocity and strength when the cement-based materials are degraded by aggressive environments and also at early stage of hydration. This is because cement-based materials depending mainly on their elastic modulus which is closely related to the mechanical strength (Panzera et al., 2011).

Ultrasonic parameters found to be successful to estimate the degradation process by ammonium nitrate, especially the drop in the degraded thickness which observed after 20 days of immersion for mortar samples, and was calculated by Phenolphthalein. Due to this drop, it is observed a drop in the decreasing of penetration depth of ultrasonic pulse, a drop in increasing of APA for both frequencies (1 and 3.5MHz), a drop in increasing of porosity and a drop in decreasing both of ultrasonic wave velocity and strength. All this show the ability of the used techniques to estimate and follow the degradation process, and the sensitivity of ultrasonic parameters to follow the changing in the microstructure of these materials due to the degradation.

## Conclusions and Future Work

---

Attenuation profile area of ultrasonic waves (APA) can be used as a good parameter to estimate the porosity and strength of cement-based materials degraded by aggressive elements. It found to be successful to distinguish the degradation steps due to sulfate attack and also to follow the degradation by ammonium nitrate solution.

In general, it is concluded that, ultrasonic parameters are very sensitive to the microstructural changes produced due to the degradation by sodium sulfate attack and ammonium nitrate. It was compared the sensitiveness of P-wave, S-wave velocities as conventional ultrasonic parameters and also the ultrasonic attenuation of backscattering noise which it is possible to get from one side access of the materials. Therefore, it is very interesting to analyse the evolution of the APA parameters and the ability of it to be correlate with microstructural changes characterized by destructive analysis or complementary testing.

The use of ultrasonic techniques with porosity, compressive and flexural strength, is not enough to follow and estimate the degradation of concrete structure subjected to marine environment but in some cases allow following the degradation process for specific periods and concentration involved in the experimental work. It is observed for the degradation by sulfate, the first step when ettringite forms and fill the pores, the obtained values of ultrasonic wave velocity, attenuation profile area, compressive strength, flexural strength and porosity, all values of these tests reveal to the good state of concrete, but in fact, this is not correct. Thus, the use of a quantitative test or semi-quantitative test as SEM is needed besides these tests, for following the degradation process.

Considering the experimental character of the research and the objective of the thesis, it is very important to analyse which ultrasonic parameter can follow the degradation process in the considered range of the porosity (microstructural changes) and the mechanical performance (compression and flexural strength losses).

One objective was to find a general non-destructive procedure to analyse and follow the degradation process due to sulphate attack and decalcification process by ammonium nitrate. The correlation analysis, carried out in Chapter 4 and Chapter 5, have led some general trends that there are useful to establish a general procedure to apply in the real cases of mortar and concrete structure inspections. In practical, it is not known the w/c ratio or the cement type in mortar and concrete structures. Therefore, it will be very useful to find some general trends for ultrasonic parameters and the porosity and mechanical strength of the degraded samples.

The achieved general trends for the both aggressive environment (SS and AM) reveals that it is possible under specific conditions use ultrasonic parameters to evaluate the degradation level of cement-based materials; these conditions would be related with the following factors:

- the concentration of the used solution,
- the exposure time of the experimental work
- the considered w/c ratio and used cement type,
- the porosity and mechanical performance ranges of the mortar and concrete samples involved in our study.

The mortar degradation by sodium sulphate attack can be followed by S-wave velocity in the considered range of porosity between (14-33%) for all studied w/c ratios. On the other hand, it is possible to estimate the porosity using the APA of frequencies 3.5 MHz when the degradation of the cementitious materials takes place (see Figures 4-106 and 4-107).

The concrete degradation by sodium sulphate attack can be followed by APA 1 MHz in the range of its porosity (9-17%). It is possible to estimate the porosity using the APA for 1 MHz for control and degraded samples. The useful trend allows evaluation the porosity with non-information about the degradation state and using ultrasonic technique for one-side access to the structure (see Figure 4-108).

On the other hand, it is possible to assess the mechanical strength loss of mortar structure during the degradation process by ammonium nitrate, when the degradation process is started and within extend range that covers high strength (close to 80 MPa) until low strength (less than 10 MPa). In the case of concrete degradation by ammonium nitrate, the P-wave can assess and the mechanical strength losses when the degradation is found (see Figures 5-50 and 5-51).

Finally it can be said, the general trends reveals the ability of ultrasonic testing as non-destructive way to assess the degradation process of cement-based materials under specific condition. This could be a useful tool in the pathology inspection procedure for mortar and concrete structures.

## 7 Future Work

Studying the degradation process of concrete with different w/c ratios (above 0.30) is needed addition to the studied concrete in this work. Thus, by using the same technique realized in this work, it could obtain a wide experimental data for concrete besides the data of this work. On the other hand, most of effort in this research has been focused on the relationship between destructive (characterisation) and ultrasonic parameters (non-destructive) in the framework of ambitious experimental plan. In this sense, future research will be realized to complete this wide experimental data for the degraded cement-based materials, with the objective to obtain a general evaluation procedure for estimation the degradation of these materials due to the marine environments.

The ultrasonic numerical simulation can be used as powerful tool to see how the ultrasonic energy (waveforms) will be affected by the microstructure along the degradation process. Obviously, some research should be performed on the degradation modelling of each structure. On the other hand, cement-based materials models, especially concrete, could be used in combination with the experimental data obtained in the current research work to achieve experimental/theoretical degradation models for marine environments. Also, the degradation process could be considered as gradual and complex change at microstructural level, therefore it is possible to use some specific

## Conclusions and Future Work

---

algorithms for the extraction of significant statistical components of the signal (waveforms) that could be used to detect and evaluate with more accuracy these microstructural changes, by the fact of the random component nature of these changes. The backscattering noise contains great part of this information and could be exploit with this kind of algorithms based on higher order statistics, nonlinear signal processing and signal processing for industrial applications.

## 8 References

Acebes Pascual, M. “Estudio y extensión de un modelo micromecánico trifásico para la caracterización ultrasónica de materiales compuestos”. Universidad Politecnica de Madrid, 2007.

Akhras, N. M. “Detecting freezing and thawing damage in concrete using signal energy”. *Cement and Concrete Research*, Vol. 28, No. 9, pp. 1275-1280, 1998.

Al-Amoudi, O.S.B. “Studies on soil foundation interaction in the sabkah environment in eastern province of Saudi Arabia”. PhD dissertation, Department of Civil Engineering, King Fahd University of Petroleum and Minerals, Dhahran, Saudi Arabia, 1992.

Al-Amoudi, O.S.B. “Sulfate attack and reinforcement corrosion in plain and blended cements exposed to sulfate environments”. *Build Environ*, Vol.33 No. 1, pp.53–61, 1998.

Aligizaki, K.K. “Pore structure of cement-based materials”. Testing, interpretation and requirements. *Modern concrete technology series 12*. Taylor & Francis, London, 2006.

Amita, Goel. “Effect of Aggressive Environment on Durability of Metakaolin Based Cement Mortar”. Master of Engineering in Civil (Structures), Thapar Institute of Engineering, Technology (Deemed University), Patiala, India, 2006.

Andrew, R. and Johnson, D. “Portland Cement in the Energy Industry”. Rice University, Houston, Texas, 2008.

Andrew, R. “Chemical composition of Portland cement”. *Visrion* 1.9,2010, <http://cnx.org/content/m16445/1.9/>

Anugonda, P.; Wiehn, J.S. and Turner,J.A. "Diffusion of ultrasound in concrete".Ultrasonics, Vol.39,pp.429-435, 2001.

Azzam, A. E. "Delayed ettringite formation, the influence of aggregate types, curing conditions, exposure conditions, alkali content, fly ash, and mix water conditioner (MWC)".Ph.D. Thesis, University of Maryland, College Park, USA,2002.

Benouis, A. and Grini, A. "Estimation of concrete's porosity by ultrasounds". Physics Procedia, Vol. 21, pp. 53-58, 2011.

Biczock, L. "Concrete corrosion, Concrete Protection". Hungarian Academy of Science, Budapest, 117, 1964.

Bratina,W.J. and Mills,D. "Study of fatigue in metals using ultrasonic technique".Canadian Metallurgical Quarterly,Vol.97,pp. 1-83, 1962.

Cao, J. and Chung, D. D. L. "Damage evolution during freeze-thaw cycling of cement mortar, studied by electrical resistivity measurement". Cement and Concrete Research, Vol. 32, No. 10, pp. 1657-1661, 2002.

Carde,C.; Francois,R.and Torrenti,J.M. "Leaching of both calcium hydroxide and CSH from cement paste: Modelling the mechanical behaviour".Cement Concrete, Vol. 26,pp. 1257-1268, 1996.

Chaix, J. F.; Garnier, V. and Corneloup, G. "Concrete damage evolution analysis by backscattered ultrasonic waves".NDT E Int ,Vol, 36,pp. 461-469, 2003.

Chekroun, M.; Le Marrec, L.; Abraham, O.; Durand, O. and Villain, G. "Analysis of coherent surface wave dispersion and attenuation for non-destructive testing of concrete" . Ultrasonics, Vol.49, pp. 743-751, 2009.



Chen, J.; Jiang, M. and Zhu, b. "Damage evolution in cement mortar due to erosion of sulfate". *Corrosion Science*, Vol. 50, pp. 2478–2483, 2008.

Chu, H.; Chen, J. "Evolution of viscosity of concrete under sulfate attack". *Construction and Building Materials*, Vol. 39, pp. 46-50, 2013.

Demirboga, R.; Türkmen, I. and Karako, M.B. "Relationship between ultrasonic velocity and compressive strength for high-volume mineral-admixtured concrete". *Cement and Concrete Research*, Vol. 34, No. 12, pp. 2329–2336, 2004.

Diamond, S. and Olek, J. (1987). *Mater. Res. Soc. Symp. Proc.* 86, 315.

Ferreira, R.M. "Probabilistic-based Durability Analysis of Concrete Structures in Marine Environment". Doctoral Thesis, Universidade do Minho, Guimarães, Portugal, ISBN 972-8692-16-1, pp.321, 2004.

Flint, E. P. and Wells, L. S. "Study of the system CaO-SiO<sub>2</sub>-H<sub>2</sub>O at 30° C and the reaction of water on the anhydrous calcium silicates". *J. Res. Nat. Bur. Stand.*, Vol. 12, No. 687, pp. 751-783, 1934.

Fuente, J. V. "Análisis Tiempo-Frecuencia para la Caracterización No Destructiva de Materiales de Construcción Mediante Ultrasonidos". Tesis doctoral, Universidad Politécnica de Valencia, 2004.

Garboczi, E. J. and Bentz, D. P. "Microstructure – property relationships in concrete: From nanometer to centimetre". Second (2nd) Canmet/ACI. *Advances in Concrete Technology. International Symposium. Supplementary Papers*, pp. 573-585, 1995.

Gartner, E. M.; Young, E. M.; Damidot, D. A. and Jawed, I. "Hydration of portland cement structure and performance of cements" 2nd edn ed J. Bensted and P. Barnes (New York: Spon Press), pp. 57–113, 2002.

Gérard, B. and Breysse, D. "Modelling of permeability in cement-based materials: Part 1. uncracked medium". *Cement and Concrete Research*, Vol. 27, No. 5, pp. 761-775, 1997.

Gi-Sung, P.; Sung-Tae, C. and Sung-Pil, C. "Predicting model for pore structure of concrete including interface transition zone between aggregate and cement paste". *International Journal of Concrete Structures and Material*, Vol. 3 No.2, pp. 81-90, 2009.

Gjørsv, O.E. "Durability and Service Life of Concrete Structures". Proceedings, The First fib Congress 2002, Session 8, Vol. 6, Japan Prestressed Concrete Engineering Association, Tokyo, pp. 1-16, 2002.

Goueygou, M.; Lafhaj, Z. and Soltani, F. "Assessment of porosity of mortar using ultrasonic rayleigh waves". *NDT & E International*, Vo. 42, No. 5, pp. 353-360, 2009.

Gregor, T.; Franci, K. and Goran, T. "Prediction of concrete strength using ultrasonic pulse velocity and artificial neural networks". *Ultrasonics*, Vol. 49, No. 1, pp. 53-60, 2009.

Gubernatis, J. E. and Domany, E. "Effects of microstructure on the speed and attenuation of elastic waves in porous materials". *Wave Motion*, Vol. 6, pp. 579-589, 1984.

Gutt, W.H. "Chemical resistance of concrete". *Concrete*, 12, 35, 1977.

Hernández, M. G.; Anaya, J. J.; Sanchez, T. and Segura, I. "Porosity estimation of aged mortar using a micromechanical model". *Ultrasonics*, Vol. 44, pp. e1007-e1011, 2006.

Hernandez, M. G.; Izquierdo, M. A.; Ibanez, A.; Anaya, J. J. and Ullate, L. G. "Porosity estimation of concrete by ultrasonic". *NDE, Ultrasonics*, Vol. 38, pp. 531-533, 2000.

[http://www.engr.psu.edu/ae/ThinShells/module%20III/concrete\\_behavior\\_text.htm](http://www.engr.psu.edu/ae/ThinShells/module%20III/concrete_behavior_text.htm)

<http://www.ndted.org/EducationResources/CommunityCollege/Ultrasonics/CalibrationMeth/Calibrationmethods.htm>

Huang, B. and Qian, C. "Experiment study of chemo-mechanical coupling behavior of leached concrete". Construction and Building Materials, Vol. 25, No. 5, pp. 2649-2654, 2011.

IAEA. "Guidebook on non-destructive testing of concrete structures" international atomic energy agency. Vienna ,training course series 17,2002.

İsmail, H. S. and Selami, M. K. "Mean grain size determination in marbles by ultrasonic first backwall echo height measurements". NDT and E International, Vol. 39, pp. 82-86, 2006.

Jacobs, L. J. and Owino, J. "Effect of aggregate size on attenuation of Rayleigh surface waves in cement-based materials". Journal of Engineering Mechanics, Vol. 126, pp.1124-1130, 2000.

Joshi, N. R. and Green, R. E. "Ultrasonic detection of fatigue damage". Journal of Engineering Fracture Mechanics ,Vol. 4, pp.527-538, 1972.

Kakali, G.; Tsivilis, S.; Skaropoulou, A.; Sharp, J. H. and Swamy, R. N. "Parameters affecting thaumasite formation in limestone cement mortar". Cement and Concrete Composites, Vol 25, No. 8, pp. 977-981, 2003.

Kalousek, G. L. and Benton, E. J. "Mechanism of Sea Water Attack on Cement Pastes". ACI Journal. 187. 364, 1970.

Kaplan, M. F. "The effects of age and Water/Cement ratio upon the relation between ultrasonic pulse velocity and compressive strength of concrete". Magazine of Concrete Research, Vol. 11, No.32, pp.85-92, 1959.

Kaplan, M. F. "The relationship between ultrasonic pulse velocity and compressive strength of concrete having the same workability but different mix proportions". Magazine of Concrete Research, Vol. 12, issue 34, pp. 3-8, 1960.

Kaplan, M.F. "The effects of the properties of coarse aggregates on the workability of concrete". Magazine of Concrete Research, Vol. 10, pp. 63–74, 1958.

Karakoç, M. B.; Demirboğa, R.; Türkmen, İ.; Can, İ. "Modeling with ANN and effect of pumice aggregate and air entrainment on the freeze–thaw durabilities of HSC". Construction and Building Materials, Vol. 25, No. 11, pp. 4241-4249, 2011.

Kozlov, V. N.; Shevaldykin, V. G. and Yakovlev, N. N. "Experimental determination of an ultrasonic wave in concrete". Scientific Research Institute for NDT, Moscow, Vol. 2, pp. 67-75, 1988.

Kucharczyková, B.; Keršner, Z.; Pospíchal, O.; Misák, P.; Daněk, P. and Schmid, P. "The porous aggregate pre-soaking in relation to the freeze–thaw resistance of lightweight aggregate concrete". Construction and Building Materials, Vol. 30, pp. 761-766, 2012.

Kumar, A.; Jayakumar, T.; Palanichamy, P., and Raj, B. "Influence of grain size on ultrasonic spectral parameters in AISI type 316 stainless steel". Scripta Materialia, Vol. 40, pp. 333-340, 1999.

Lafhaj, Z. and Goueygou, M. "Experimental study on sound and damaged mortar: Variation of ultrasonic parameters with porosity". Construction and Building Materials, Vol. 23, pp. 953–958, 2009.

Lafhaj, Z.; Goueygou, M.; Djerbi, A., and Kaczmarek, M. "Correlation between porosity, permeability and ultrasonic parameters of mortar with variable water / cement ratio and water content". *Cement and Concrete Research*, Vol. 36, pp. 625 – 633, 2006.

Landis, E. N. and Shah, S. P. "Frequency-dependent stress wave attenuation in cement-based materials". *Journal of Engineering Mechanics*, Vol. 121, pp. 737-743, 1995.

Lee, S.T.; Moon, H.Y. and Swamy, R.N. "Sulfate attack and role of silica fume in resisting strength loss". *Cem. Concr. Compos.* Vol. 27, No. 1, pp. 65–76, 2005.

Lin, J. M.; Sansalone, M. J. and Poston, R. "Impact-echo studies of interfacial bond quality in concrete: Part II—Effects of bond tensile strength". *Material journal*, Vol. 93, No. 4, pp. 318-326, July 1996.

Lin, L. M. and Sansalone, M. "Impact-echo studies of interfacial bond quality in concrete: Part 1-effect of unbonded fraction of area". *Material Journal*, Vol. 93, No. 3, pp. 223-232, May 1996.

Mal, A. K.; Bar-Cohen, Y. and Lih, S. S. "Wave attenuation in fiber-reinforced composites". *ASTM Special Technical Publication*, Vol. 1169, pp. 245-261, 1992.

Malhotra, V. M. and Carino, N. J. "Handbook on nondestructive testing of concrete". *CRC Press LLC*, 1991.

Mather, B. "Effects of sea water on concrete". *Army Engineer Waterways Experiment Station Vicksburg Miss. Report N. AEWES-Misc paper 6-690 AD.739 -563*, 1964.

Mehta, P. K. "Concrete in marine environment". *Taylor & Francis Books*, 206 pp. 2003.

Mehta, P. K. "Effect of cement composition on corrosion of steel in concrete". *Proc. Symp. Corrosion of Steel in Concrete*, ASTM, 1975.

Mehta, P. K. "Durability of Concrete in Marine Environment-A Review". ACI Publication SP- 65. 1980.

Mehta, P. K. and Monteiro, P. J. M. "Concrete: Microstructure, properties, and materials". Second Edition. Prentice Hall, Englewoods Cliffs, NJ. ISBN 0-13-175621-4. 548 pp. 1993

Mehta, P. Kumar, and Paulo J.M. Monteiro. Concrete Microstructure, Properties and Materials. 3rd ed. New York: Mc Graw-Hill, (2006).

Mehta, P.K., Concrete in Marine Environment, Taylor & Francis Books, 2003, 206 pages.

Molero, M.; Aparicio, S.; Al-Assadi, G.; Casati, M. J.; Hernández, M. G. and Anaya, J. J. "Evaluation of freeze–thaw damage in concrete by ultrasonic imaging". NDT & E International, Vol. 52, pp. 86-94, 2012.

Molero, M.; Segura, I.; Aparicio, S.; and Fuente, J .V. "Influence of aggregates and air voids on the ultrasonic velocity and attenuation in cementitious materials". European Journal of Environmental and Civil Engineering, Vol. 15, No. 4, pp. 501 – 517, 2011.

Molero, M.; Segura, I.; Izquierdo, M. A. G.; Fuente, J. V. and Anaya, J. J. "Sand/cement ratio evaluation on mortar using neural networks and ultrasonic transmission inspection". Ultrasonics, Vol. 49, No.2, pp. 231-237, 2009.

Naffa, S. O.; Goueygou, M.; Piwakowski, B. and Buyle-Bodin, F. "Detection of chemical damage in concrete using ultrasound". Ultrasonics, Vol. 40, pp. 247–251, 2002.

Nair, S. M.; Hsu, D. K. and Rose, J. H. "Porosity estimation using the frequency dependence of the ultrasonic attenuation". Journal of Nondestructive Evaluation, Vol. 8, pp. 13-26, 1989.

Neuenschwander, J.; Schmidt, T.; Lüthi, T. and Romer, M. "Leaky rayleigh wave investigation on mortar samples". *Ultrasonics*, Vol 45, pp. 50-55, 2006.

Neville, A. M. "Properties of concrete". 4th Edition, New York, John Wiley and Sons Inc. 1996

Neville, A.M. "Properties of concrete". 4th ed. Longman, 1995.

Neville, A.M. "Properties of concrete". Fourth Edition, Longman group UK limited, 1997.

Nyame, B. K. and Iuston, I. M. "Relationships between permeability and pore structure of hardened concrete paste". *Magazine of Concrete Research*, Vol. 33, No. 116, pp. 139-146, 1981.

Ould Naffa, S.; Goueygou, M.; Piwakowski, B. and Buyle-Bodin, F. "Detection of chemical damage in concrete using ultrasound". *Ultrasonics*, Vol 40, pp. 247-251, 2002

Panet, M.; Cheng, C.; Deschamps, M.; Poncelet, O. and Audoin, B. "Microconcrete ageing ultrasonic identification". *Cement and Concrete Research*, Vol. 32, No. 11, pp. 1831-1838, 2002.

Panzer T. H.; Rubio J. C.; Bowen C. R.; Vasconcelos W. L.; Strecker K. "Correlation between structure and pulse velocity of cementitious composites". *Advances in Cement Research*, Vol. 20, No. 3, pp. 101-108, 2008.

Panzer, T. H; Christoforo, A. L.; Cota, F. P.; Borges, P. H. R.; Bowen, C. R. "Ultrasonic Pulse Velocity Evaluation of Cementitious Materials, *Advances in Composite Materials-Analysis of Natural and Man-Made Materials*". Dr. Pavla Tesinova (Ed.), ISBN: 978-953-307-449-8, 2011. InTech, Available from:

<http://www.intechopen.com/books/advances-in-composite-materials-analysis-of-natural-and-man-made-materials/ultrasonic-pulse-velocity-evaluation-of-cementitious-materials>

Papadakis, E. P. "Ultrasound attenuation caused by scattering in polycrystalline metals". Journal of the Acoustical Society of America, Vol. 37, pp. 711-717, 1965.

Piwakowski, B.; Fnine, A.; Goueygou, M.; Buyle-Bodin, F. "Generation of rayleigh waves into mortar and concrete samples". Ultrasonics, Vol 42, pp. 395-402, 2004.

Poblete, A.; Acebes Pascual, M. "Thermographic measurement of the effect of humidity in mortar porosity". Infrared Physics & Technology, Vol. 49, No. 3, pp. 224-227, 2007.

Popovics S.; Rose J.L. and Popovics J.S. "The behaviour of Ultrasonic Pulses in Concrete". Cement and Concrete Research, Vol. 20, pp 259-270, 1990.

Popovics, J. S. and Rose, L. J. "A survey of developments in ultrasonic NDE of concrete". IEEE Transactions on Ferroelectrics and Frequency Control, Vol. 41, No. 1, pp. 140– 143, 1994.

Popovics, S.; Bilgutay, N.; Karaoguz, M. and Akgul, T. "High frequency ultrasound technique for testing concrete" .ACI Material Journal, Vol. 97, pp. 58-65, 2000.

Pospíchal, O.; Kucharczyková, B.; Misák, P. and Vymazal, T. "Freeze-thaw resistance of concrete with porous aggregate". Procedia Engineering, Vol. 2, No. 1, pp. 521-529, 2010.

Qasrawi, Y.H. "Concrete strength by combined non-destructive methods simply and reliably predicted". Cement and Concrete Research, Vol. 30, No. 6, pp. 739–746, 2000.



Rajagopalan, P. R.; Prakash, J. and Naramimhan, V. "Correlation between ultrasonic pulse velocity and strength of concrete". *Indian Concrete Journal*, Vol. 47, No. 11, pp. 416-418, 1973.

Rathinam, P.S. "Potential application of nanotechnology on cement based materials". Ph.D, Department of Civil Engineering, University of Arkansas, 4190 Bell Engineering Center, 156pp, 2009.

Regourd, M.; Hosnairn, H.; Morlureaux, B.; Bisseny, P. and Evers. G. "Ettringite and Thausmasite in Mortar of the Offshore Dike in the Chebourg Port". No. 358, 1978.

Richardson, A. E.; Coventry, K. A.; Wilkinson, S. "Freeze/thaw durability of concrete with synthetic fibre additions". *Cold Regions Science and Technology*, Vol. 83-84, pp. 49-56, 2012.

RILEM Recommendations. "Absorption of Water by Immersion under Vacuum", *Materials and Structures*, RILEM CPC 11.3, Vol. 101, pp. 393-394, 1984.

Robeyst, N.; Grosse, C. U. and De Belie, N. "Measuring the change in ultrasonic p-wave energy transmitted in fresh mortar with additives to monitor the setting". *Cement and Concrete Research*, Vol. 39, No. 10, pp. 868-875, 2009.

Roney, R. K. "The influence of metal grain structure on the attenuation of an ultrasonic acoustic wave". Dissertation (Ph.D.), California Institute of Technology, 1950.

Sahmaran, M.; Erdem, T.K. and Yaman, I.O. "Sulfate resistance of plain and blended cements exposed to wetting-drying and heating-cooling environments". *Constr. Build. Mater.*, Vol. 21, pp. 1771-1778, 2007.

Sansalone, M. "Impact-echo: The complete story" *.ACI Structural Journal*, Vo. 94, No. 6, November-December, pp. 777-786, 1997.

Sansalone, M. and Carino, N. J. "Detecting delaminations in concrete slabs with and without overlays using the impact-echo method". *ACI Materials Journal*, Vol. 89, No. 2, pp. 175-184, 1989.

Santhanam, M. and Cohen, M.D. "Cracking of mortars subjected to external sulfate attack." *Materials Science of Concrete: The Sidney Diamond Symposium*, Ed. M. Cohen, S. Mindess, and J. Skalny. Westerbok, Ohio: American Ceramic Society, 1998.

Santhanam, M. and Cohen, M.D. "Cracking of mortars subjected to external sulfate Sayers, C. M. and Smith, R. L. "The propagation of ultrasound in porous media. *Ultrasonics* ,Vol. 20, No. 5 pp. 201–205, 1982.

Schickert, M. "Ultrasonics NDE of concrete". *IEEE Ultrasonics Symposium. Proceedings (Cat. No.02CH37388)*, Vol. 1, pp. 739-748, 2002.

Schneider, U. and Chen, S. W. "Deterioration of high-performance concrete subjected to attack by the combination of ammonium nitrate solution and flexure stress". *Cement and Concrete Research*, Vol. 35, pp. 1705– 1713, 2005.

Schmidt, T.; Lothenbach, B.; Romer, M.; Neuenschwander, J. and Scrivener, K. "Physical and microstructural aspects of sulfate attack on ordinary and limestone blended portland cements". *Cement and Concrete Research*, Vol. 39, No. 12, pp. 1111-1121, 2009.

Skalny, J.; Marchand, J. and Odler, I. "Sulfate attack on concrete". *Modern Concrete Technology Series*, Spon Press, London. (2002).

Skaropoulou, A.; Kakali, G. and Tsivilis, S. "Thaumasite form of sulfate attack in limestone cement concrete: The effect of cement composition, sand type and exposure temperature". *Construction and Building Materials*, Vol. 36, pp. 527-533, 2012

Skaropoulou, A.; Sotiriadis, K.; Kakali, G. and Tsivilis, S. "Use of mineral admixtures to improve the resistance of limestone cement concrete against thaumasite form of sulfate attack". *Cement and Concrete Composites*, 2013.

Skaropoulou, A.; Tsivilis, S.; Kakali, G.; Sharp, J. H. and Swamy, R. N. "Thaumasite form of sulfate attack in limestone cement mortars: A study on long term efficiency of mineral admixtures". *Construction and Building Materials*, Vol. 23, No. 6, pp. 2338-2345, 2009.

Skaropoulou, A.; Tsivilis, S.; Kakali, G.; Sharp, J. H. and Swamy, R. N. "Long term behavior of portland limestone cement mortars exposed to magnesium sulfate attack". *Cement and Concrete Composites*, Vol. 31, No. 9, pp. 628-636, 2009.

Smith, E. H. "Mechanical engineers reference book". 12th ed. 1998: Butterworth Heinemann. 1248.

Smith, R. L. "The effect of grain size distribution on the frequency dependence of the ultrasonic attenuation in polycrystalline materials". *Ultrasonics*, Vol. 20, pp. 211-214, 1982.

Soltani, F.; Goueygou, M.; Lafhaj, Z. and Piwakowski, B. "Relationship between ultrasonic rayleigh wave propagation and capillary porosity in cement paste with variable water content". *NDT & E International*, Vol. 54, pp. 75-83, 2013.

Song, H.; Chen, J. "Effect of damage evolution on poisson's ratio of concrete under sulfate attack". *Acta Mechanica Solida Sinica*, Vol. 24, No. 3, pp. 209-215, 2011.

Song, H., C. J. "Effect of damage evolution on poisson's ratio of concrete under sulfate attack". *Acta Mechanica Solida Sinica*, Vol. 24, No. 3, pp. 209-215, 2011.

Sun, C.; Chen, J.; Zhu, J.; Zhang, M. and Ye, J. "A new diffusion model of sulfate ions in concrete". *Construction and Building Materials*, Vol. 39, pp. 39-45, 2013.

Tamn, R. N. and Malhotra, V. M. "The ultrasonic pulse velocity method," *Handbook on non-destructive testing of concrete*". CRC Press, Boca Raton, Edited by Malhotra, V. M. and Carino, N.J., pp. 169-188, 1991.

Taylor, H. F. W. "Cement chemistry". 2nd edition, Thomas Telford Publishing, London, ISBN: 0 7277 2592 0, 1997.

Trtnik, G.; Kavcic, F.; Turk, G. "Prediction of concrete strength using ultrasonic pulse velocity and artificial neural networks". *Ultrasonics*, Vol. 49, pp. 53–60, 2009.

Truell, R. and Hikata, A. "Fatigue in 2S aluminum as observed by ultrasonic attenuation methods". *Special Technical Publication*, No. 213, 1957

Tsivilis, S.; Kakali, G.; Skaropoulou, A.; Sharp, J. H. and Swamy, R. N. "Use of mineral admixtures to prevent thaumasite formation in limestone cement mortar". *Cement and Concrete Composites*, Volume 25, No. 8, pp. 969-976, 2003.

Turgut, P. and Kucuk, O. F. "Comparative relationships of direct, indirect, and semi-direct ultrasonic pulse velocity measurements in concrete". *Russian Journal of Nondestructive Testing*, Vol. 42, No. 11, pp. 745–751, 2006.

UNE-EN 196-1:2005: "Métodos de ensayo de cementos. Parte 1: Determinación de las resistencias mecánicas", 2005.

Uysal, M. and Akyuncu, V. "Durability performance of concrete incorporating class F and class C fly ashes". *Construction and Building Materials*, Vol. 34, pp. 170-178, 2012.

Van Hauwaert, A.; Thimus, J. and Delannay, F. "Use of ultrasonics to follow crack growth". *Ultrasonics*, Vol. 36, pp. 209-217, 1998.

Vegas, I.; Urreta, J.; Frías, M. and García, R. "Freeze-thaw resistance of blended cements containing calcined paper sludge". *Construction and Building Materials*, Vol. 23, No. 8, pp. 2862-2868, 2009.

Verbeck G. J. "Mechanism of corrosion in concrete". *Corrosion of Metals in Concrete*. ACI SP-49, 1975. 21.

Vergara, L.; Fuente, J.V.; Gosálbez, J.; López Buendía, A.M and Domínguez, L.E. "Nondestructive testing on ornamental rock blocks". *Materials Evaluation (American society of Nondestructive Testing)* ISSN: 0025-5327, Vol. 62, pp. 73-78, 2004.

Vergara, L.; Gosálbeza, J.; Fuente J, V.; Miralles, R. and Boscha, I. "Measurement of cement porosity by centroid frequency profiles of ultrasonic grain noise". *Signal Processing*, Vol. 84, pp 2315–2324, 2004.

Vergara, L.; Miralles, R.; Gosálbez, J.; Juanes, F. J.; Ullate, L. G.; Anaya, J. J., et al. "NDE ultrasonic methods to characterise the porosity of mortar". *NDT & E International*, Vol. 34, No. 8, pp. 557-562, 2001.

Vergara, L.; Miralles, R.; Gosálbeza, J.; juanes, F. J.; Ullate, L. G.; Anaya, J. J.; Hernández, M. and Izquierdo, M. "NDE ultrasonic methods to characterise the porosity of mortar". *NDT&E International*, Vol. 34, pp. 557-562, 2001.

Wonsiri, P. "Cement-based materials' characterization using ultrasonic attenuation". PhD, GEORGIA INSTITUTE OF TECHNOLOGY, 2006.

Wonsiri, P.; Jarzynski, J.; Qu, J.; Kim, J.; Jacobs, L. J. and Kurtis, K. E. "Characterization of multi-scale porosity in cement paste by advanced ultrasonic techniques". *Cement and Concrete Research*, Vol. 37, No. 1, pp. 38-46, 2007.

Woodson, R. D. (2009). Chapter 3 - causes of distress and deterioration of concrete. *Concrete structures* (pp. 19-29). Boston: Butterworth-Heinemann.

Yang, D. and Luo, J. (2012). "The damage of concrete under flexural loading and salt solution". *Construction and Building Materials*, Vol. 36, pp. 129-134, 2012.

Yang, R. B. and Mal, A. K. "Multiple scattering of elastic waves in a fiber-reinforced composites". *Journal of mechanical physics and solids*, Vol. 42, pp. 1945-1968, 1994.

Yim, H. J.; Kim, J. H.; Park, S. and Kwak, H. "Characterization of thermally damaged concrete using a nonlinear ultrasonic method". *Cement and Concrete Research*, Vol 42, No.11, pp. 1438-1446, 2012.

Young, J. F.; Mindess, S. and Darwin, D. "Concrete". 2nd Edition, Prentice Hall Inc. 2002.

Zuquan, J.; Wei, S.; Yunsheng, Z.; Jinyang, J. and Jianzhong, L. "Interaction between sulfate and chloride solution attack of concretes with and without fly ash". *Cement and Concrete Research*, Vol. 37, No. 8, pp. 1223-1232, 2007

